The Utilisation of Bio-Platform Molecules in the Green Synthesis of Renewable Surfactants

Rachael Louise Castle

Doctor of Philosophy

University of York

Chemistry

September 2016

Abstract

Biomass utilisation for synthesis of renewable surfactants has many advantages. The development of alternatives to petrochemically derived products is key, as well as reduction in waste sent to landfill. This thesis focused on two surfactant types and took two approaches towards improving their green credentials.

The first investigation aimed at reducing the environmental impact of the synthesis of existing surfactants, alkyl polyglucosides. Zeolites were used as green catalysts to improve product separation and enable catalyst reuse. The key properties of the zeolites were identified as pore size and Lewis acid site strength and density enabling further optimisation to be carried out. Levoglucosan, a glucose-based anhydrosugar, was used as an alternative starting material; the acetal ring improved reaction rate and stereoselectivity compared to the current synthesis from glucose.

The second investigation created a range of novel surfactants with potential as drop-in replacements for current surfactants, sulfo-succinates. Itaconic acid, a bio-derived platform molecule, was used in an environmentally friendly synthesis of sulfo-methylene-succinates; they were tested for surface activity and critical micelle concentration against the market standards. These compounds were shown to have higher surface activities than the equivalent sulfo-succinates, indicating they would make more efficient surfactants. In addition, they exhibited lower critical micelle concentration values meaning the replacements could be employed in smaller amounts in formulations, reducing economic along with environmental impact.

The use of waste biomass, specifically waste paper, was also investigated to source levoglucosan, for alkyl polyglucoside synthesis. Microwave pyrolysis was tested on waste paper and shown to successfully produce levoglucosan in short reaction times; chemical production from this waste stream is a higher value alternative to recycling.

The work detailed within highlighted how a whole process approach is key for future development and that petrochemical depletion does not have to be detrimental to the chemical industry.

Contents

List of Figures

List of Tables

List of Schemes

Acknowledgements

Firstly I would like to thank my supervisors, Professor James Clark and Dr. Avtar Matharu from the University of York as well as Professor Dave Thornthwaite from Unilever. All three have provided me with valuable support and advice throughout my project and encouraged me to develop both within their teams and as an independent researcher. I have learned a lot from them during the last four years.

I am very grateful for the financial support from the Department of Chemistry and from Unilever without which, this project could not have taken place. I also would like to thank the undergraduate labs technical team for their support throughout my teaching scholarship, with a special mention to David Pugh who supported me through all my teaching endeavours.

A thank you is also due to the technical support throughout the department, to Heather Fish for NMR help; to Karl Heaton for mass spec; and especially to Paul Elliott for everything, in particular the help throughout my time as GC Equipment Champion and for allowing Lyndsay and myself to be 'formidable'.

Thank you to the green chemists who made the last four years fun, especially Helen, Lucie, Andy, Fergal, Stiofan, Katie, Rob and Toms A and F. To Julia, Neil and Lyndsay, without you three I would not have got this far, thanks for being great friends and knowing when to back away and throw chocolate. Finally, a special mention goes to my partner Adam, without whom I would definitely have never finished writing this thesis; thank you so much for all the bullying, tea making and patience it took from you to get me here, I owe you many holidays now.

A last thank you goes to my parents who have given me continued support and encouragement through everything; for that I will always be very grateful.

Author's Declaration

I confirm that all the work within this thesis is my own except where clearly referenced or acknowledged. This work was carried out at the University of York between October 2012 and September 2016 and during a visit to Unilever Port Sunlight research centre in August 2015. This thesis has not been submitted for any other award at this or any other institution.

Chapter 1

Introduction

The world as it works today is one that relies heavily on the chemical industry and hence on oil and other fossil reserves. Nearly every aspect of life benefits from the work of this industry; food, medicines, clothes, building, electronics, transport. With reserves of fossil fuels rapidly depleting, the current way of living is becoming, or is already, unsustainable and this is starting to have a major negative impact on the planet and its inhabitants. In order to ensure that the world is maintained in a habitable state for future generations, the principles on which society was built must be evaluated and improved.[1,2]

1.1　Green Chemistry

Green chemistry is a discipline devoted to ensuring the future of the chemical industry is favourable within society and the environment, as well as the future of society and the environment alongside the chemical industry. The relationship must become not only mutually beneficial but sustainable.

There are twelve main ideas within the green chemistry sector which outline the basic objectives to be worked towards and these are listed below.[3]

1. It is better to prevent waste than to treat or clean up waste after it is formed.

2. Synthetic methods should be designed to maximise the incorporation of all the materials used in the process into the final product.

3. Wherever practical, synthetic methodologies should be designed so that they use and generate substances that possess little or no toxicity to human health and the environment.

4. Chemical products should be designed to preserve efficacy of function while reducing toxicity.

5. The use of auxiliary substances (e.g. solvents, separation agents etc.) should be made unnecessary wherever possible and, innocuous when used.

6. Energy requirements should be recognised for their environmental and economic impacts and should be minimised. Synthetic methods should be conducted at ambient temperature and pressure.

7. A raw material or feedstock should be renewable rather than depleting wherever technically and economically practical.

8. Unnecessary derivatisation (blocking group, protection/deprotection, as well as temporary modification of physical/chemical processes) should be avoided whenever possible.

9. Catalytic reagents (as selective as possible) are superior to stoichiometric reagents.

10. Chemical products should be designed so that at the end of their function they do not persist in the environment and break down into innocuous degradation products.

11. Analytical methodologies need to be further developed to allow real-time and in-process monitoring and control prior to formation of hazardous substances.

12. Substances and the form of a substance used in a chemical process should be chosen so as to minimise the potential for chemical accidents including releases, explosions and fires.

The overall green chemistry ideal is not remedial but preventative; minimise waste production, avoid hazardous chemicals, maximise renewable resource utilisation.[1,4]

1.1.1 Motivations

The benefits of adopting green chemical approaches are wider than simply ensuring the future supply of chemicals for modern living. The habits of humans are affecting all life as well as the condition of the planet.[1,5,6]

Environment

Climate change or global warming is a growing threat and stems from the unsustainable use of fossil fuels with no plan for retrieving the carbon back from the atmosphere. With increasing atmospheric

concentrations of greenhouse gases, such as CO_2, the atmosphere is increasing in temperature and this is predicted to have a profound effect of the world's eco- and weather systems in the future. Habitats will struggle to survive in the rapidly changing world causing species to become extinct. Rising ocean levels from melting polar ice caps, decreasing ocean pH from increasing dissolved CO_2 and increasing ocean temperature will mean that the depletion of life will not be limited to just land environments. [4–8]

Another consideration is the growing need for space to dispose of the waste generated from this culture of disposable products. Landfill has many negative impacts on the environment, from leaching of toxic material into the ground and water to endangering wildlife with physical hazards such as sharps objects. But it also has many negative social implications too; complaints of bad smells, ruined views and unstable land left behind once the site is full are just a few. In addition to these resulting effects, the entire idea is based upon the burial of resources which were previously highly valuable, and into which a great deal of time, energy and engineering was invested, and could be utilised for a new generation of products. [1,2,4–6,9]

Legislation and Hazards

A major driver for many behind green chemistry is the reduction of the hazards of the chemical industry. Not only for the chemists who research the idea and the plant workers who manufacture the product, but for the consumer who eats out of, or washes in said product. Finally, also for the environment into which it is disposed and the wildlife who must live amongst it once humans are through with it. Registration, Evaluation, Authorisation and Restriction of Chemicals (REACH) was introduced by the EU Commission to improve the standard of information about all the chemicals in use by industry with the aim of improving the health of humans, animals and the environment through better understanding chemical potential or real hazards. [10,11] The improved clarity of the hazards posed by the chemicals popular with the industry gives green chemistry a good opportunity to provide replacements with lower hazards which are bio-derived and sustainable. [2,4,5] And REACH is not alone, many other leglisative changes concerning the chemical industry have recently or soon are coming into force and imposing ever tightening restrictions on the hazards which are deemed acceptable. In 2009, Classification, Labelling and Packaging of substances and mixtures (CLP) legislation came in to force to ensure all hazards posed by chemicals are clearly established and communicated to all workers and consumers by standardised pictograms

and statements. Also, in 2012, Biocidal Product Regulation (BPR) legislation came into force, ensuring the protection of humans and the environment during the marketing and use of products aimed at protection of humans, animals or the environment against harmful organisms such as pests or bacteria. [12–14]

With concern over these numerous issues growing among consumers, chemical companies have a final incentive for becoming 'green'. Customers are necessary for businesses and the public appetite for environmentally friendly, natural, bio-derived and organic alternatives has never been greater. [2,5]

1.1.2 Methods

There are many approaches to green chemistry which have been adopted, focussing on the various aspects of the chemical manufacturing process, from raw material sourcing, to energy efficient heating, and even novel reactions.

Biomass

Starting at the beginning of a process, use of bio-derived molecules, obtained from biomass or waste products, has many benefits. Synthesis of chemicals from waste not only reduces the amount of material sent to landfill but this is a renewable resource. Growing biomass for the singular purpose of chemical manufacture is also renewable and helps the removal of CO_2 from the atmosphere however careful consideration must be taken for this approach. The biomass needs space to be grown which means it directly competes with food production. Additionally, the land must be properly managed to ensure nutrients and minerals remain renewable and hence the land remains fertile. Use of any biomass, be it waste or produced with chemical manufacture in mind, can be more complex and expensive than use of traditional resources.

Biomass is comprised of a wide mix of materials and the main components are starch, cellulose, hemicellulose and lignin. Starch, cellulose and hemicellulose are similar in structure; all three being polysaccharides arranged in a heirarchical array of fibrils and microfibrils. Lignin is also a polymer however is made up predominantly of aromatic molecules, .

Starch contains two polymers; amylose and amylopectin in up to a 30:70 ratio, Scheme 1. Amylose is a straight chain polymer in which the D-glucose monomers are linked *via* α-1,4-glycosidic bonds, Scheme 1. Amylopectin is a chain of amylose which also contains around 5% α-1,6-glycosidic

linkages creating a branched polymer. The molecular weights of these branched amylose chains can be up to 5×10^8 g mol^{-1} making amylopectin one of the largest natural polymers.[15]
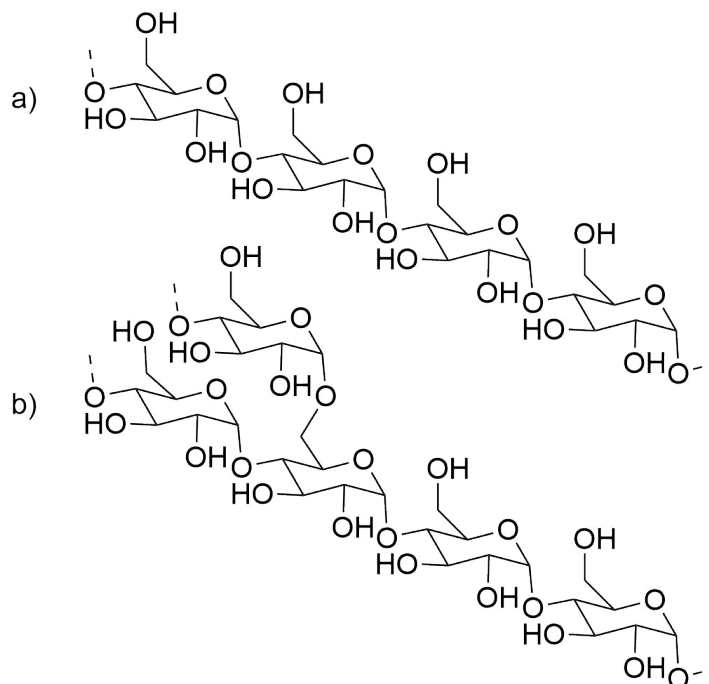
Scheme 1: The structure of starch, comprised of a) straight amylose chains and b) branched amylopectin chains[15]
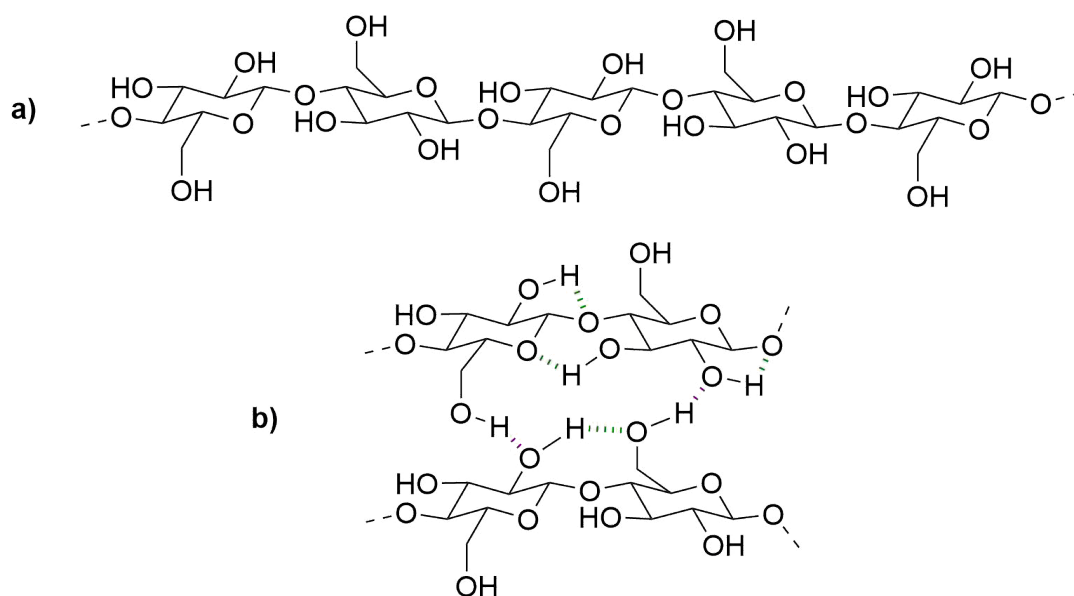
Scheme 2: The structure of cellulose with a) the backbone and b) the hydrogen bonding network between the chains where green are inter-chain and purple are intra-chain[16,17]

Cellulose is the most abundant carbohydrate polymer and consists of D-glucose polymer chains

with β-1,4-glycosidic linkages, Scheme 2. The straight chains interact through various types of hydrogen bonding and form a network of structures with crystalline and amorphous regions. Inter-sheet, inter-chain and intra-chain hydrogen bonds can be observed in cellulose making the polymer strong and rigid and difficult to depolymerise without high temperatures. [16]
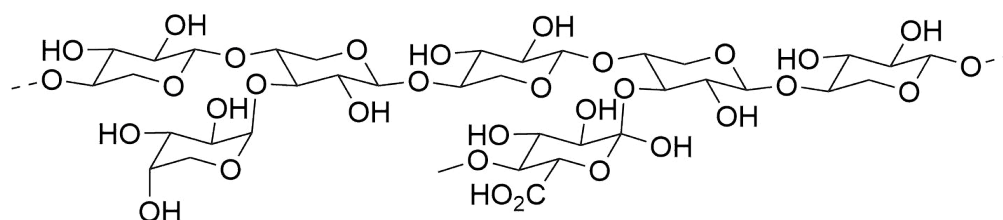
Scheme 3: The structure of hemicellulose with a xylose based backbone and example side chains[18]

Hemicellulose is a polysacharride containing a variety of both hexose and pentose sugar monomers. Xylose, arabinose, glucose, galactose and mannose are the primary components and glucuronic and galacturonic acids can also be present. The xylan backbone of pentose sugars has β-1,6-glycosidic linkages the same a cellulose but is highly substituted with side chains and tends to be crosslinked, Scheme 3. Hemicellulose is found in the cell walls of all terrestrial plants and a few certain types of plants have additional β-1,3-1,4-glucans present too. [18]
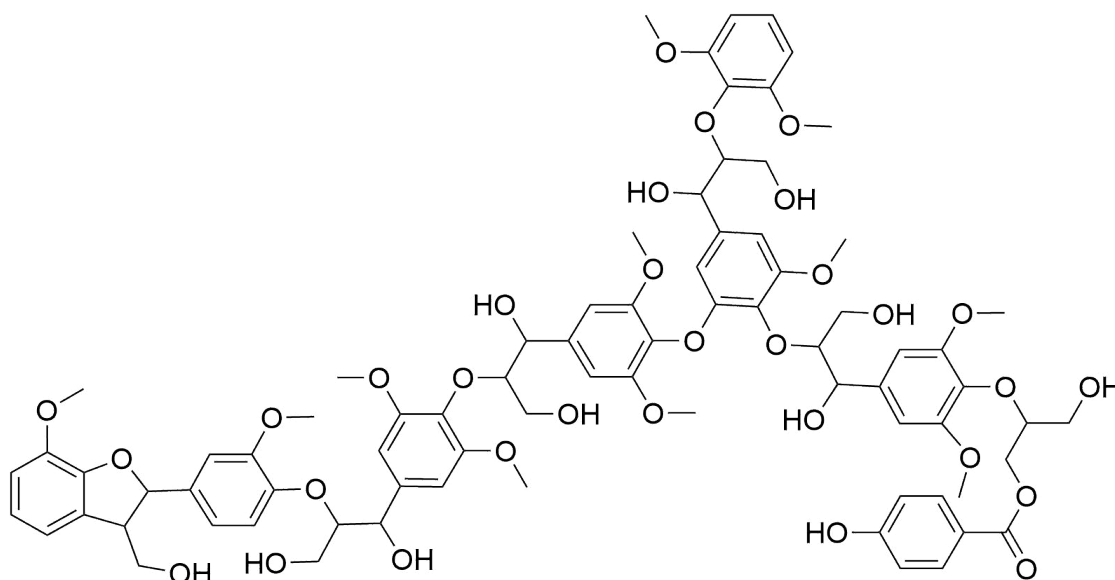
Scheme 4: The structure of a section of lignin[19]

Lignin makes up around 15-30% of woody biomass and is the only biopolymer discussed here which is not a polysaccharide. [5] Lignin protects the polysaccharides in the cell walls of plants and hence is rigid and robust. The monomers in lignin are aromatic molecules, mainly hydroxy-cunnamyl

alcohols, coniferyl alcohol and sinapyl alcohol. Lignin forms from the radical polymerisation of these aromatics and hence the structure is complex and varied depending on the plant, Scheme 4.[19]

Due to this complex nature of biomass, processing can be lengthy and sometimes inefficient. Water content, for example, can be a particular difficulty.[1,4,5,20–22] Despite these challenges, biomass utilisation is enjoying a high degree of interest not only from academic research but also from industry; there are many existing examples of chemicals and products being synthesised from biomass on the market, such as itaconic acid (IA) from corn stover, mesoporous catalysts from starch processing and polyvinyl chloride (PVC) plasticisers from vegetable oils.[5,23–25]

Platform Molecules

The United States Department of Energy (U.S. D.O.E.) has identified platform molecules as an area of green chemistry research with great opportunity and has made a list of the top chemicals for investigation, Table 1. All the molecules chosen were shown to already have potential, not only in the synthesis/production but also in the application. The focus of the research which the report was to encourage, is to improve the economic outlook for the bio-platform molecules which currently acts as a significant deterrent for the majority of the chemical industry.[26]
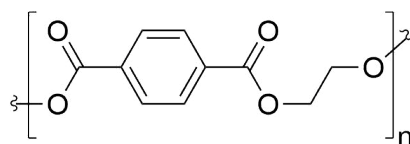
Scheme 5: Structure of polyethylene terephthalate (PET)[4]

The platform molecule approach can be tackled from two angles; looking at molecules to be used as drop in replacements for existing oleochemicals to save on infrastructure upgrades, or to design new products based on the new platform molecules which gives scope to improve on the existing products.[4,5] An example of these two competing approaches can be found in plastic bottles; PET, Scheme 5, is a plastic which has found uses in a large number of applications and consequently >50 million tonnes is produced each year. Bio-based PET is increasingly sought after by companies wishing to advertise their use of a 'plant-bottle'.[4]

The ethylene is readily available from bio-ethanol however the terephthalic acid is made from *p*-xylene which is derived from petrochemicals. The development of bio-based routes to *p*-xylene

for direct replacement has been carried out however all the various syntheses are multi-step, energy intensive processes, Scheme 6.[4,27]

Table 1: U.S. D.O.E.'s top value added chemicals from biomass[26]

Chemical	Structure	Chemical	Structure
1,4-succinic acid		Glutamic acid	
Fumaric acid		Itaconic acid	
Malic acid		Levulinic acid	
2,5-furan dicarboxylic acid		3-hydroxy butyrolactone	
3-hydroxy propionic acid		Glycerol	
Aspartic acid		Sorbitol	
Glucaric acid		Xylitol / arabinitol	

An alternative to the use of *p*-xylene is to produce polyethylene furandicarboxylate (PEF), Scheme 7; instead of terephthalic acid, 2,5-furan dicarboxylic acid (FDCA) is used which is a bio-derived molecule identified by the U.S. D.O.E., Table 1.[4,28–30] The PEF bottles have many improvements on PET, they have lower permeability to gases meaning the contained drinks have a longer life; they have higher glass transition temperature making them easier to handle during the manufacture and filling; and they have lower melting points reducing energy consumption during recycling and processing.[4,31]
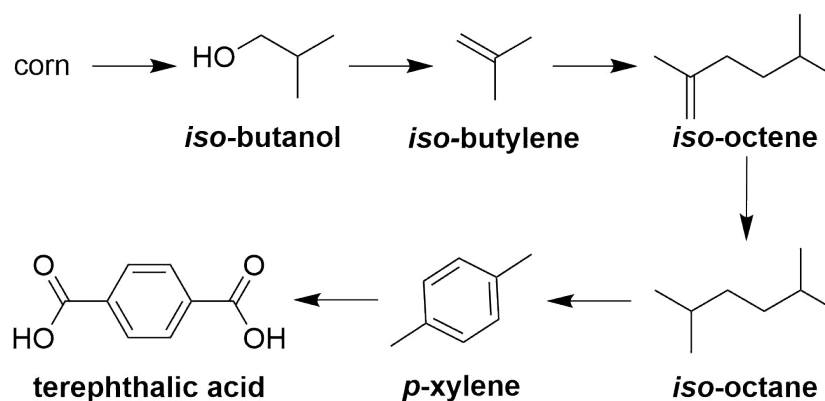
Scheme 6: Example route of synthesis to bio-based terephthalic acid[4,27]
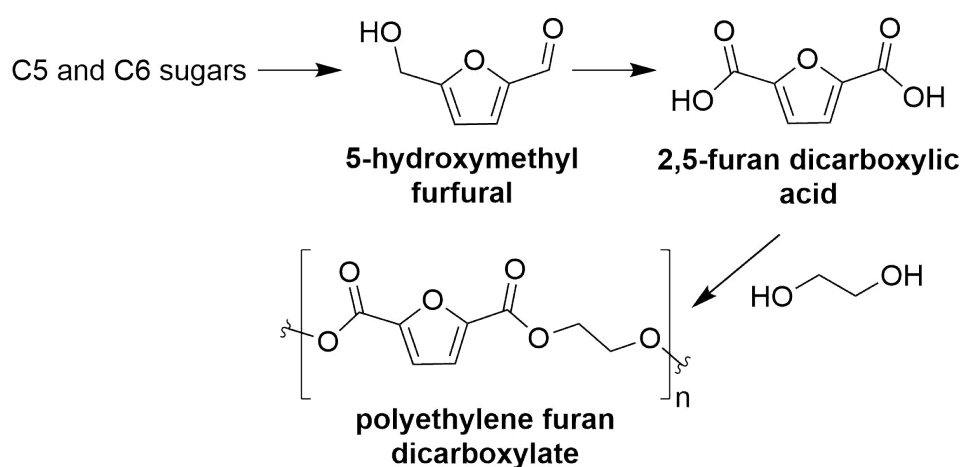
Scheme 7: Structure and example synthesis of renewable PEF, a replacement for PET[4,28–30]

Clean Synthesis

Moving on to the process itself introduces the idea of a clean synthesis. Process optimisation to include alternative solvents, flow chemistry or new catalysts is highly effective in making existing reactions or processes more environmentally friendly and sustainable, but even simple changes such as reducing reaction times or temperatures can improve the energy consumption greatly. The idea is to examine every aspect of a synthesis, even if only small changes can be made.[22,32,33]

Alternative Solvents

Alternative solvents include a wide range of different molecules and solvent properties and can be termed 'green' for large number of reasons. Bio-derived solvents such as *p*-cymene and *D*-limonene, Scheme 8, can be useful for reactions such as esterifications and amidations as they

exhibit properties similar to toluene. Being bio-derived, they are by definition sustainable and their synthesis from waste biomass, such as citrus peel, means that they do not pose any competition to food production. Clark *et al.*[34] tested these two citrus derived solvents against traditional petrochemical solvents in an example of ester synthesis and found that the rate of butyl butanoate synthesis, Scheme 9, was faster in both of the bio-derived solvents than in any of the traditional solvents tried; 84.1×10^{-6}, 106×10^{-6}, 62.6×10^{-6} and 59.7×10^{-6} dm^3 mol^{-1} s^{-1} for *p*-cymene, *D*-limonene, toluene and chlorobenzene, respectively.[34]

a)   **b)**
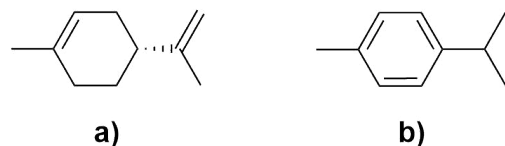
Scheme 8: Two examples of bio-derived solvents synthesised from citrus waste.[34] a) is *p*-cymene and b) is *D*-limonene

a)   **b)**   **c)**   **d)**
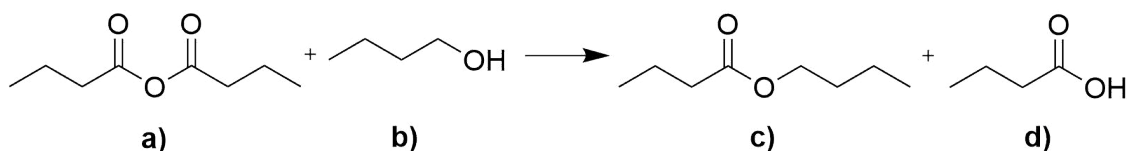
Scheme 9: Model ester formation to test two bio-derived solvents, *p*-cymene and *D*-limonene.[34] a) is butanoic anhydride b) is butanol c) is butyl butanoate and d) is butanoic acid

A problem associated with such solvents often includes the boiling point which can be high, resulting in tricky product separation. To avoid this difficulty, using supercritical CO_2 (scCO_2) is an option. A supercritical fluid is one which has been heated above its critical temperature and compressed above its critical pressure, Figure 1.[35] CO_2 becomes a supercritical fluid above 73.8 bar and 31.1 °C and exhibits behaviours from both the liquid and the gaseous phases. scCO_2 behaves as a gas, though is denser than liquid CO_2 and has improved solvent properties from its liquid counterpart, with higher diffusivity, lower surface tension and viscosity as well as increased polarity. scCO_2 is often utilised as a solvent in organic reactions because of these properties, which are also tailorable to the needs of the reaction simply by altering the temperature and pressure conditions. A change in pressure can alter the polarity of the solvent and switch the solubility of a reactant or product at any given time during the process. Once the reaction is finished, releasing the pressure turns the CO_2 into a gas and hence no separation of product from solvent is required. Becoming supercritical at conditions close to ambient temperature means that the application of this solvent

is relatively inexpensive in terms of energy usage and the lack of any separation reduces process time and additional solvent waste. The inert nature of CO_2 and its low flammability, especially when compared with traditional organic solvent, are also distinct advantages.[4,33,36,37]

Using alternative solvents such as $scCO_2$ is not without its challenges however. Although $scCO_2$ is versatile and its solvating power is tailorable, the solvating power of many traditional organic solvents is stronger. Also, due to the large variety and availability of these existiing solvents, the range of their solvation affinities is wider than that of $scCO_2$. Finally, reactions must be conducted under pressure in order to ensure the CO_2 is supercritical and this can increase process costs and reduce process safety.[4,33,36,37]
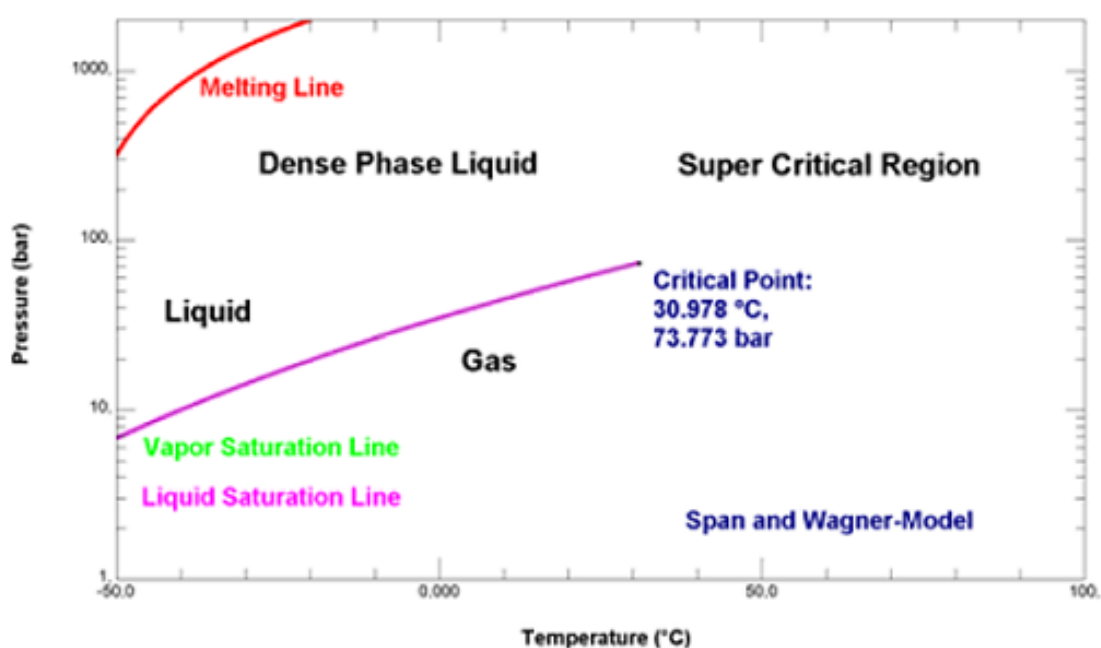
Figure 1: Phase diagram of CO_2[35]

Catalysis

Catalysts are green because they are non-stoichiometric and often re-usable, reducing their impact on the reaction atom efficiency; they improve reaction rate, reducing the energy usage of the process; and they improve reaction yield and often selectivity, which reduces the waste produced by the process.[38,39] Catalysts work by offering an alternative reaction pathway which as a lower activation energy compared with the original reaction pathway, Figure 2.[40] Often, activation of the starting material or stabilisation of key intermediates is the catalysts' role. For example, the rate of acid catalysed esterification is increased because the acid protonates the carbonyl oxygen

in the acid which withdraws electron density from the carbonyl carbon, making it more prone to attack from the oxygen of the alcohol.[41]
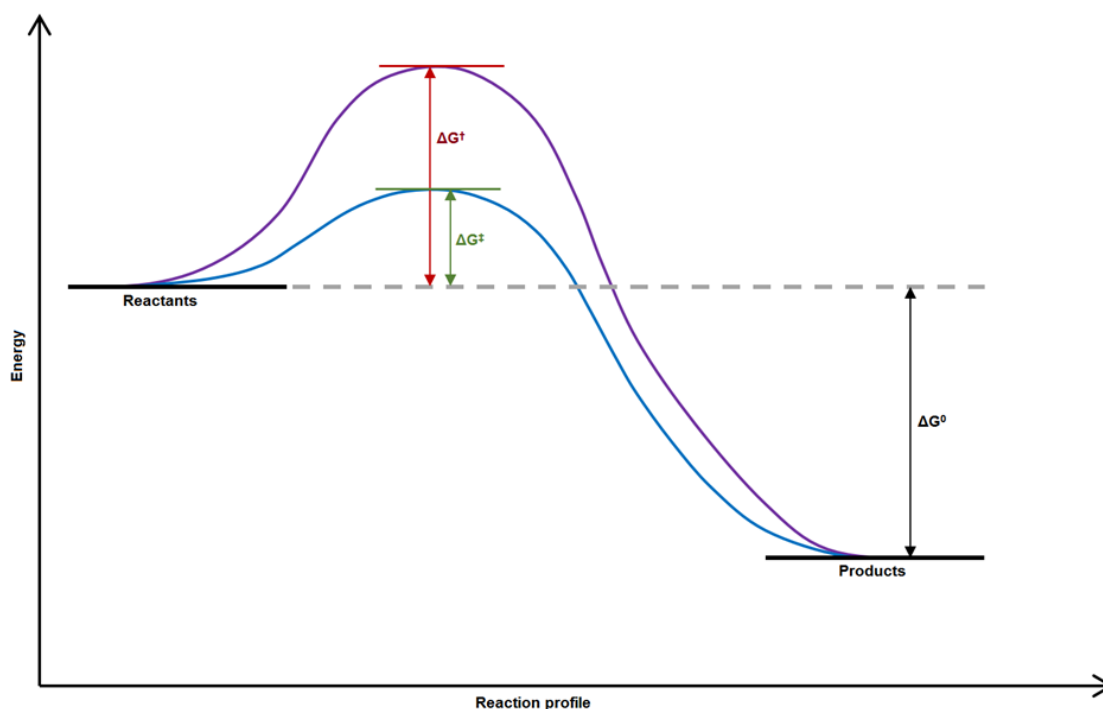
Figure 2: Reaction profiles of a catalysed (blue) and uncatalysed (purple) reaction, showing the difference in activation energy between the two. ΔG^0 is the change in Gibb's Free Energy of the reaction, $\Delta G^\dagger$ is the Gibb's Energy of Activation of the uncatalysed reaction and $\Delta G^\ddagger$ is the Gibb's Energy of Activation of the catalysed reaction

Solid catalysts or solid supported catalysts are important in green chemistry because they can be easily separated from the reaction medium after use and often activated and re-used in subsequent reactions, which reduces waste and cost.[2,39,42]

In the case of esterification, solid acid catalysts such as zeolites are often used. There are two mechanisms proposed for heterogeneous catalysis, the Eley-Rideal (E-R) single site mechanism; and the Langmuir-Hinshelwood (L-H) dual site mechanism. In the E-R mechanism, one substrate adsorbed onto the surface of the catalyst and the other substrate reacts with it while remaining in solution. Esterification catalysed by zeolites has been shown to proceed through this mechanism with the acid substrate entering the pores of the catalyst and complexing to the acid sites of the zeolite. This creates the same δ^+ on the carbonyl carbon as protonation of the carbonyl oxygen does with the traditional acid catalyst, Figure 3.[43–45]
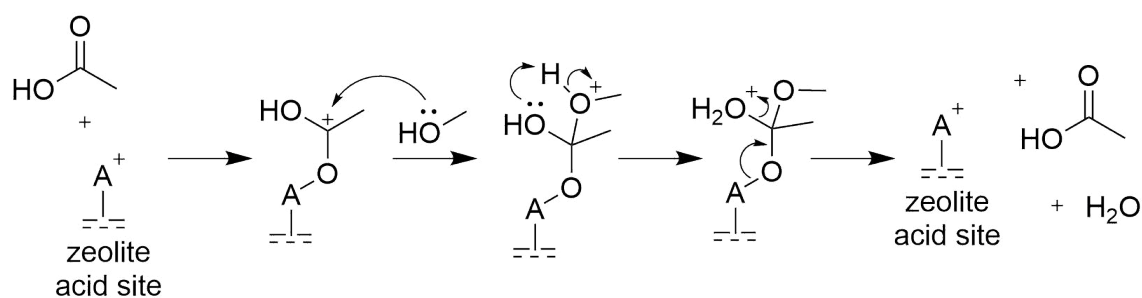
Figure 3: E-R mechanism of heterogeneous catalysis; esterification by zeolites[43]

In the L-H mechanism, both substrates get adsorbed onto the surface of the catalyst and then react together. Esterification catalysed by solid supported acids such as propylsulfonic acid, has been shown to proceed *via* this mechanism. The acid substrate adsorbs onto the surface and is protonated, creating the δ^+ on the carbonyl carbon which can then be attacked by the adsorbed alcohol on a neighbouring or nearby catalyst site, Figure 4.[46,47]
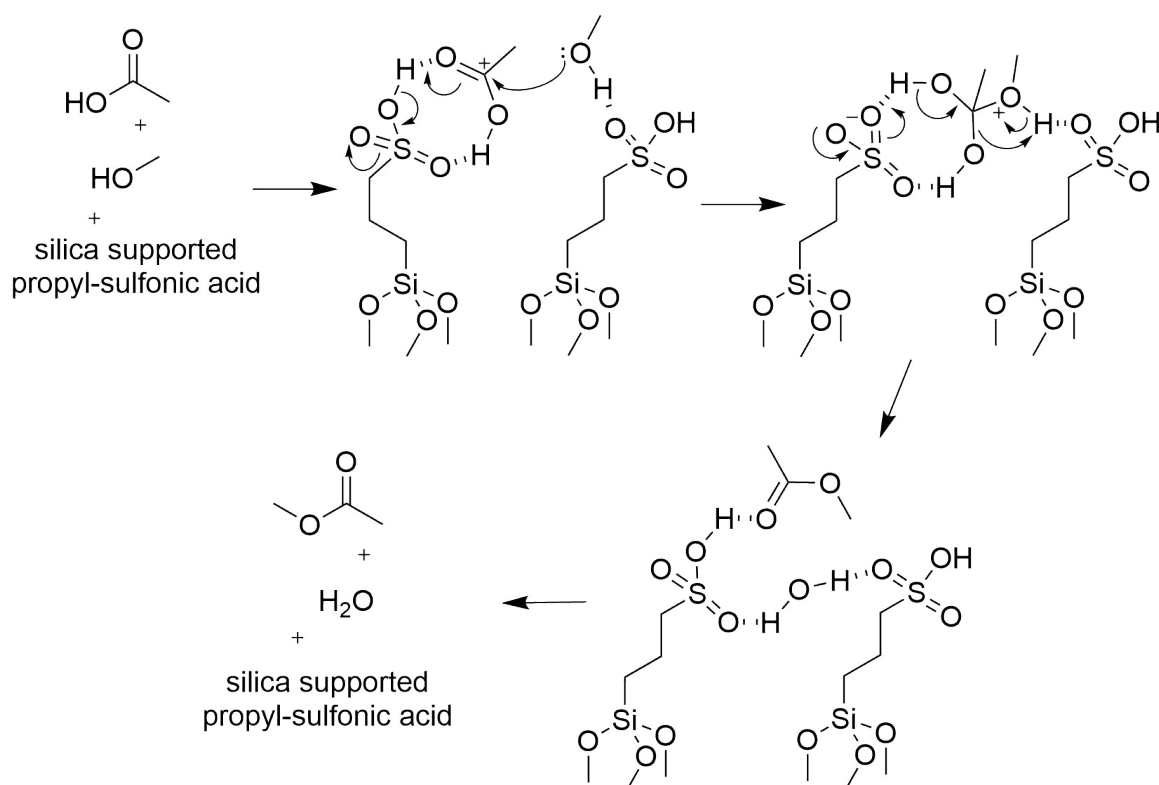
Figure 4: L-H mechanism of heterogeneous catalysis; esterification by silica supported propylsulfonic acid[46]

The cause of the mechanistic differences between the two esterifications is reported to be due to the structure of the heterogeneous catalyst. In zeolites, both substrates must diffuse into the pores

of the catalyst to reach the bulk of the active sites. This means the substrate which remains in solution is close enough to the adsorbed substrate to react. For catalysts which have the bulk of the acid sites on the external surface, both substrates adsorb before they react because any substrate remaining in solution is not restrained in a small pore close to the active site and hence has a low chance of reacting with the adsorbed substrate prior to adsorption. [43–47]

Microwave Technology

The use of microwave heating is a key technique in green chemistry because it has the potential to improve syntheses in a variety of ways. Microwaves which are used in chemical applications are either 2450 or 915 MHz, which are within the range of frequencies that cause rotation of molecules or bonds and hence microwave absorption. The energy dissipates out as heat to other molecules; this process occurs homogeneously throughout the sample (assuming the sample is homogeneous) and so microwaves heat more efficiently and quickly than conventional heating. This has many benefits, more controllable heating improves the safety of the process; more efficient heating reduces the cost of the process by reducing energy consumption; and due to the interaction of the microwaves with the molecules directly, many reactions occur much faster, in a matter of minutes as opposed to hours. [16,48–50]

Different materials absorb the microwave energy by different amounts, dependent on the dielectic loss factor of that material; this is related to the capability of the material to absorb electromagnetic radiation and convert this into heat energy. Many variables effect a material's dielectric loss factor including the polarity and how flexible the molecule or material is; the ability to interact with the microwave radiation and to vibrate or rotate on absorption is important for energy conversion and heat dissipation. Biomass poses many potential problems when it is used with microwave heating as it primarily comprises large rigid structures which are crystalline, such as cellulose or lignin, hence, the molecules cannot move. Pre-treatment of biomass is often used to help microwave increase adsorption, such as use of a chemical or physical process to breakdown the crystallinity and obtain an amorphous structure. [51,52]

Integrated Bio-refinery

Taking all these ideas together, gives the concept of an integrated bio-refinery. Based on similar principles used in the production and processing of crude oil, the bio-refinery takes raw biomass

and puts it through various processes and technologies to obtain a range of products, utilising as much of the biomass as chemically and physically possible.[4,6,9,22] There are many examples of the bio-refinery concept being investigated in the literature, for example the valorisation of food waste such as citrus peel or lignocellulosic biomass such as wheat straw.[6,33,53–57] Citrus peel is obtained from the juicing industry and is composed mainly of cellulose, sugars and flavonoids. Microwave processing yields four product fractions from this waste material, high-value flavonoids such as *D*-limonene; pectin used as a gelling agent; sugars which are important bio-derived building blocks for many chemicals; and mesoporous cellulose which can be useful for synthesis of heterogeneous catalysts.[56,57] Lignocellulosic biomass can be sequentially processed to produce a larger range of products due to the more complex nature, than citrus peel. An overview of one such bio-refinery process which is presented in the literature is shown below, Figure 5.[33]
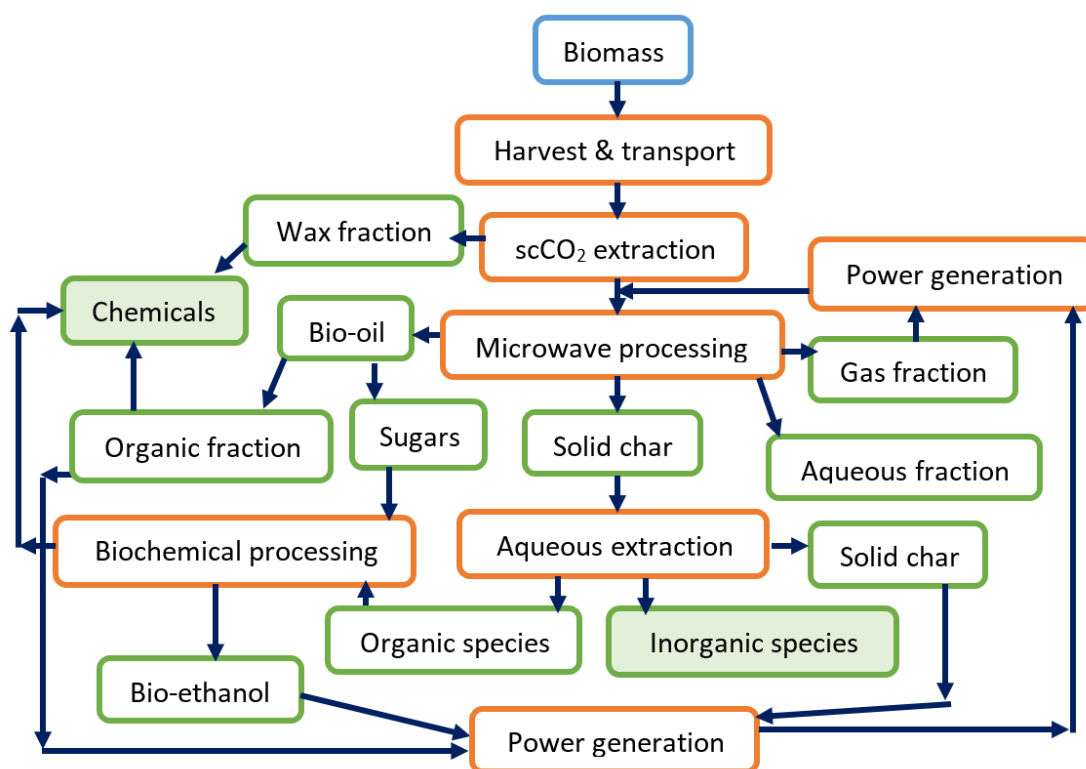
Figure 5: Example of an integrated biorefinery process based on lignocellulosic biomass[33]

A wide range of products were obtained from this bio-refinery. Gaseous products, CO_2 or CH_4 for example, can be utilised in power generation, as can the solid char residue while the organic compounds are useful bio-platform molecules. Fatty acids and alcohols from the wax fraction, along with sugars, can be used for detergents and cosmetics while smaller molecules such as formic acid or acetaldehyde can be used to produce bulk production chemicals of low value.[33]

1.2   Surfactants

Surfactants are produced on a large scale, with currently >14 million tonnes being produced per annum and a consistent annual increase observed.[58] They are used in many sectors including cosmetics, household cleaners, agrochemicals and pharmaceuticals.[58,59] This versatility is due to the fact that surfactants are able to alter the interaction between various liquid phases. They can be utilised for many purposes such as the stabilisation of foams, the solubilisation of one phase into another and the altering of a liquid's surface tension.[59]

1.2.1   Chemistry

Surfactants, or amphiphiles, typically have a hydrophilic head group with a hydrophobic tail and it is this unique combination that affords them so many of their useful properties, Figure 6.[60]

Figure 6: The structure of a surfactant with the hydrophilic head group (shown in red) and the hydrophobic tail (shown in black)[60]

As the two parts of the molecule have opposing affinities to water, in aqueous solutions the behaviour of the surfactants is controlled primarily by the need to reduce the exposure of the hydrophobic section to that solution. When free in solution the hydrophobic tail of the surfactant is surrounded by water molecules and this is entropically unfavourable. Since the hydrophobic tail cannot hydrogen bond with the solvent, the water molecules are forced to rearrange to maximise the hydrogen bonding, Figure 7, which restricts their movement and decreases the entropy of the system. The removal of the hydrophobicity from the water restores the freedom of movement to the water molecules as they can again hydrogen bond in all directions; entropy is therefore gained and Free Energy minimised.[60]
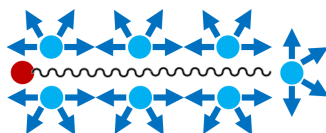
Figure 7: A 'cage' of water molecules around the hydrophobic tail of a surfactant[60]

To remove the hydrophobic tails from solution, the surfactants first localise at the surface,

orientated so that their hydrophobic tails are out of the solution. This behaviour is what causes the reduction in surface tension which is a known and well exploited property of surfactants. Surface tension is due to the cohesive forces between molecules at the surface of a liquid. These forces cannot act in all directions as they do in the bulk liquid and hence the net force on the surface molecules has a direction. Surfactants disrupt this cohesion when they localise at the surface and hence reduce the surface tension, Figure 8.[60]

(a) Pure solvent   **(b)** Solvent plus surfactant
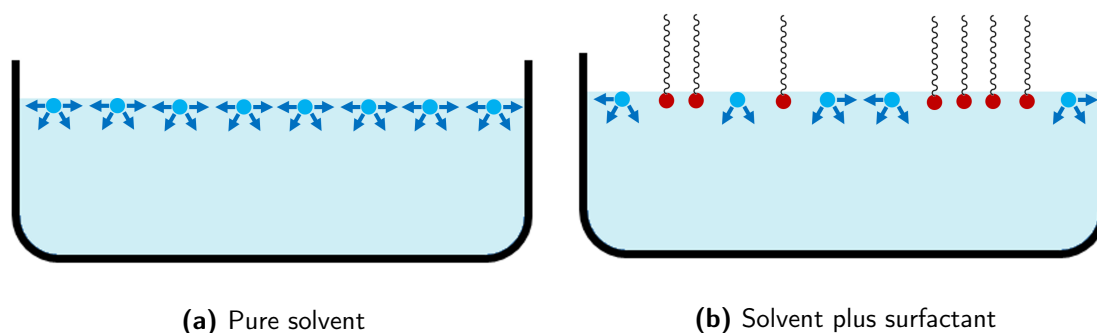
Figure 8: Mode of surface activity of surfactants[60]

What is exceptionally useful about surfactants is that they have a range of behaviours that occur over a range of concentrations and so they can be controlled. On increasing the concentration of surfactant in solution, the surface eventually becomes full and any additional surfactants stay in the bulk solution. This is when micelle formation occurs; the surfactants orientate themselves in groups, with the tails pointing towards the centre of the group. The free energy of the system is therefore minimised by arranging the hydrophobicity inside a shell of hydrophilic head groups, Figure 9.[60,61] The surfactant concentration above which the micelles form is known as the critical micelle concentration (CMC) and is dependant upon the ratio of hydrophobicity to hydrophilicity of the surfactant.[62,63]

Micelles form when the entropic gain from restoring the freedom to the water molecules outweighs the entropic loss of ordering the surfactant monomers into the micelle; this is known as the hydrophobic effect.[60,61]

The concentration of one phase in another immiscible phase, such as oil in water, can also affect the behaviour of the surfactants in that solution. The secondary phase is located inside the micelles, the surfactants in which stabilise the surface of this 'bubble' and hence the maintains mix between the two phases; this is the interfacial activity of surfactants. As the concentration of the secondary phase increases, the micelles get too big to sustain their own size and start to accumulate until the

structure becomes one large macromolecular arrangement, instead of many smaller ones.[60,61] This is outside of the limits of this thesis and so will not be explained in detail however this concept is important in order to stress the versatility and importance of surfactants.

(a) Below CMC: free surfactant   **(b)** Above CMC: a micelle
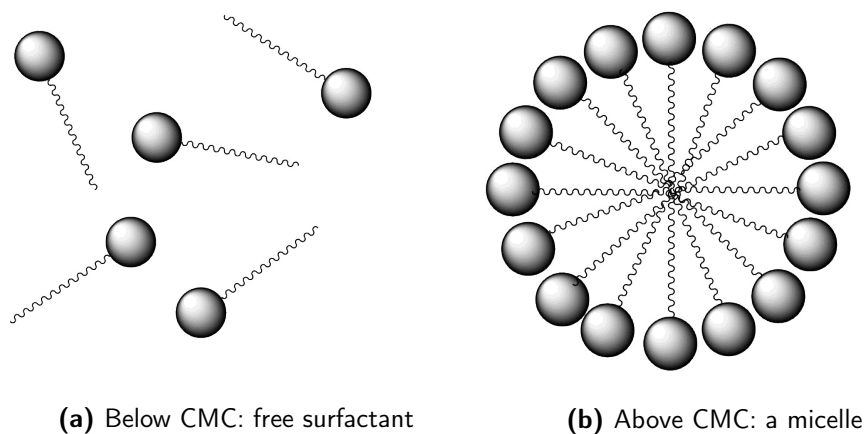
Figure 9: Behaviour of surfactants in solution[60,61]

1.2.2   Green Surfactants

Given the large size of the market, only a small proportion of surfactants are synthesised from renewable sources and so this sector represents a large opportunity, for improvement but also for bio-platform chemical research to take advantage of. Currently, renewable surfactants are split down the middle. Renewable hydrophobes are easy to come by and synthesise; the availability of plant oils and fatty animal derived by-products is huge. Renewable hydrophiles, on the other hand, are more complex with higher functionality and so less available; this means however that there is a wider variety of sources and structures available for research and a larger opportunity for design and implementation of new molecules.
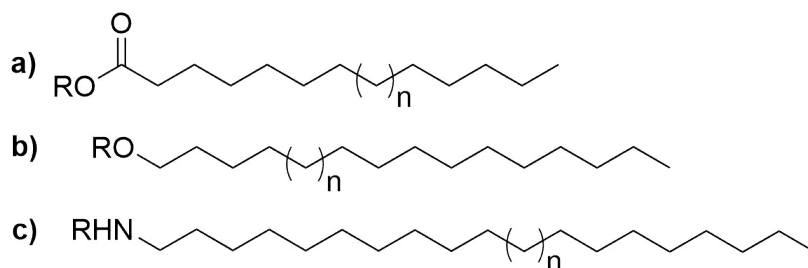
Scheme 10: Examples of hydrophobes used in renewable surfactants, R is a hydrophilic head group, a) is a fatty acid, b) is a fatty alcohol and c) is an amine[58]

The hydrophobic tails are almost exclusively obtained from triglycerides, Scheme 10. Fatty acids and alcohols, and after modification esters too, are readily available and are perfectly suited to the application of long hydrophobic chains and they have a functional group with which to attach a hydrophobic moeity.[58]

Many platform molecules can be utilised as hydrophilic head groups for surfactants; by nature they are hydrophilic and have in-built functionality with which to react the hydrophobic tail. Glycerol, carbohydrates, organic acids and amino acids have all been investigated for utilisation in surfactant synthesis as well as molecules obtainable from pyrolysis such as furfurals, Scheme 11.[58,63–68]

glycerol   **glutamic acid**   **furfural**
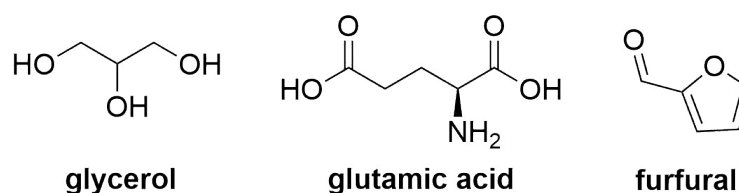
Scheme 11: Examples of bio-platform molecules used as hydrophiles in renewable surfactants[58,63–68]

The large number of applications for surfactants and the industry's dependence on petrochemicals presents a large and pressing opportunity for renewable surfactant synthesis and investigation.

1.3   Summary and Aims

Green chemistry is far reaching; not only in its potential applications but also in its necessity. It has been shown in this section that there are many areas for improvement and many options to explore in doing so. Waste reduction and utilisation are key and should be used in conjunction with the optimisation of novel products to fill the gaps in the green products on the market today. Surfactants are a key area for study, not only because of their large market share but because of the potential for bio-derived molecules within the area and because of the lack of renewable surfactants on the market.

The aim of this thesis as a whole was to utilise the ideas and concepts of green chemistry to investigate novel renewable surfactants and their syntheses. The surfactants were to be based on bio-derived platform molecules and the processes used in their syntheses were to be as clean and sustainable as possible.

The primary aim was to investigate and synthesise renewable, bio-derived surfactants using two different approaches. Firstly, the synthesis of existing surfactants was to be investigated and hence optimised; the chosen surfactants being glsplapg from levoglucosan (1,6-β-D-glucopyranose) (LG). The catalysis of the process and the source of the raw material were the two key areas for improvement. Secondly, the synthesis of novel bio-derived surfactants as drop-in replacements for current market surfactants was to be researched. The similarity between itaconic acid (IA) and maleic acid (MalA) was to be exploited, alongside the bio-derivable nature of IA, to synthesise a range of replacements for the commonly used detergents, sulfo-succinates.

To complement these aims, two supporting investigations were to be undertaken. Firstly, a range of tests designed to determine the surface active properties of the IA based molecules were to be carried out; the objective was to show the potential that these novel surfactants had. Secondly, to examine the potential for LG synthesis from waste material, the microwave pyrolysis of waste and recycled paper was to be studied.

By achieving these objectives, this thesis would provide two approaches to renewable product development, as well as demonstrate the enhanced properties available from novel materials and the scope for valorisation of a waste material.

Chapter 2

Synthesis of Surfactants from Levoglucosan

2.1 Introduction

2.1.1 Alkyl Polyglucosides

There are an increasing number of green, renewable surfactants on the market but one of the most common and well established group is alkyl polyglucosides (APGs), Scheme 12.[58] Based on glucose with a long chain hydrocarbon these surfactants can be synthesised easily from bio-based sugars and triglycerides.[59] The glucose monomer can be obtained from the hydrolysis of bio-polymers such as starch and commercially this is obtained from crops such as wheat, with the hydrophobic moiety being obtained from crops such as palm oil.[58,59] These biomass sources are controversial because of competition with food crops and habitat destruction.
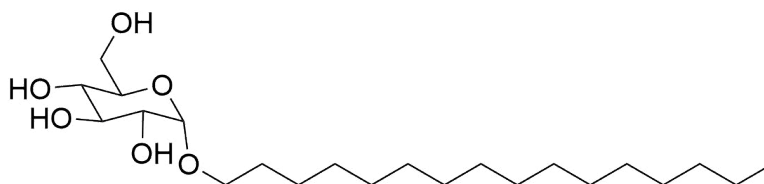
Scheme 12: Structure of an APG, a common renewable surfactant on the market[58,59]

APGs are non-ionic and have many applications in cosmetics, laundry detergents, agrochemicals and hard surface cleaners.[58,59] They are especially popular in personal care formulations due to

their low toxicity, high biodegradability and mildness to skin, especially when compared to other available surfactants.[69] By varying the length of the hydrophobic chain attached to the sugar monomer, the properties of the surfactant can be modified for varying applications. With shorter chains, APGs have good detergent properties whereas the longer chains impart good emulsifying properties to the surfactants; these changes are due to the changing hydrophilic-lipophilic balance (HLB) of the surfactant.[59–61] They are also used to aid the biodegradation of hydrophobic organics in water treatment through increased solubilisation.[70]

Emil Fischer documented the first synthesis more than 100 years ago and Fischer glycosylation is still the main synthetic process used today.[58,59,65] Glycosylation involves the nucleophilic attack of an alcohol onto the acetal of the sugar resulting in substitution, Scheme 13.[59]
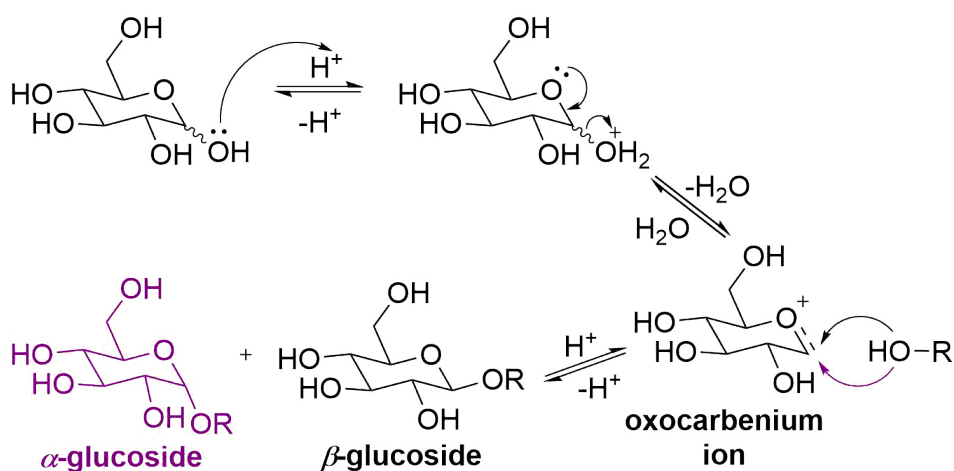
Scheme 13: Mechanism of Fischer Glycosylation of glucose[59]

To produce APGs with longer chains attached poses some synthetic problems, namely solubility and reactivity. There are ways to overcome this, including glycosylation first with a short chain alcohol such as butanol followed by transglycosylation to form the desired APG.[6,58,71] This, along with high costs of production of renewable starting materials, can push up the price of APGs and is a good example of why the renewable products market is slow to take off.[71]

APGs are versatile surfactants with wide ranging applications and many variations have been investigated to extend this further. Use of other sugar monomers is common, such as xylose, as well as functionalisation of the sugar monomer to produce cationic surfactants.[72,73] Use of betaines to crease positively charged surfactants introduces a new range of properties to APGs which increases their application, especially in the cosmetics industry, Scheme 14.[73]
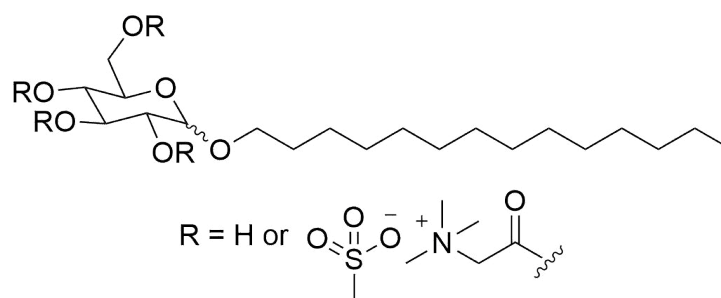
Scheme 14: Structure of an APG functionalised with a cationic betaine[73]

Cationic surfactants can resist being rinsed off the skin meaning the product works for longer but many current cationic surfactants are acutely toxic and have poor biodegradability.[73] Incorporation of alternative hydrophobic tails is also of value. Use of thiols instead of alcohols increases the stability of the surfactant meaning it can be used in a wider range of formulations, Scheme 15.[74]
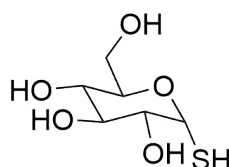
Scheme 15: Structure of an APG functionalised with a thiol group[74]

2.1.2 Levoglucosan

Levoglucosan (1,6-β-D-glucopyranose) (LG) is an anhydrosugar of glucose, with a cyclic acetal between carbons 1 and 6, Scheme 16.[75–77]
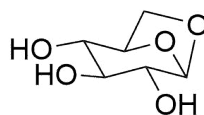
Scheme 16: Structure of LG, an anhydrosugar of glucose[55]

LG is synthesised from cellulose degradation reactions, such as pyrolysis, as discussed in later Chapters.[75–77] Due to the abundance of cellulose in waste biomass, LG has potential for utilisation in the production of bio-derived molecules, such as APGs. Being so similar to glucose in structure, LG is applicable in the synthesis of APGs and with the acetal in LG being cyclic, the ring strain makes the reactivity of carbon 1 high, which means that reaction with alcohols can occur faster.

Not only this but the presence of the ring promotes stereospecific attack on this carbon producing only the α-glucoside. [74]

2.1.3   Solid Acid Catalysis

As mentioned in the Introduction, section 1.1.2, solid or heterogeneous catalysts are a green alternative to conventional homogeneous catalysts as they are reusable and easily separated from the products at the end of a reaction. In addition, the presence of complex pore structures within which the catalysis takes place, means that higher selectivity can be achieved through restriction of available reactants and possible transition states that fit in the pores. [39] The type of heterogeneous catalysts that were focussed on in this thesis were solid acid catalysts due to the nature of the reactions studied and they come in a variety of types; these can include zeolites, clays, silicas, zirconias, and ion exchange resins, and given the diverse structure of these catalysts, they therefore can be applied to a wide range of reactions and substrates.

In general, the mechanism of catalysis by solid catalysts is similar to the counterpart homogeneous catalysts only diffusion and physisorption play important roles in the process too, due to the catalysts' pores. The structure, size and chemical nature of the surface of the catalysts' pore network varies largely between the different solid acid catalysts', as does the origin of the acidity and so the main groups of catalysts investigated in this study have been discussed individually below. The acids tend to have both Brönsted and Lewis acidity, Brönsted acids are molecules capable of donating a proton or hydrogen ion to a base; and Lewis acids are molecules that are electron-pair acceptors and form a Lewis adduct on reaction with a Lewis base through electron-pair sharing. [78]

Zeolites

Zeolties are one of the most common and most widely industrially applied of the solid acid catalysts and are based on structured mesoporous silica doped with different amounts of aluminium. [79] There are a wide range of structures of zeolites but all have at least one network of channels of various sizes which can be interlinked; the structures are characterised as either 1-, 2- or 3-dimensional depending on the cross-linking of the various channel networks. The channels arise because the structures are made of series' of rings of atoms. The number of atoms in each of the rings determines the size of that channel network; ring size can range from 8 to 20 atoms but typically

is between 8–12.[80] β-zeolite, the zeolite type used in this thesis, has channel networks of 12, 6, 5 and 4 rings, Scheme 17.[81]
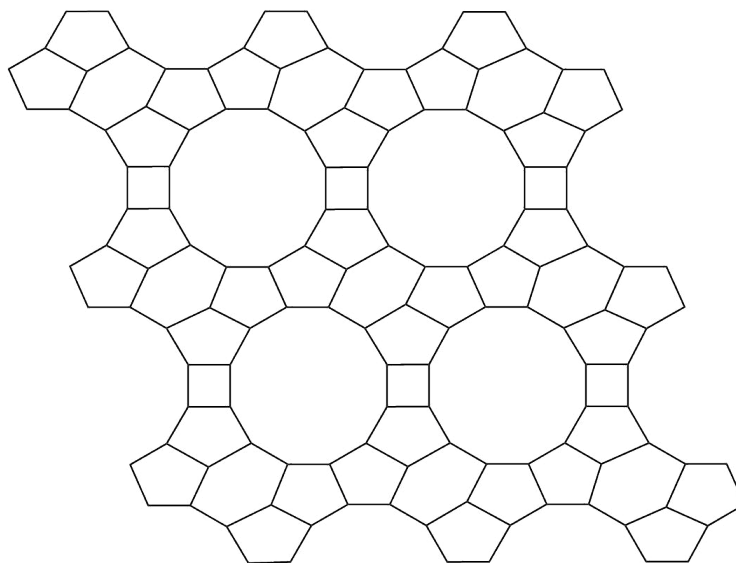
Scheme 17: Structure of polytype B projection 100 through β-zeolite[81]

The acidity in zeolites is produced by multiple sources and there are often both Brönsted and Lewis sites present, of varying strengths.[82–84] As the silicon is 4^+, it sits in a tetrahedral framework of oxygen ions; when silicon is substituted with 3^+ aluminium, there is a surplus negative charge which must be balanced by cations or protons.[85] Metal cations act as weak Lewis acid sites and the protons acts as Brönsted acid sites.[85] This type of Brönsted acidity can be introduced by doping the zeolite with ammonium ions and subsequently calcining; the temperature drives off ammonia and leaves behind extra protons on the zeolite, in the form of bridging hydroxyl groups between silicon and aluminium.[82–84] The external surface of zeolites, or defects from dealumination caused by calcination or steaming are terminated with silanols which are a second, weak type of Brönsted acid site and the third type of Brönsted acid site is a hydroxyl group on an extra-framework aluminium (EFAL); an EFAL is a displaced aluminium atom, removed from the structure, again by calcination or steaming, Figure 10.[82–85]

Lewis acidity is due primarily to the aluminium present in the zeolite. Compensation cations of aluminium, which are extra-framework, have at least one free orbital meaning they act as weak Lewis acids, as mentioned above. Alternatively, dehydroxylation at EFALs, leaves behind aluminium sites with empty orbitals which act as the primary Lewis acid sites. Dehydroxylation of bridging or structural hydroxyls also gives rise to Lewis acid sites, this time with more locality on the silicon

than aluminium, Figure 10.[82,84,85]
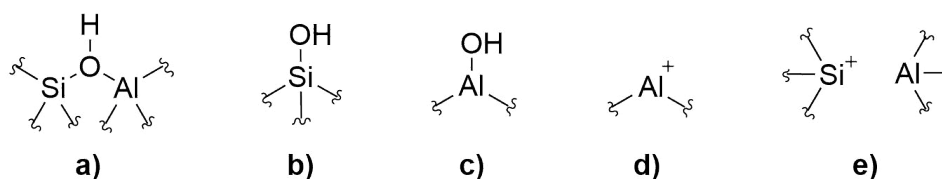
Figure 10: The structures of Lewis and Bönsted acid sites in zeolites. a) is a structural/bridging hydroxyl which is a Bönsted acid site; b) is a silanol which is a Bönsted acid site; c) is a hydroxyl on an EFAL which is a Bönsted acid site; d) is an EFAL which is a Lewis acid site; and e) is a Lewis acid site formed by dehdroxylation of a bridging or structural hydroxyl group[82–85]

The strength of the acid sites is dependant on many factors. For Brönsted acidity the angle of the $Si-O(H)-Al$ bond determines the bond strengths; as the angle increases, the silicon and aluminium bonds to the oxygen get stronger, weakening the $O-H$ bond and increasing the strength of the acid. In the Lewis acid sites, the density of the aluminium within the structure determines the acid site strength. The more isolated the aluminium sites are, the stronger the acid sites are.[85]

Aluminium content has a high impact on the acid strength of the overall zeolite because the effects are two-fold. Increasing aluminium content means more acid sites but a higher density of aluminium means weaker acid sites. Consequently, zeolite acidity tends to peak around a certain alumina:silica molar ratio (Al:Si) ratio and drops off at the two extremes; this peak will vary with the different structures of zeolites and the impact on catalysis will vary with reaction.[84]

Clays

Clays are natural materials which can be modified for use as solid acid catalysts. They are often made up of a range of minerals and the compositions vary greatly; montmorillonite will be focussed on here as it was used in this Chapter. Montmorillonite has a general composition of $Al_2Si_4O_{10}(OH)_2 \cdot nH_2O$ and as with all clays, has a layered structure. The layers are made up of alternating structures; octahedral alumina sheets sandwiched between two tetrahedral silica sheets, Figure 11.[86] The layer spacing can be a variety of sizes, often depending on the amount of water present in the clay but can also be artificially controlled by pillaring. Pillaring is the doping of the clay with ions to sit between the layers and prop them apart from each other giving easier access to the internal clay structure to potential reaction substrates.[86]

Similar to the zeolites, the acidity in clays can be from both Brönsted and Lewis sites. Brönsted sites derive from protons in the interlamellar (between the layers) water which becomes polarised by the aluminium ions in the surrounding sheets. Lewis sites originate from tri-coordinated aluminium with a free orbital.[86–89] These aluminium ions are usually located at the edges of the sheets and can be increased with calcining. Calcining a clay drives out the water, causing collapse of the layers and more unsaturated metals.
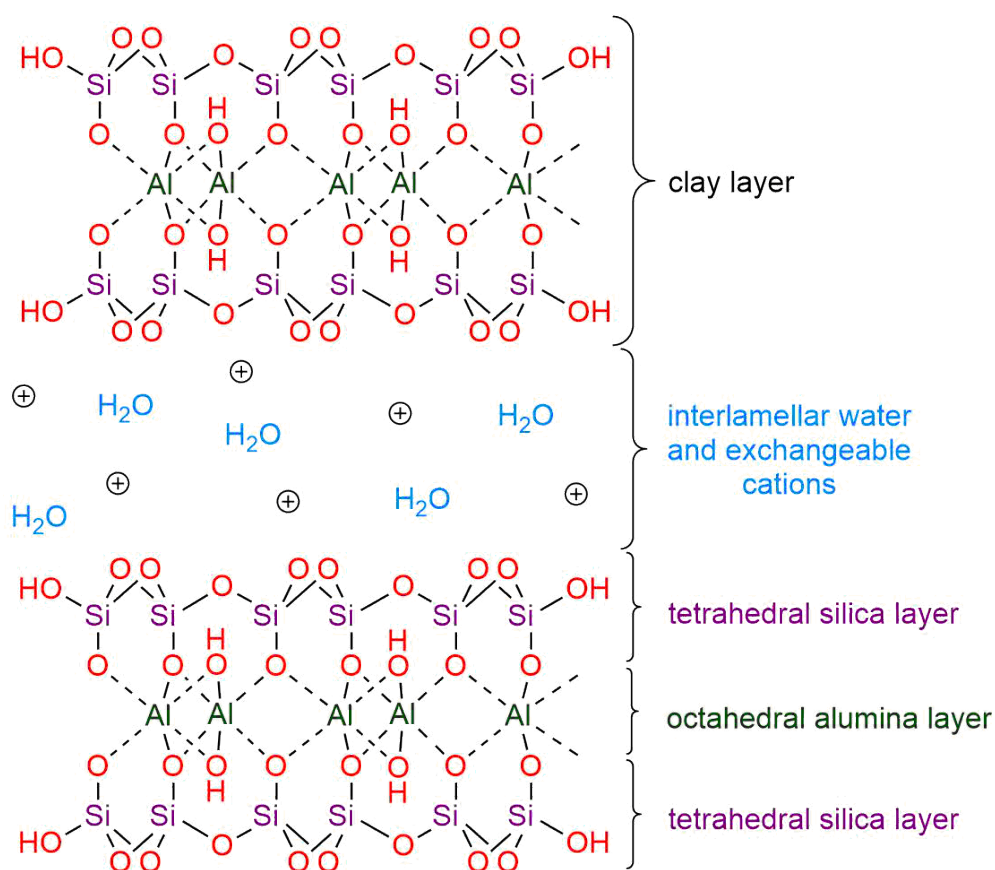
Figure 11: Typical structure of montmorillonite clay with alternating tetrahedral silica and octahedral alumina[86]

To increase the acidity of clays, they can be treated with acid which causes the structure to swell and hence increases the acidity through increased surface area; montmorillonite clay K10 (MK10) and montmorillonite clay K30 (MK30) are two examples of such clays.[86]

Sulfated Zirconia

Sulfated zirconia is an acid catalyst often likened to a superacid, composed of zirconium oxide impregnated with sulfuric acid.[90,91] The structure of the zirconium oxide, on doping with the sulfate groups, becomes more crystalline as the sulfate groups stabilise the tetragonal oxide structure.[92,93] The main acid group on the sulfated zirconia is shown in Scheme 18, however hydrated sulfate groups and coordinately unsaturated zirconium sites are also present, giving a range of acid sites for a variety of catalytic applications.[90–94]
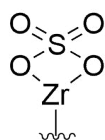
Scheme 18: The main type of acid site observed in sulfated zirconia; a sulfate group coordinated *via* a bridging structure[90–94]

2.1.4   Aims of the Chapter

APGs are renewable bio-derived surfactants which have an increasing share of the market for cosmetics and detergents, with production >85,000 tonnes in 2012.[58,59,70,95–99] Their popularity stems from their potential 100% derivation from biomass,[70,95] alongside their low toxicity[98,99] and biodegradability.[100] In order to maintain this growth, there must be continual improvement in the methods used for deriving the starting materials from biomass, as well as in the synthesis of the APGs themselves. Many of the commercial APGs are synthesised from glucose,[58,59,96] in Fischer glycosylation catalysed using corrosive acids such as *para*-toluene sulfonic acid (*p*-TSA).[58,97] Areas for improvement can easily be identified, such as the current need for high reaction temperatures and strongly acidic catalysts.[58,59] As there is already an established market for these green surfactants, the aim of this Chapter was to investigate avenues of synthesis which could reduce the environmental impact of the synthesis as well as the impact on the growth of crops for food and utilise the biomass waste sent to landfill. The area chosen for investigation in this thesis was acid catalysis; solid acid catalysts are gaining in popularity and application and have been shown to be well suited for alcoholysis reactions.[101] Solid acid catalysts are known for high selectivity, low corrosiveness, easy product separation and extensive catalyst reuse which could result in a wider substrate scope for APG synthesis as well as improved green credentials and lower costs.

2.2 Catalyst Screen

The first stage of the investigation into the synthesis of APG surfactants from LG was to do a screen of potential catalysts, all acidic. The model reaction chosen was ring opening of LG with methanol to form methyl-α-D-glucopyranoside (MGP), Scheme 19.
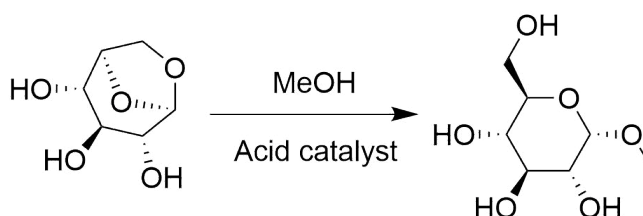
Scheme 19: The acid catalysed ring opening of LG with methanol to form MGP

2.2.1 Side Products
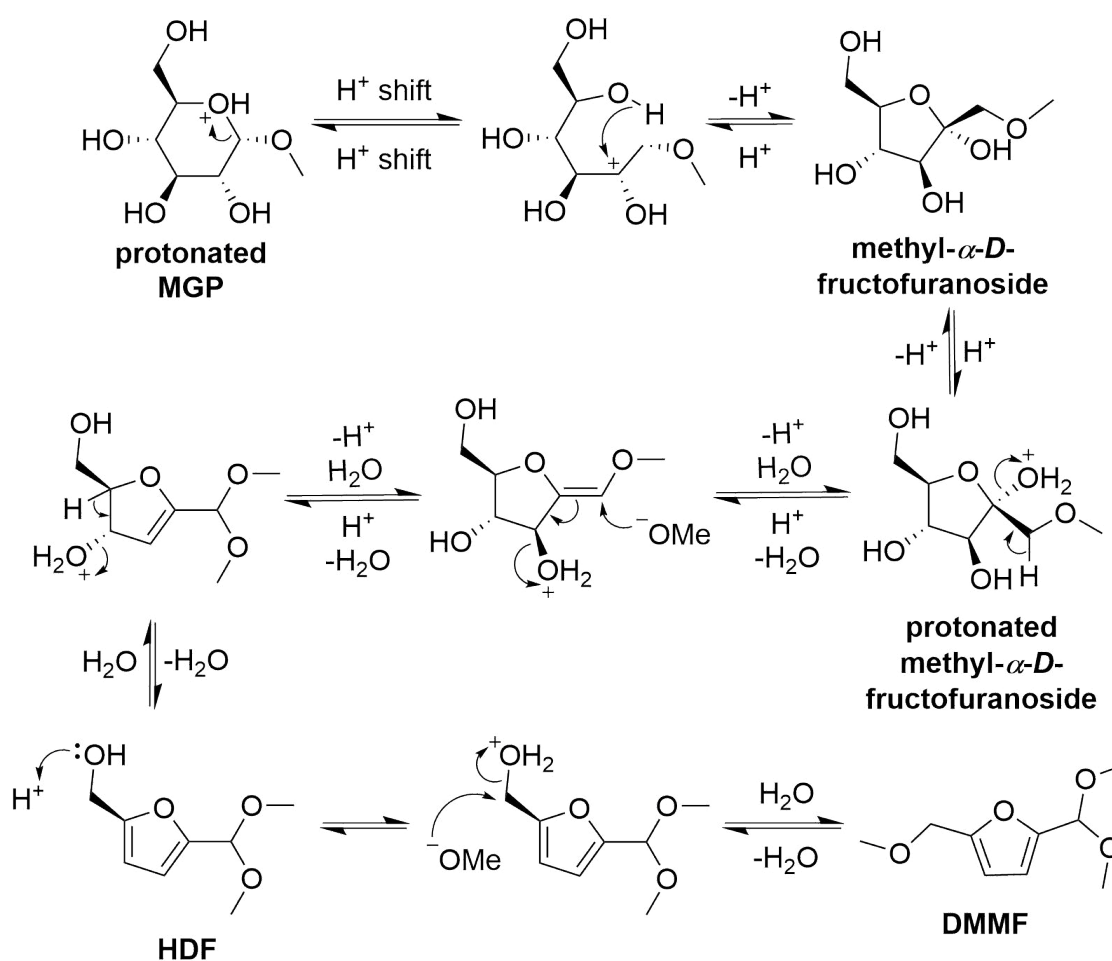
Scheme 20: Mechanism of formation of side products, HDF and DMMF, from isomerisation of MGP, observed in the acid catalysed ring opening of LG with methanol[55,102–107]

This reaction was monitored using gas chromatography (GC) and the side products were identified by comparison to standards together with gas chromatography-mass spectrometry (GC-MS) and nuclear magnetic resonance (NMR) spectroscopy where necessary. The side products identified for this reaction were 5-(hydroxymethyl)-2-(dimethoxymethyl)furan (HDF), methyl levulinate and 2-(dimethoxymethyl)-5-(methoxymethyl)furan (DMMF), Schemes 20 and 21, as well as small LG oligomers; although it was suspected that larger oligomer chains were also formed but identification of these was not possible due to their large size, low concentration and co-elution.
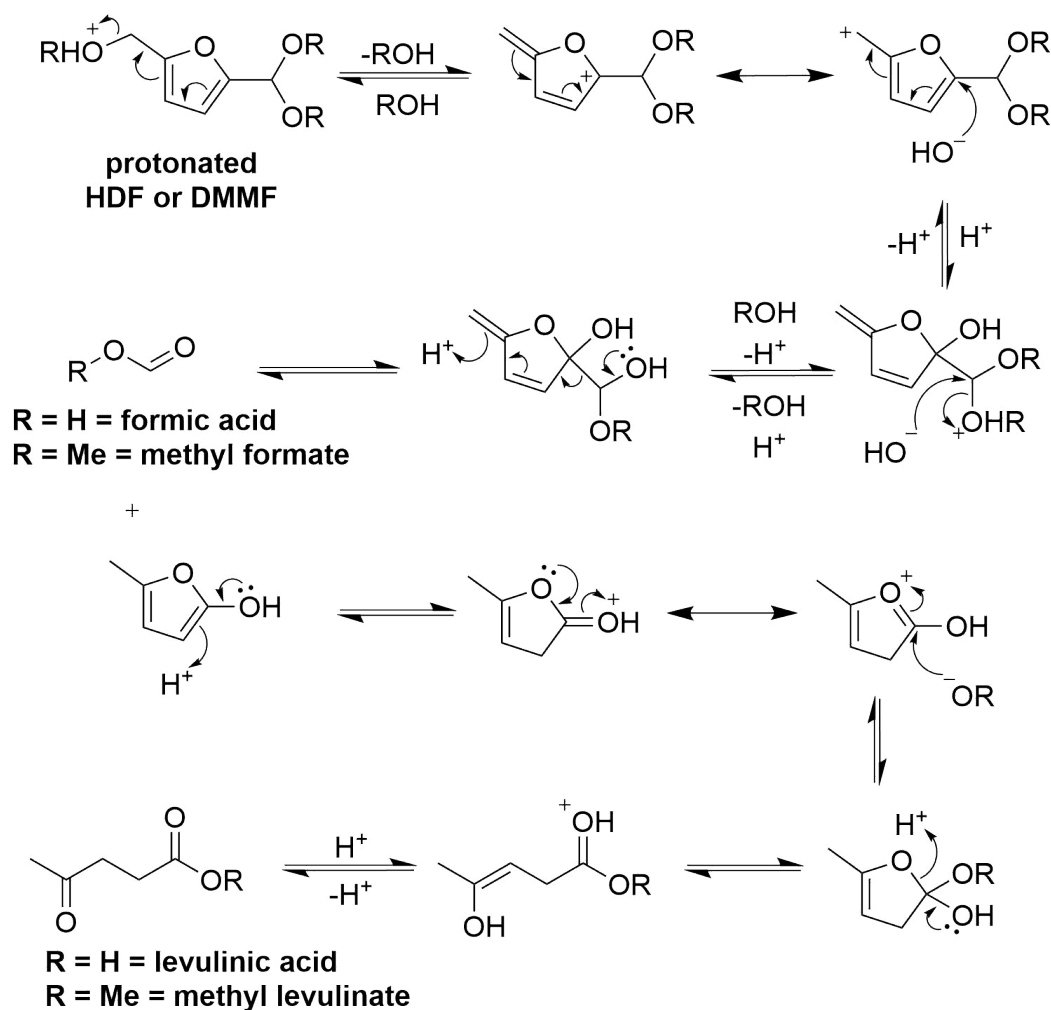
Scheme 21: Mechanism of formation of side products, methyl levulinate, levulinic acid, formic acid and methyl formate, observed in the acid catalysed ring opening of LG with methanol[55,103–106,108,109]

Methyl formate would also be formed alongside the methyl levulinate but this was not confirmed due to co-elution with methanol in the GC and GC-MS. It is known that in aqueous acidic conditions glucose can be isomerised to fructose and then dehydrated to form 5-hydroxymethyl furfural (HMF)

which can breakdown to form levulinic and formic acid;[103,104,107–112] it has also been shown that in the presence of methanol the same acid catalysed reactions can occur to form methylated variants of the same products.[55,105,106,108,109] Proposed mechanisms for the formation of these side products are shown in Schemes 20 and 21.[55,102–106,108]

2.2.2   Initial Screens

The screen of acids that was carried out investigated a range of homo- and heterogeneous acids of varying strengths. Currently, many of the industrial processes still use homogeneous acids such as sulfuric acid or p-TSA so it was important that homogenous acids be tested to act as a comparison for the heterogeneous catalysts; these are more desirable for many reasons, namely ease of separation and reuse.[58,65,101] The familiarity and existing infrastructure have meant that homogeneous acids have remained popular for longer than necessary.

Homogeneous Acids

The two homogeneous acids chosen were phosphoric acid (H_3PO_4) (PAcid) and tungstosilicic acid ($H_4[W_{12}SiO_{40}]$) (TAcid) and the results, shown in comparison to an uncatalysed reaction, are presented below, Figure 12.

It is clear from these results that TAcid performed well, achieving high conversion and selectivity, both 98%, whereas PAcid gave both lower conversion and lower selectivity,13% and 72% respectively. Heteropolyacids like TAcid are known for being strong acids, stronger than most mineral and solid acids, and TAcid in particular has been compared to superacids.[113,114] PAcid has pK_a values of 2.12, 7.20 and 11.9 for the three proton dissociations whereas TAcid has pK_a values of 2.0, 4.0 and 6.3 which are much lower. This would account for the higher activity of the heteropoly acid for this ring opening reaction.[113] In addition to this higher acid strength, heteropoly acids are known to have higher catalytic activities than other acids due to the ability of the large polyanionic complex, formed by the deprotonation of the heteropoly acid, to stabilise cationic reaction intermediates;[113] in this reaction this would be the protonated LG, prior to attack from $^-$OMe, Scheme 22.

TAcid showed great potential for the catalysis of this reaction however use of a heterogeneous acid would be preferable to enable easy separation, regeneration and reuse of the catalyst. The use of supported heteropoly acids would be an interesting avenue to investigate as TAcid has often

been supported on silica for catalytic purposes as well as on other materials such as filamentous carbon.[113] The investigation of supported heteropoly acids fell outside of the scope of this thesis however given the promising results obtained, would be interesting to investigate further in the future.
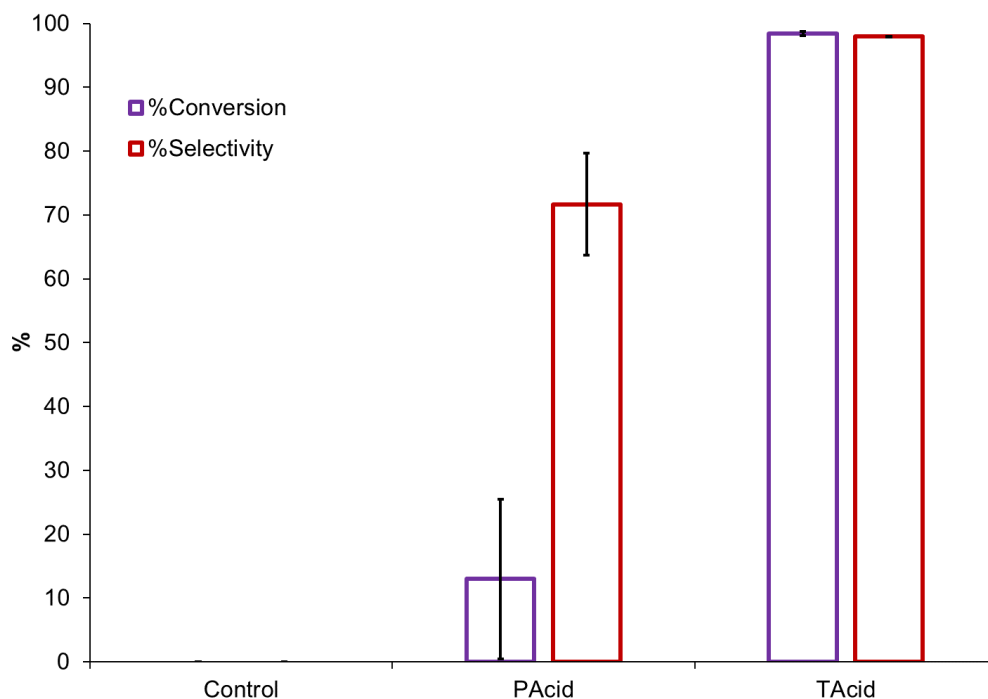
Figure 12: Initial catalyst screen for ring opening of LG with homogeneous acids. PAcid is phosphoric acid (H_3PO_4) and TAcid is tungstosilicic acid. Selectivity is to LG
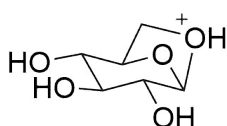
Scheme 22: Protonated LG; an intermediate in the acid catalysed ring opening of LG by methanol

Heterogeneous Acids

The heterogeneous acids chosen for investigation were a β-zeolite, a range of clays and sulfated zirconia, Figure 13.

H-β-zeolite (H-β-Z) was the best performing heterogeneous catalyst screened in the first instance, with both conversion and selectivity at >98%. Sulfated zirconia (SZ) also performed well, again with high selectivity and only a small drop in conversion to >80%. The montmorillonite clays

did not show as much promise with conversions <45%, however, as the selectivity for MK10 was >98% this clay was selected alongside H-β-Z and SZ to be taken forward for further investigations. MK30 and montmorillonite clay KSF (MKSF) were disregarded as both the yields and selectivities of these two catalysts were lower than the other three catalysts tested.
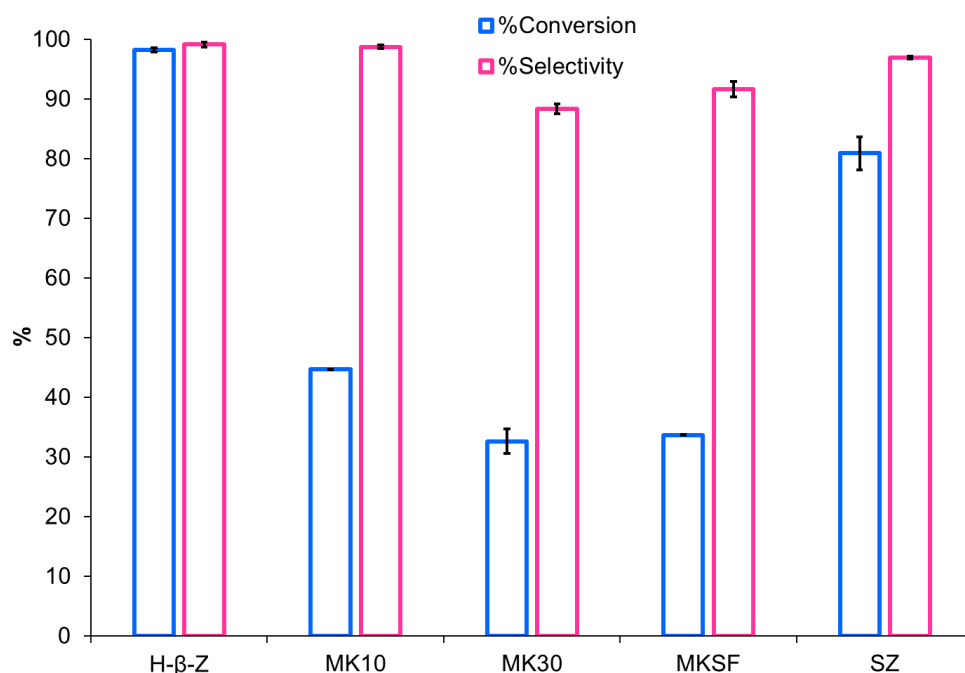
Figure 13: Initial catalyst screen for the ring opening of LG with heterogeneous acids. H-β-Z is H-β-zeolite, MK10 is montmorillonite clay K10, MK30 is montmorillonite clay K30, MKSF is montmorillonite clay KSF and SZ is sulfated zirconia

To better understand the reasons behind the low catalytic activities of the clays, characterisation of all the heterogeneous catalysts was carried out.

Characterisation of Potential Catalysts

Acidity   To measure the acidity of solid acid catalysts, they were doped with a pyridine probe molecule which bonds to the catalysts' surface differently depending on the surface acid site present. The various bonds formed between the pyridine probe and the acid sites on the surface can be differentiated by their fourier transform infra-red (FT-IR) stretches.[84,115,116] The FT-IR spectra resulting from the pyridine doping of the solid acid catalysts tested in this section are shown below, Figure 14.

SZ was not assessed by this method because it is reported that overestimation of the number of Lewis acid (LA) sites on the surface occurs; this is due to the interaction with sites other than the acidic sites of interest. [90,117–119]
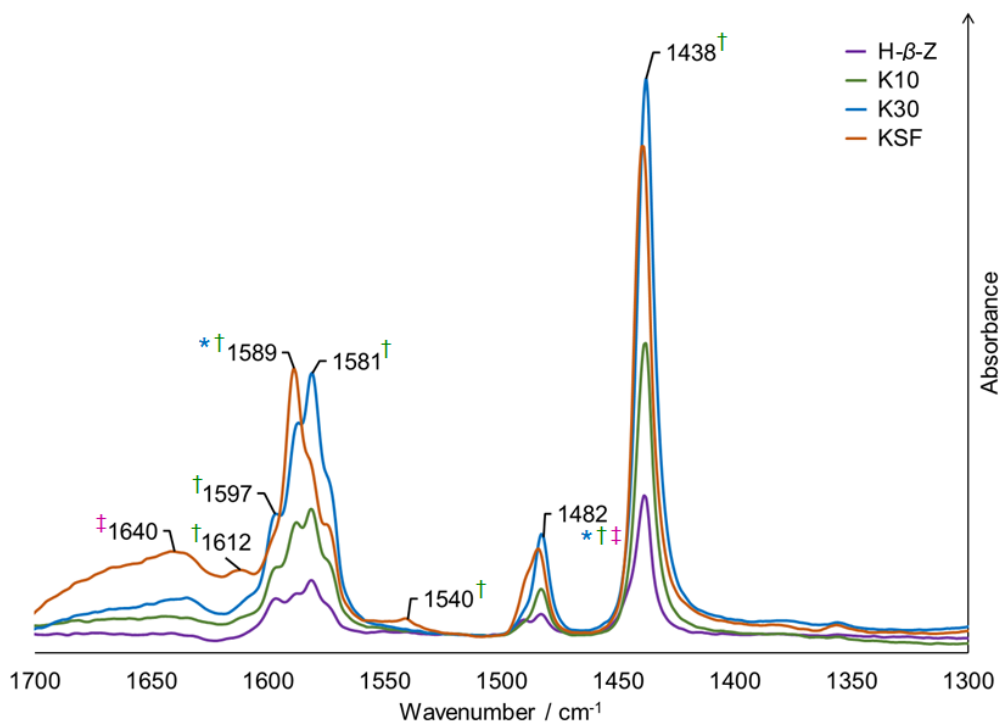
Figure 14: FT-IR spectra indicating acidity of various solid acids; shown by the shifting pyridine stretches representative of the pyridine bonding modes. ∗ corresponds to a H-bonding mode, † corresponds to a Lewis acid bonding mode and ‡ corresponds to a Brönsted acid bonding mode
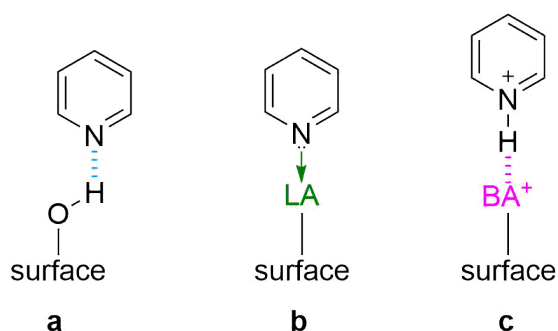
Scheme 23: Bonding modes of pyridine to the surface of a solid acid catalyst. a) is the hydrogen bonding mode, b) is LA bonding mode and c) is Brönsted acid (BA) bonding mode [87,88]

The different stretches correspond to the different bonding modes of pyridine and hence were used to determine the types of acid sites on the surface of the catalysts. [84,115] There are three types of bonding modes between the pyridine and the catalyst surface, the hydrogen bonding mode; the

LA bonding mode, from the lone electron pair on a pyridine nitrogen to the empty orbital on a metal in a LA site; and the BA bonding mode, of a pyridinium ion to a BA site, Scheme 23.[87,88]

The key stretches that can be identified in the FT-IR spectra and the bonding modes of pyridine with which they correspond are listed below, Table 2.

It can be seen in Figure 14 that the types of acid sites in each of the catalysts studied are similar. MKSF has the most BA sites, shown by the peak at 1640 cm^{-1}, which is due to this clay being treated with acid to exchange the interlamellar cations for protons. All three clays showed predominantly Lewis acidity, 1438 and 1580 cm^{-1}, with MK30 appearing to have more acid sites than MK10. This will be due to the higher aluminium content of the MK30 compared to the MK10; as discussed above, section 2.1.3, the Lewis acidity is due primarily to the presence of aluminium in the clay.[120] The lack of Brönsted acid sites in MK10 and MK30 will be due to the calcination carried out at 400 °C which will have driven out interlamellar water and caused layer collapse. There is no clear difference in the type of acid sites of these clays, when compared to the H-β-Z, indicating that this property is unlikely to be the reason behind the lower conversions these clays achieved in the studied reaction. This suggests that the clay structure is important.

Table 2: FT-IR stretches of pyridine bonded to the surface of solid acid catalysts[82,87–89,121,122]

Bonding modes	H	LA	BA
		1445	
	1485	1485	1485
		1490	1490
			1540
		1578	
	1590	1590	
	1595		
		1610	
			1640

Porosimetry Surface characteristics were measured using porosimetry whereby the samples were degassed before being exposed to increasing nitrogen pressure at 77 K.[123–125] Relative pressures

and adsorption volumes allow for calculation of surface area using the BET (Brunauer, Emmett and Teller) theory [126] and pore size and pore diameter using the BJH (Barrett, Joyner and Halenda) theory. [127,128] The surface characteristics of the catalysts screened are summarised below, Table 3.

Table 3: Porosimetry results for potential catalysts of the ring opening of LG

Catalyst	BET surface area / $m^2\ g^{-1}$	Pore volume / $cm^3\ g^{-1}$	Pore diameter / nm
H-β-Z	450	0.147	6.08
MK10	212	0.00	N/A
MK30	177	0.00	N/A
MKSF	2.06	0.00	N/A
SZ	148	0.0564	2.80

These porosimetry results show that there is no one property that is key in understanding the activities of the catalysts. H-β-Z has large pore diameters with high surface area which could indicate why it produced a higher conversion compared to the montmorillonite clays which have lower surface areas. The clays do not contain pores; they have layered structures [86,120] with cations present between the layers to balance the charge. [89] In MK10 and MK30 these cations are aluminium and in MKSF they have been exchanged for protons. [86,120] During calcination, the interlamellar water is driven out and the layers collapse [86] which could be the reason for the poor activities of the clays. If the Lewis acid sites, created through the interlamellar water removal, [86] are inaccessible to the substrates of the reaction then the conversion will be low. MK10 and MK30 have higher surface areas than MKSF because they are acid washed which causes swelling and hence an increase in the surface area. [129] The SZ has much lower surface area and pore diameter than H-β-Z and the clays but still produces high conversion and selectivity. Catalysts doped with sulfuric acid, such as SZ, are known to leach and with sulfuric acid consequently in solution, the origin of catalysis must be questioned with the likely origin in this circumstance being the free sulfuric acid. This not only explains why the low surface area and narrow pores did not affect catalyst activity but also poses concern; with sulfuric acid leaching into the reaction mixture, separation and reuse of the catalyst becomes much more difficult. This leaching will be an important consideration when evaluating the results of the further investigations carried out on the three chosen catalysts.

2.2.3   Further Investigations

Three of the initially screened catalysts were taken forward for further investigations to look at the reaction time, Figures 15 and 16.
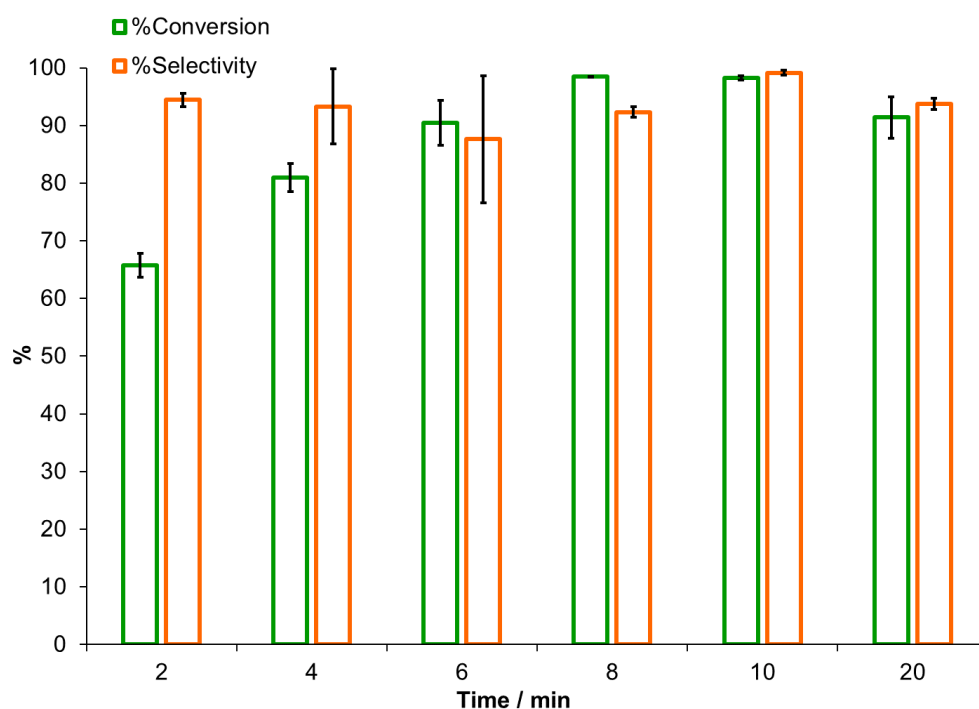
Figure 15: Effect of reaction time on the ring opening of LG with H-β-Z

H-β-Z and SZ were chosen because they produced the highest conversion and selectivity in the first screen and hence appeared to be the most promising catalysts. MK10 was chosen because the selectivity was high and although the conversion was relatively low, compared with the other catalysts tested, it was speculated that a longer reaction time may lead to an increase in conversion.

Using MK10, Figure 16a, while the selectivity remained high, the conversion only increased to 60% after 60 mins compared with 45% after 10 mins. It was decided that any increase gained by longer reaction times would be outweighed by the extra energy used for the reaction, given the small increase seen in these results. The drop in conversion observed between 10–30 minutes for MK10 catalysis is within the error of the experiment and can be disregarded. On the grounds of low conversion, the MK10 can be ruled out as a catalyst for this reaction, especially when compared to the alternative two catalysts tested.
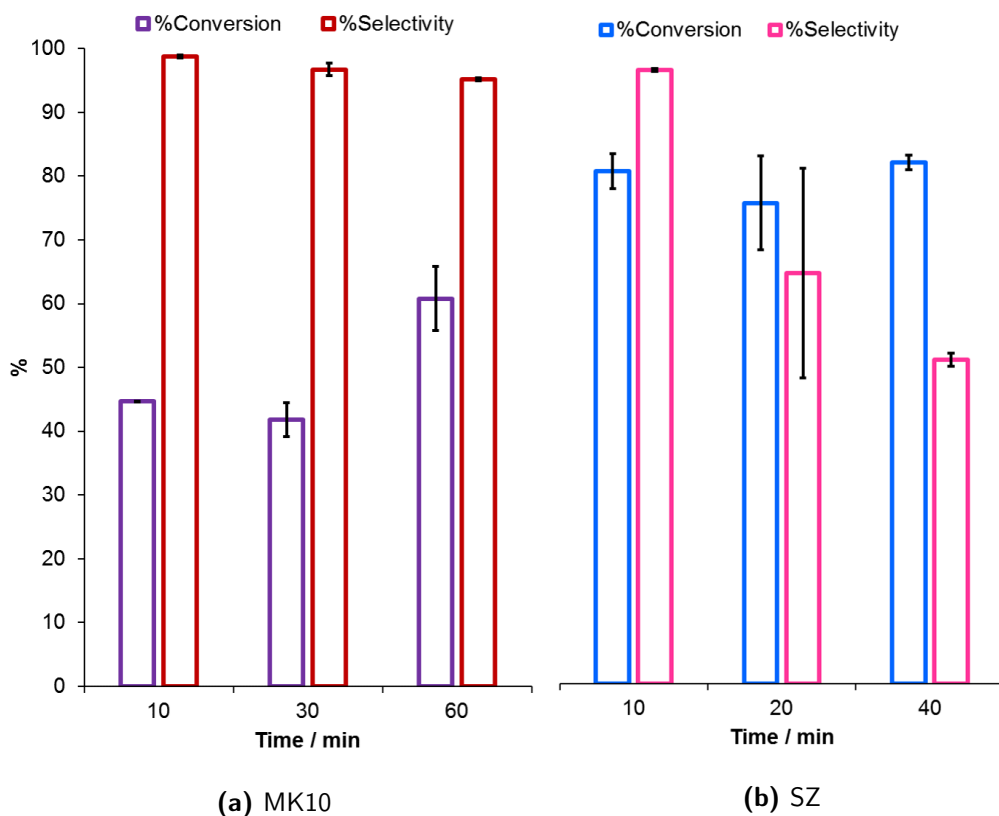
Figure 16: Effect of reaction time on the ring opening of LG with two solid acid catalysts

SZ showed higher conversion than the MK10 however, at only 82%, still lower than the H-β-Z, Figure 16b. The selectivity seen in the SZ catalysed reaction decreased steadily with time and after 40 mins was as low as 50%; this is likely to be due to sulfuric acid leaching which appears to be catalysing MGP formation as well as dehydration and subsequent breakdown of the MGP, as discussed earlier in section 2.1.3, resulting in increasing conversion but decreasing selectivity.[55,105] Given the decreasing selectivity and the lower conversion observed, compared with the H-β-Z, SZ can also be ruled out as a suitable catalyst for the ring opening of LG.

The aim of these further investigations into H-β-Z was to reduce the reaction time and hence energy use for the synthesis, Figure 15. It can be seen from these results that H-β-Z was the most promising catalyst of those studied; a conversion of >98% was achieved in a reaction time of only 8 minutes.

Additionally, this high reaction rate could enable further optimisation of the process. With only a short residence time necessary for the reactants in this reaction it shows potential for testing in a flow reactor which would improve the catalyst turnover number as well as reduce the process waste. Packing the zeolite into a flow reactor and passing the reagents over the catalyst would also

reduce the energy consumption of the reaction as the heating would be more efficient. Additionally, higher selectivity through fewer side reactions is likely to be achieved. This would be an interesting avenue for further investigations as it can also be seen that the selectivity remains high, >87%, throughout the full 20 mins indicating the process would be robust in a flow system.[32]

2.3 Investigations into Zeolite Catalysts

2.3.1 Methanol as a Test Substrate

To further optimise the reaction and understand the properties important for catalysis, the same model reaction was used to investigate zeolite Al:Si, under various reaction conditions.

Table 4: Effect of Al:Si and zeolite calcination temperature on the ring opening of LG with methanol at various reaction times

Zeolite	Activation temperature / °C	Reaction time / min	C* / % (error)	S† / % (error)
25z	UC	5	21.7 (± 8.18)	77.8 (± 7.01)
		20	96.7 (± 0.87)	92.2 (± 0.01)
	c400 °C	5	97.1 (± 0.45)	90.5 (± 1.23)
		20	94.1 (± 1.31)	67.3 (± 12.8)
	c550 °C	5	97.4 (± 0.25)	94.8 (± 0.56)
		20	97.8 (± 0.12)	91.5 (± 0.61)
30z	UC	5	96.9 (± 1.20)	92.2 (± 0.78)
		20	96.1 (± 1.61)	79.1 (± 12.4)
	c400 °C	5	96.5 (± 1.53)	81.7 (± 8.03)
		20	95.9 (± 0.92)	75.0 (± 7.55)
	c550 °C	5	98.1 (± 0.25)	93.4 (± 0.40)
		20	97.0 (± 0.16)	91.5 (± 1.12)

*Conversion of LG   †Selectivity to MGP

Three zeolites were chosen with a range of Al:Si ratios and they were, zeolite25 (Al:Si molar ratio 25:1) (25Z); zeolite30 (Al:Si molar ratio 30:1) (30Z); and zeolite150 (Al:Si molar ratio 150:1)

(150Z). The effect of different calcination temperatures was also investigated and each zeolite was calcined at 400 °C (c400 °C) or calcined at 550 °C (c550 °C) then compared against uncalcined (UC) material, Tables 4 and 5.

Table 5: Effect of Al:Si and zeolite calcination temperature on the ring opening of LG with methanol at various reaction times

Zeolite	Activation temperature / °C	Reaction time / min	C* / % (error)	S† / % (error)
150z	UC	5	83.4 (± 11.9)	92.3 (± 0.76)
		20	96.4 (± 1.41)	88.1 (± 5.06)
	c400 °C	5	87.7 (± 9.84)	92.3 (± 1.66)
		20	92.5 (± 0.19)	65.5 (± 0.59)
	c550 °C	5	88.6 (± 1.57)	93.1 (± 0.32)
		20	97.4 (± 0.03)	93.1 (± 0.87)

*Conversion of LG   †Selectivity to MGP
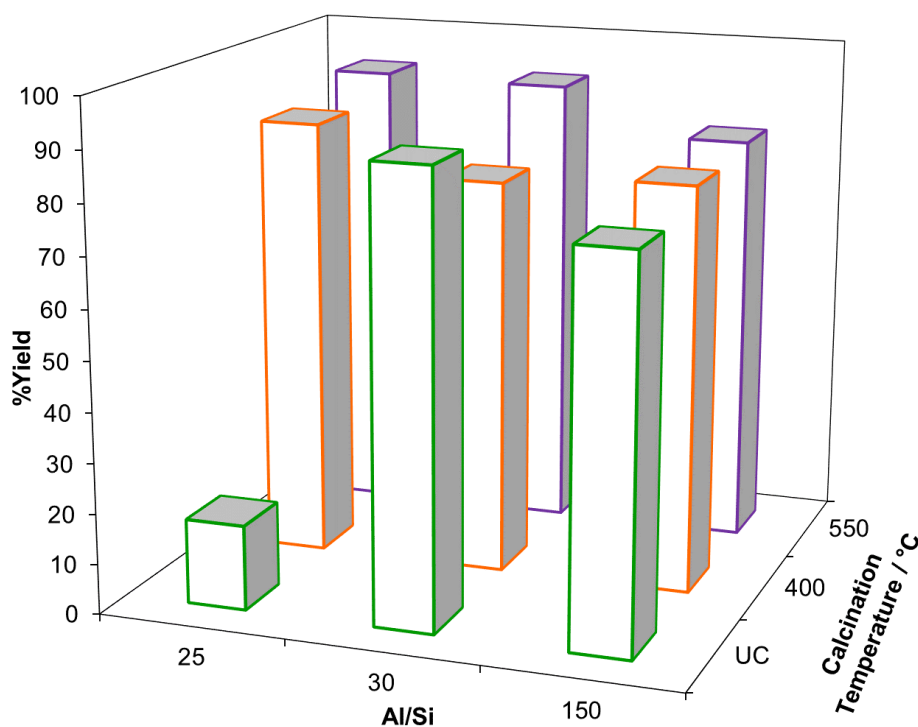
Figure 17: Effect of Al:Si and zeolite calcination temperature on the ring opening of LG with methanol after 5 mins
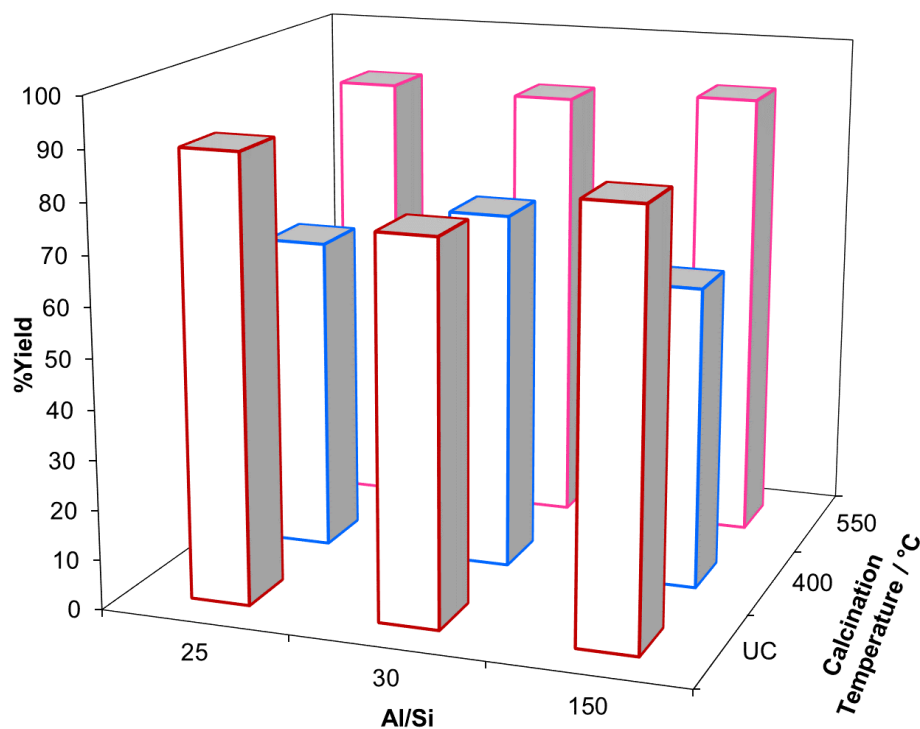
Figure 18: Effect of Al:Si and zeolite calcination temperature on the ring opening of LG with methanol after 20 mins

All three catalysts, calcined at the three temperatures, performed well over a reaction time of 5 mins with the only exception being UC/25Z for which a low conversion was observed, Figure 17. After 20 mins, two trends can be seen to be emerging, Figure 18, zeolites c400 °C produced lower yields than the other two calcination temperatures; and the relationship between activity and Al:Si is non-linear.

2.3.2   Zeolite Characterisation

As with the catalysts from the initial screen, characterisation of the three zeolites after calcination at the three temperatures was carried out.

Acidity

Analysis of the acidity of the zeolite surface was carried out, again with the use of a pyridine probe as described in section 2.2.2. The results were evaluated against two variables and are presented below, Al:Si in Figure 19, and calcination temperature in Figure 20.
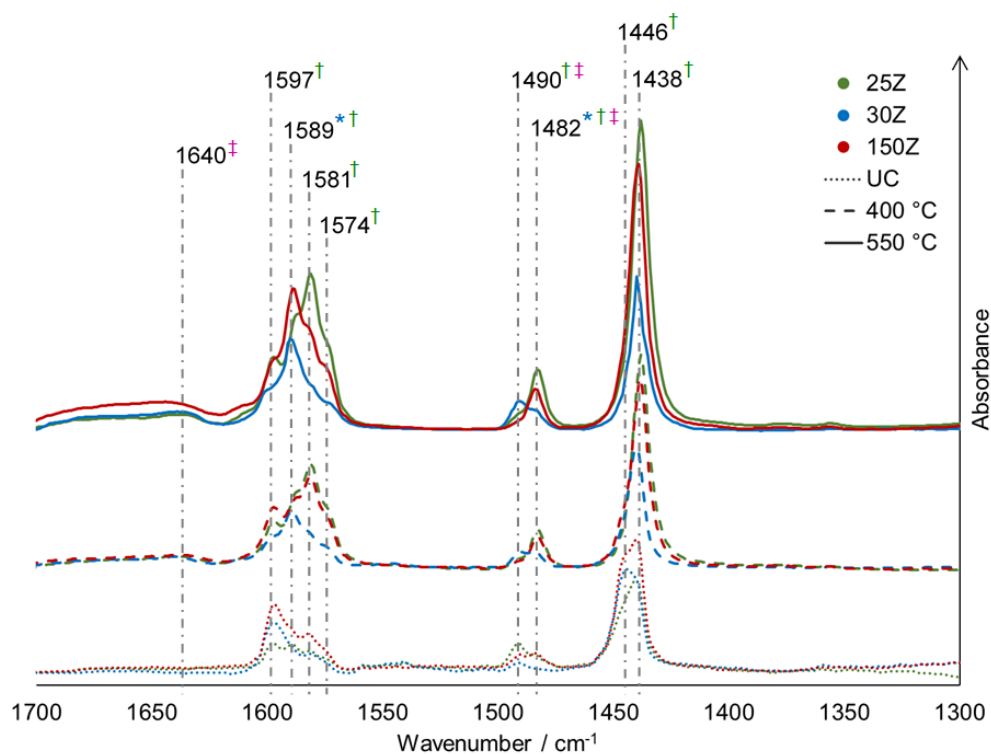
Figure 19: FT-IR spectra indicating changes in zeolite acidity with varying Al:Si; shown by the shifting pyridine stretches representative of the pyridine bonding modes. ∗ corresponds to a H-bonding mode, † corresponds to a Lewis acid bonding mode and ‡ corresponds to a Brönsted acid bonding mode

It is known that the changing Al:Si has an effect on the acidity of the zeolites, as discussed in section 2.1.3, and this can be seen in Figure 19. 25Z and 150Z show similar acidity profiles with 25Z nearly always showing higher amounts of acidic sites. The only significant difference between the two can be seen in the c550 °C/150Z spectrum where the largest peak in the 1580–1590 cm^{-1} region shifts from 1581 to 1589 cm^{-1}; this shift changes the profile so it is similar to 30Z instead of 25Z. Throughout the entire profile, 30Z shows peaks slightly higher in wavenumber to 25Z.

By examining the spectra in a different order, the effect of the calcination temperature can be seen, Figure 20. Firstly, concentrating on the area 1580–1590 cm^{-1}, 25Z shows an increase in the peak at 1581 cm^{-1} with increasing calcination temperature whereas 30Z shows an increase in the peak at 1589 cm^{-1}. 150Z shows an initial increase in the peak at 1581 cm^{-1}, at c400 °C, but then a shift to a peak at 1589 cm^{-1} at c550 °C. Throughout the rest of the spectra, increasing calcination temperature increases the acidity, with a more pronounced affect observed for 25Z. Small peaks can be seen to shift from 1490 to 1482 cm^{-1}, for 25Z and 150Z, after an increase in

calcination temperature, but 30Z maintains a peak at 1490 cm^{-1} even at the higher calcination temperatures.
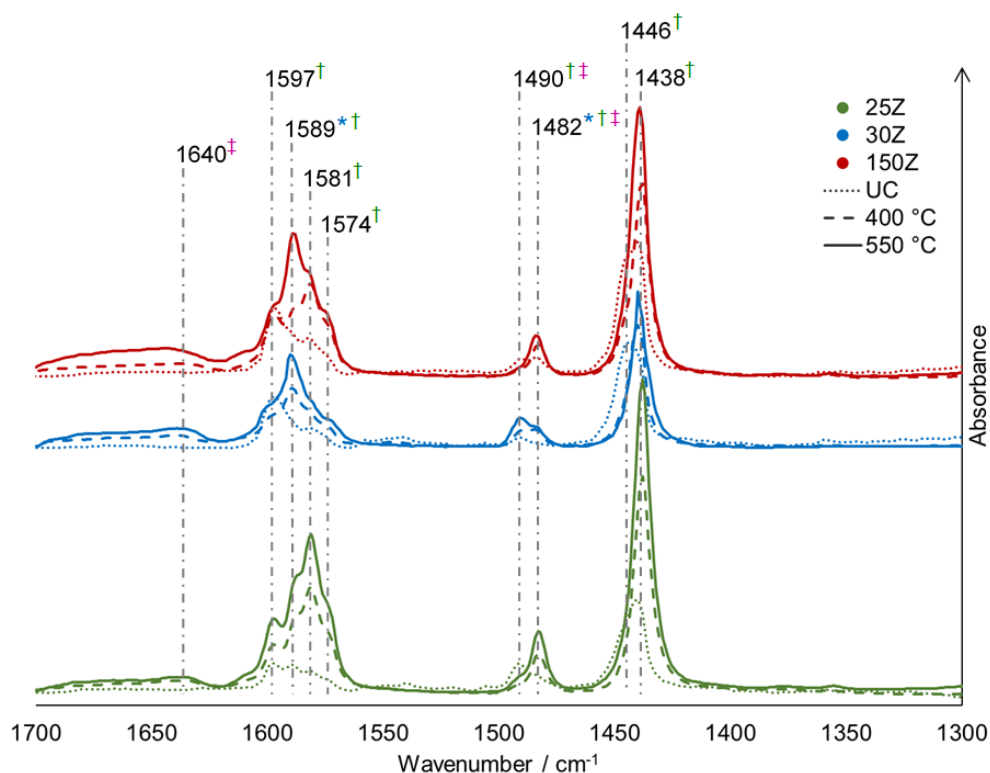
Figure 20: FT-IR spectra indicating changes in zeolite acidity with varying calcination temperature; shown by the shifting pyridine stretches representative of the pyridine bonding modes. ∗ corresponds to a H-bonding mode, † corresponds to a Lewis acid bonding mode and ‡ corresponds to a Brönsted acid bonding mode

Referring back to Table 2 from section 2.2.2, it can be seen that many Lewis acid sites are present in these zeolites. The two stretches known to be indicative of Lewis or Brönsted acidity are 1440 and 1540 cm^{-1}, respectively, and hence, looking at the spectra, it can be said that only Lewis acidity is present in the zeolites.[82,87–89,121] The shifting of peaks in the region of 1580–1590 cm^{-1} could indicate a shift in the pyridine bonding mode from LA to hydrogen bonding, however, the 1590 cm^{-1} peak has been associated with pyridine -hydrogen and -LA bonding and so this shift could indicate a change in the Lewis acid sites.[87–89] A change in the Lewis acid sites is more likely to be the cause because a decrease, not an increase, in hydrogen bonding with increasing calcination temperature is expected. Hydroxyl groups are driven off the surface to a larger extent at higher temperatures, hence the decrease in hydrogen bonding.[84] The peak at 1597 cm^{-1} is lowest in the UC/25Z spectrum which corresponds with the lowest yield in the reaction. In addition, in

the other two zeolites, this peak is lowest in the c400 °C spectra, also corresponding to the lowest yields for those zeolites. The acid site associated with this wavenumber is likely to be important in the catalysis of the ring opening of LG and around this wavenumber, many peaks associated with various LA sites are found.[88,89,122]

Porosimetry

Nitrogen adsorption porosimetry was carried out on the zeolites, as on the earlier solid acid catalysts, section 2.2.2, and the adsorption isotherms are shown below, Figures 21 to 23.
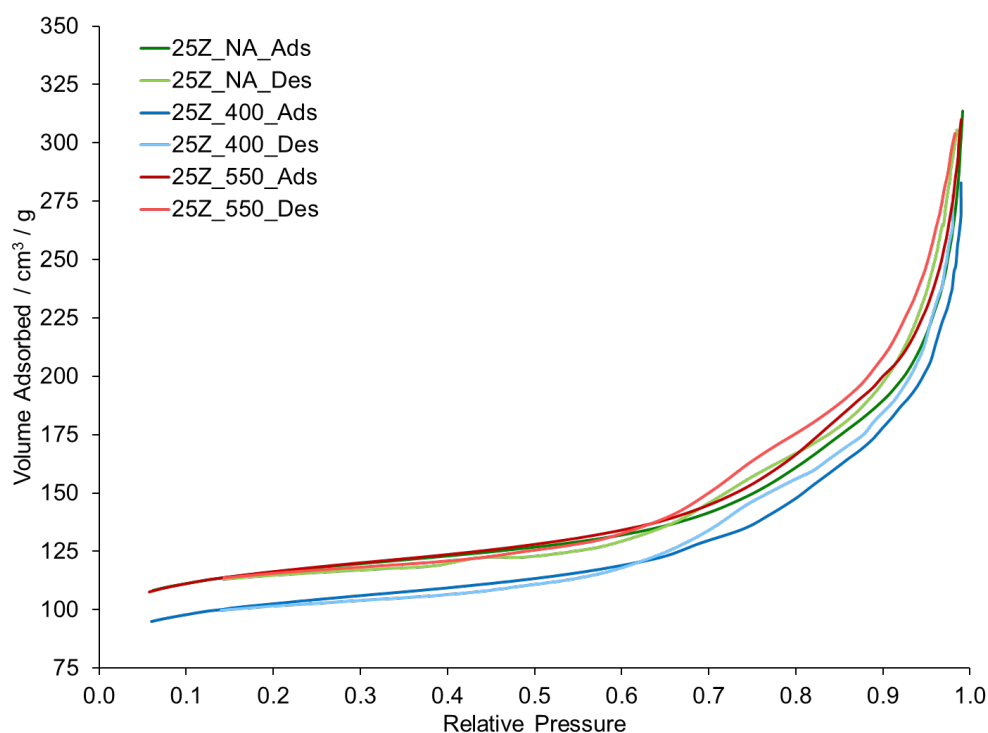
Figure 21: Nitrogen adsorption isotherm of 25Z, uncalcined and calcined at 400 and 550 °C. Relative pressure is P/P^0

It can be seen from these isotherms that the three zeolites exhibit Type IV isotherms which indicates that the zeolites are mesoporous and that the interactions between the surface and the adsorbent play a significant role. The first part of the isotherm follow the Type II isotherm and is due to the monolayer-multilayer adsorption on the surface and the pore walls. The second half of the isotherm is where capillary condensation occurs and this is indicated by the presence of a hysteresis loop; where the desorption branch does not follow the adsorption branch of the isotherm. This phenomenon is observed in mesopores when the adsorbent gas condenses to a

liquid-like phase and the pore fills. This filling occurs once the capillary width (taking into account mono- and multi-layers of adsorbed gas on the pore walls) is equal to the radius of the liquid meniscus. Consequently, the desorption requires a lower pressure than adsorption required due to the cohesive forces in the liquid and the surface tension of the meniscus. [130–133]
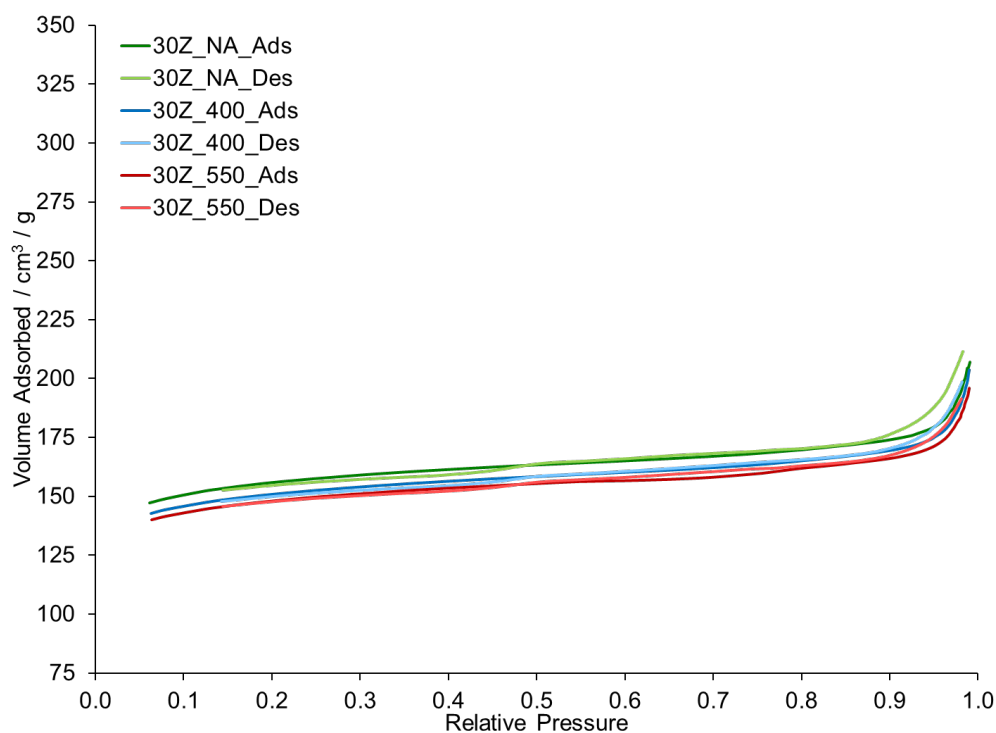
Figure 22: Nitrogen adsorption isotherm of 30Z, uncalcined and calcined at 400 and 550 °C. Relative pressure is P/P^0

These three adsorption isotherms show the monolayer formation at the lower relative pressures followed by the hysteresis loop upon capillary condensation in the pores, Figures 21 to 23. It is clear from the isotherms that 25Z and 150Z are very similar however 30Z has a distinctly different profile. A smaller volume of nitrogen is adsorbed and the hysteresis loop is significantly smaller. What can also be seen from the isotherms of 25Z and 150Z is that the c400 °C isotherms indicate lower volumes of nitrogen were adsorbed than c550 °C and UC. This could indicate a reduction in absorbant-adsorbate affinity and occurs alongside a drop in reaction yield for the zeolites, as seen in section 2.3.1. Comparing these results with the analysis on the acidity profiles of the zeolties, it can be seen that a change occurs in the zeolite surface at this temperature in relation to the other two. This reduction in the peak at 1597 cm^{-1} could be having an affect on the nitrogen adsorption; 30Z consistently has a lower peak at this wavenumber than the other two zeolites. From these isotherms, the surface characteristics were calculated and are shown below, Table 6.
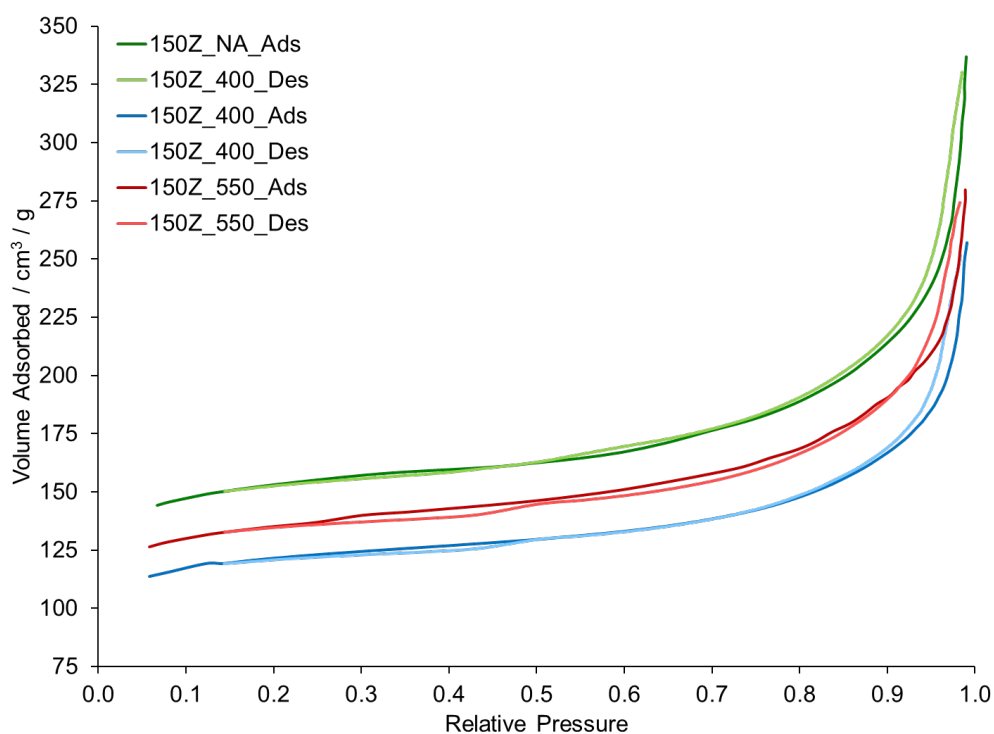
Figure 23: Nitrogen adsorption isotherm of 150Z, uncalcined and calcined at 400 and 550 °C. Relative pressure is P/P^0

Table 6: Porosimetry results for potential zeolite catalysts for the ring opening of LG

Calcination temperature / °C	Al:Si	BET surface area / $m^2\,g^{-1}$	Pore volume / $cm^3\,g^{-1}$	Pore diameter / nm
UC	25	378	0.139	4.55
	30	503	0.231	2.44
	150	494	0.202	3.77
400	25	334	0.114	4.74
	30	486	0.222	2.46
	150	394	0.163	3.64
550	25	380	0.133	4.63
	30	477	0.218	2.43
	150	439	0.180	3.58

30Z has a consistently narrower pore diameter compared with the other two zeolites which appears

to be the only main difference between the three zeolites. The catalytic activity could be lowered by the inaccessibility of the pores which would prevent substrates from reaching the acid sites; Lewis acid sites in zeolites are located, primarily, inside the pores.[82] The narrow pores of the 30Z did not reduce the activity of this zeolite in the reaction with methanol but this effect was carefully considered when investigations with longer alcohols were carried out later in the Chapter.

2.4   Scope of Hydrophobic Tails

2.4.1   Decanol

For synthesis of surfactants from LG using this ring opening reaction, longer alcohols would be required to ensure the resulting surfactants had a suitable HLB. Decanol was chosen as a representative example to test the zeolite catalysis. HLB is an indication of the distribution of hydrophilicity and hydrophobicity of surfactants and as this index increases, the micelle formation becomes less favourable and hence critical micelle concentration (CMC) increases. Larger head groups in surfactants result in too much unfavourable electrostatic and steric interaction between them in the micelle; smaller hydrophobic tails in surfactants reduce the entropic gain that arises from shielding the tails from the water within the micelle.[62,63] Depending on the application, various CMCs are desirable, for example in detergents the micelles trap dirt within them to allow them to be easily rinsed away by water and so lower CMC allows lower surfactant concentration to be used. However in applications where surface stabilisation is the desired effect, such as foaming agents, a higher CMC is important to ensure surfactants are free in solution to act at the surfaces of the bubbles, not trapped as micelles.[60]

Increasing Conversion with Calcination Temperature

In general, the conversion increases with increasing zeolite calcination temperature. This trend can be clearly seen when turnover frequency (TOF) is calculated for each zeolite and compared to the TOFs for the methanol reactions, Figure 24. TOF is the moles of reactant converted per mole of catalyst per second and is a common industry metric used to measure catalyst efficiency.

The TOFs for the reactions with 30Z do not show any change over the various calcination temperatures for either alcohol which could be explained by the low pore diameter observed by

porosimetry. This would also explain the significant drop in TOF from methanol to decanol. The reaction with c400 °C/150Z and decanol shows lower conversion than the other calcination temperatures with 150Z and with methanol, which could be explained by looking at the acidity. The acidity profile shows a peak at 1597 cm^{-1} which dips at c400 °C and could be responsible for the lower activity of this zeolite after calcination at this temperature. The lack of a dip in the methanol results could not be a true result given the large error margin seen on this result. This peak would be expected to be the hydrogen or LA bonding mode of pyridine and as there is such an impact on the activity of the catalysts, it is speculated that this site is an LA site. No correlation was observed between these results and the porosimetry data collected for the zeolites.
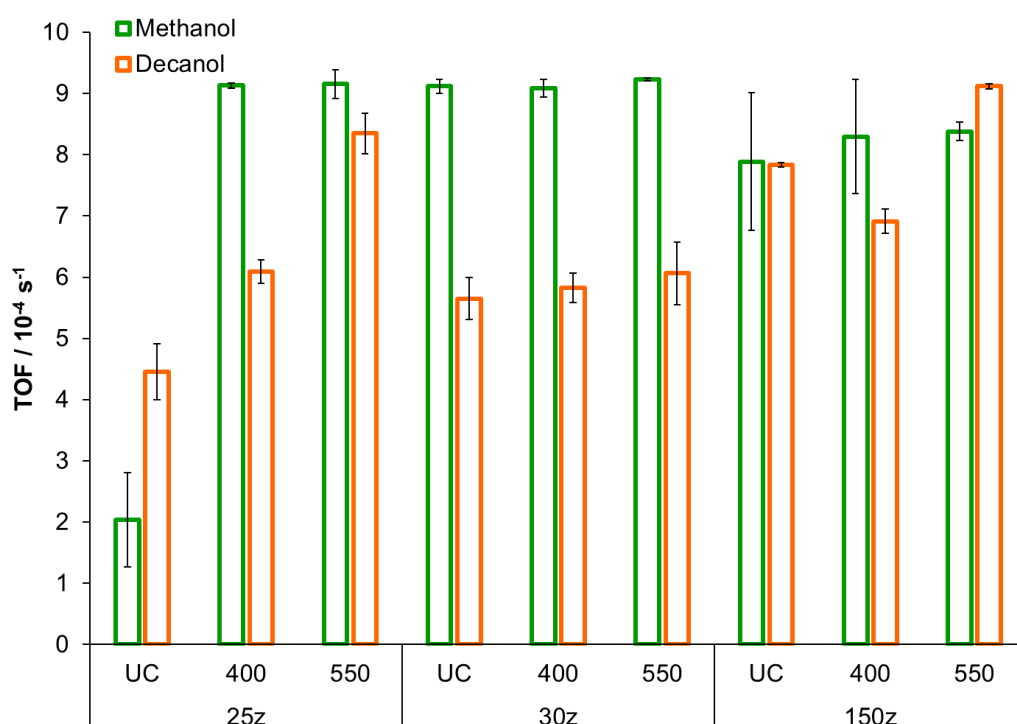
Figure 24: Effect of zeolite calcination temperature on catalytic TOF for LG ring opening with methanol and decanol

Increasing Selectivity with Aluminium Content

It can be seen that the selectivity to decyl-α-D-glucopyranoside (DGP) increases with both higher alumina content and higher calcination temperature, Table 7 and Figures 25 and 26. This trend appears to correlate with the acidity profiles observed of the zeolites. The UC/25Z has much lower acidity aside from the peak at 1490 cm^{-1} which could correspond to some Brönsted acidity on

the surface; this type of acid site exhibits lower selectivity than the Lewis acid sites.

Table 7: Effect of Al:Si and zeolite calcination temperature on the selectivity to DGP in the ring opening of LG with dethanol at various reaction times

Activation temperature / °C	Reaction time / min	Selectivity to DGP / % (error)		
		25Z	30Z	150Z
UC	5	38.5 ($\pm$ 7.60)	50.0 ($\pm$ 1.86)	61.9 ($\pm$ 2.05)
	20	18.5 ($\pm$ 0.561)	32.8 ($\pm$ 4.00)	42.5 ($\pm$ 4.42)
c400 °C	5	78.1 ($\pm$ 3.65)	62.1 ($\pm$ 1.12)	63.9 ($\pm$ 12.1)
	20	56.4 ($\pm$ 3.84)	40.9 ($\pm$ 9.98)	58.0 ($\pm$ 2.73)
c550 °C	5	83.4 ($\pm$ 5.72)	72.1 ($\pm$ 1.37)	59.9 ($\pm$ 2.03)
	20	41.5 ($\pm$ 12.4)	48.5 ($\pm$ 0.180)	44.5 ($\pm$ 13.8)
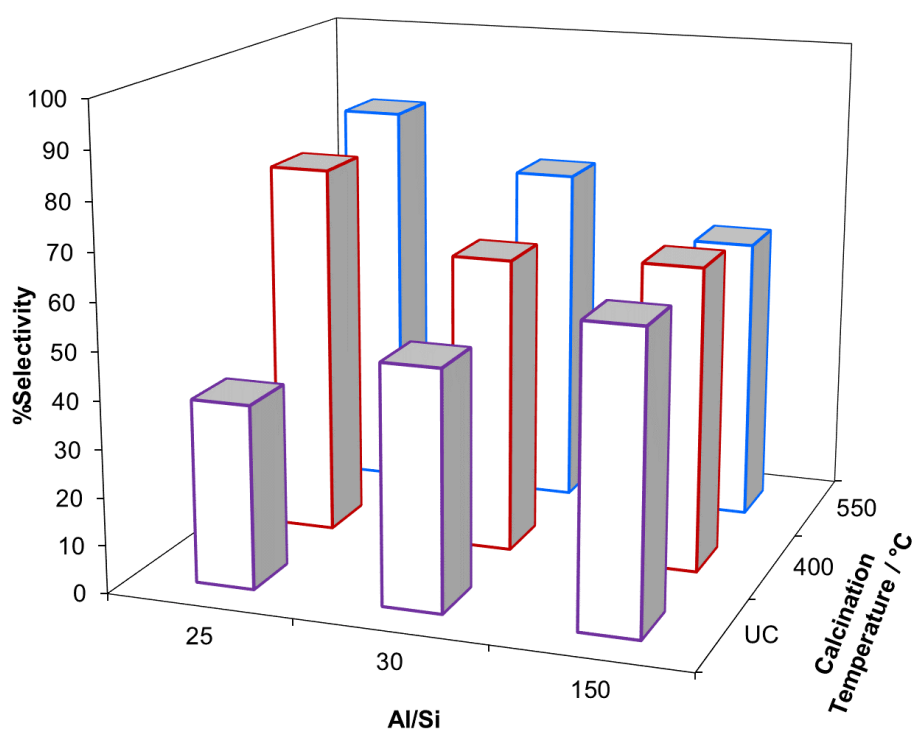
Figure 25: Effect of Al:Si on the selectivity of the ring opening of LG with decanol after 5 mins

When the zeolites are calcined at increasing temperatures, the peaks at 1482 and 1581 cm^{-1} grow in 25Z to a greater extent than the other two zeolites and this could be responsible for the increased activity of this zeolite. 25Z has smaller peaks at 1490, 1589 and 1597 cm^{-1} than

the other two zeolites at the higher calcination temperatures which could account for the higher selectivity of 25Z, if the acid sites those peaks represented were BA or strong LA sites. In addition, 25Z has much wider pores than 30Z or 150Z which would again account for the higher activity of this zeolite in this reaction. Again, no correlation was observed between these results and the porosimetry data collected about the zeolites. This could mean that there is no link between the catalyst activity and the porosity characteristics or it could indicate that a larger range of zeolites needs to be investigated for the trend to be clear. As discussed later in Section 2.6, a more thorough investigation would be useful to carry out in order to determine whether the surface characteristics are important to the catalysts' activity.
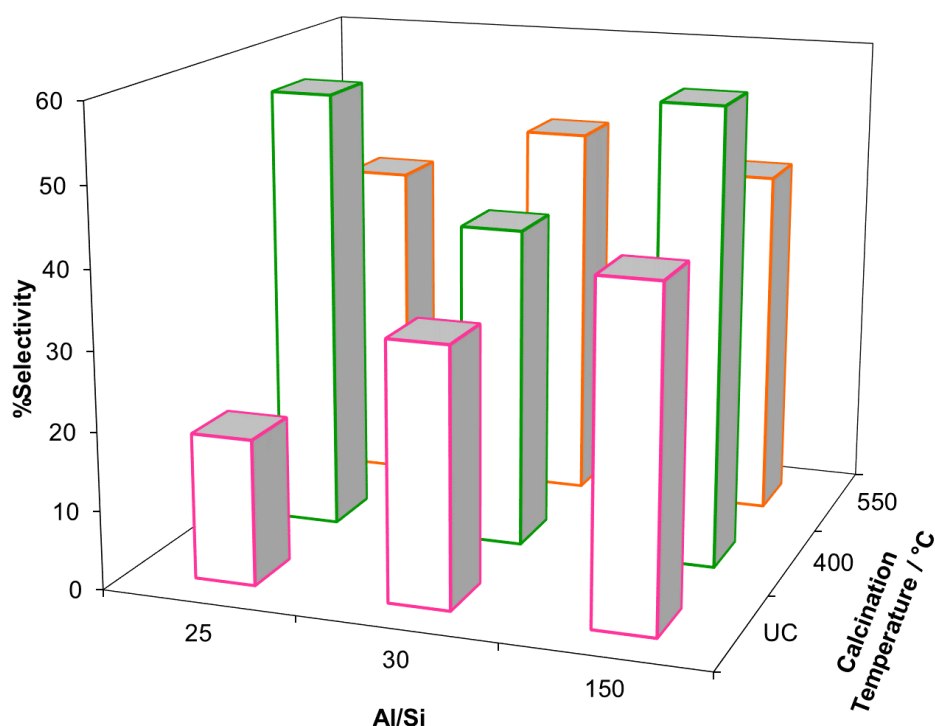
Figure 26: Effect of Al:Si on the selectivity of the ring opening of LG with decanol after 20 mins

Overall zeolite acidity is a balance between the number of acidic sites and the strength of the sites. The acid sites exhibit stronger acidity the more isolated they are from each other, as discussed earlier, section 2.1.3. This means the overall zeolite strength peaks between too few acid sites and too weak acid sites.[84,85] The strength of the acid sites can not be determined by pyridine adsorption alone and so this property is unknown however the Lewis acid sites in 25Z will be the weakest because they will be closer together than in the other two zeolites, as there is more aluminium in 25Z. The weakness of the acid sites could explain the high selectivity of this zeolite

while the increased number of sites could explain the high conversion, when compared with the other zeolites. A combination of the correct strength of the Lewis acid sites, the amount of sites as well as large pore widths are clearly necessary for successful catalysis of the ring opening of LG.

2.4.2 Octanol Isomers

In order to facilitate the synthesis of useful surfactants *via* this method, compatibility of the catalysts with secondary alcohols would be necessary. These reactions were carried out with the optimum zeolite calcined at the optimum temperature, c550 °C/25Z, as identified in the previous section.
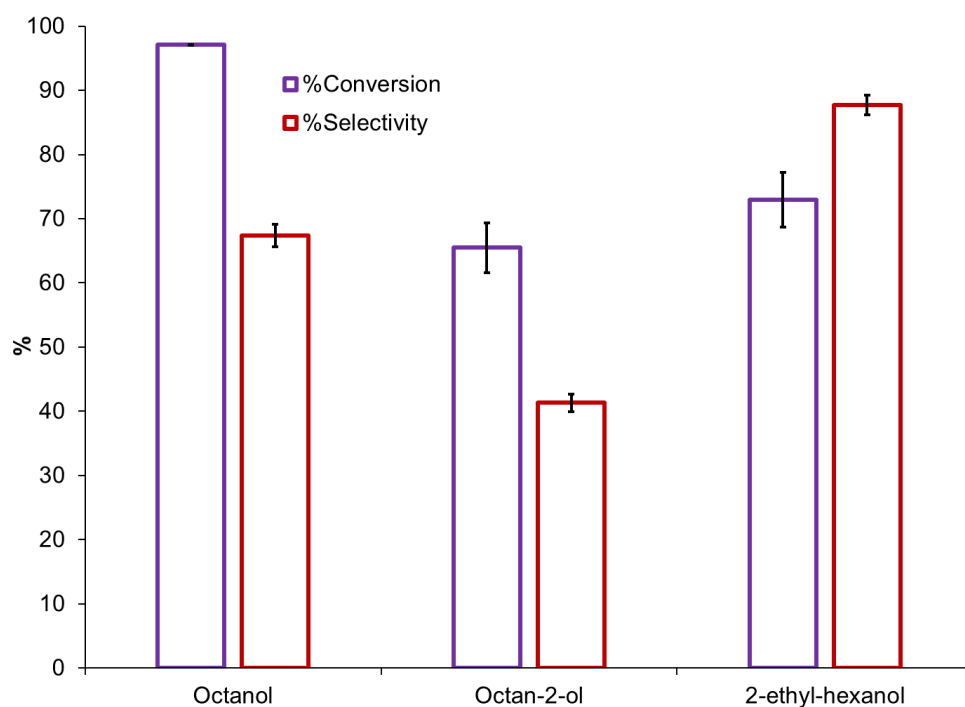
Figure 27: Ring opening of LG with isomers of C_8 alcohols

Branched hydrophobic tails impart a large variety of properties to the surfactants and their micellisation which widens their potential for industrial use. Branched chains will have a larger volume meaning that in the micelle, the head groups won't be large enough to completely shield the hydrophobicity from the water. This will decrease the Free Energy advantage of micelle formation; shielding the hydrophobic tails from the water releases the water from a cage like structure around the tails which is entropically favourable however if not all water molecules are released, the entropic benefit of micelle formation will not be as large.[60,61]

Good conversion, >65%, was achieved for both the secondary alcohol and the sterically hindered primary alcohol showing that this catalyst has potential for synthesis of a variety of APG surfactants, Figure 27. Lower conversion was expected for bulkier substrates as diffusion through the pores to acid sites would be slower. In addition, attack from the OH in the alcohol would be slower as it would be more hindered the longer and more branched the attached chain is.

2.5   Conclusions

This Chapter investigated the use of various solid acid catalysts in the ring opening of LG and highlighted a set of catalysts with the greatest potential. Zeolites have been shown to be active and selective in the synthesis of APGs from LG and through characterisation of these catalysts, an understanding of the important/defining properties has started to develop. LG is a good starting material for APGs because it is readily obtained from biomass; LG is the primary product of cellulose pyrolysis. In addition, the anhydro-ring of the LG acts to promote attack from the alcohol; ring strain increases reaction rate and steric hindrance produces a preference for one stereoisomer, the α-glucopyranoside.[74] Lewis acidity was shown to be important for the catalysis and it was found that certain Lewis acid sites were associated with lower selectivity; these were speculated to be the stronger acid sites. Using porosimetry, zeolite structure was probed, and wide but defined pores were shown to be key in the catalyst activity, as it was deduced that they allowed the substrates access to the active acid sites contained within the zeolite structure.[84]

The synthesis developed has highlighted some improvements to be made in the existing process. This route from LG means that direct esterification with the desired alcohol can be carried out. Currently, due to solubility and reactivity difficulties, the APGs are synthesised *via* the butyl ester which is then transesterified with the longer chain alcohol. As mentioned above, LG's anhydro-ring allows for direct stereospecific reaction with longer alcohols which means there is potential to reduce the current multi-step process to a selective single step one.[58,59,74] In addition, the change to solid catalysts from the currently favoured homogeneous acids means that product separation would be much easier and there would be a possibilty for catalyst reuse. This would improve the process from both an environmental and economic viewpoint.

Zeolites have been shown to be active with long and branched chain alcohols, namely decanol and 1− and 2−octanol and 2−ethyl hexanol, although the conversion decreased for the longer and sterically hindered substrates. This trend in conversion indicates that there will be a limit to the use of zeolites in this reaction however the variability seen with changing zeolite properties indicates that further investigation of a wider range of solid acids could reduce this. This represents an opportunity for future work on this project.

This project has shown that solid acid catalysts, especially zeolites, can be successfully utilised for the synthesis of green renewable surfactants, APGs. The implications of this are wide ranging; increased substrate scope as well as improved cost and green credentials will increase the applications

available to APGs and hence increase production.

2.6 Future Work

Complete understanding of the mechanism of catalysis and the catalyst properties which are key for the catalyst activity would be of interest and it is recommended that further study be to this end. Zeolite acidity has been shown to be important for catalytic activity and screening of a larger number of zeolites with a more comprehensive range of Al:Si ratios would enable evaluation of the relative importance of acid site density *vs.* strength. Synthesis of templated aluminosilicates could provide this range of Al:Si ratios and also allow for control over the pore size and shape. Modification of the template used in the synthesis would enable the modification of the zeolite pores and would improve the understanding of the effect of the catalyst structure on the activity. Characterisation of the strength of the zeolite acid sites by use of a range of probes of varying basic strength coupled with FT-IR would compliment this work.

As mentioned early on in the Chapter, TAcid performed well and as it is a suitable catalyst to load onto a solid support, this would be an interesting avenue to investigate as an alternative to zeolite catalysis.[113] Silica or carbon based supports for TAcid are previously documented and would give this homogeneous acid all the benefits of a heterogenous solid acid catalyst.[113] By loading the TAcid onto the surface of a solid support the restrictions of zeolite pore size would not be applicable and improved results may be seen with longer and more hindered alcohols.

For any solid acid catalyst, the main benefits are ease of catalyst separation, regeneration and reuse. Testing of these zeolites in repeated reactions to assess their robustness and recyclability would be an important future study. The zeolites would need to be calcined prior to reuse but then the number of cycles of use could be studied which would have implications for the industrial applications of the catalyst.

Chapter 3

Synthesis of Itaconate Surfactants

3.1 Introduction

3.1.1 Sulfo-succinates

Sulfo-succinates are common anionic surfactants which have a hydrophilic head group composed of a C_4 diacid with a sulfonate group, which is attached to one or two hydrophilic hydrocarbon chains of various lengths and functionalities *via* the carboxylic acid groups, Scheme 24.[134]
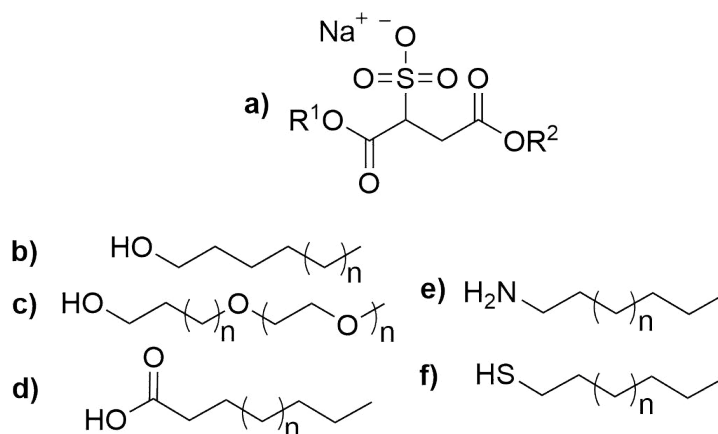
Scheme 24: Structure of a) sulfo-succinates on the market with examples of hydrophobic groups; where R1 and R2 can be a proton, a metal cation, b) a fatty alcohol, c) an ethoxylated fatty alcohol, d) a fatty acid, e) an amine, or f) a thiol[63,134,135]

Developed in 1939, these surfactants make up around 49% of all anionic surfactants as they have such a wide range of applications.[134] They have a reputation for being safe and mild as well as

versatile and efficient.[136]

Generally there are two categories of sulfo-succinates, monoesters and diesters. The monoesters are good foamers and detergents while being mild to the skin and eyes which lends them well to applications in personal care and cosmetics; household cleaners and shampoos; textiles, paints and coatings; leather treatment, printing and agriculture.[134,137] They are also known for having, good emulsifying and solubilising properties; good surface tension reduction and low critical micelle concentrations (CMCs); and high biodegradation rates.[134] The diesters can be irritants and suffer from low solubility in aqueous solutions and so find applications in wetting, antistatic and dispersants. Examples include the dyeing industry for improved colour dispersal; the agricultural industry for better spreading, wetting and penetrating abilities of fertilisers and pesticides; and as corrosion inhibitors in a large range of industries.[134,137]

Gemini sulfo-succinates are also popular due to their unique range of properties, different to single sulfo-succinates, Scheme 25.[138]
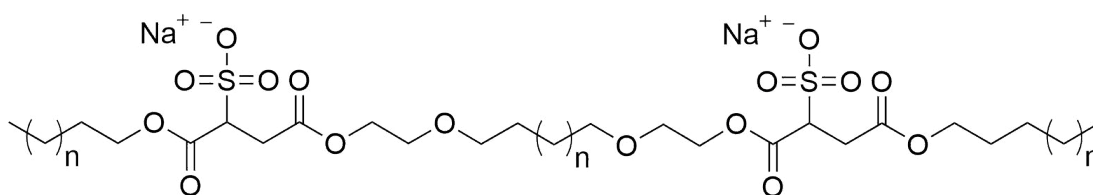
Scheme 25: Structure of a gemini sulfo-succiante[138]

Due to their size and their additional hydrophilic groups, they have improved water solubility and surface activity as well as increased aggregation and rheological activity.[138]

Sulfo-succinates have the additional benefit of being chiral molecules, Scheme 26, which opens up avenues for even more applications.[139] Many separation techniques such as capillary electrophoresis or membrane separation use chiral additives to remove diastereomers and when used in reactions they can increase rates and selectivities. This occurs through their ability to aggregate and interact with the chiral reactants or products.[139]
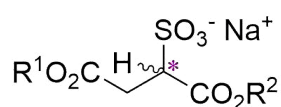
Scheme 26: The chirality in the structure of a sulfo-succinate[139]

3.1.2 Synthesis

Sulfo-succinate synthesis is straightforward. Esterification with an alcohol of maleic acid (MalA) or maleic anhydride (MalAnh) followed by sulfitation with sodium sulfite, Scheme 27.[134,137,138,140]
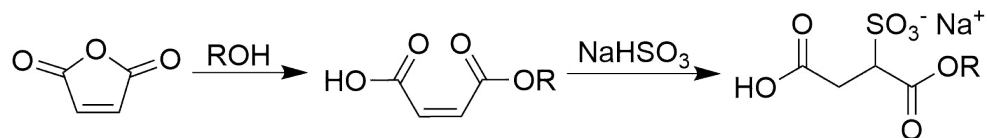
Scheme 27: Synthesis of current market monoalkyl sulfo-succinates from MalAnh using sodium bisulfite[134,137,138,140]

With a small number of synthetic steps, limited purification and minimal waste produced, this synthesis has good green credentials. However, with its use of non-renewable petrochemicals coupled with the irretrievable nature of the products after use, there are improvements to be made.

3.1.3 Itaconic Acid

Itaconic acid (IA) is very similar in structure and properties to MalA and was named in the list of top value added chemicals from biomass from the United States Department of Energy (U.S. D.O.E.).[26] This bio-derived acid has an additional CH_2 group with a terminal double bond unlike MalA's internal, Scheme 28.[26]
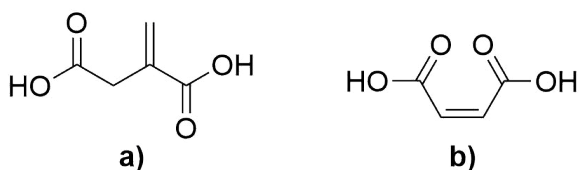
Scheme 28: Structure of a) bio-derived IA and b) petrochemical derived MalA[26]

IA was first discovered as a by-product of citric acid pyrolysis by Baup[141] and since then much research has been carried out on its production and use.[54,142–146] IA can be produced from many types of biomass, xylose from wood, glucose from corn, levoglucosan (1,6-β-D-glucopyranose) (LG) from cellulose, to name a few.[54,143]

Currently, commercial production is from 6-carbon sugars as the process is higher yielding however

it is more expensive than from 5-carbon sugars.[144] Originally isolated from *Aspergillus Itaconicus* in 1932, IA is now known to be overproduced by *Aspergillus Terreus* and commercial production uses this fungal strain today, Scheme 29.[144–146]
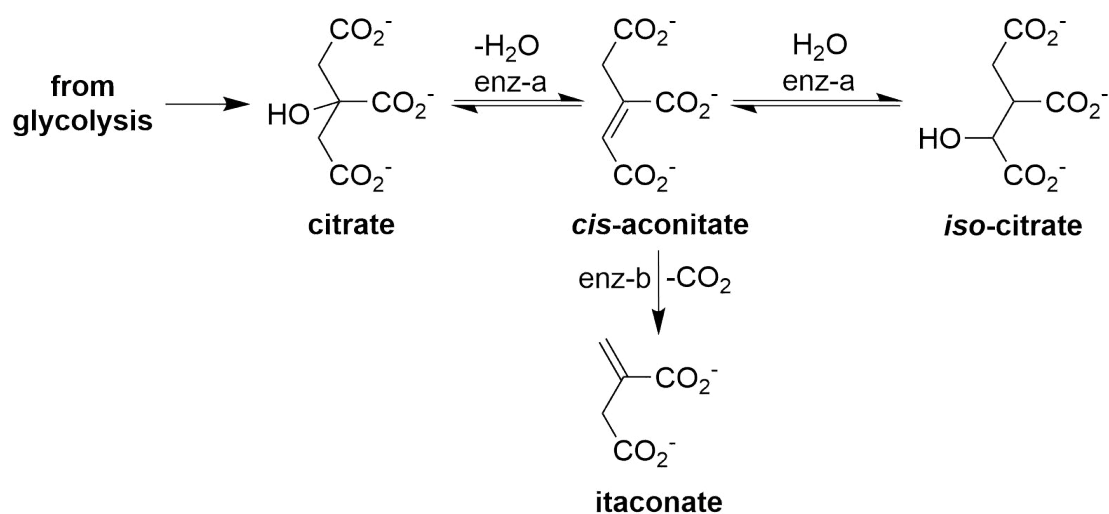
Scheme 29: Route of biosynthetic production of IA by *Aspergillus Terrus* from glucose *via* citric and aconitic acids. enz-a is aconitase and enz-b is aconitase-decarboxylase[145,146]

IA production is almost exclusively from fungi due to the problematic and expensive chemical synthesis. The synthetic routes to IA are dry distillation of citric acid to the anhydride followed by hydrolysis; oxidation of mesityl oxide and isomerisation of resultant citric acid; or oxidation of isoprene, all of which are multi-step and energy intensive.[146]

Market production was >15,000 t in 2001 but the high price has been a factor in keeping this low.[146] The predicted market production for IA by 2020 is from 200-–414 kt per annum with the potential to increase this up to 6163 kt per annum if all avenues for use are exploited.[144]

Synthesis of surfactants using IA in place of MalA has the potential to create a range of renewable surfactants, which can replace the current sulfo-succinates and improve the green credentials of the surfactant industry greatly. The options for renewable anionic surfactants on the market today are scarce and so these molecules have lots of potential.

IA and MalA have enough structural similarities to enable sulfo-methylene-succinates to be drop-in replacements for sulfo-succinates but also have enough differences to ensure they exhibit enhanced properties. The symmetry of the MalA enables faster reaction rates than the IA as there are two esters reactive enough to esterify; in IA one is strongly conjugated with the double bond which makes esterification unfavourable.[147,148] On the other hand, the terminal position of the

double bond and the additional CH_2 in the IA lower the hydrophilic-lipophilic balance (HLB) of the resultant surfactant; this improves the surface activity and lowers the CMC, as shown in Chapter 4.[60,62,63]

3.1.4 Sulfo-methylene-succinates

Currently there are many examples of itaconate esters in the literature as surfactants which compare to commercial sodium dodecyl sulfate (SDS).[149] The first example of an itaconate-based surfactant was potassium dodecyl itaconate which has improved surface activity than SDS with similar sized micelles and interfacial properties.[149] Monododecyl itaconate and monohexadecyl itaconate have since been utilised as polymerisable surfactants; an advantage of the double bond being terminal.[150] These surfactants are useful in synthetic rubbers, paints, adhesives and binders as well as additives in paper, textiles and leather treatment. The ability to bind to a surface gives them better activity as they have greater stability. This is important in emulsion polymerisation as they are used to govern the particle size and distribution of the polymer product, as well as in coatings, when they are used as emulsifiers, better coverage can be achieved when the emulsifier is chemically bound to a polymer as this prevents migration and coagulation.[150,151]

Among these many examples of itaconate ester surfactants there are only a few examples of sulfonates or of exploitation of the terminal double bond for attachment of functionality.[152,153] One of these examples is mono-nonylphenol ethoxylate(10) sulfo-methylene-succinate, Scheme 30.[142] These surfactants exhibit low CMC values and are aimed at competing with gemini surfactants as emulsifiers and dispersants.[142]
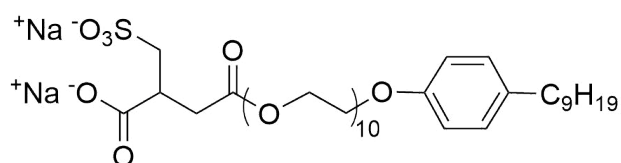
Scheme 30: Structure of mono-nonylphenol ethoxylate(10) sulfo-methylene-succinate[142]

The most recent and relevant example of sulfo-methylene-succinates in the literature is comparable to the surfactants synthesised in this Chapter, except has two hydrophobic chains. Di-*n*-octyl sulfo-methylene-succinate, Scheme 31, is comparable to commercial Aerosol-OT-1 (AOT-1).[67] This surfactant, coupled with the ones developed within this Chapter demonstrates the importance and potential of these molecules in the improvement of the renewable surfactants market. This

thesis focusses on mono-ester variations of the sulfo-methylene-succinate surfactants and therefore is complemented by the work done by Xu *et al.*[67].
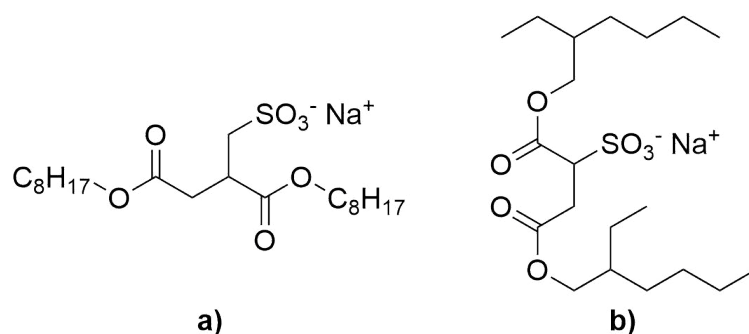
Scheme 31: Structure of a) di-*n*-octyl sulfo-methylene-succinate and b) AOT-1 an existing market sulfo-succinate[67]

3.1.5 Aims of the Chapter

As seen, sulfo-succinates represent a large proportion of the surfactant market however these types of surfactant are under-represented in the renewable side of the market. With a solid base to work from, in terms of existing similar surfactants and complimentary potential renewable surfactants, this chapter aimed at developing a range of sulfo-methylene-succinates from a bio-derived platform molecule, IA. Importantly, the synthetic methods utilised were to be as clean as possible.

3.2 Chain Addition

3.2.1 Esterification of Itaconic Acid

The first investigations were carried out using standard esterification of IA in order to add the hydrophobic chain to the hydrophilic head group of the potential surfactant. The esterification trialled was acid catalysed which is an equilibrium and follows a well established mechanism, Scheme 32.[154,155] Both homogeneous and heterogeneous acid catalysts are used for esterifications. Traditionally hetergoeneous catalysts such as sulfuric acid and *para*-toluene sulfonic acid (*p*-TSA) are used however during the current green chemistry drive, a large increase in the use of solid acid catalysts has been seen.[46,101,134,156,157] Montmorillonite clays, sulfated zirconias, functionalised silicas, zeolites and ion exchange resins such as amberlite have been documented as successful

esterification catalysts and these have many advantages over the traditional, as discussed in the Introduction, section 1.1.2 and in Chapter 2, section 2.1.3.[43,46,47,92,101,148,155,157]
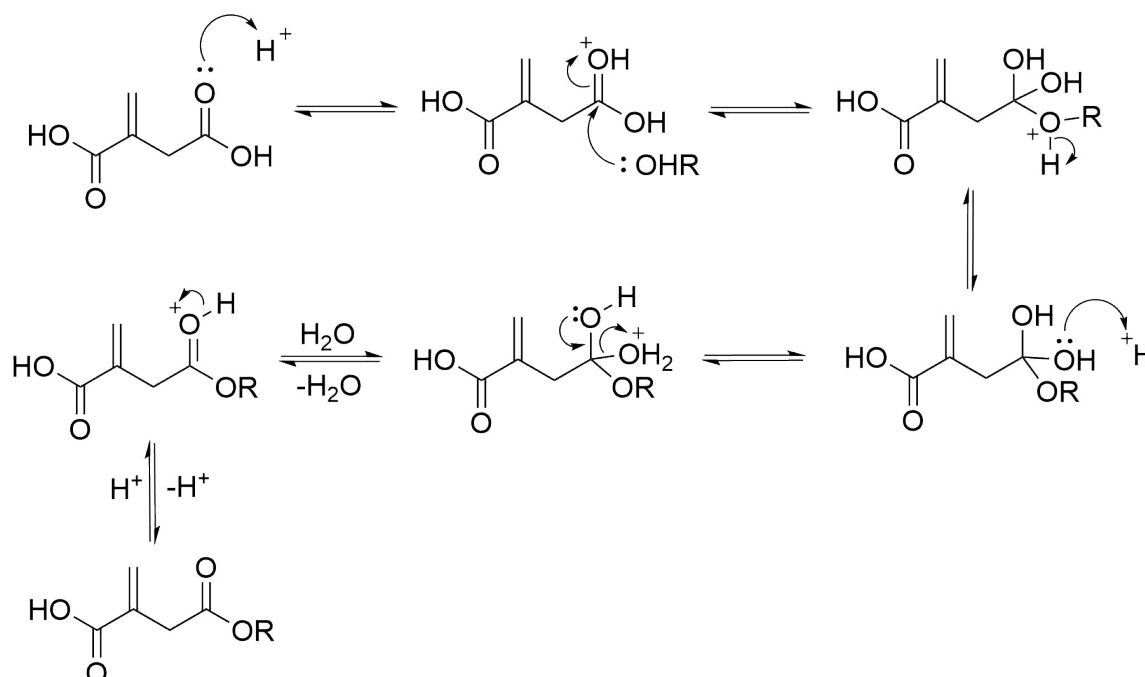
Scheme 32: Mechanism of acid catalysed esterification[154,155]

The difficulty faced in this thesis was the conjugation of the second carboxylic acid group with the double bond in IA. This conjugation decreases the electrophilicity of the carbonyl carbon and reduces the chances of attack on it by the alcohol oxygen, Scheme 33. IA almost exclusively esterifies at the non-conjugated carboxylic acid first and diester formation poses a significant challenge.[147,148,157,158]
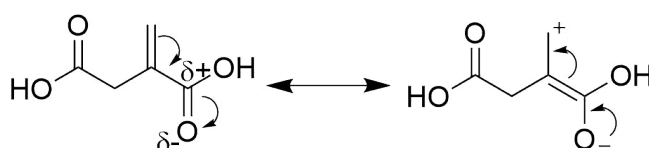
Scheme 33: Conjugation of the carboxylic acid with the double bond in IA[147,148]

Finding alternative, green catalysts for this reaction is difficult if di-esterification is required and therefore not many examples are to be seen in the literature. Montmorillonite clays and porous zeolites have both been found to be highly successful catalysts for the esterification of diacids, however, the former to di-esters only without conjugation and the latter, while of conjugated diacids, only to the mono-ester.[155,157] Li *et al.*[158] succeeded in finding solid acid catalysts, based

on TiO_2-SiO_2 (Ti:Si 25:1), capable of producing >91% yields of the di-methyl, di-butyl and di-isooctyl itaconates. Unfortunately, these catalysts required the addition of rare earth metals (Si:Ln up to 1:1) and the reactions required 6 h at 100 °C in an autoclave.[158]

This choice between clean synthesis and diester production is important to address for the future production of dialkyl sulfo-surfactants and hence was investigated later on in this Chapter.

Octanol

Octanol was selected to be the test alcohol for this esterification, Scheme 34, because the resultant surfactant produced from the reaction and subsequent sulfitation would have a suitable HLB for potential applications.
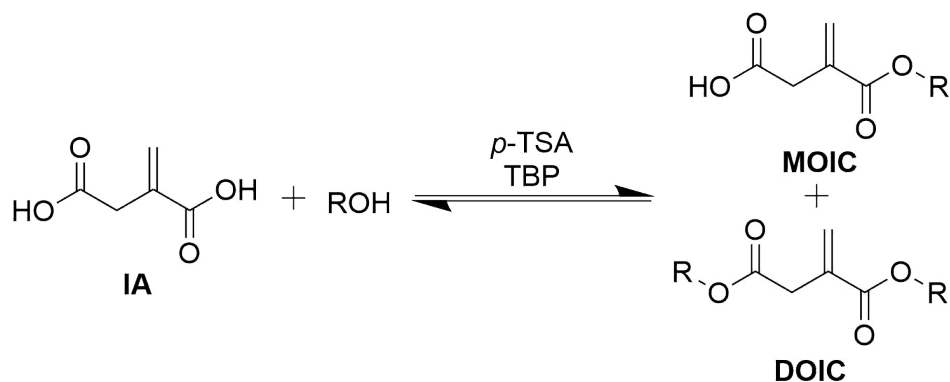
Scheme 34: Esterification of IA with an alcohol, a *p*-TSA catalyst and a *tert-tri*-butyl phenol (TBP) radical inhibitor to produce mono-octyl itaconate (MOIC) and dioctyl itaconate (DOIC). R is C_8H_{17}

Standard esterification conditions were chosen and a screen of some temperature/time combinations was carried out. The results were determined by ^{1}H nuclear magnetic resonance (NMR) spectroscopy, Figure 28, and products, MOIC and DOIC, identified by mass spectrometry (MS) where necessary.

It can be seen in Figure 28 that the reaction proceeded in under 2 h to a conversion of >90% and unexpectedly, due to the conjugation of one of the carbonyl groups, to a high selectivity of the diester. At the higher temperature, 140 °C, and longer reaction times, the proportion of diester continued to grow, to up to 90%, but limited effects can be seen beyond this. The reason behind this high conversion and diester formation can be attributed to the strongly acidic catalyst.[154,155]
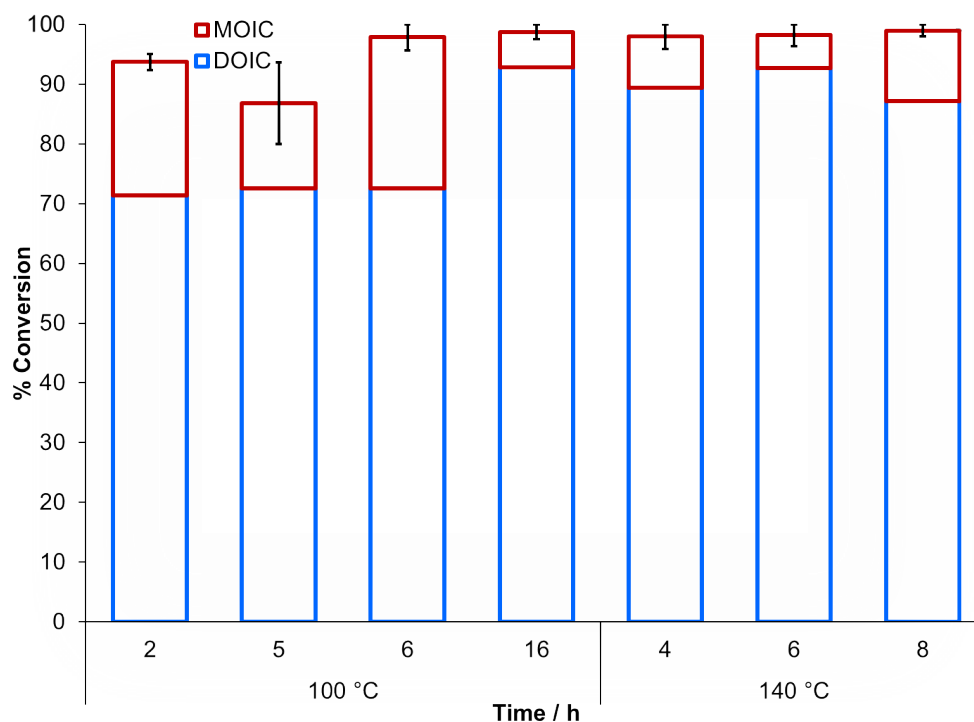
Figure 28: Effect of temperature and time on the esterification of IA with octanol

These results show promising conversion and yields of the desired products, especially DOIC, because the formation of diester of conjugated diacids is usually difficult.[147,148] *p*-TSA is a good catalyst for these reactions, in terms of producing high conversion and selectivity, however it is highly acidic, non-selective, homogeneous and corrosive.[101] In IA there are not any acid sensitive functional groups and so no negative effects of the acid's indiscriminate attack are seen, however, this restricts the acid's use to hardy substrates. In addition, removal or separation of the *p*-TSA from the mixture post reaction is difficult given its state, and the disposal of the consequently acidic waste is complicated due to the potential for high environmental effects.
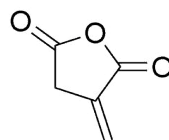
Scheme 35: Structure of itaconic anhydride (IAnh)[159]

Due to these concerns about homogeneous catalysts, the investigation was shifted to focus of improving the green credentials of the ester synthesis; this consequently meant the shift towards producing mono- instead of diester however they too have potential in the synthesis of interesting surfactants.[62]

The ring opening of IAnh, a cyclic dehydrated IA, Scheme 35, which is comparable to MalAnh currently used in sulfo-succinate synthesis, was investigated because the need for catalysis in that reaction is low.

3.2.2   Ring Opening of Itaconic Anhydride

Anhydrides *vs.* Acids?

Cyclic anhydrides are readily ring opened due to their ring strain and hence high reactivity and so formation of the itaconate monoester from IAnh has the potential to be performed quickly, without the need for a catalyst.[160,161] The ring opening of IAnh is also stereospecific and only the ester on the saturated side of the itaconate moeity is formed, Scheme 36; the conjugation hinders the formation of the ester on the unsaturated side of the itaconate moeity for the same reasons as previously discussed for IA esterification.[161,162]
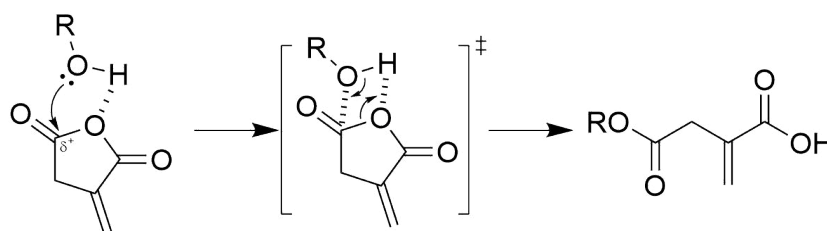
Scheme 36: Mechanism for the ring opening of IAnh with an alcohol[160]

Traditionally, anhydride synthesis is energy intensive and requires the use of dehydrating reagents such as acetic anhydride or acetyl chloride and many of the reports of IAnh synthesis use such chemicals.[163,164] IAnh has also been synthesised without the need for other reagents, however the energy requirement is still present; dry distillation of citric acid or heating of IA has been documented to produce IAnh and while this synthesis is not entirely green, the absence of excess reagents is positive.[165,166] Use of IAnh for the formation of monoesters has the potential to reduce the need for long reaction times at high temperatures and remove the need for a catalyst and so in this case these advantages could be seen to compensate for the compromise in starting material.

The ring opening of IAnh with an alcohol was carried out with octanol which, as before, was chosen as the test alcohol, Scheme 37.
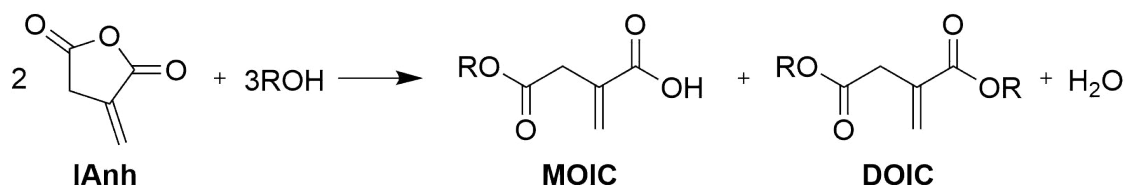
Scheme 37: Ring opening of IAnh with an alcohol to form MOIC and DOIC. R is C_8H_{17}

Microwave Reactions

Microwave (MW) reactions are often seen as quick and efficient alternatives to their conventionally heated counterparts and so the first investigations carried out were of this nature. Again, octanol was used as the test substrate so that the reactions and products could be comparable to the previous investigations.

Product Identification ^{1}H NMR spectra showed that four products were present. Following optimisation with supercritical fluid chromatography (SFC), the four products were successfully isolated for further analysis. It was determined that alongside the MOIC and the DOIC expected, there was also some IA and citraconate and mesaconate isomers being produced.

Itaconate isomerisation is well established in the literature; the double bond migrates and two isomers form, the mesaconate (carbonyl groups *trans*) and citraconate (carbonyl groups *cis*), Scheme 38. [167–170]
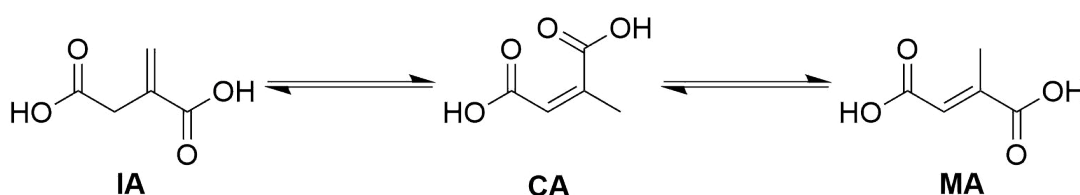
Scheme 38: Structures of IA and its two isomers, mesaconic acid (MA) (carbonyl groups *trans*) and citraconic acid (CA) (carbonyl groups *cis*) [167,168,170]

The mechanism of isomerisation, shown below, is dependant on the presence of water and involves deprotonation/reprotonation of allylic carbons and migration of the unsaturated bond, as well as deprotonation of the carboxylic acid group for *cis/trans* (with respect to the carbonyl groups) isomerisation, Scheme 39. [168]

or

IA

CA

or

tautomerism

tautomerism
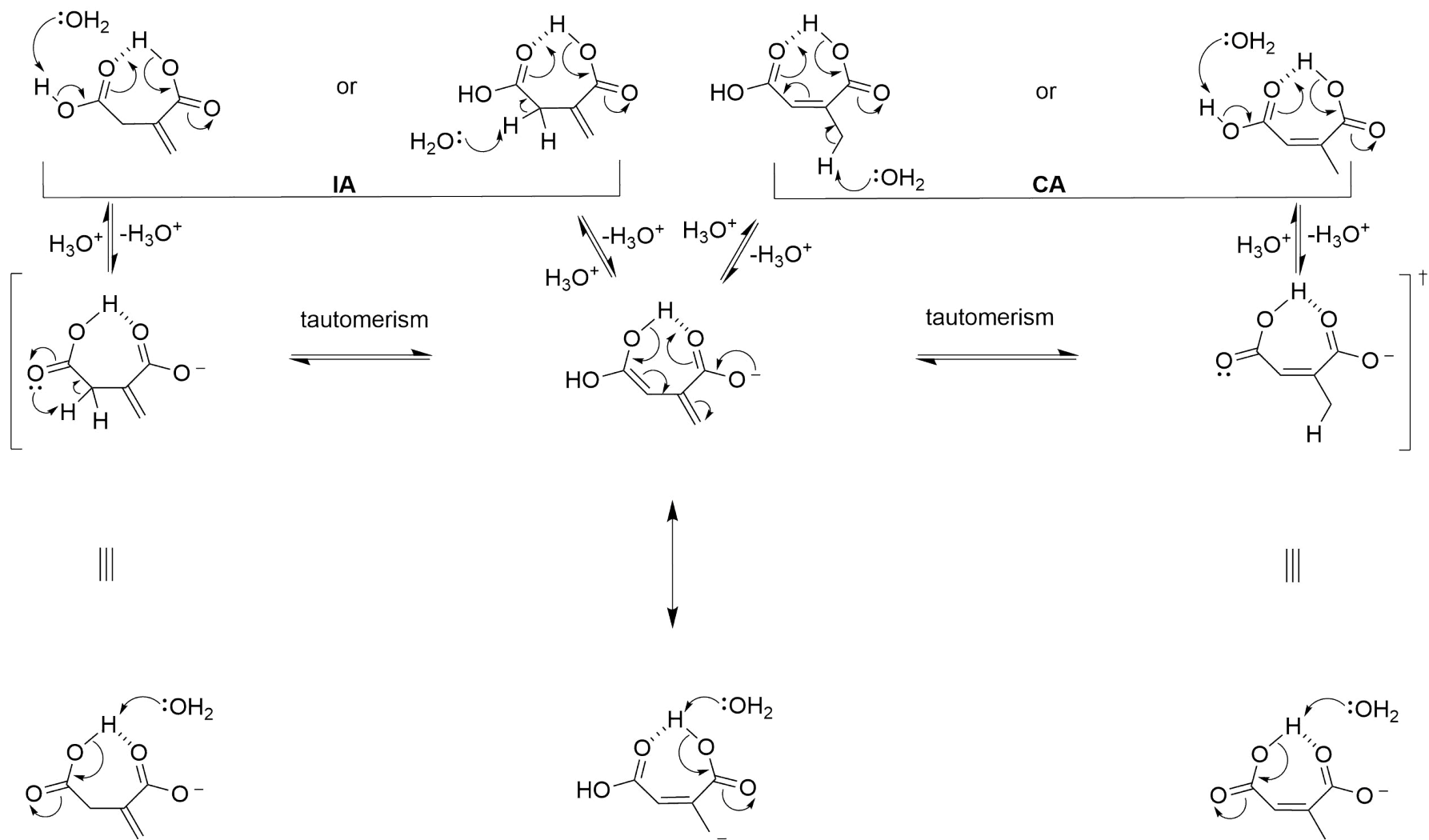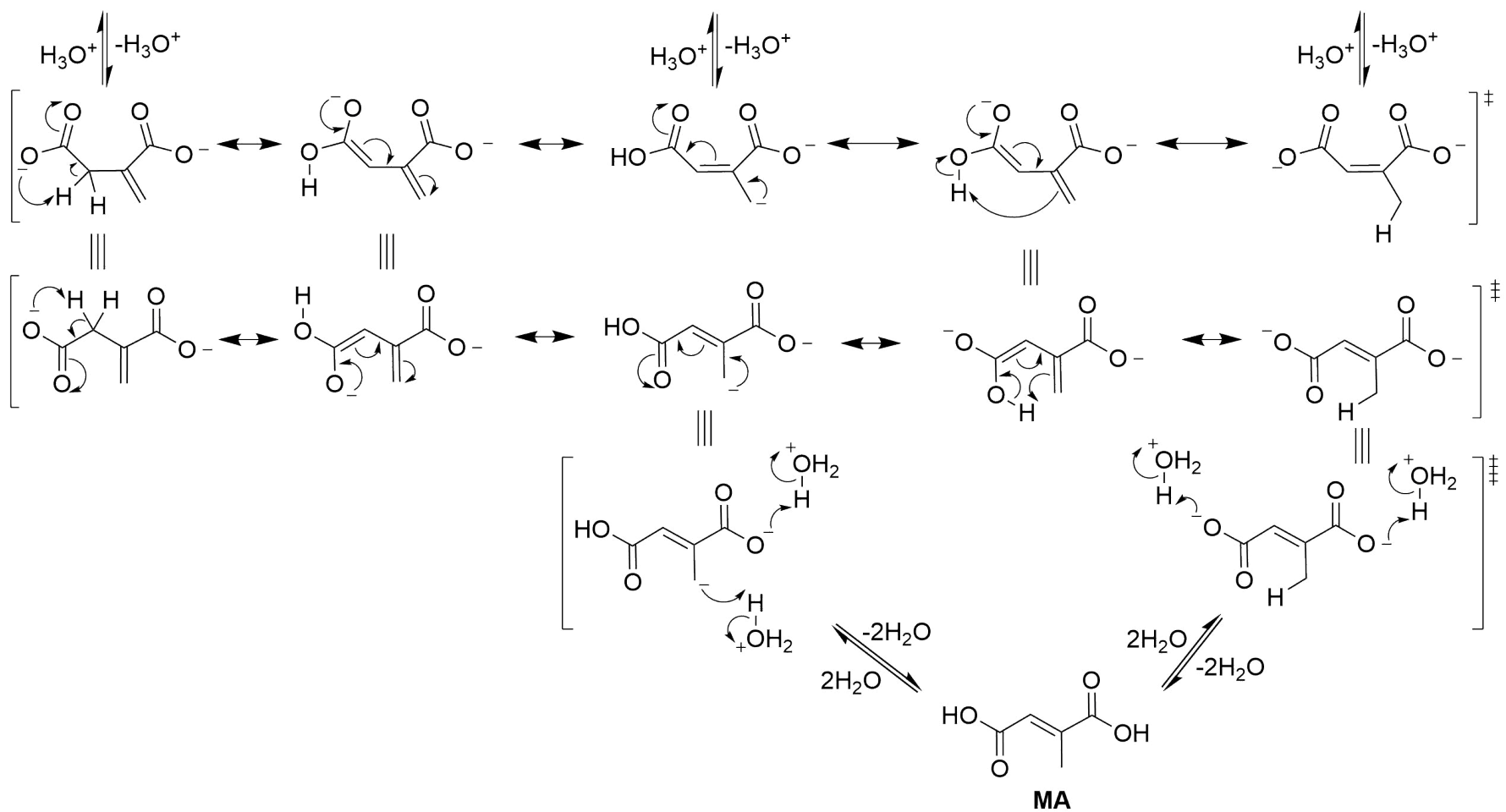
Scheme 39: Isomerisation mechanism of IA to CA and MA in water[168]

With the double bond in the terminal position itaconic acid is the most stable isomer and the equilibrium ratios of the three isomers were first determined by Sakai [168] to be 80, 17 and 3% for IA, CA and MA, respectively. The isomerisation between itaconate and citraconate is known to be fast, with the equilibrium between the *cis-* and *trans-* isomers (with respect to the carbonyl groups) forming slower due to the energy barrier to rotation. [168,170,171] Cody *et al.* [170] suggested that the equilibrium reported by Sakai [168] did not form instantaneously, instead the ratios of the three isomers developed over time. It was proposed that the citraconate isomer established itself quickly first, as the kinetically favourable product, with the mesaconate isomer becoming more prominent over time. This is due to the ease of isomerisation between the terminal and the *cis* isomers but the *trans* isomer being the most stable and hence the thermodynamically favoured product. [170,171]

This is seen in polymerisation reactions conducted over long reaction times where the isomer ratios are observed as 46, 49 and 5 % for itaconate, mesaconate and citraconate, respectively. [172,173] The kinetic favourability of the citraconate arises from hydrogen bonding between the two carboxylic acid groups; this forms a cyclic intermediate which holds the *cis* configuration in place during the double bond migration. Additional deprotonation of the molecule, at an acid group, is required to break the hydrogen bonding and allow free rotation of the central $HO_2CHC\text{-}C(CH_2)CO_2H$ bond during isomerisation to form the mesaconate isomer. [168] In the case of the diacids, CA forms over MA.

MOCC   **DOCC**

MOMC   **DOMC**
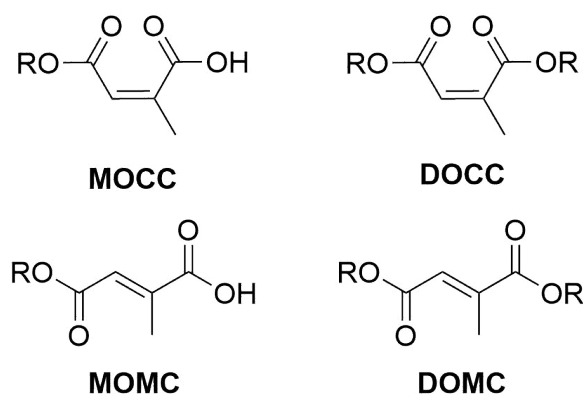
Scheme 40: Isomers of mono- and di-esters of IA

This hydrogen bonding is disrupted when esterification of one or both of the carboxylic acid groups has taken place and so in the case of the mono- and di-esters, only the mesaconate is seen, because the kinetic favourability of the citraconate is lost. [169] In these cases, mono-octyl

mesaconate (MOMC) and dioctyl mesaconate (DOMC) form over mono-octyl citraconate (MOCC) or dioctyl citraconate (DOCC), Scheme 40.

Temperature Effects The initial optimisations were carried out to determine the best conditions for further investigations into the reaction, with temperature being the first variable.
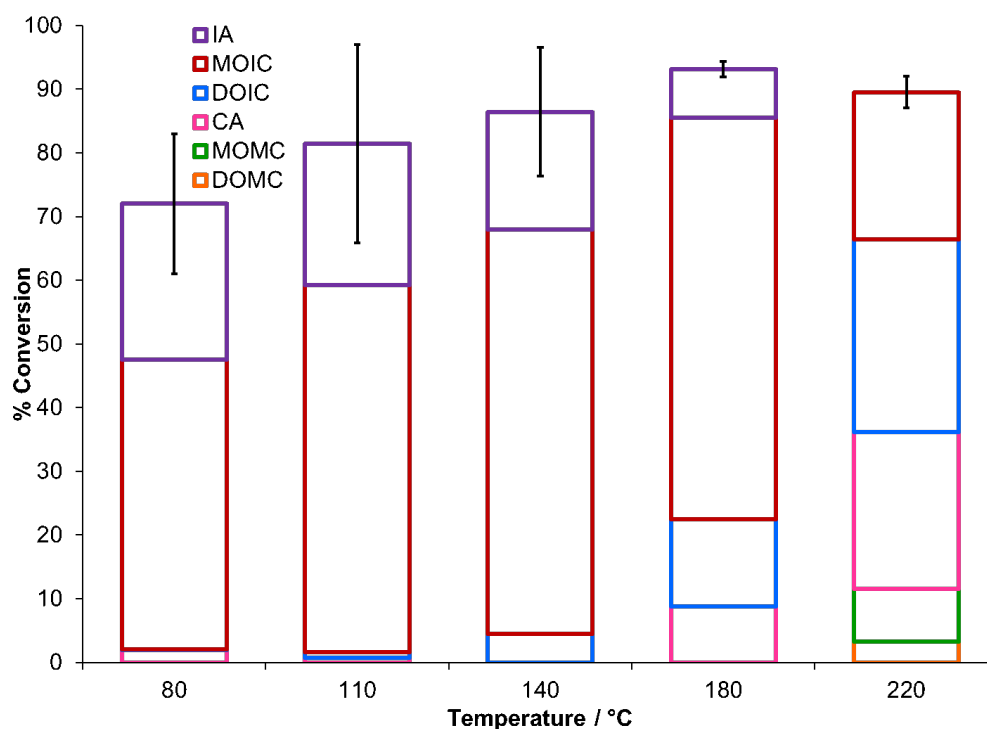
Figure 29: Effect of temperature on the MW induced ring opening of IAnh by octanol

It can be seen, from Figure 29, that conversion of IAnh increases with temperature and there is a maximum of up to 95% at 180 °C. In terms of selectivity to MOIC, this is lower at the higher temperatures with a significant change at 220 °C; at this temperature there is a lower preference for a particular product due to isomerisation. The esterification of the conjugated carboxylic acid will be encouraged by the high temperature and the MOIC will itself be reacting to form the DOIC. Isomerisation of IAnh and IA will form the citraconate isomer and isomerisation of MOIC and DOIC will form their respective mesaconate isomers.[168,169]

IA is present up to 25% at the low temperatures and drops off sharply as the temperature increases from 140–220 °C; this will be reacting with octanol at the higher temperatures to MOIC and then further to DOIC, or isomerising to CA.

Effect of Time Reaction time was the second variable investigated for this reaction and two representative temperatures where chosen for this study. Length of reaction time has little effect on conversion or selectivity of ring opening, Figure 30. The most pronounced trend seen is a slight increase in conversion. The increase is only 10% indicating that full conversion to MOIC or DOIC would be unachievable with any reasonable MW conditions.
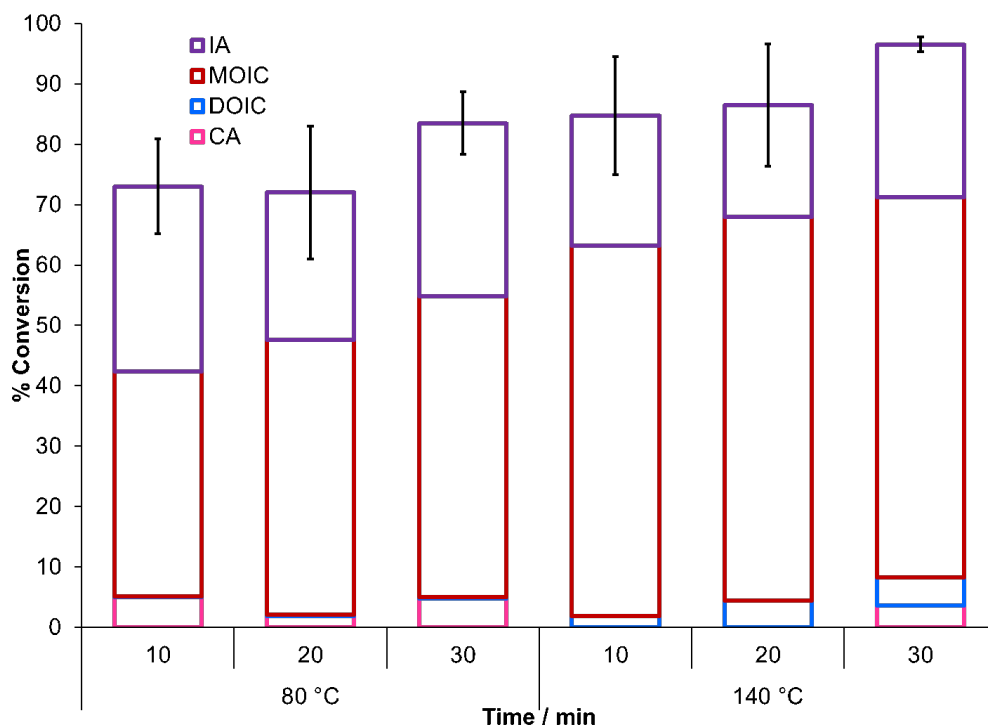
Figure 30: Effect of reaction time on the MW induced ring opening of IAnh by octanol

Forcing Conditions

The conditions of 80 °C, 20 min were chosen to test further variables in an attempt to push the reaction through to full conversion, *i.e.* no remaining IA. These conditions were used because lower temperatures reduce energy use of the reaction, and after 20 mins there was the lowest isomerisation.

Pre-warming the reaction to aid substrate dissolution, the use of Lewis acids in order to encourage nucleophilic attack and an excess of octanol to push the reaction forwards faster, were all trialled, Figure 31. The two pre-warming attempts, by observation, had no effect on solubility however an increase in conversion can be seen due to pre-warming on a hot-plate. Pre-warming in the microwave was tested because the direct interaction of the microwaves with the molecules in the solution was proposed to aid dissolution. This is in comparison with conventional heating whereby

the reaction is heated through conduction and convection not molecular excitement. Additionally, the homogeneity arising form the mechanism of microwave heating, alongside the speed with which heating occurs would be advantageous if an additional dissolution step was necessary in the process. However, this method appears to have had little or no effect, potentially due to the lower temperature used.[16,48–50]
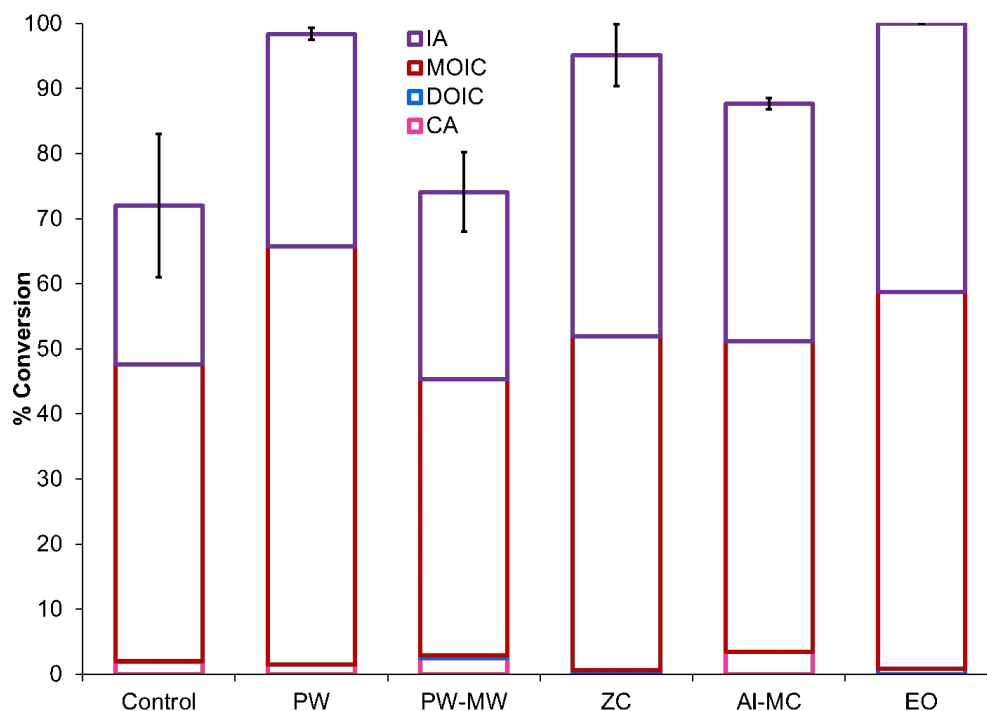
Figure 31: MW induced ring opening of IAnh with octanol. PW involved heating on a hotplate (80 °C, 15 min) prior to reaction, PW-MW involved heating in the MW (40 °C, 10 min) prior to reaction, ZC involved addition of $ZnCl_2$ (10 percent by weight (wt%)), Al-MC involved addition of aluminium pillared montmorillonite clay (Al-MC) (10 wt%) and EO involved addition of an excess of octanol (2 molar equivalents (mol equiv.))
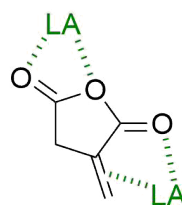
Scheme 41: Coordination of a Lewis acid (LA) to IAnh[174]

Lewis acids co-ordinate to anhydrides through a carbonyl oxygen and the central oxygen atom, Scheme 41, which increases the electrophilicity of the carbonyl carbon, encouraging attack from

the alcohol oxygen.[174] The $ZnCl_2$ and the Al-MC can both act as Lewis acids by co-ordination of the cation, however the Al-MC is a weaker Lewis acid and hence has a less pronounced effect on the conversion.[89] Lewis acid sites in montmorillonite clays are located inside the clay structure making it harder for co-ordination and subsequent nucleophilic attack than the homogeneous $ZnCl_2$, especially if layer collapse occurred after calcination.[175]

The excess of octanol, predictably from Le Chatelier's principle, increased conversion but still there was no evidence of DOIC. 80 °C is evidently not a high enough temperature for formation of the ester at the conjugated carbonyl.[176] The formation of MOIC does not produce water however the formation of DOIC does and hence would require removal of this water from the reaction set-up to pull the esterification forwards.[176]

Anhydrous Reactions
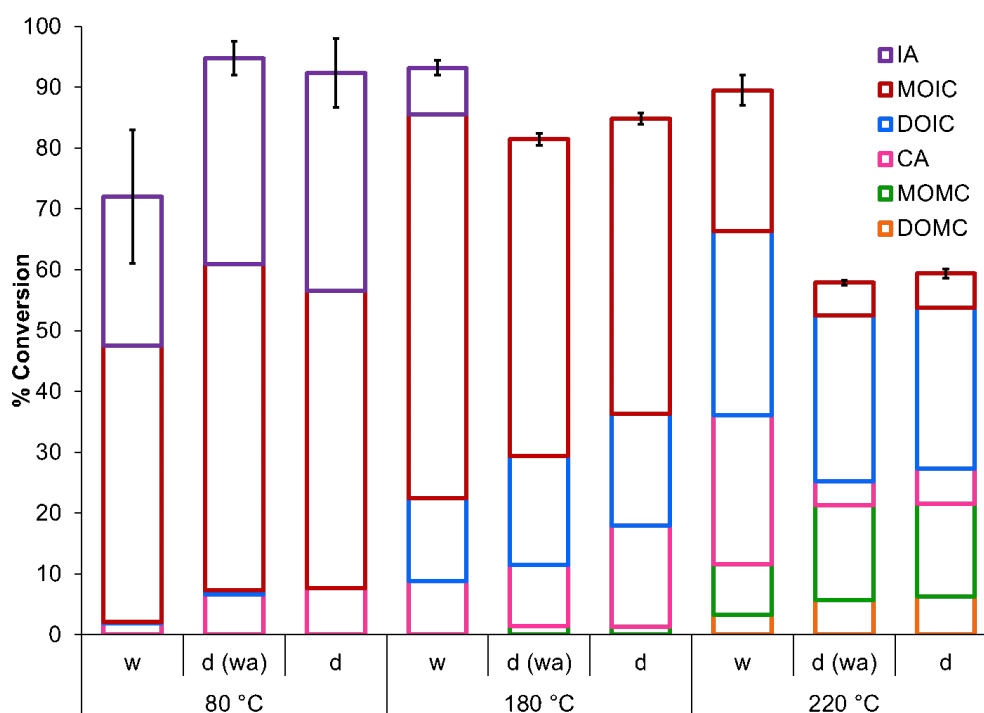
Figure 32: MW induced ring opening of IAnh with octanol under various anhydrous reaction conditions. w was all solvents as received, d (wa) was reaction over 4 Å molecular sieves with octanol previously dried over 4 Å molecular sieves but ^{1}H NMR solvents (DMSO$-$d$_6$ and CDCl$_3$) as received and, d was reaction over 4 Å molecular sieves with octanol and all ^{1}H NMR solvents (DMSO$-$d$_6$ and CDCl$_3$) previously dried over 4 Å molecular sieves

Removal of water from the reaction was tested to reduce isomerisation and to reduce the IA present, the test reaction was carried out under a number of conditions.[160,168]

With no trends seen and no consistent explanations as to the reasons for the results obtained, Figure 32, the suitability of the ^{1}H NMR solvent was called in to question. DMSO$-$d$_6$ is a very hygroscopic solvent and the difficulty in assuring that the analysis is anhydrous, and remains so throughout analysis, is very high.[177] It was considered that an alternative ^{1}H NMR solvent should be tested.

Acetone$-$d$_6$

Acetone$-$d$_6$ *vs.* DMSO$-$d$_6$ It is clear from these results, Figure 33, that the use of different solvents for the analysis has a significant impact on the products observed.
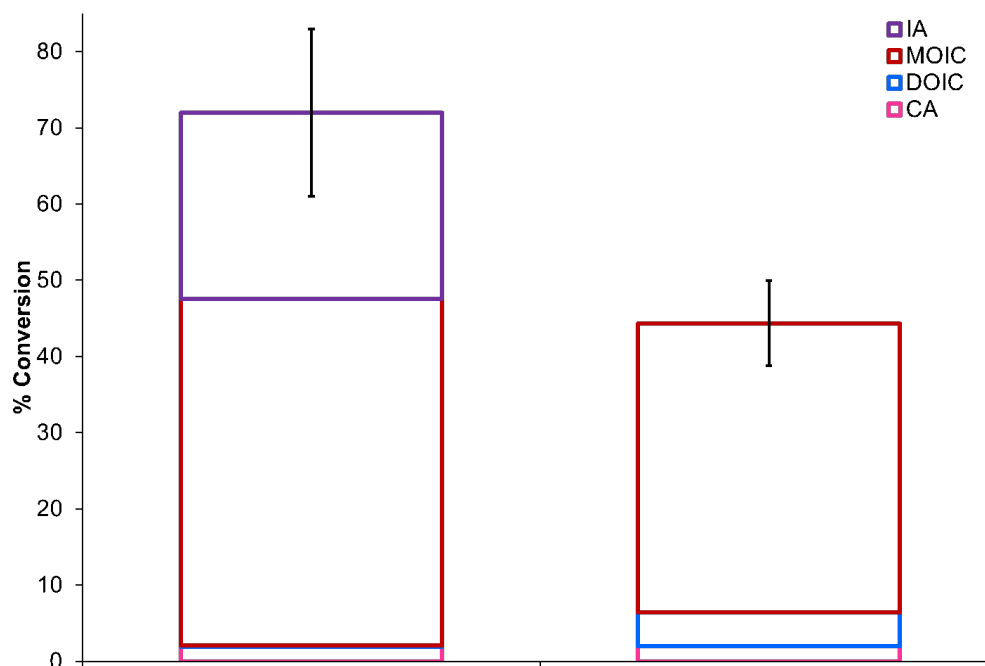
Figure 33: The effect of using alternative deuterated solvents for ^{1}H NMR spectroscopy of the MW induced ring opening of IAnh with octanol

Using acetone$-$d$_6$, it can be seen that no IA was present, which indicates that it was forming in the analysis, not the reaction. The implications of this are that the range of product distributions observed were formed during the analysis step and the results in DMSO$-$d$_6$ do not reflect the reaction itself. It is probable that the DMSO$-$d$_6$ will be wet, even after treatment with 4 Å

molecular sieves because it is very hygroscopic. [177] The length of time that the bottle of DMSO$-$d$_6$ used for the analysis had been open will have varied significantly and so it follows that the water levels in the DMSO$-$d$_6$ would also vary substantially; this would have impacted the results. The water will react with IAnh to IA, and will encourage isomerisation of the itaconate, forming MOMC and MOCC. [160,167–169]

The ^{1}H NMR spectrum of IAnh was examined to determine whether residual water in DMSO$-$d$_6$ would be enough to cause the ring opening to IA. Four spectra were run, one in each of D$_2$O, DMSO$-$d$_6$, DMSO$-$d$_6$ with extra water added and acetone$-$d$_6$. The D$_2$O, as expected, showed only 4% IAnh with 96% IA, and no evidence of isomerisation. The acetone$-$d$_6$ was similar, showing only IAnh and IA, 72 and 28%, respectively. The DMSO$-$d$_6$ however showed not only much more IA than the acetone$-$d$_6$, indicating that the solvent was holding more water, but also evidence of isomerisation to CA and MA. [169] The ratios of products shifted dramatically, not only from acetone$-$d$_6$ to DMSO$-$d$_6$ but also from DMSO$-$d$_6$ to DMSO$-$d$_6$ with extra water. In DMSO$-$d$_6$ straight from the bottle, the product ratio was 60, 35, 5 and 0% and with the added water was 28, 48, 15 and 9% for IAnh, IA, CA and MA respectively, Figure 34.

These product ratios show that while the water does ring open the IAnh, and it is previously shown that the water is necessary for the isomerisation of the IA, at room temperature (r.t.) it would seem it is the presence of the DMSO$-$d$_6$ that is causing or facilitating the isomerisation. DMSO$-$d$_6$ can act as a nucleophile and is also shown to strongly H-bond with water. [178,179] This H-bonding, Scheme 42, will enhance the nucleophilicity of the water due to the electron density being donated by the DMSO$-$d$_6$ and this will increase the likelihood of nucleophilic attack from water causing ring opening and/or isomerisation.
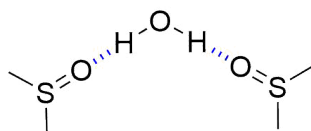
Scheme 42: Hydrogen bonding of DMSO with water

Dry acetone$-$d$_6$ was consequently used as the solvent for analysis from this point onwards.
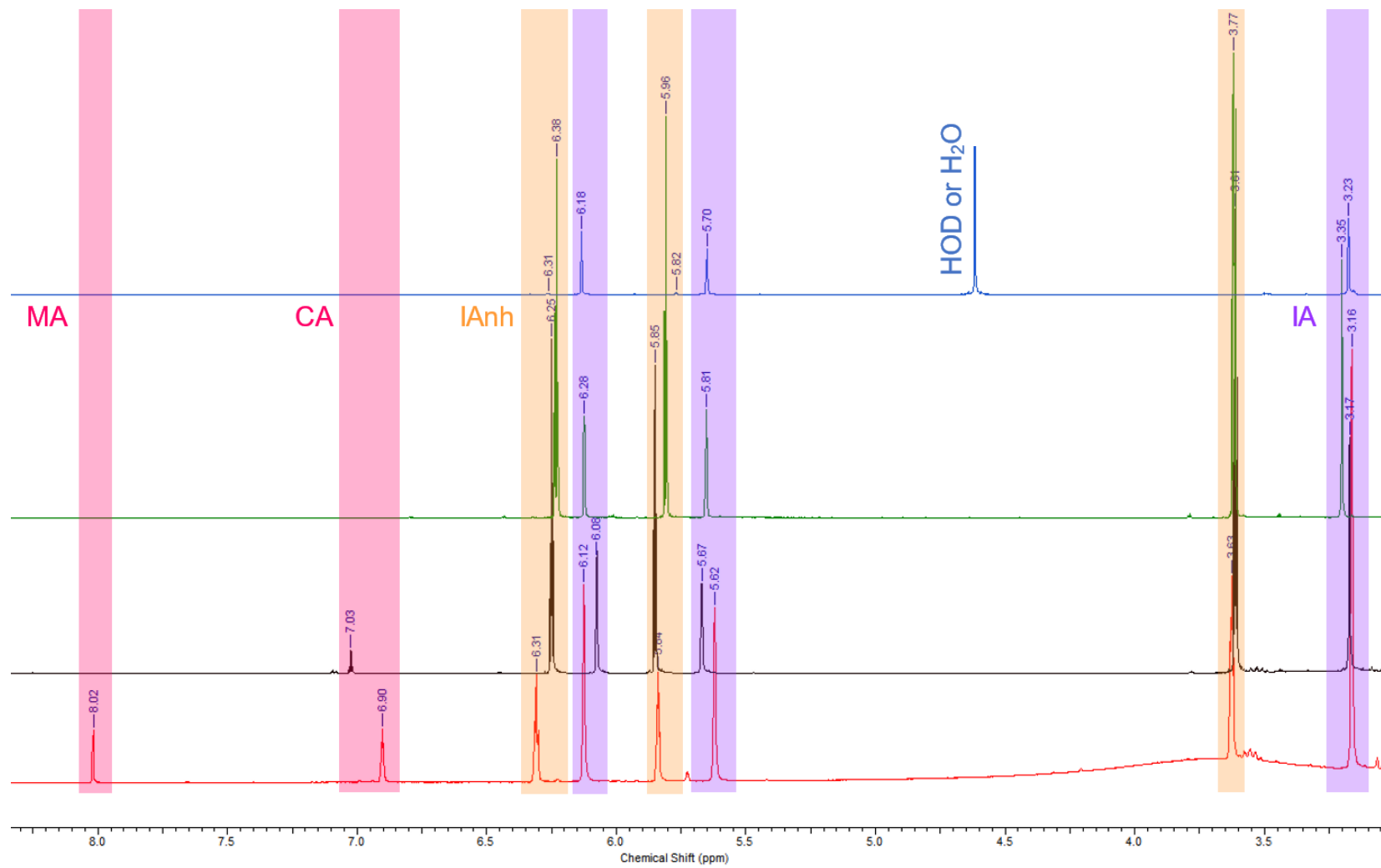
Figure 34: IAnh ^{1}H NMR spectroscopy in various deuterated solvents. Top to bottom; D$_2$O, acetone$-$d$_6$, DMSO$-$d$_6$ and DMSO$-$d$_6$ plus H$_2$O

Harsh Conditions   To push the MW induced ring opening to full conversion, a higher temperature and an excess of octanol were employed.
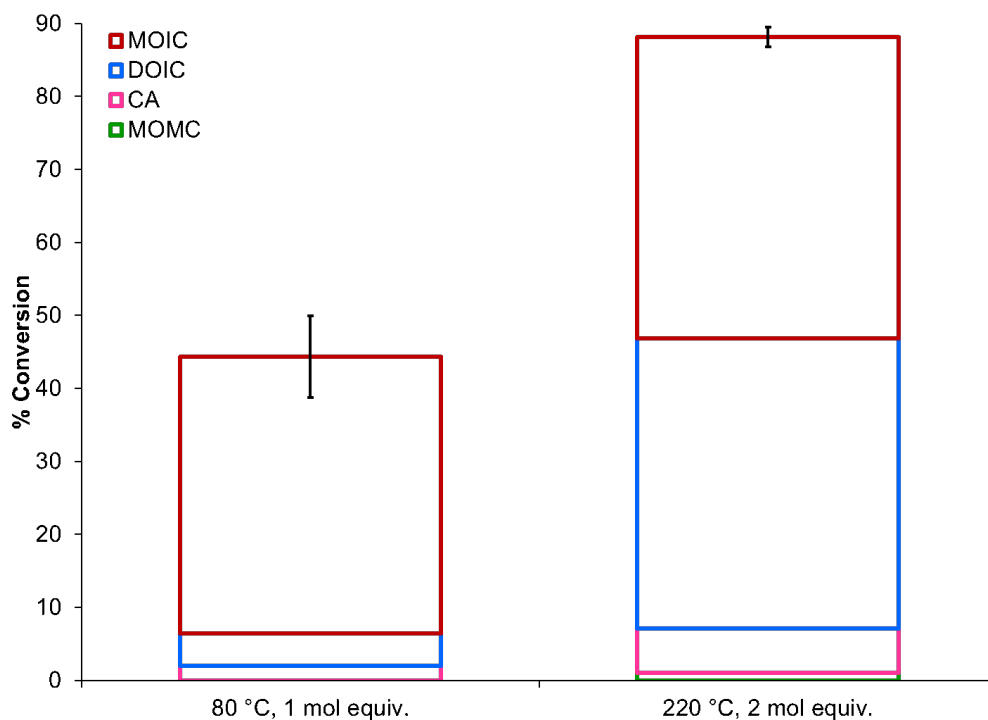
Figure 35: Effect of harsh reaction conditions on the MW induced ring opening of IAnh with octanol using acetone$-$d$_6$ for ^{1}H NMR spectroscopy

On increasing the temperature, Figure 35, there was a large increase in the conversion and an increase in the amount of DOIC. However, the reaction still did not proceed to full completion and the ratio of DOIC to MOIC was at best 1:1 which is not selective enough to be useful. Due to these poor results, the MW conditions were considered to be not appropriate for this reaction.

Conventional Reactions

With the reactions in the microwave unsuccessful, some experiments were trialled using conventional methods of heating, namely a hot-plate. An array of alcohols were tested to see if the chain length had an effect on the conversion and selectivity to monoalkyl itaconate (MAIC) and dialkyl itaconate (DAIC).

High conversion was achieved with 80% selectivity to MAIC, and there was minimal drop in either conversion or selectivity with the increase in chain length; these conditions can be used for the synthesis of surfactants. It would be expected for the conversion to drop with increased chain

length due to the increased immiscibility of the two substrates. In addition, it would be expected that secondary alcohols would have a decreased conversion and high selectivity due to the increased steric hindrance for attack towards the IAnh. This effect was observed however the conversion was still high enough for the synthesis of surfactants to be carried out using these conditions.
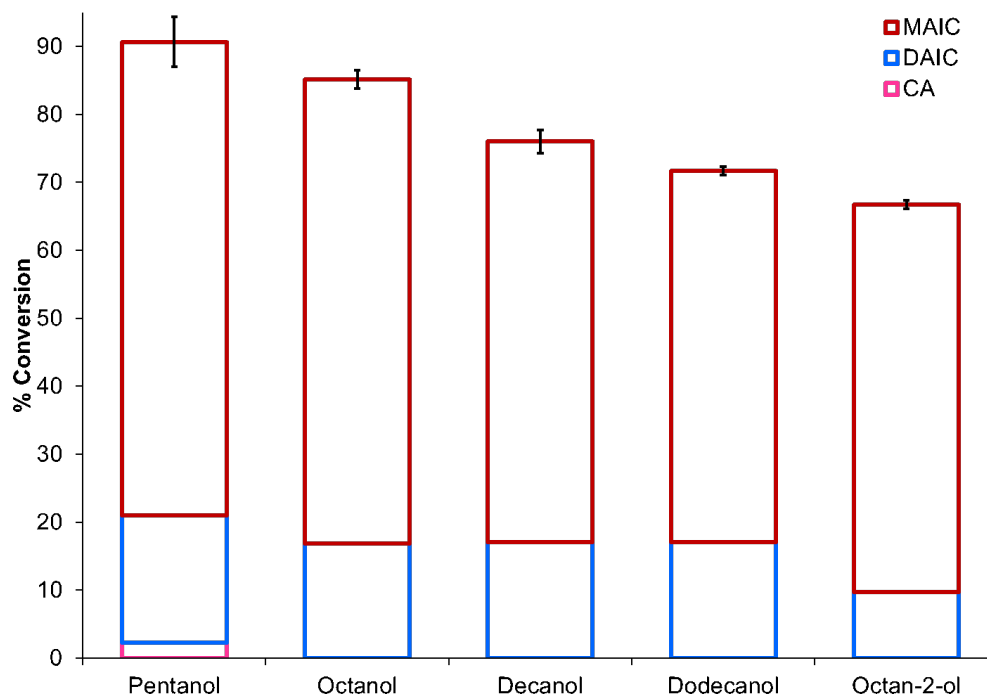
Figure 36: Ring opening of IAnh with various alcohols

Surfactant properties are highly dependant on, among other factors, the hydrophobic chain quantity and length. It was therefore desirable to push the reaction towards DAIC for comparison against the MAIC. An excess of alcohol and a Lewis acid catalyst, iron chloride, were tested. Iron (III) chloride was chosen, over the zinc chloride used earlier in the Chapter, because it is a stronger Lewis acid due to the higher charge density on the metal.[175]

With an excess of octanol and the presence of a Lewis acid the conversion was pushed to 100% however selectivity to DAIC remained low, Figure 37. No impact was seen of the $FeCl_3$ compared with just 2 mol equiv. of octanol suggesting that the conjugation between the carbonyl and the alkene is more favourable than the coordination with the Lewis acid.

Although selectivity towards DAIC was not achieved with the opening of IAnh, a catalyst and solvent free synthesis for MAIC was identified; this reaction can be used as a key step in the green synthesis of bio-derived surfactants.
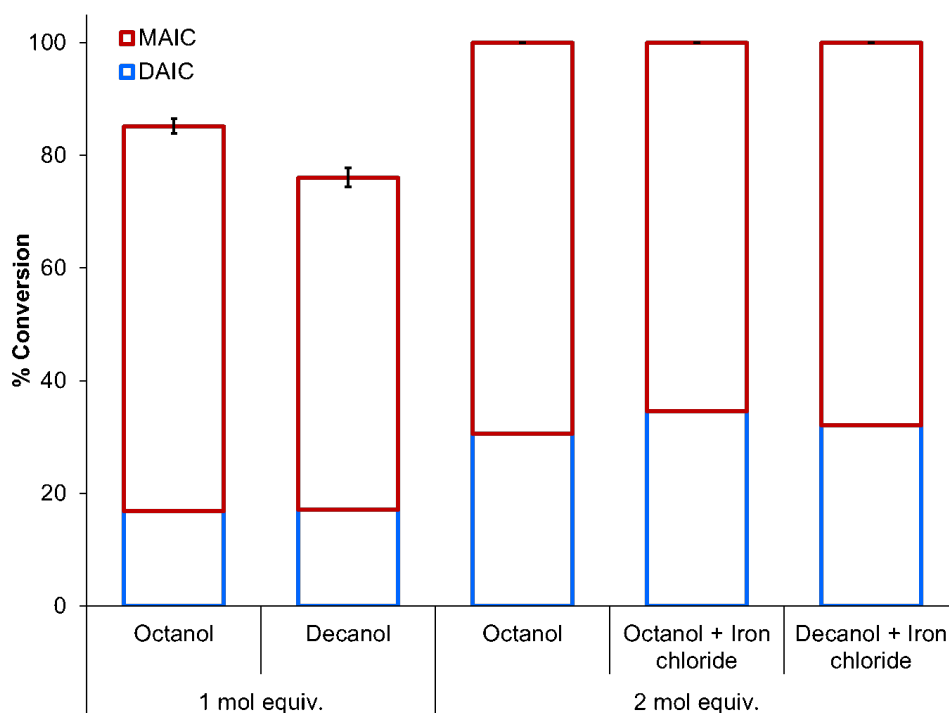
Figure 37: The effect of various conditions to push ring opening of IAnh with various alcohols to DAIC

3.3 Pendant Addition

Addition of pendants is necessary to ensure the surfactant head group is hydrophilic enough to balance the hydrophobicity of the tail. The itaconate moiety is useful because of the terminal alkene that can be used in addition/substitution reactions; there is less steric hindrance not only during the synthesis of the surfactant but also in the micelles of the surfactant, when compared with the existing sulfo-succinates.

3.3.1 Sulfitation

Sulfitation can be achieved with a number of reagents; sodium sulfite and sodium bisulfite are two of the most commonly used. In this thesis, sodium metabisulfite was chosen due to its availability and stability. Sodium bisulfite is frequently chosen in both the literature and in industry however is less stable than the metabisulfite in the solid state. Synthesis of metabisulfite is also simpler as solutions of sodium bisulfite crystallise out as sodium metabisulfite and often bisulfite is sold as a mixture with metabulfite present up to 50%.[180]

As it is produced in the scrubbing process of flue-gases on chemical production plants, sodium metabisulfite could be considered a green reactant to choose. The SO_2 in the gases is reacted with aqueous sodium hydroxide, sometimes sodium carbonate or bicarbonate, then the solution is gently cooled to allow the sodium metabisulfite to crystallise. The product can then be easily collected by filtration.[181–183] Excess SO_2 is needed to prevent formation of sodium sulfite, which is favourable for efficient SO_2 removal.

Mechanism

Sulfitation is the addition of the bisulfite ion across a double bond and can be achieved with many functional groups including internal and terminal alkenes, α-β-unsaturated carbonyls and even aldehydes; the addition results in a saturated sulfonate compound.[184–187] The mechanism of sulfitation was investigated throughout the 1930s and 1950s but the most conclusive study published was in 1975 when Bright *et al.*[185] described in detail a radical mechanism which built on the original idea from Kharasch *et al.*[184] Morton and Landfield[186] proposed an ionic mechanism based on a reaction carried out under nitrogen with a radical inhibitor present, the rate of which was apparently unaffected. This conclusion is questionable because they only "remove(d) *most* of the dissolved oxygen" and as sulfite is so readily autoxidised this would not have been enough to prevent radical formation.[186] The support for the radical mechanism arises from the structure of the product; this reaction gives the anti-Markovnikov addition product as the proton gets added to the most hindered side of the alkene.[184,188] In ionic mechanisms, the proton adds first and hence, adds to the least hindered side of the alkene; this is favourable for two reasons, attack is easier because it is less hindered and the anion which results from this attack is more stable due to the surrounding groups, Scheme 43.[184]
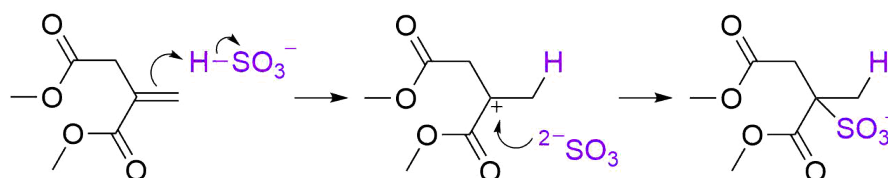
Scheme 43: Possible ionic addition of bisulfite to give the Markovnikov addition product[184]

In a radical mechanism the proton addition is second and so takes place on the most hindered side of the alkene; the first addition, in this case of the sulfite radical, is to the least hindered side of the alkene, again for steric and stabilisation reasons, Scheme 44.[184]

No Markovnikov addition products are seen in the sulfitation of double bonds which strongly suggests the mechanism could not be ionic.[184,185] To back this up, Kharasch *et al.*[184] also observed a dramatic decrease in rate when oxygen was removed and radical inhibitors were employed. Although some product did form, the rate was slow and there was no sign of Markovnikov addition; this still supports the theory of a radical mechanism but suggests that oxygen exclusion had not been stringent enough.
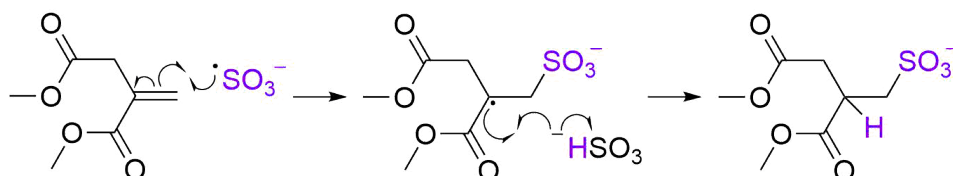
Scheme 44: Radical addition of bisulfite to give the anti-Markovnikov addition product[184]

The mechanism thus proposed was as follows, Scheme 45.[184,185]

Initiation

$$HSO_3^- + In^\bullet \longrightarrow SO_3^{-\bullet} + HIn$$
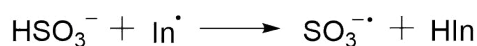
Propagation

Termination

$$2SO_3^{-\bullet} \longrightarrow S_2O_6^{2-}$$
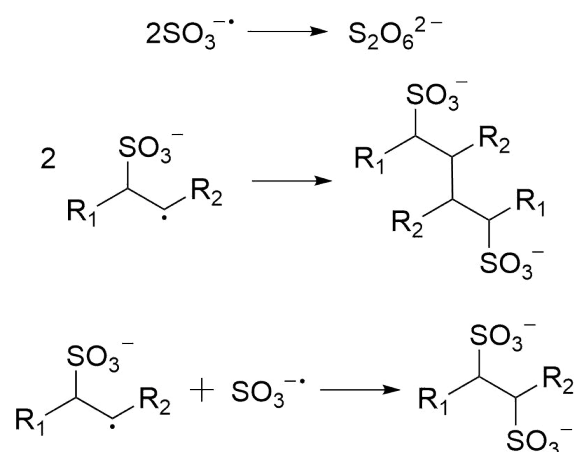
Scheme 45: Radical mechanism for sulfitation of an alkene with bisulfite[184,185]

The mechanism follows the standard three radical mechanism steps, initiation, propagation and

termination. The initiation step occurs easily due to how readily sulfite and bisulfite undergo autoxidation.[189] In this thesis, sodium metabisulfite (SMBS) is used as the sulfitation agent and so the initiation will be discussed with reference to that; the reactions can however also be applied to many other compounds, sodium bisulfite, sodium sulfite etc. The dissociation of the metabisulfite ion in water, Scheme 46, is rapid, and occurs to produce the bisulfite ion and then on to the sulfite ion and a proton.[189] This proton can cause the bisulfite to form sulfur dioxide, which removes the sulfur from solution or causes unwanted side reactions, as discussed later along with the propagation steps. The K_a for the dissociation of bisulfite to sulfite is small (6.4×10^{-8}), so the bisulfite ion will be the major ion present at the pH of the reactions in this thesis.[190]

$$S_2O_5{}^{2-} + H_2O \rightleftharpoons 2HSO_3{}^-$$

$$HSO_3{}^- \rightleftharpoons SO_3{}^{2-}$$

$$HSO_3{}^- + H^+ \rightleftharpoons SO_2 + H_2O$$
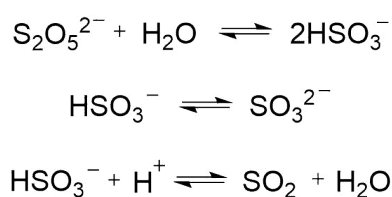
Scheme 46: Dissociation of SMBS in water to bisulfite, sulfite and sulfur dioxide[189]

The autoxidation of the bisulfite ion can proceed through several steps to many products and can be initiated by a range of compounds; molecular oxygen, the OH radical, ozone and peroxides are all capable, as well as NO_x, metals such as iron/manganese, chloride and many organic compounds.[189,191–195] Some examples of these autoxidation steps which are key for the sulfitation initiation are shown below, Scheme 47.[189,191,193,194]

$$HSO_3{}^- + O_2 \longrightarrow SO_3{}^{-\bullet} + O_2{}^{-\bullet} + H^+$$

$$HSO_3{}^- + {}^\bullet OH \longrightarrow SO_3{}^{-\bullet} + H_2O$$

$$HSO_3{}^- + H_2O_2 \longrightarrow SO_3{}^{-\bullet} + H_2O_2{}^{\bullet-} + H^+$$
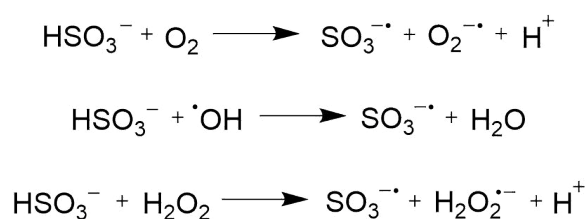
Scheme 47: Example reactions of the autoxidation of bisulfite with molecular oxygen, the hydroxyl radical and hydrogen peroxide[189,191,193,194]

The propagation steps of the mechanism involve the addition of the sulfite radical and the abstraction of a proton by the resultant alkyl radical.[185] The sulfite addition is known to be the rate determining step (RDS) and this can be supported by the study of reaction rates with various alkenes. Firstly, the observation that *cis*-alkenes react faster than *trans*-alkenes, which

is due to the higher reactivity of *cis*-alkenes; this is known as the *cis*-effect, is due to the lower energy ground state of the *trans*-alkenes and would not impact the reaction rate if the RDS was the hydrogen abstraction. The second supporting observation is that alkenes producing a tertiary radical in the addition step react fast than those producing a secondary radical. If the hydrogen abstraction was the RDS, this rate difference should be reversed.[185] The secondary radicals are more reactive due to the reduced inductive effects present, Scheme 48, and hence will abstract a proton faster than the tertiary radicals will. By contrast, the tertiary radicals are more stable, again due to inductive effects, and hence will lead to a faster addition.

secondary   **tertiary**
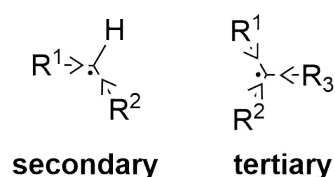
Scheme 48: Stabilisation of secondary and tertiary alkyl radicals by inductive effects

The last supporting evidence is the reaction of bisulfite and styrene.[185] In the absence of oxygen, this reaction leads to a 1:1 adduct of the two reactants and no telomerisation occurs. This shows that the hydrogen abstraction is fast otherwise telomerisation would have time to occur, Scheme 49.
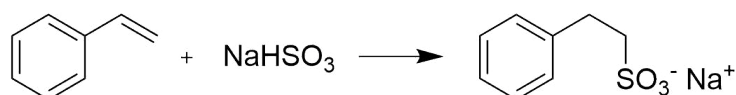
Scheme 49: Addition of sodium bisulfite to styrene forming a 1:1 adduct

With the addition being the RDS, the sulfite radical accumulates and so once above a certain 'lower limit' of concentration, the reaction rate is independant of bisulfite concentration. It is, however dependant, in the first order, on the alkene and also on the concentration of the initiator, Equation (1).[185]

$$\frac{-\mathrm{d[alkene]}}{\mathrm{d}t} = k[\mathrm{alkene}][\mathrm{initiator}]^{1/2} \tag{1}$$

k is the rate constant for the sulfitation of an alkene

This stage in the mechanism is when the sulfitation is most susceptible to side reactions; the alkyl radical can react with other species aside from undergoing proton abstraction. Presence of SO_2

in solution is a primary source of side reactions as it adds to the alkyl radical and forms alkyl sulfonate-sulfinates, Scheme 50. This reaction is common with long straight chain alkenes but is slow to occur when there is any steric hindrance. This is an advantage as the diacids used in this thesis are sterically hindered enough to prevent formation of this unwanted product. Another advantage of the reactions discussed here is that a high temperature is used which also makes production of these side products unfavourable. At temperatures above 80 °C the alkyl radical from the sulfite addition and SO_2 are more thermodynamically stable and hence more favourable than the resulting sulfonate-sulfinate radical formed from the potential SO_2 addition.[185] The sulfitation products were monitored closely but no side reactions were observed.[185]

$$HSO_3^- + H^+ \rightleftharpoons SO_2 + H_2O$$
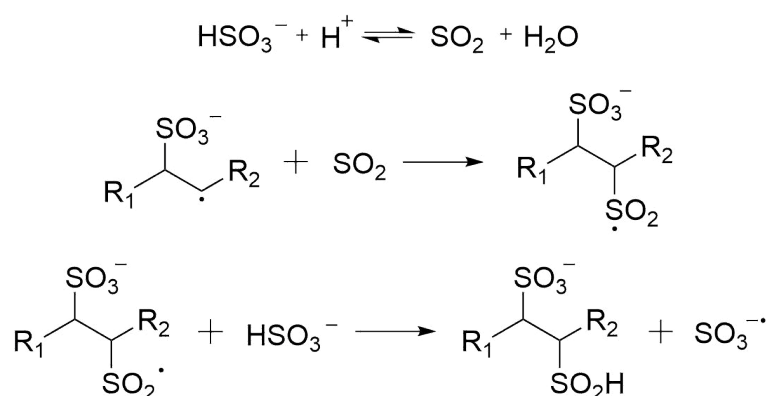
Scheme 50: Formation of side products, alkyl sulfonate-sulfinates, from the addition of SO_2[185]

The termination step can occur between any two radicals present but given that there is significant accumulation of the sulfite radical, two of these are most likely to combine.[185]

3.3.2 Dimethyl Itaconate as a Test Substrate

As dimethyl itaconate (DMIC) is a readily available starting material, it was chosen to be the substrate used in the testing of the sulfitation reaction. The model reaction to produce dimethyl sulfo-methylene-succinate (DMSMS) is shown below, Scheme 51.
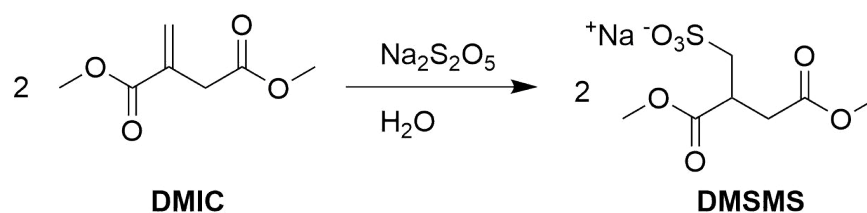
Scheme 51: Sulfitation of DMIC with SMBS to DMSMS

SMBS was used for the sulfitation as previous studies have shown the bisulfite ion to be efficient in the addition to α-β-unsaturated compounds and every mole of SMBS produces two moles of bisulfite, Scheme 52.[185,186,189]

$$S_2O_5{}^{2-} + H_2O \rightleftharpoons 2HSO_3{}^-$$

Scheme 52: Dissociation of the metabisulfite ion to two bisulfite ions in aqueous solution [189]

Optimisation was carried out with DMIC and various factors were investigated; temperature and time were the first two and the reaction was seen to proceed quickly.
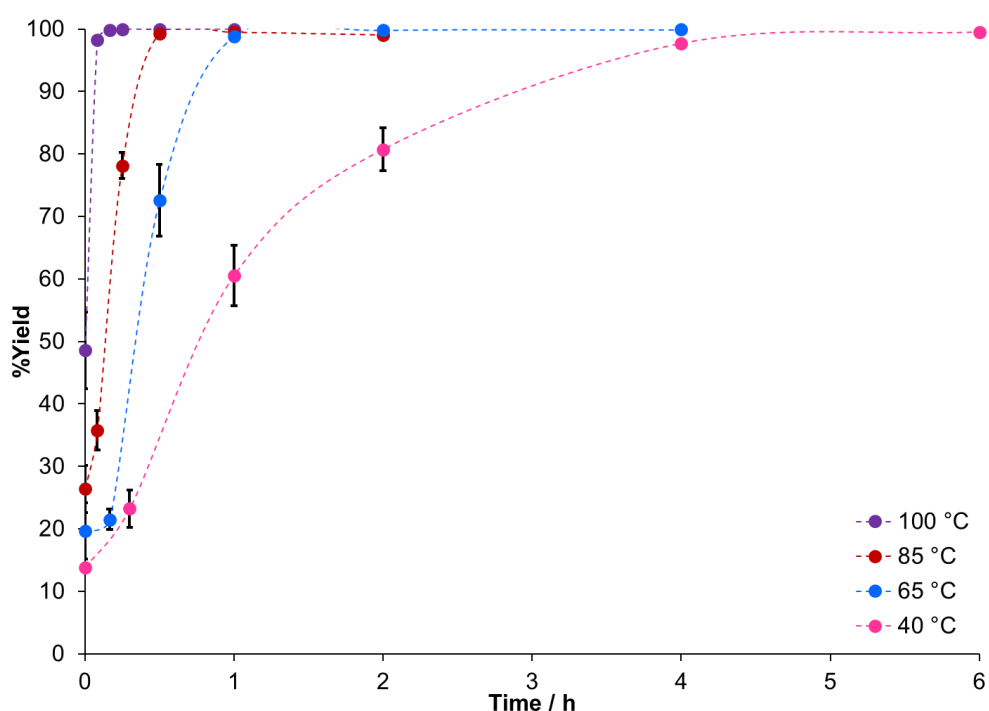
Figure 38: The effect of temperature on the sulfitation of DMIC with 2 mol equiv. SMBS

It can be seen from the results of these tests, Figure 38, that the temperature is the most important factor in these reactions. At 100 °C, complete sulfitation is achieved within 5 mins but a drop of just 15 °C increases this time to 30 mins. This is due to the initiation of the radical mechanism, Scheme 53, the autoxidation of the bisulfite, which slows at low temperatures. The rate equation for the reaction, Equation (1), shows that the rate depends on the concentration of the radical initiator because the RDS in the mechanism is the addition of the sulfite radical to the double bond, Scheme 54.[185] When initiation is fast, accumulation of this radical occurs but if initiation slows, accumulation doesn't occur and hence reaction rate also slows.[185,186]

$$In^\bullet + HSO_3^- \longrightarrow SO_3^{-\bullet} + InH$$
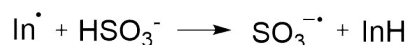
Scheme 53: Initiation of the sulfitation mechanism from the bisulfite ion to the sulfite radical.[185,186] In is the initiator
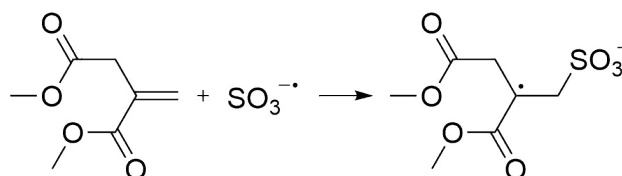
Scheme 54: RDS of the sulfitation of an alkene with bisulfite[185,186]

Two further substrates, with different R groups, Scheme 55, were tested in the sulfitation to gain an indication for the substrate scope of the reaction.
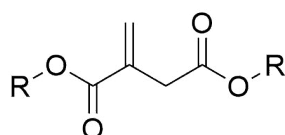
Scheme 55: Structures of itaconate substrates for sulfitation screening. When R = H structure is IA, Me structure is DMIC and Bu structure is dibutyl itaconate (DBIC)

Table 8: Time taken for 100% conversion (by ^{1}H NMR) sulfitation of substrates with various R groups with SMBS

Substrate	Time / mins
IA	5
DMIC	5
DBIC	60

The results show that the longer alkyl chains lead to slower reaction times, Table 8. This decreased reaction rate will be due to the lower solubility of the long alkyl chains in the aqueous reaction medium. *Iso*propyl alcohol (IPA) is necessary with the longer chains to increase solubility however this can also lead to an undesirable separate aqueous phase where the (bi)sulfite ions/radicals are located. In addition, larger proportions of IPA give slower reaction rates and this is postulated to be down to a highly polar reaction transition state which becomes less favourable when in the

alcohol.[185] With increased time and stirring, complete sulfitation was achieved so this reduction in reaction rate was not deemed to be an issue.

3.3.3   Mono-octyl Itaconate

The next step was to optimise the reaction for a substrate that would be useful in surfactant synthesis, in this case MOIC. The model reaction with octanol, shown below, Scheme 56, produces mono-octyl sulfo-methylene-succinate (MOSMS) .
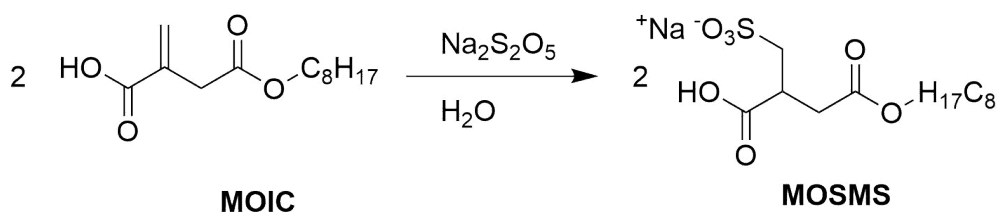
Scheme 56: Sulfitation of MOIC with SMBS to MOSMS

The reaction was trialled and required longer times at higher temperatures to achieve completion with the longer chains Figure 39.
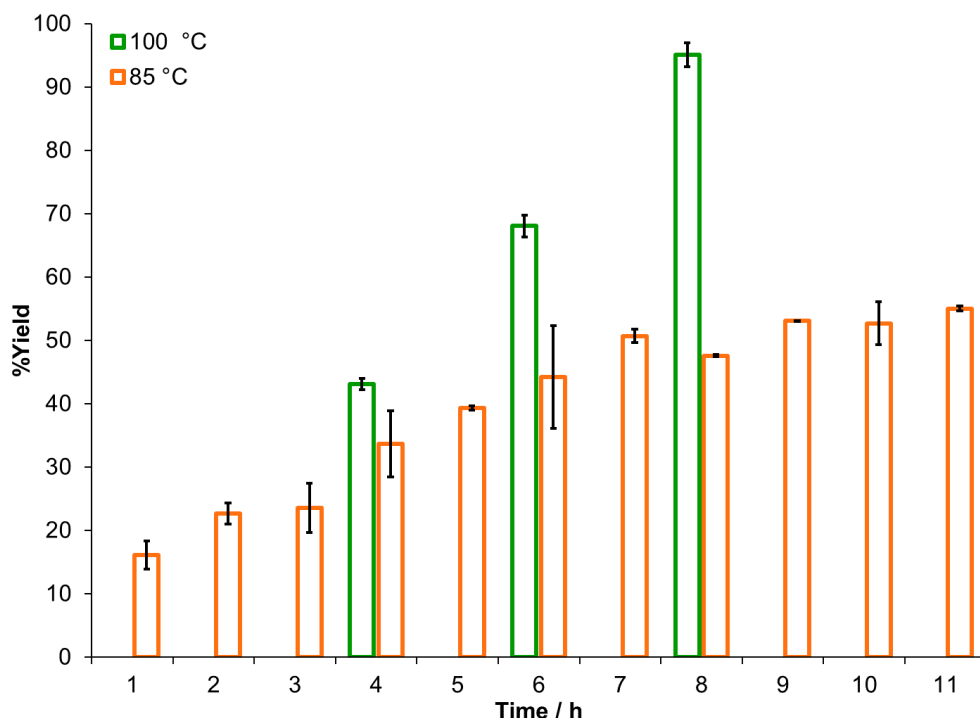
Figure 39: The effect of temperature on the sulfitation of MOIC with 2 mol equiv. SMBS

As previously discussed, the lower water solubility of the longer alkyl chains slows the reaction and

this can be seen clearly in these results. The higher temperature would have been needed to help maintain enough solubility between the two substrates and hence at 85 °C the reaction stalls.[185]

Sulfitation has been shown to be a versatile reaction for addition of a sulfite group onto an α-β-unsaturated carbonyl. The conditions for sulfitation onto compounds with high potential for use as surfactants have been optimised and sulfitation to an example of these compounds has been demonstrated. This reaction was suitable to be coupled with the anhydride ring opening from Section 3.2 and a range of compounds were synthesised and subsequently tested for physical properties which could be used to assess surfactant potential.

3.3.4   Other Mono-alkyl Itaconates

The synthesis of monoalkyl sulfo-methylene-succinates (MASMSs) was developed in this Chapter in order to produce a range of compounds which could be tested for their potential to be utilised as surfactants. Sulfo-succinates are existing surfactants widely used in consumer products[62,134,136,196] and so a range of monoalkyl sulfo-succinates (MASSCs) were also synthesised *via* this method, Scheme 57, to provide a comparison.
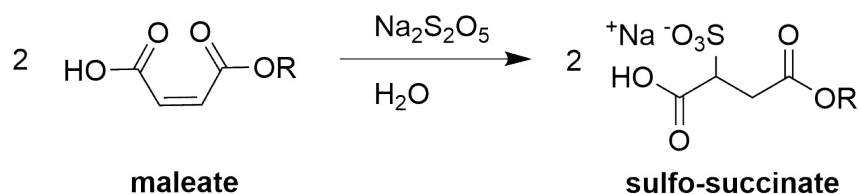
Scheme 57: Sulfo-succinate synthesis *via* the sulfitation of maleate esters

The time taken for sulfitation of the various mono-esters is shown below, Table 9, and as was observed earlier, the longer alkyl chains give slower reaction rates.

Table 9: Range of sulfo-surfactants synthesised for physical surfactants testing and time taken for complete sulfitation with SMBS

			Time / h		
Hydrocarbon chain	hexyl	octyl	decyl	dodecyl	tetradecyl
Methylene-succinate	7	8	12	14	24
Succinate		12	14	20	30

In addition, it was seen that the maleate esters react slower than the itaconates and this is due to the extra steric hindrance of the maleate moeity and the type of radical intermediate produced in the RDS with each compound. Addition of the sulfite radical to the itaconate double bond gives a tertiary radical whereas addition to the maleate moeity produces a secondary radical, Scheme 58, which is not as stable.[185]

a)   **b)**
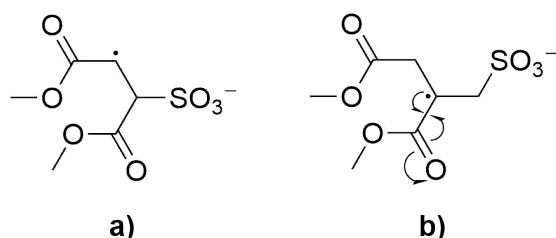
Scheme 58: The different radicals produced in the RDSs of maleate and itaconate sulfitation. a) a succinate radical from a maleate and b) a methylene-succinate radical from an itaconate

The radicals both gain mesomeric stabilisation from the carbonyl group and inductive stabilisation from the surrounding alkyl groups however the secondary radical from the addition to the maleate has only one such group whereas the tertiary itaconate radical has two, Scheme 59.
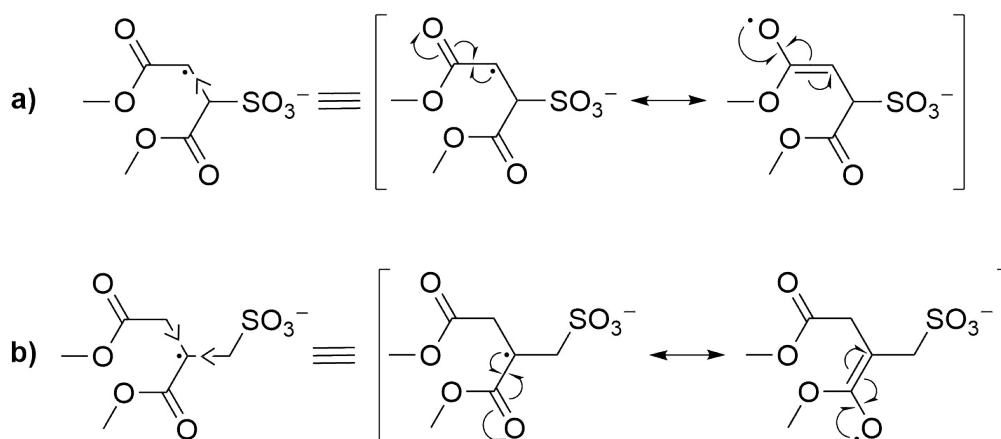
Scheme 59: Stabilisation of the two intermediate radicals from the RDSs of maleate and itaconate ester sulfitation. a) a succinate radical from a maleate and b) a methylene-succinate radical from an itaconate

3.4 Green Metrics

3.4.1 Theory and Calculations

There are a number of metrics available for assessing reactions with the simplest and most widely recognised being yield, conversion and selectivity. These will not be discussed here as they have been extensively examined throughout this thesis. The next set of metrics focuses on the reaction efficiency with respect to the input mass and includes atom economy (AE) and reaction mass efficiency (RME), Equations (2) and (3), respectively.[197]

$$AE = \frac{Molar\,Mass\,of\,Products \; / \; g \; mol^{-1}}{Molar\,Mass\,of\,Reactants \; / \; g \; mol^{-1}} \tag{2}$$

$$RME = \frac{Mass\,Isolated\,Product \; / \; g}{Total\,Mass\,of\,Reactants \; / \; g} \times 100 \tag{3}$$

These two metrics are an indication of how efficient the reaction is in terms of mass; the AE shows the theoretical efficiency and the RME shows this in practice. Comparison of the two gives optimum efficiency (OE), Equation (4), which shows how close to the theoretical maximum efficiency of the reaction, the process is.[197]

$$OE = \frac{RME}{AE} \times 100 \tag{4}$$

The third set of metrics to be considered in this thesis concentrates on how mass intensive the reaction or process is and includes (process) mass intensity (MI/PMI) and waste intensity (WI), Equations (5) and (6), respectively. MI relates to a single reaction step and PMI relates to a whole process.[197]

$$MI/PMI = \frac{Total\,Mass\,Input \; / \; g}{Mass\,of\,Isolated\,Product \; / \; g} \tag{5}$$

$$WI = \frac{Total\,Mass\,of\,Waste \; / \; g}{Total\,Mass\,Input \; / \; g} \tag{6}$$

MI/PMI measures how much mass is needed to produce one unit mass of product and WI measures the mass of waste produced per unit mass needed. Taking these metrics together yields waste

percentage (WP), Equation (7), which indicates the proportion of the MI/PMI that goes directly to waste. [197]

$$WP = \frac{WI}{PI} \times 100 \qquad (7)$$

Assessing all these metrics together, the green credentials of reactions and processes can be quantitatively, not just qualitatively assessed.

3.4.2   Results

The synthesis developed in the Chapter was assessed using the metrics discussed above, section 3.4.1, both as two separate steps and as one whole process. The results are shown below, Table 10.

Table 10: Green metrics for sulfo-methyl-succinate synthesis

Metric	IAnh ring opening	Sulfitation	Complete Process
AE	100.0	100.0	100.0
RME	83.0	90.6	87.4
OE	83.0	90.6	87.4
MI/PMI	10.0	1.67	8.87
WI	0.899	0.402	0.805
WP	9.09	24.0	9.07

These results show that both the individual reaction steps and the process as a whole perform well when evaluated using green metrics. The high AEs show that the reactions that were chosen are as efficient as they could theoretically be, stoichiometrically, and the OEs show that the process has been optimised to within 14% of the ideal.

In terms of the intensity of the process, the results are promising however potential improvements can clearly be observed. The high MI/PMIs arise from the washing stages of the reactions which involve excess organic solvents. Product isolation and purification without the need for these solvents, or reduction in the volume of solvent required, would address this. The WIs, importantly, are low and hence the WPs are also low, showing that the process adheres to the first green

chemistry principle; that it is better to prevent waste than to treat or clean up waste after it is formed.[3]

The high efficiency, low waste output and the low percentage of the intensity that ends up in that waste are all promising results when considering the synthesis for future work and possible scale-up options. The most important next step to consider would be the reduction in hazardous and/toxic chemicals in the various washing stages of the process.

3.5 Conclusions

The aim of this chapter was to identify a synthesis for potential surfactants using bio-based starting materials. With fossil resources for current surfactants at imminent risk of decline and the surfactants industry being one of the largest producer of synthetic organic chemicals, with >12 Mt / annum[58] being produced every year, the motivation behind this research is clear. Many investigations into green surfactants are promising, and progressing along quickly towards industrial scale production and use. Sulfo-succinates are a large portion of the surfactant market however the current options for renewable production are limited; anionic surfactants, especially containing sulfur, have been largely overlooked in terms of environmentally friendly alternatives. IA was identified by the US Department of Energy as a target for research as they deemed it a Top Value Added Chemical from Biomass and this diacid is structurally similar to the building blocks needed for sulfo-succinate synthesis, such as MalA or MalAnh.[26] Due to this similarity, and the fact that it is obtainable from biomass *via* the use of fungi, IA has the potential for use in the synthesis of alternatives and importantly drop in replacements for common sulfo-succinates.[71]

A synthetic route to sulfo-methylene-succinates has been achieved in this Chapter and consists of only two, green and straightforward steps from bio-derivable itaconates. The first washing step is however problematic; the use of hexane and methanol for recrystallisation poses health and flammability risks before taking into account the volume of waste produced in this type of purification. There is potential for the two washing steps to be combined however and complete removal of the washing solvents is achievable, which would improve the green credentials of the synthesis. Importantly, there are no catalysts for either stage, no unusable side products are observed and the only solvents for the synthetic steps are water/IPA. Overall, the synthesis is very clean and simple and holds great potential for scale up and industrial use.

While there are many examples in the literature of similar synthetic routes to sulfo-succinates to the route described in this chapter, none as yet that use SMBS as a the sulfitation agent and only one that utilises the similarity between MalAnh and IAnh. Xu *et al.*[67] synthesised a sulfo-methylene-succinate diester which compliments this work and provides useful comparison in the analysis carried out in Chapter 4. The majority of synthetic routes in the literature use acid catalysts, namely *p*-TSA, and higher temperatures for sulfitation than the route presented here.[67] While this means that there are only small advantages of the route developed in this Chapter in terms of synthetic methods and green credentials, there are large advantages in the synthesis of

novel sulfo-methylene-succinates as drop-in replacements for sulfo-succinates; not only in the end use and application but also in the industrial synthetic process and production.

3.6   Future Work

To complete the study of sulfo-methylene-succinates, dialkyl sulfo-surfactants should be synthesised and tested. Sulfo-methylene-succinates with two hydrophobic chains will have lower CMCs, than the corresponding surfactants with singular chains, due to a lower HLB. This will mean micelle formation is more favourable which will benefit applications such as detergents.[60] Starting with MAIC, standard Fischer esterification would be required, conducted with Dean-Stark apparatus and many solid acid catalysts are proven to be suitable for this transformation, such as clays and zeolites.[101] It has been shown in this chapter that sulfitation onto the DAIC occurs readily and so a range of dialkyl sulfo-methylene-succinates (DASMSs) can be synthesised for testing and comparison with the MASMSs.

It would be of interest to create a range of surfactants with varying properties and hence the use of muconic and aconitic acids should also be investigated. Muconic acid has two central, internal double bonds suitable for sulfitation, meaning that longer chains would need to be used to maintain a suitable CMC value. The great size of the head group with the extra charge density would mean higher electrostatic repulsion in the micelle and potentially much higher CMC values for equivalent surfactants. Aconitic acid is a tri-carboxylic acid and has potential in the synthesis of a wide variety of surfactants. Inclusion of three hydrophobic chains would dramatically increase the CMC of the resulting surfactant due to the difficulty this surfactant would have in folding the tails for micelle formation.[61] Alternatively, an increased number of anionic groups in the head group, by leaving COO^- groups unaltered, coupled with fewer, longer chains would also achieve a high CMC value. The high charge density of the head group would destabilise the micelle through charge repulsion.[61] For both of these acids, their structures would enable the resulting surfactants to remain in solution longer than those investigated here, which would be useful in applications such as foaming agents where the surfactants are needed at the surface of the bubbles for stabilisation.[60]

Chapter 4

Surfactant Testing

4.1 Introduction

4.1.1 Chemistry and Applications

As discussed in the Introduction, section 1.2.1, the useful properties of surfactants derive from their amphiphilic nature and the requirement to minimise the free energy of the system they are in. The wide variety of applications in which surfactants are useful is possible because the behaviour of the surfactants can be modified by altering the concentration of the surfactant.

For applications that merely require a surface tension reduction, such as foaming agents, keeping the concentration low is preferable unless using a surfactant with a high critical micelle concentration (CMC) is practical.[60] Often though, micelles are required as they can collect other hydrophobic groups inside them, as this helps keep the free energy of the system to a minimum.[61,134] In this case, surfactants with low CMCs, are important to reduce the need for a high surfactant concentration, which is undesirable not only for economic reasons but also to protect the consumer who will use the product and the environment into which it will be disposed.

Micelles are useful for many applications of surfactants, as cleaning agents, micelles can collect dirt, such as oils and fats, inside them; as emulsifiers, they can distribute the secondary phase evenly within the bulk solution and stabilise it; and in pharmaceuticals they can act as carriers of active pharmaceutical ingredients (APIs) within the excipient mixture.[60]

4.1.2 Tests

Given the variety of industries in which surfactants are used, and the range of properties on which these applications depends, the measurement of the effectiveness of a surfactant is carried out with a large number of physical tests. Only three will be discussed here in detail because they were used in this Chapter to assess the sulfo-methylene-succinates, CMC, dynamic surface tension and dynamic interfacial tension.[60]

Critical Micelle Concentration

First and foremost, CMC measurement is important because it determines not only the applications in which the surfactant can be used but also the concentration range at which the surfactant is efficient; micelles only form above the CMC and so it follows that detergency is only achieved in the same concentration range.

CMC is calculated from a plot of surface tension over a range of surfactant concentrations. The data for these plots are collected on a tensiometer, in this thesis this was a Krűss force tensiometer K100; there are a number of methods to measure the surface tension but in this case the Wilhelmy plate method was used alongside the Wilhemy equation, Equation (8), and so this will be the only method discussed here. The Wilhelmy plate, usually made of platinum and attached to a tensiometer, is dipped into the surfactant solution to allow the force acting from the liquid onto the plate to be measured by the tensiometer, Figure 40. Using this, and the fact that the liquid will have a contact angle of 0 °, the surface tension is calculated with the Wilhelmy equation.[60]

$$\sigma = \frac{F}{L \times \cos \theta} \tag{8}$$

σ is the surface tension / mN / m
F is the force acting on the Wilhelmy plate / mN
L is the wetted length of the plate / m (equal to the perimeter of the plate)
θ is the contact angle and is 0 °

As the surfactant is dosed in to incrementally increase the concentration, the surface tension is measured, once the system has reached equilibrium after each concentration change. When the data are collated, liner regression analysis on the curves before and after the CMC, Figure 41, followed by simultaneous equation calculations results in the CMC.
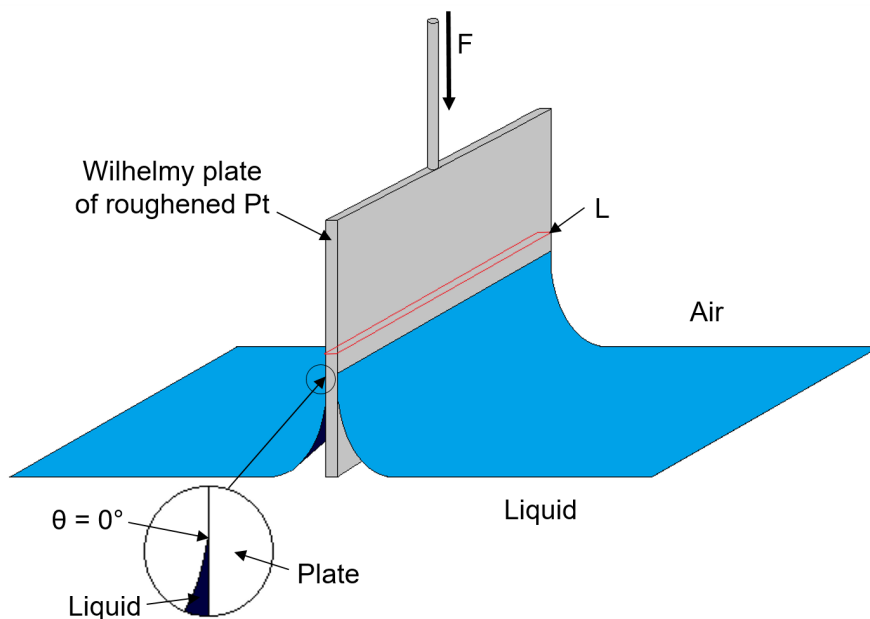
Figure 40: Measurement of surface tension for CMC determination using the Wilhelmy plate method. Where the terms relate to the equation above
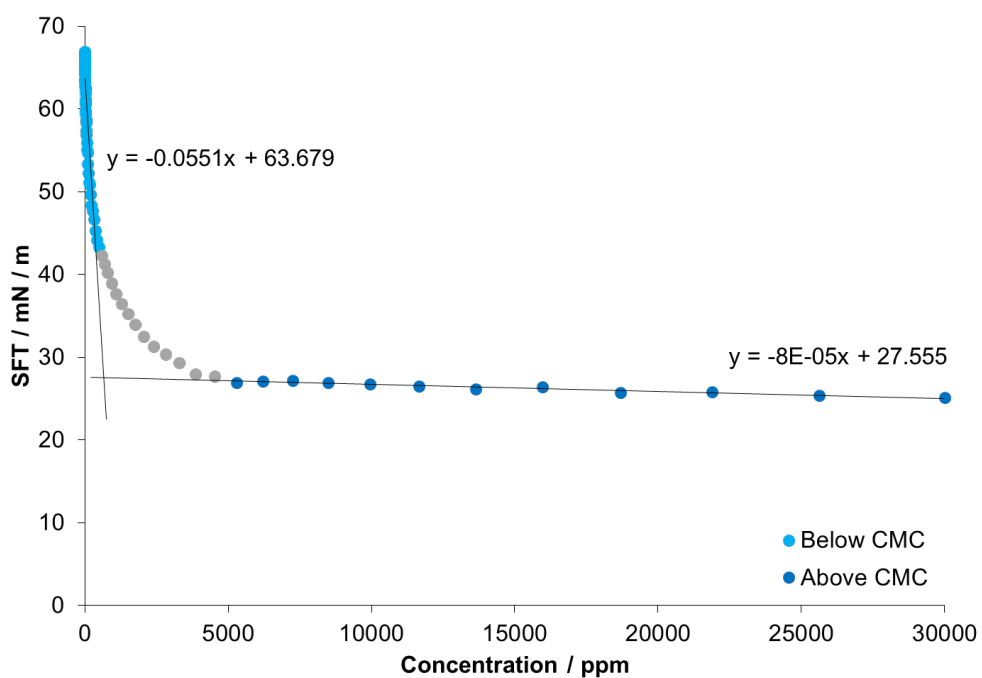
Figure 41: Example calculation of CMC for surfactants. SFT is surface tension

Surface Tension

Surface tension is the second important property to test and must be evaluated in a number of ways, the amount by which the surfactant reduces the surface tension; the capability of surfactants

to reduce the tension at different types of surfaces/interfaces; and the speed with which the surfactant stabilises the surface/interface and reaches equilibrium. The dynamic surface tension of a surfactant is the surface tension at the interface between the surfactant solution, in this case aqueous, and air, at a given time. In this case these measurements were carried out on a Sinterface maximum bubble pressure tensiometer BPA-1S which uses the Young-Laplace equation, Equation (9), to calculate the surface tension at regular intervals over a period of time.

$$\sigma = \frac{(p_{\text{max}} - p_0) \times r}{2} \tag{9}$$

σ is the surface tension / mN / m

p_{max} is the maximum pressure (when the bubble radius equals the capillary radius) / Pa

p_0 is the hydrostatic pressure at a given surface age / Pa

r is the radius of the bubble / m

The instrument flows air from a capillary into the surfactant solution and measures the hydrostatic pressure inside the bubbles produced. The radius of the capillary, which is known, dictates the radius of the bubble hence surface tension at a given surface age can be calculated.

The dynamic interfacial tension is similar to the dynamic surface tension but at the surface between the surfactant solution, in this case again aqueous, and an oil, in this case hexadecane. A Krűss drop volume tensiometer DVT50 was used for the measurement of the dynamic interfacial tension and uses the following equation, Equation (10).

$$\sigma = \frac{V \times \Delta\rho \times g}{\pi \times d} \tag{10}$$

σ is the surface tension / mN m^{-1}

V is the drop volume / cm^3

$\Delta\rho$ is the density difference between the phases / g cm^{-3}

g is the acceleration due to gravity / m s^{-2}

d is the diameter of the capillary / m

The instrument sends a flow of lighter oil into the heavier aqueous surfactant solution, from the bottom upwards. The bubble which consequently forms, is a balance of the upwards force caused by its own weight against the inward interfacial tension which decreases with increasing bubble volume. The interfacial pressure can therefore be calculated if the volume of the bubble is known at the point of bubble detachment; this can be determined using the known oil flow rate and the

bubble or surface age.

Low surface tension is necessary for many applications, one example being laundry detergents. With a high surface tension, the water cannot effectively 'wet' the whole surface of the fabric, especially in small spaces, due to the high contact angle between the water drop and the fabric, Figure 42. This is also know an wettability and benefits any application which requires a surfactant solution to act on a surface; examples include surface cleaners, laundry detergents and soap.[60]

(a) low surface tension and high wettability   **(b)** high surface tension and low wettability
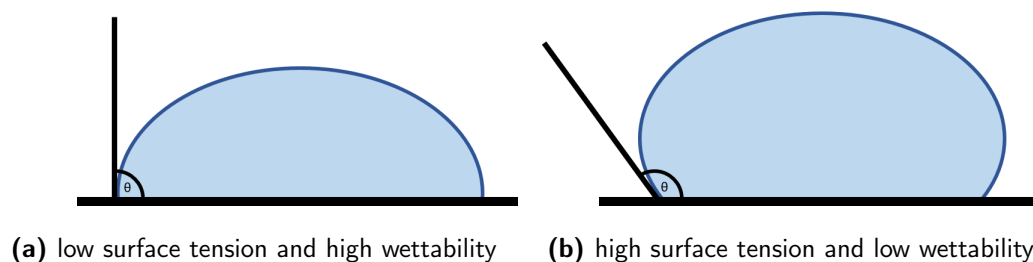
Figure 42: The wettability of solution with different surface tensions; measurable by determining θ, the contact angle between the droplet and the surface[60]

Other important measurements for surfactants are foaming ability, micelle sizing, toxicity and biodegradiability. The foaming ability arises from the stabilisation of air bubbles within the solution by the surfactant and is important for a variety of reasons. In shampoos and soaps, high foam is desirable not only for function but also for consumer satisfaction; in laundry detergents however, low foam is necessary to prevent overflow of water from the washing machine and damage to the appliance occurring. Micelle size and interfacial tension are important for emulsifiers, to ensure the dispersion of phase two throughout phase one is within desired limits, and to ensure the droplets of phase two are stable within phase one respectively. The necessity of low toxicity and high biodegradability does not need any explanation.[60]

4.1.3   Aims of the Chapter

Sulfo-succinates are know to be efficient as well as mild surfactants which is why they have become such an integral part of the surfactant market. This Chapter aimed at evaluating whether the novel molecules synthesised in Chapter 3, firstly, had useful properties for applications as surfactants; and secondly, whether they were comparable to the common sulfo-succinates to enable their consideration as drop-in replacements or greener alternatives.

4.1.4   Compounds of Interest

The synthesis which was developed in the previous chapter was utilised for the production of a range of sulfo-methylene-succinates, the properties of which were to be investigated with the view to evaluating their potential as surfactants. Sulfo-succinates, discussed in the Introduction, are similar existing surfactants widely used in consumer products and so a range of these compounds were also synthesised to provide a comparison.[62,134,136,196] The key difference between the two sets of compounds is the additional $-CH_2$ group present in sulfo-methylene-succinates. This increases the size of the head group and hence reduced charge density; reduces electrostatic interactions, favouring micelle formation but bulkier head groups effect the packing and sizing of micelle. The impact of this difference will be discussed with the results from the testing, further into this Chapter.

The sulfo-methylene-succinates all had the general structure shown in Scheme 60, with chain lengths ranging from C_6--C_{14}.
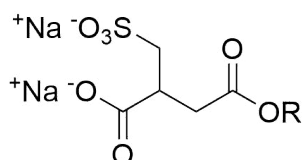
Scheme 60: General structure of the sulfo-methylene-succinates synthesised for evaluation as surfactants. $R = C_6H_{13}$, C_8H_{17}, $C_{10}H_{21}$, $C_{12}H_{25}$ or $C_{14}H_{29}$

The sulfo-succinates synthesised for comparison all had the general structure shown in Scheme 61, with chain lengths ranging from C_8--C_{14}.
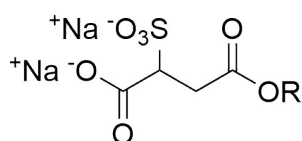
Scheme 61: General structure of the sulfo-succinates synthesised for comparison with the novel surfactants being evaluated. $R = C_8H_{17}$, $C_{10}H_{21}$, $C_{12}H_{25}$ or $C_{14}H_{29}$

4.2   Critical Micelle Concentration

CMC was the first characterisation carried out on the synthesised surfactants as commercial sulfo-succinates have a wide range of CMCs. Also, as explained previously, section 4.1.1, CMC has implications for the surfactant application. The CMCs were determined using the Whilhelmy plate method as described above, section 4.1.2, and the results are shown below, Figure 43.
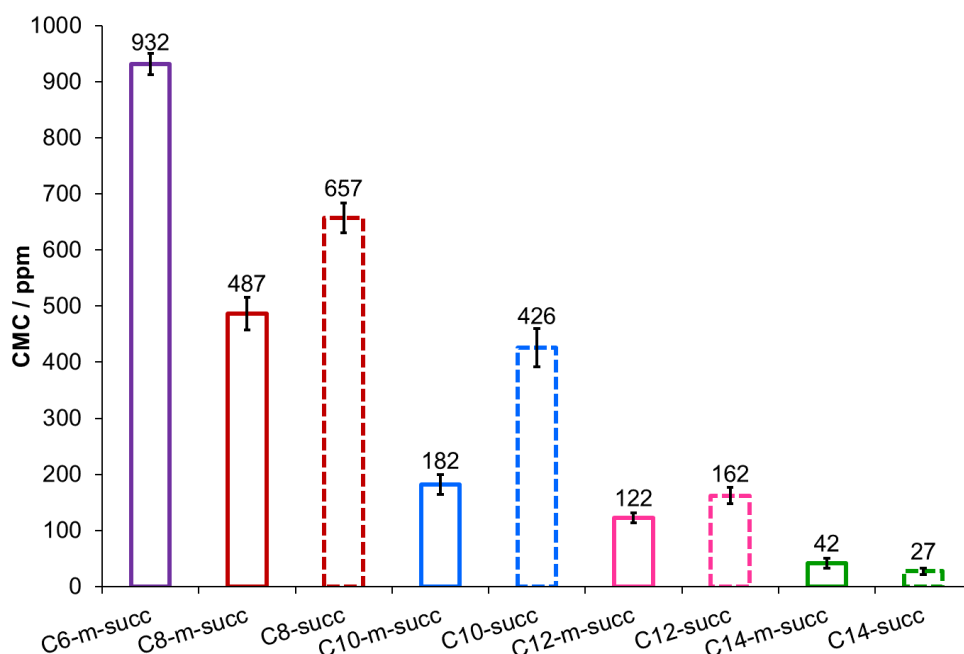
Figure 43:   CMCs of novel sulfo-methylene-succinates (Cx-m-succ) compared to common sulfo-succinates (Cx-succ)

Clear trends for the two sets of surfactants can be seen in the collected data. Both sets of CMCs for the two surfactant ranges decrease steadily with increasing chain length and throughout the entire range, the sulfo-methylene-succinates have lower CMCs than the sulfo-succinate equivalents. The decrease in CMC with increasing chain length is expected as the longer chain will have an increased hydrophobic effect; the entropy will be decreased by a greater amount when the longer chain is in solution as discussed in the Introduction, section 1.2.1.[63,198] This is because there will be more water molecules restricted in movement due to contact with the hydrophobic tail, and therefore the micelle formation will become favourable at lower concentrations.[60]

To explain the lower CMCs of the sulfo-methylene-succinates compared to the sulfo-succinates, the concept of hydrophilic-lipophilic balance (HLB) is necessary. HLB indicates the distribution of hydrophilicity and hydrophobicity of surfactants and as this index increases, the micelle formation

becomes less favourable. Sulfo-methylene-succinates contain an extra $-CH_2$ in the head group which reduces the charge density and hence lowers the HLB relative to the sulfo-succinate equivalent. Micelle formation is therefore more favourable at lower concentrations as there would be less electrostatic interaction between the head groups when in the micelle, to cause destabilisation, Figure 44.[62,63]

(a) low charge density hydrophilic groups   **(b)** high charge density hydrophilic groups
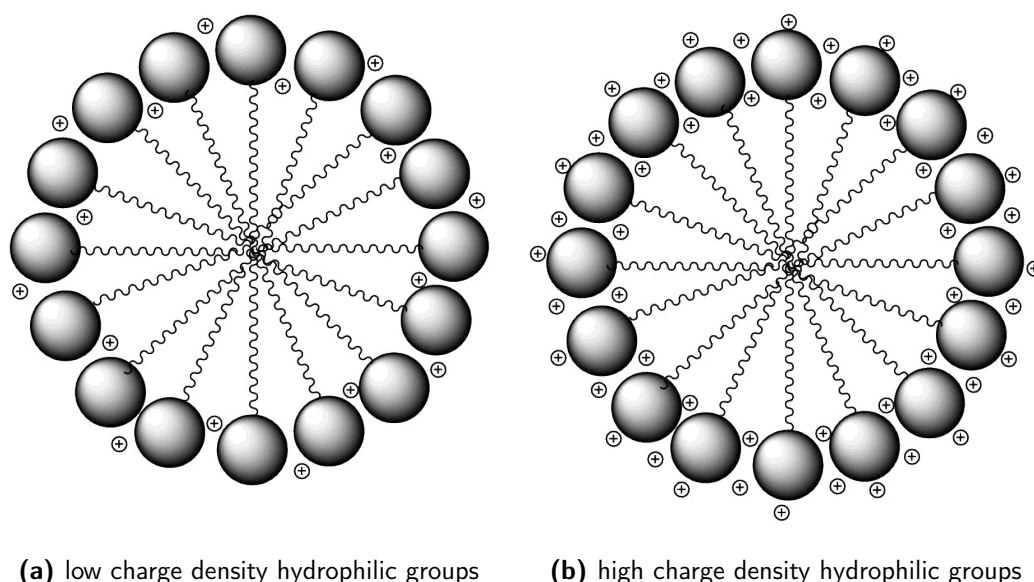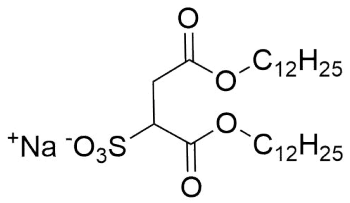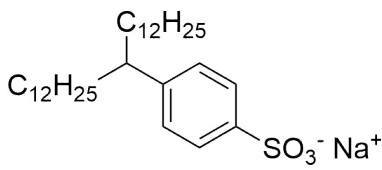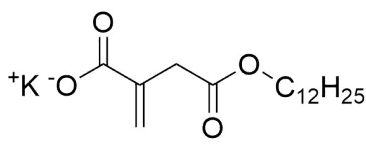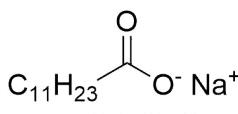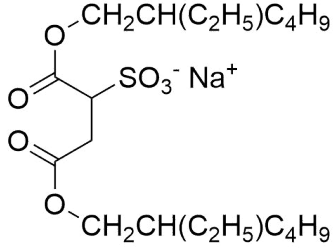
Figure 44: Electrostatic interactions in micelles of surfactants with various charge densities[60]

Commercial sulfo-succinates have a wide range of CMCs and a selection of these are shown in Table 11.[63,71,135,139,142,149,199] Sodium laurate, sodium dioctyl sulfo-succinate (SDOSS) and sodium dodecyl sulfate (SDS) all have much higher CMCs than any of the surfactants investigated in this work. For sodium laurate and SDS this is unsurprising, with only one hydrophobic chain and head groups with high charge densities, the HLBs are high. For SDOSS this is somewhat surprising given the diester nature of this surfactant however this is likely to be due to the awkward folding of the molecule necessary for micelle formation, Scheme 62.[60]
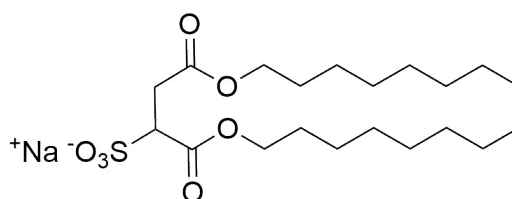
Scheme 62: Folding of an SDOSS molecule to allow for packing into a micelle[60]
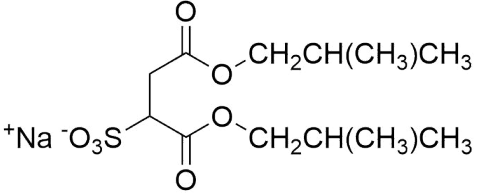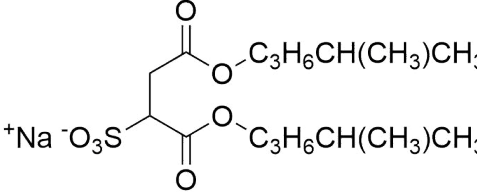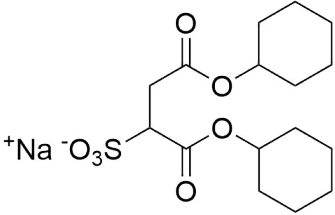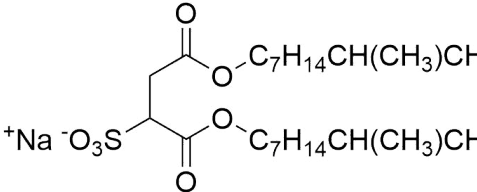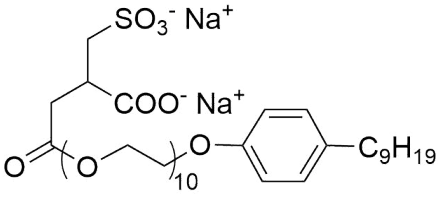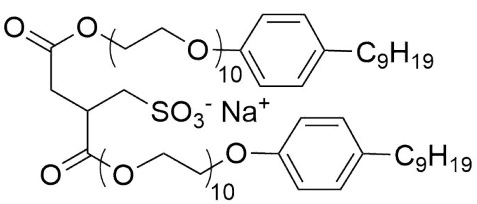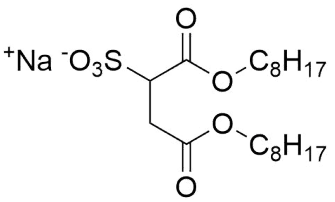
Table 11: CMC values for commercial surfactants similar in structure to sulfo-methylene-succinates

Surfactant	Structure	CMC / ppm
SDOSS		2223 [135]
Sodium dodecyl benzene sulfonate		637 [142]
Potassium dodecyl itaconate		101 [149]
SDS	$H_{25}C_{12}OSO_3^- Na^+$	2192 [71]
Sodium laurate		5602 [63,199]
Aerosol-OT-1 (AOT-1)		445 [139]

Recently this field has progressed in the literature and many surfactants similar to those synthesised in this thesis have been documented. Below are CMC values for similar literature sulfo-succinates as well novel sulfo-methylene-succinates from recent literature, Table 12. [67,134,142]

These literature CMC values all fit with the trends observed in the CMC data obtained in this thesis. It is interesting to note the impact that the highly branched or high volume chains have on the CMC values; even with two long chains, the CMCs are high due to the difficulty in forming micelles which would be able to fit the chains inside them. If the hydrophilic head groups do not occupy enough volume with respect to the volume of the chains then the micelle exterior will have gaps through with water can penetrate, Figure 45. [61] This situation reduces the entropic gain from micelle formation and so it becomes less favourable. [61]

Table 12: CMC values for other sulfo(-methylene)-succinate similar in structure to those synthesised in this thesis

Surfactant	Structure	CMC / ppm
Di-*iso*-butyl sulfo-succinate		17000[134]
Di-*iso*-hexyl sulfo-succinate		1000[134]
Dicyclohexyl sulfo-succinate		3000[134]
Di-*iso*-decyl sulfo-succinate		80[134]
Monononylphenol ethoxylate(10) sulfo-methylene-succinate		27[142]
Dinonylphenol ethoxylate(10) sulfo-methylene-succinate		218[142]
Dioctyl sulfo-methylene-succinate (DOSMS)		183[67]
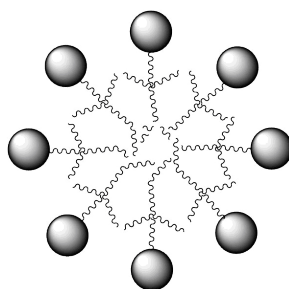
Figure 45: A micelle formed of surfactants with high volume hydrophobic tails[61]

The CMC of the literature DOSMS, 183 ppm, is shown to be comparable in value to one synthesised here, monodecyl sulfo-methylene-succinate (MDSMS) at 182 ppm. These two differently structured surfactants have similar CMC values due to the balance from the lower charge density head groups brings against the lower hydrophobic effect of a smaller hydrophobic group(s). Another similar CMC can be seen when comparing monononylphenol ethoxylate(10) sulfo-methylene-succinate from the literature and mono-tetradecyl sulfo-methylene-succinate (MTDSMS) which both have CMC values of 27 ppm. This literature example contains a hydrophobic phenol ring on the end of the chain which is the cause of a large enough hydrophobic effect to balance out the higher charge density head group. The comparison of these two data sets clearly shows the versatility of surfactants and how easy they are to tailor to the specific application. In addition, the possibility of obtaining a wide range of CMC values with the surfactants synthesised in this thesis has been highlighted.[61,67,142]

From the literature results, it is clear that a full investigation of a range of di-esters as well as investigation of di-esters with larger hydrophilic head groups, such as obtainable through the use of muconic and aconitic acids, would be interesting. The literature surfactants include examples with CMC values higher by a factor of 19, than of those tested in this Chapter. For applications where surface acitivity is desired but micelles are not, high CMC values are important and the comparison discussed here has highlighted this potential for improvement in the range of surfactants synthesised.

These CMCs for the literature sulfo-methylene-succinates were found to be over a wide range but all relatively low with respect to some commercial surfactants. This is positive as there are many benefits of surfactants with a lower CMC, when considering them for applications such as detergency.[134] The main advantage is that the lower the CMC, the lower the concentration of surfactant needed for effective detergency in consumer products; this reduces environmental

concerns in the end of life stage of the product.[58] Also, as mentioned previously, this is a positive potential area for expansion of range of surfactants investigated within this thesis.

4.3   Dynamic Surface/Interfacial Tension

All measurements were taken at the same concentration, 5000 ppm, which is not only above the CMC of every surfactant but high enough above the CMC for there to be a significant concentration of micelles in each case alongside the free surfactants that will be in equilibrium with the surfactants in the micelles. The absolute concentration is a more important factor to consider than the ratio of the solution concentration to the CMC of the surfactnat because the concentration of the micelles and free surfactants in the bulk liquid will directly impact the surface/interfacial tension value as well as the equilibration time.

4.3.1   Dynamic Surface Tension

The dynamic surface tension was important to measure because the surface tension is important for applications such as foaming agents where the surface of the bubbles within the foam need stabilisation gained from surfactants. It is also important for equilibrium to be reached quickly, for example to ensure the foam is stabilised quickly.[60] The dynamic surface tension was determined using a maximum bubble tensiometer, as described previously, section 4.1.2, and the results for both surfactant sets are discussed below.

It can be clearly seen that the sulfo-methylene-succinates not only reduce the surface tension by a greater amount, Figure 46, than the sulfo-succinates, Figure 47, but they also stabilise the surface quicker, Figures 48 and 49. These results suggest that the sulfo-methylene-succinate are more efficient surfactants than the sulfo-succinates.[63]

Sulfo-methylene-succinates, with their lower HLB, will be less stable in the bulk solution and so will localise at the surface and hence reduce the surface tension faster than their sulfo-succinate equivalents. In addition, the sulfo-methylene-succinate head group, with its lower charge density, will have weaker interactions with the surrounding water molecules which will reduce the surface tension further than the sulfo-succinate equivalents.[60]
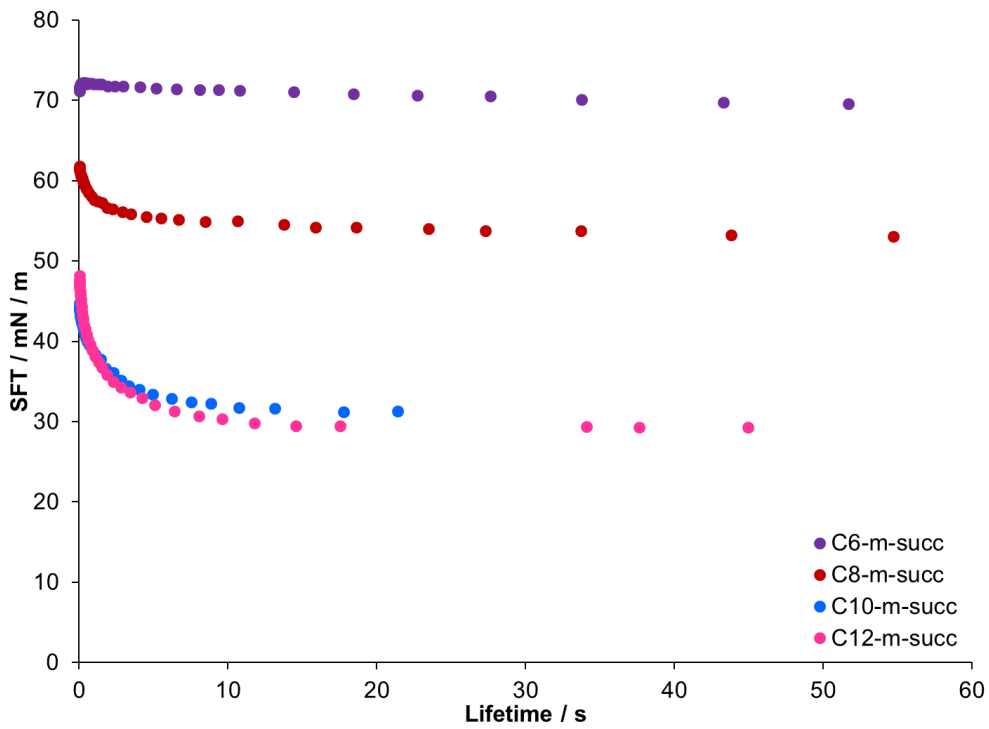
Figure 46: Reduction of surface tension at the air-water interface by sulfo-methylene-succinates. SFT is surface tension
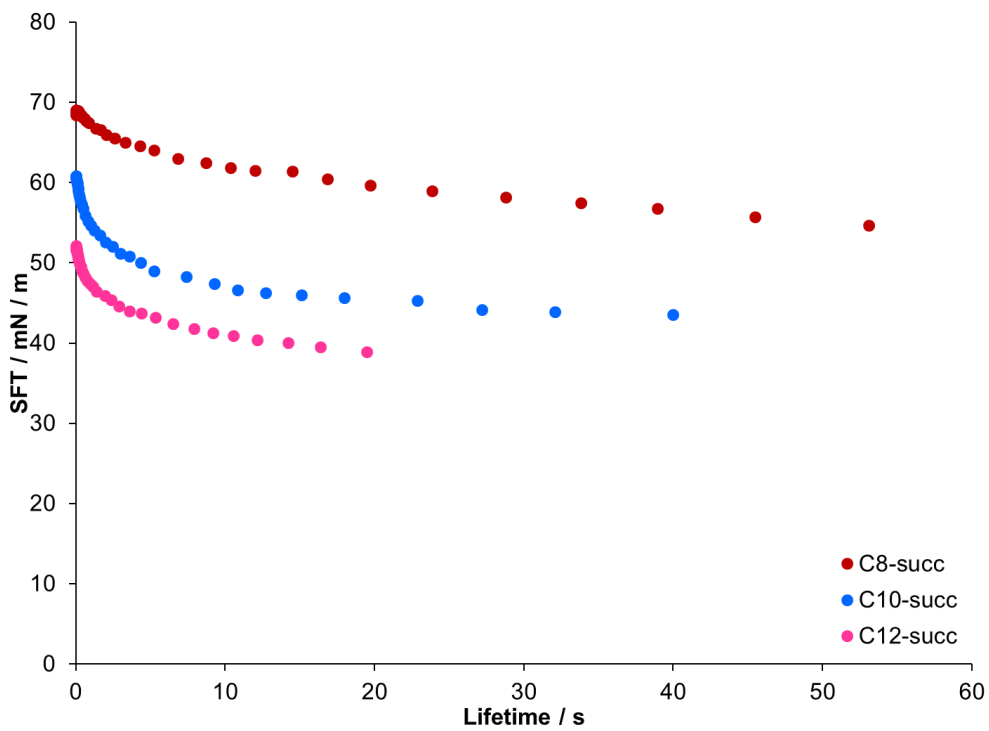
Figure 47: Reduction of surface tension at the air-water interface by sulfo-succinates. SFT is surface tension
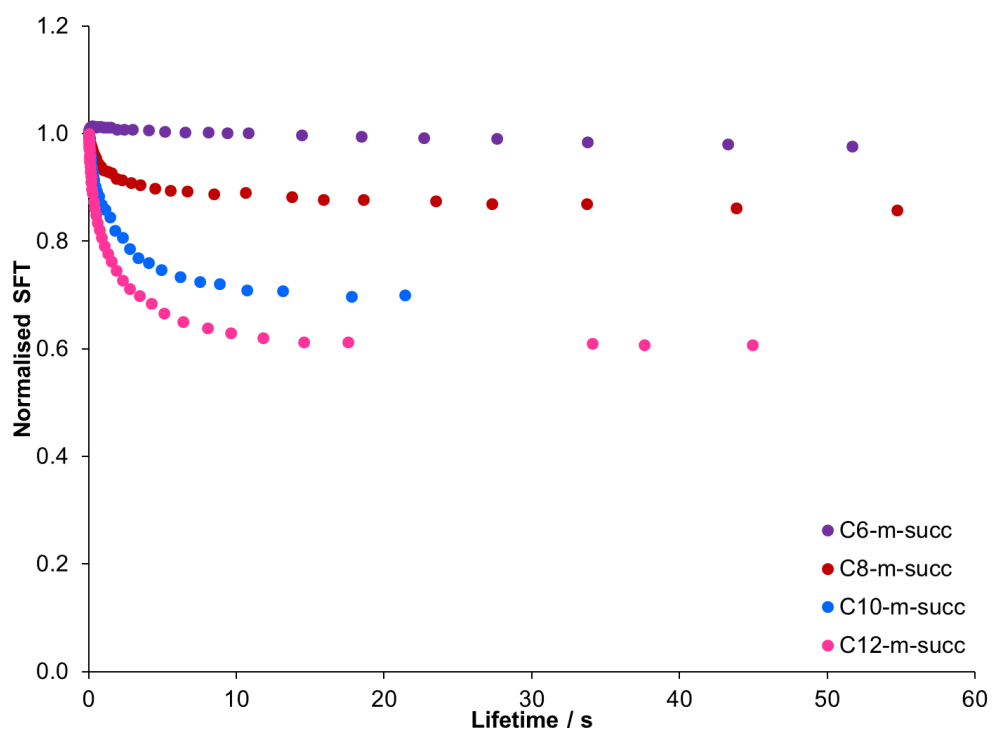
Figure 48: Normalised surface tension reduction at the air-water interface by sulfo-methylene-succinates. SFT is surface tension
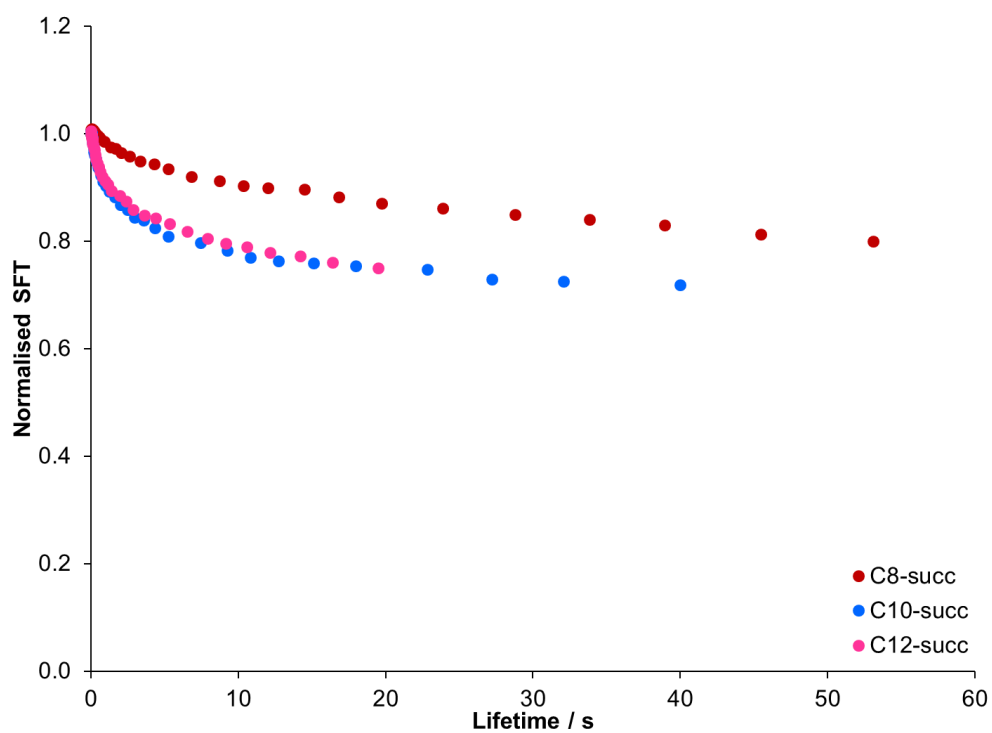
Figure 49: Normalised surface tension reduction at the air-water interface by sulfo-surfactants. SFT is surface tension

4.3.2   Dynamic Interfacial Tension

As emulsifiers, surfactants are required to stabilise droplets of a secondary phase within the main solution phase and hence it is important for this application that they have high interfacial activity. As with surface tension, the speed with which the surfactants can stabilise the interface is as important as the degree of reduction in interfacial tension they can achieve.[60] The dynamic interfacial tension was measured using a drop volume tensiometer, as described in section 4.1.2, and the results obtained for the two sets of surfactants are discussed below.
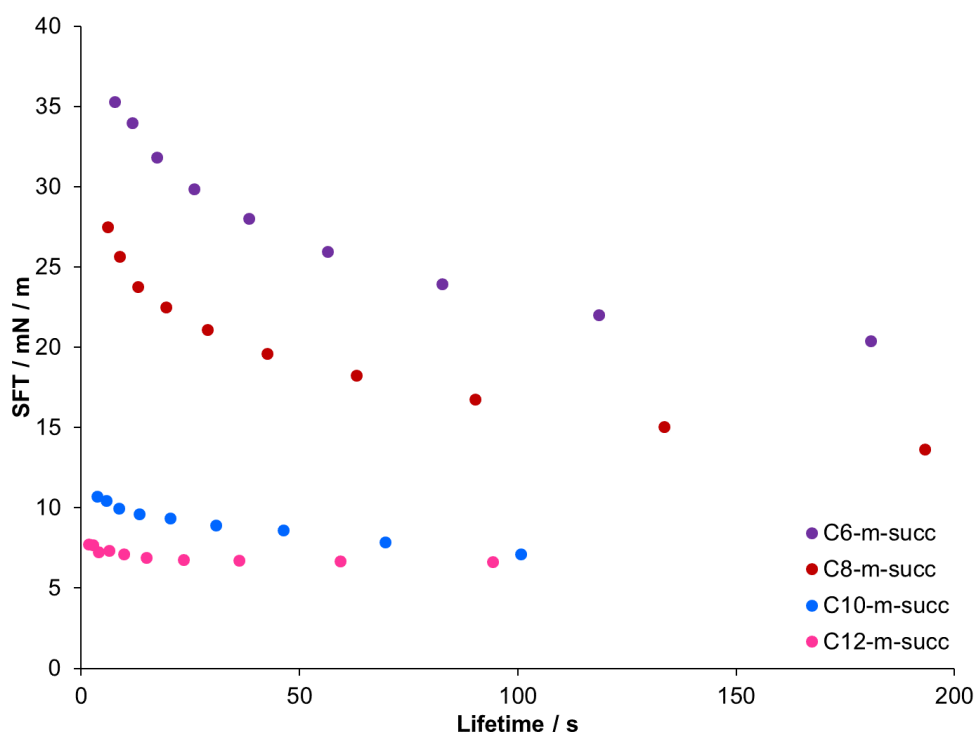
Figure   50:   Reduction   of   interfacial   tension   at   the   oil-water   interface   by sulfo-methylene-succinates. SFT is surface tension

It is clear from these results, Figures 50 and 51, that the same trends in interfacial tension are observed as were evident in the surface tension results. The sulfo-methylene-succinates reduce the interfacial tension to a greater extent than the sulfo-succinates do for the same length chain. It can also be seen that equilibrium in interfacial tension is reached quicker by the sulfo-methylene-succinates than by the sulfo-succinates. This difference in activity will be due to the lower HLB of the sulfo-methylene-succinates compared to the sulfo-succinates, which is due to the lower charge density in the head group of the surfactants.[60] This reasoning is the same as was applied for the surface tension results earlier in this Section.
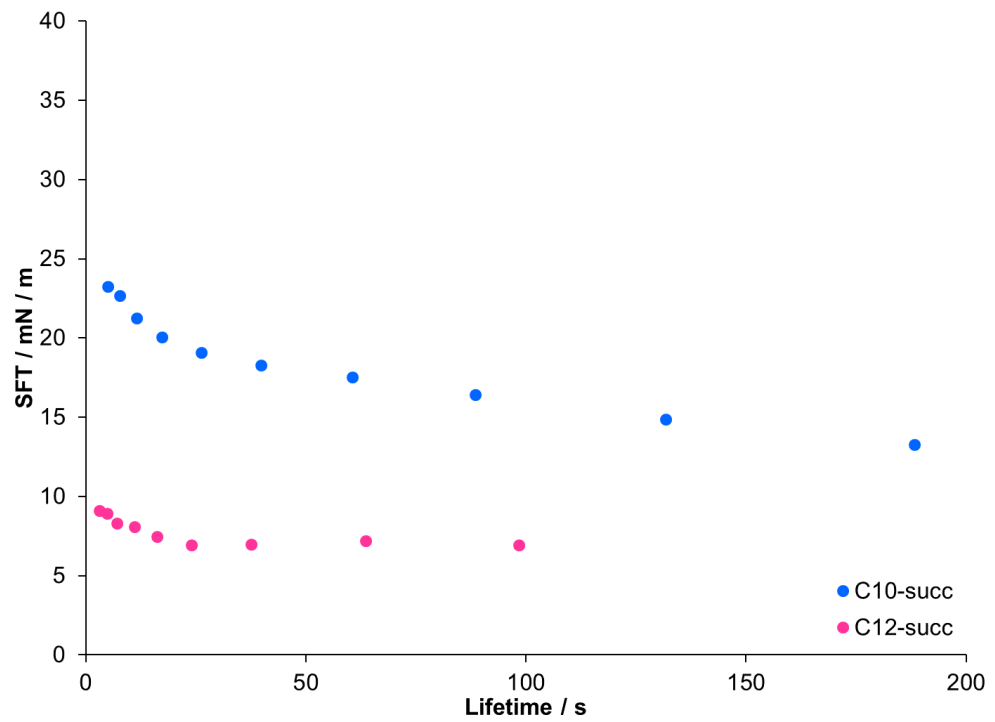
Figure 51: Reduction of interfacial tension at the oil-water interface by sulfo-succinates. SFT is surface tension

4.4   Conclusions

The surfactant industry is a large, primarily petroleum based industry, hence, the need and opportunity for increasing its environmental and sustainability credentials are huge.[58] Aside from the obvious, the problems associated with fossil derived surfactants are generally toxicity and biodegradability; the problems with bio-derived surfactants are generally efficiency and production costs.[58] Finding a renewable alternative to an existing surfactant which is already proven to be not only of low toxicity and mild on the consumer but also highly biodegradable would seem the easiest of solutions.[58,134,136] There are currently limited renewable alternatives to sulfur-based surfactants available at the industrial scale and with sodium metabisulfite (SMBS) obtainable as a by-product of industrial sulfur dioxide scrubbing, the bio-derived sulfo-methylene-succinates evaluated in this chapter appear promising.[58,181–183]

The results presented cover only a few of the properties that the sulfo-methylene-succinates would need to succeed as commercial surfactants however the indication is that further investigations would be worth carrying out. Two assessments were made, CMC, the minimum concentration needed for detergency action; and surface/interfacial tension, an indicator of the efficiency of action of the compounds as surfactants. It was shown that the sulfo-methylene-succinates exhibit the ability to reduce surface tension quicker and more effectively than sulfo-succinates and this stands them in good stead for commercial applications. Additionally, these novel surfactants showed low CMCs which will enable their use at lower concentrations in any consumer products they were included in, compared to the existing options, with no loss of efficiency. This would reduce the environmental impact of the products using sulfo-methylene-succinates in place of sulfo-succinates which already have a head-start as biodegradable and low toxicity compounds.

The similarity in structure and properties to the exisiting sulfo-succinates that the surfactants tested in this chapter exhibit would enable these new compounds to use the high popularity and esteem of the sulfo-succinates to facilitate their widespread production and application. This good publicity, along with the favourable results presented here, means the sulfo-methylene-succinates could have the potential to replace sulfo-succinates as one of the most common surfactants in detergents and cosmetics.

4.5   Future Work

The results obtained in this Chapter show that the sulfo-methylene-succinates have potential for use as industrial surfactants. Therefore, more testing should be carried out to further assess their properties and the potential applications they could be utilised for.

Firstly, testing to determine a wider range of physical properties of the surfactants should be carried out. Micelle sizing is important for any application which relies upon the solubilisation of a substrate within the micelle; the relative sizes of the micelle and the substrate must be compatible. These applications cover not only detergents and emulsifiers but also drug delivery systems and micelle templated polymerisations. The wettability or contact angle is related to surface activity and is important for applications which rely on the action of the surfactant containing solution on a surface; the smaller the contact angle between the solution droplet and the surface then the larger the area of the surface which is in contact with the solution, which is beneficial. The foaming ability of surfactants is important in personal care products and household cleaners. This list of important surfactant properties is not exhaustive but focusses on the most important next steps for this investigation.[60]

There are also many properties of these surfactants which are important for all of the potential industrial applications of sulfo-methylene-succinates and these should be investigated in further stages of testing. Low toxicity and high bio-compatability of the surfactants is a priority as exposure to consumers, for example in cosmetics or even detergents, will be high.[136] In addition, biodegradability, eco-toxicity and other environmental factors such as the eutrophication potential will need to be assessed as the volume of surfactant which is disposed into the drains and consequently into the environment by the consumers will also be high.[59] Sulfo-succinates have reputations of being mild yet effective as well as inexpensive so it is important that the same properties are exhibited by the sulfo-methylene-succinates.[134]

Chapter 5

Paper Pyrolysis

5.1 Introduction

Biomass processing is carried out using many techniques, gasification, the heating of biomass at temperatures high enough, typically >800 °C, to transform it into gaseous products;[200] combustion or incineration for energy production;[1,201] and fermentation, treatment with bacteria or yeast to produce chemicals;[1,54] but one of the most increasingly popular techniques is pyrolysis. Pyrolysis is thermal decomposition of a material and can be tailored to produce gaseous, liquid and solid products. Heating rate is an important factor in the products of pyrolysis; slow pyrolysis results in more solid, char based products whereas fast pyrolysis yields more bio-oil based products and hence is becoming more prevalent in the literature for biomass processing.[202]

Pyrolysis is carried out in a variety of ways, depending on the products desired but the popularity of microwave pyrolysis is increasing because there are a few distinct advantages to using microwaves. Conventional pyrolysis is carried out at high temperatures, 300–700 °C, but microwave pyrolysis can be carried out at lower temperatures 100–200 °C.[50,51,203] It has been shown that microwaves interact with biomass, such as cellulose, and induce structural changes which allow for better breakdown at lower temperatures; the hydrogen bonding network of the cellulose breaks down in both the cystalline and amorphous regions and hence the cellulose chains are more able to absorb the microwave energy as they have functional groups and side chains which are free to rotate, Figure 52.[16,57,204]
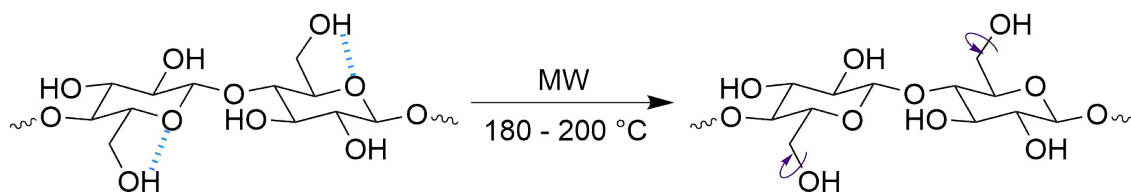
Figure 52: The interaction of microwaves with cellulose inducing activation of certain functional groups[16]

In addition, the energy consumption of biomass processing is reduced when microwave pyrolysis is utilised. The reason is not just because a lower temperature is needed but also because heating is more efficient and there are fewer requirements for biomass pre-treatment. Firstly because, with uniform heating that does not rely on conduction, the particle size of the biomass does not need to be as small as for conventional pyrolysis, and secondly because drying of biomass is unnecessary as the microwaves directly heat water; it is a small polar molecule and hence has a high dielectric constant.[51,52,57]

For the purpose of this thesis, given the composition of the biomass in question, all discussion will refer only to cellulose pyrolysis.

5.1.1 Pyrolysis Mechanism

Levoglucosan Formation

The mechanism of cellulose pyrolysis, by the nature of the process, is complex and difficult to investigate. There are many competing theories as to the exact reactions that occur in the breakdown of cellulose but it is widely accepted that cellulose depolymerises at the glycosidic bonds between the monomers.[203] The Broido-Shafizadeh model is one of the first pyrolysis mechanisms to be presented in the literature and comprises three steps, cellulose activation, followed by two routes, to either volatiles or char.[202,205,206] This general scheme is largely still supported however it is now widely believed that the first step is cellulose breakdown to levoglucosan (1,6-β-D-glucopyranose) (LG); there is substantial evidence for the primary formation of LG as high yields of pure LG are easy to observe at the start of pyrolysis.[17,77,207–212] Mechanisms for the LG formation from

cellulose that have been proposed and scrutinised in the recent literature fall into three camps, a concerted mechanism, a radical mechanism and an ionic mechanism.[17,209]

A variety of radical mechanisms, such as the example presented below, have been suggested; this type of mechanism is the least likely of the three main suggestions.[213–217] Aside from the lack of supporting evidence presented in the literature for radical involvement and the limited provision of any detail, the mechanism involves many steps, which seems unlikely to occur with such predictability given the complexity of the system in question and the high reactivity of the radicals. The high yields of LG that are obtainable from cellulose pyrolysis, mean that the radicals would have to almost exclusively follow a multistep pathway to form LG, Scheme 63, in preference to any number of alternative reactions.[17,210,213,218]
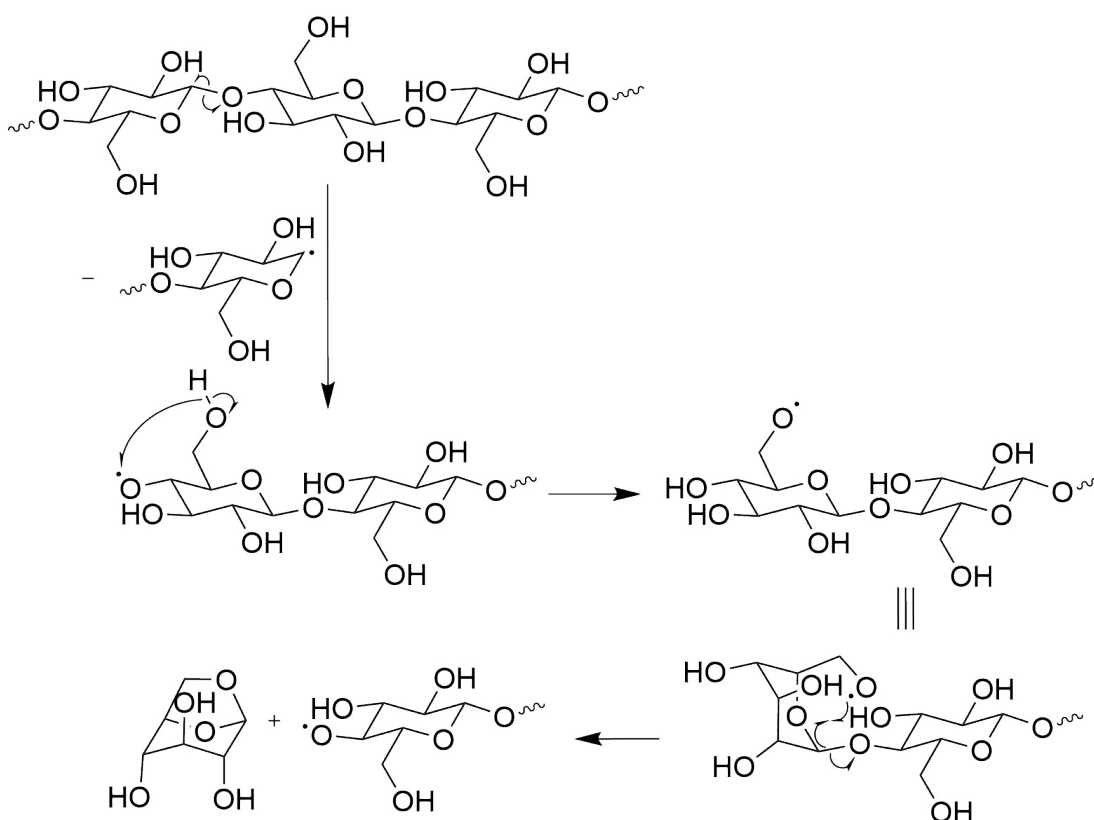
Scheme 63: Example mechanism of a radical based pathway from cellulose to LG[213]

The other two mechanisms do not have much to tell between them, they proceed *via* very similar pathways, with sequential heterolytic cleavage of glycosidic bonds. The ionic mechanism as proposed by Ponder *et al.*[212] is shown below, Scheme 64, and they suggested the glycosidic bonds break at similar rates given the temperatures involved in pyrolysis, meaning the LG forms with limited side products. In addition, at these temperatures, >250 °C, the LG is immediately

volatilised and hence removed from the remaining chains, preventing LG breakdown.[212]

In the concerted mechanism, the anhydro ring of the LG forms as the glycosidic bond breaks and hence the intermediates have no charges. The mechanism, shown below in Scheme 65, was proposed by Mayes and Broadbelt[17] and was based upon theoretical calculations carried out on a variety of mechanisms. The experimental evidence for differentiating between the ionic and the concerted mechanisms is difficult to obtain due to the complexity of the system involved. The two mechanisms are very similar and any intermediates cannot be isolated due to the speed of the reactions taking place.[17,209]
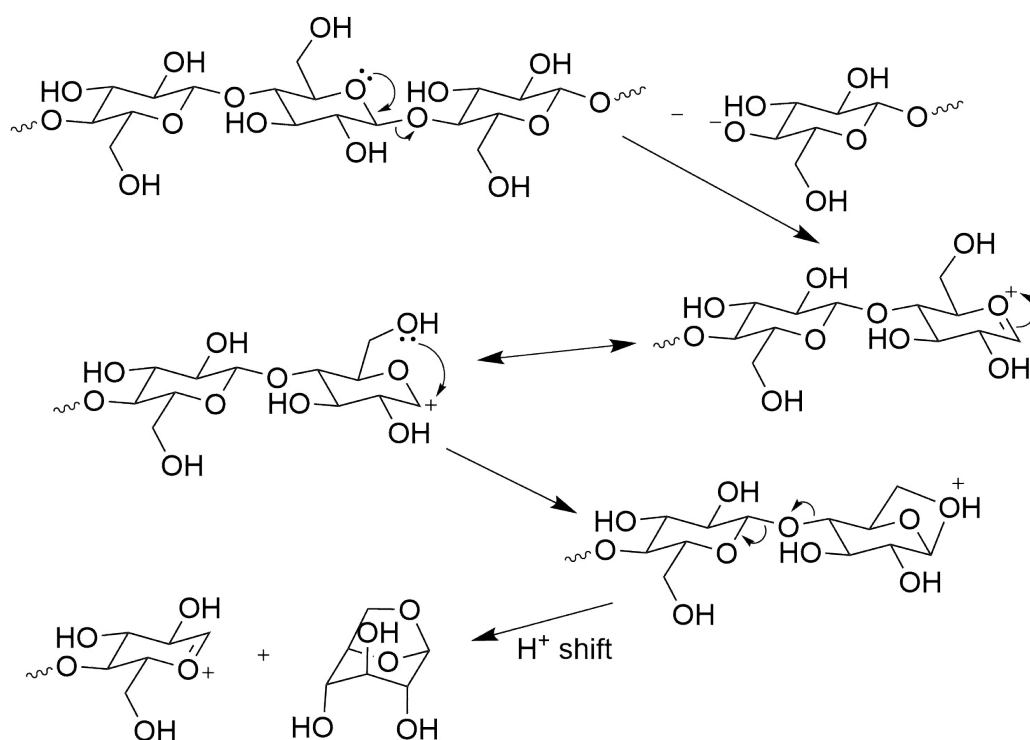
Scheme 64: Mechanism of proposed ionic pathway from cellulose to LG[212]

Mayes and Broadbelt[17] calculated the activation energies for the three mechanisms and these clearly indicate the most favourable reaction pathway is the concerted mechanism. The three theoretical values were 94.5–97.8, 78.6–167.2 and 53.5–55.2 kcal mol^{-1} for the respective mechanism pathways, radical, ionic and concerted.[17] The value for the ionic mechanism varied by a substantial amount due to the electrostatic interactions which were designed to simulate real cellulose pyrolysis. In addition to the concerted mechanism having the lowest theoretical activation energy, this value was close to the experimental value determined by Antal Jr *et al.*[219] of 54.5 kcal mol^{-1}. The experimental value was measured for pyrolytic weight loss but as the weight loss is due to the first

pyrolysis step, which is the formation and evaporation of LG, these two values can be considered comparable. [17]

While the investigations carried out by Mayes and Broadbelt [17] are not conclusive, they indicate that the concerted mechanism is the most probable pathway for the formation of LG from cellulose during pyrolysis. This mechanism only accounts for the first reaction in pyrolysis which is only a small part and more work is needed on the more complex secondary reactions that occur during the latter stages; not least to determine conclusively whether they are indeed secondary.
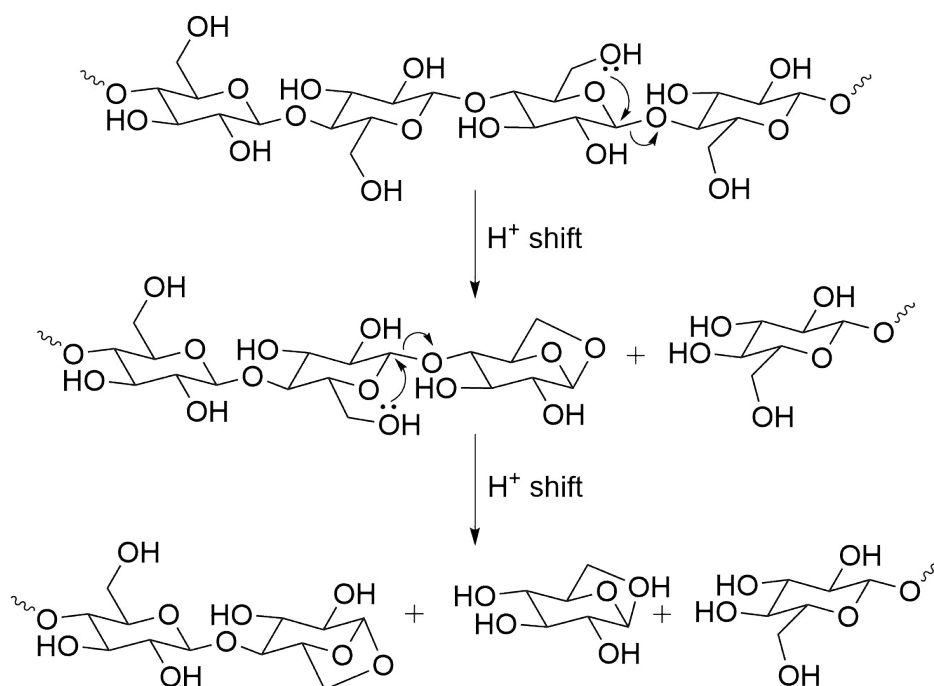
Scheme 65: Mechanism of proposed concerted pathway from cellulose to LG [17]

Secondary Reactions

Assuming LG is the primary pyrolysis product, many subsequent products form and the mechanisms of their formation are unclear. There are many investigations into these mechanisms in the literature and there is dispute as to whether all of these reactions start with LG or some originate from oligomers of LG, Figure 53. [210,211,218,220–223] Due to the fast rate that pyrolysis mechanisms occur at, isolation of products from individual stages of the process is difficult.

Many investigations into the pyrolysis of pure LG have been carried out to determine whether it breaks down to the secondary pyrolysis products but the results have been interpreted in a number of ways. When pyrolysed alone, LG can be quantitatively recovered, but when cellulose or other

pyrolysis products such as vapours or char are introduced, recovery of LG drops significantly.[210] This has been used as evidence to show both that, LG does not break down to the other pyrolysis products, only cellulose does; but also that cellulose and/or char, catalyse the degradation of LG and hence none of these products form with LG alone.[208,210,211,222,224]

a) Cellulose ⟶ Levoglucosan ⟶ LMW species, char and volatiles

b) Cellulose ⟶ Levoglucosan ⇌ Oligosaccharides ⟶ LMW species, char and volatiles
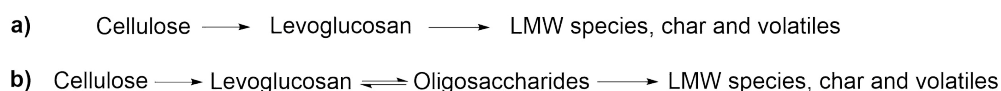
Figure 53: Competing theories of formation of other pyrolysis products from LG or oligosaccharides. a) is breakdown directly of LG and b) is the breakdown of LG *via* formation of oligosaccharides[210,220,222]

Additionally, it has been shown that pyrolysis of pure LG forms oligomers of varying sizes dependant on the temperature and also that this process is reversible.[200] The results of this investigation show that the amounts of oligosaccharides and polysaccharides, formed from the LG, decrease as volatiles and char begin to appear; LG was shown not to decrease at this point. This research appears to prove that the degradation occurs *via* the oligomerisation of LG however it does not disprove the catalysis of LG breakdown by char.

On the other hand, if the oligomers can breakdown to form the alternative pyrolysis products, and do not just depolymerise to re-form LG, then it follows that cellulose can too. If that is the case, then this evidence suggests the whole theory under discussion is incorrect; cellulose pyrolysis does not only produce LG in the first step.

The reports are conflicting and each case presents evidence which strongly supports its own proposed theory. If the LG forms from subsequent glycosidic bond cleavage of LG as Mayes and Broadbelt[17] have concluded, then it follows that the secondary reaction products are from LG. If the LG forms oligomers at high temperatures which then form the volatiles and char as Hosoya *et al.*[200] conclude, it then follows that the cellulose will also produce the alternative pyrolysis products, hence, LG cannot be the only primary product. However, it has been shown that pyrolysis under conditions which encourage LG evaporation and hence removal from the pyrolysis conditions achieves yields of LG >70%. It therefore follows that removal of LG prevents or drastically slows the formation of the alternative pyrolysis products; if the products were forming from cellulose then these would still form regardless of the presence of LG.[210,218]

Clearly, further investigation is needed but the results suggest that potentially all of the pathways

proposed can occur and the conditions of pyrolysis need to be tailored to force the degradation down the desired route.

5.1.2 Paper as a Waste Stream

Sources of cellulosic biomass which do not compete with the food production market are highly desirable and one such of these is waste paper. The paper industry produced more than 393 million tonnes of paper and cardboard in 2010 and up to 70% of this is cellulose.[225,226] Recycling of paper is so widespread, in 2010, more than 223 million tonnes of paper was collected worldwide which is more than 50% of the global production, and this is consistently on the increase.[225,227] Globally, improvements are still necessary but in certain areas, such as Europe, the theoretical maximum for paper recovery is being approached; an estimated 20% of paper and cardboard is not recyclable due to its use, such as sanitary products or cigarette papers.[225,228] The demand for recovered paper has increased due to various legislative changes on the required minimum recycled paper content for certain types of packaging and the ability for the system to meet demand has been supported by further legislation; separate collection of paper to prevent contamination along with the de-classification of recovered paper as waste.[227–229]

Recovered paper is well utilised in new paper production and recovered fibres account for 50% of the total papermaking fibres used globally, however, virgin fibres will always be necessary to maintain the required paper quality as the cellulose fibres degrade during the recycling process.[228] The different grades of recovered paper exhibit various rates of use with recovered newspaper being used up to 93% of the time whereas recovered graphics paper only being used up to 11% of the time.[228] This disparity is mainly due to the heavy contamination of certain paper types with inks, adhesives and coatings. The de-inking process causes many problems for the recycling industry and the development of new technologies is worsening the issue; the development of water soluble inks has meant traditional methods of deinkingare no longer efficient.[228] Contamination from all sources is detrimental to the recycling process unfortunately is increasing consistently year on year.[228] Higher amounts of contamination increase the energy and water consumption of the recycling process as well as the air and water pollutants produced, and the quantity of rejected end product. Acidification, eutrophication, human toxicity and photochemical ozone production potential were also all shown to increase with higher contamination in recovered paper.[230]

While paper production and recycling is a streamlined, self-contained system, alternative options

can be more environmentally and economically viable. In addition, as the utilisation of all recovered paper is increasingly difficult due to contaminants and paper quality restraints, different uses for the remaining recovered paper are becoming necessary.[201] Minor uses of pulp such as in building materials are increasingly well researched but two main options are available; incineration and chemical synthesis.[201,231] The use of waste paper in chemical synthesis is realistic due to the high cellulose content of the paper and because of the high value of the chemicals produced which mean the processing costs do not need to be as low as for production of low quality/value recycled paper.[226] Much research has already been carried out into chemical production from waste paper and a variety of end products have been identified such as bio-ethanol, adhesives and bio-platform molecules.[20,201,226,232–234]

Challenges

In this thesis, waste paper was investigated for its utilisation in pyrolysis to produce LG. Therefore, the focus for the following discussion on paper contaminants was their effect on the mechanism of LG production. It is however important to note that paper contamination causes difficulties in all application of waste paper.

The most common contaminants found in recovered paper are from the manufacturing industry. High quality paper requires fillers and coatings to ensure the aesthetics of the paper meet the desired standards and most recovered paper will have ink or adhesive contamination from the original application. Office paper has the highest contamination content, with large amounts of alkali or alkaline earth metal salts such as $CaCO_3$ or clays such as kaolinite or TiO_2 for colour reduction; silica or organosilanes for improvement of particle size in pulping for finer paper production; inks from office use; and adhesives and waxes for reduced water permeability.[226,228,233,235]

In terms of interference with chemical synthesis from waste paper, alkali or alkaline earth metal salts were the most important contaminants to consider. Presence of alkali or alkaline earth metal salts during pyrolysis have been shown to alter the product profiles by as much as 30% and specifically affect LG production.[235–238] It has been speculated that the metal ions complex with the cellulose and stabilise alternative intermediates in the cellulose breakdown mechanism, Scheme 66.[235]

The products seen to be most affected by this complexation were LG which decreased from 59 to 26 percent by weight (wt%); glycolaldehyde which increased from 7 to 28 wt%; formic acid which increased from 7 to 18 wt%; and acetol which increased from 0.3 to 2 wt%.[235–238] As well as

the complexation of the metal with the cellulose, the dehydrating nature of some of the salts has also been considered as a factor, especially in production of 5-hydroxymethyl furfural (HMF) and levoglucosenone. [235,239,240]
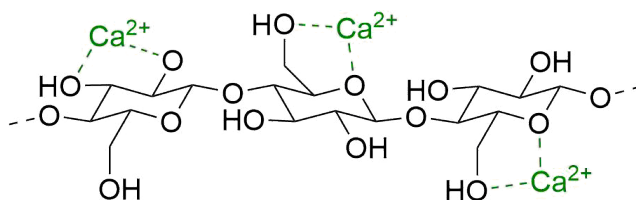
Scheme 66: Complexation of calcium ions to cellulose during pyrolysis [235]

This research can be utilised for the reduction in impact of the fillers and additives from paper manufacture on the pyrolysis of the resulting waste; by understanding the mechanism and its key factors, solutions can be found. An important note is the different amounts of influence the various salts had on LG; it was shown that the most influencial metal ions were K > Na > Ca > Mg and $Cl^- > NO_3^- \approx OH^- > CO_3^{2-} \approx PO_4^{2-}$ were the most influential counter ions. [235,241] Currently, as one of the most common paper fillers is $CaCO_3$, the impact is low compared with other potential additives which is good news for pyrolytic applications of recovered paper.

Many investigations into the removal of the alkali or alkaline earth metal salts prior to pyrolysis, usually by acid-washing the paper have been carried out and the results indicate that this could improve the yields of desirable products obtained. [212,224,236,242] It has to be considered, however, the value in this extra treatment, in terms of added end products, when compared with the additional cost, both environmental and economical, of pre-treatment of the waste biomass.

5.1.3   Aims of the Chapter

Chapter 2 demonstrated that alkyl polyglucosides (APGs) could successfully be synthesised from LG, a compound produced in paper pyrolysis, as described above, section 5.1.1. Paper has been shown to be a high volume waste stream with potential for higher value use than recycling. This Chapter investigated the possibility of bringing together the synthesis of renewable surfactants with the valorisation of a non-food based waste biomass stream to not only improve the renewable surfactant market but also the utilisation of waste.

5.2   Paper *vs.* Cellulose

In order to identify a baseline for future optimisation and to evaluate differences between cellulose pyrolysis and that of paper, microwave pyrolysis was carried out on microcrystalline cellulose and waste paper under identical conditions. These experiments also allowed the identification of the products of pyrolysis, by gas chromatography (GC), gas chromatography-mass spectrometry (GC-MS) and nuclear magnetic resonance (NMR) spectroscopy.

Table 13: Mass balance of cellulose and paper microwave pyrolysis (0.7 g material, 250 W, <250 $^\circ$C, <5 mins)

	Yield* / % (error)			
Fraction	Cellulose		Paper	
Gas	8.331	($\pm$ 3.8)	11.15	($\pm$ 1.4)
Bio-oil	21.90	($\pm$ 1.3)	15.22	($\pm$ 0.90)
Char	69.77	($\pm$ 2.6)	73.63	($\pm$ 1.6)

*wt% of initial mass

The pyrolysis of the two materials gave a number of product streams, separated and collected for individual analysis, Table 13. The results show that the paper produced less of the desired bio-oil, as a wt% of initial mass, than the pure cellulose, with char and gaseous products increasing to compensate. This is expected due to the presence of fillers used in the paper industry. [201,226,232] As discussed previously, section 5.1.2, many of these fillers are inorganic salts, such as $CaCO_3$ up to 8 wt%, which can act as Lewis acid catalysts in the pyrolysis of cellulose and aid the breakdown to low molecular weight (LMW) species and gaseous products. [226,235]

Identification of the pyrolysis products contained in the bio-oil was carried out using GC-MS, standards for comparison and literature where necessary. This allowed for a more complete understanding of the effects of fillers and additives on the pyrolysis.

Table 14: Products observed[†] by GC in bio-oil from microwave pyrolysis of cellulose and paper[209,210,235]

| Compound | Average* / % (error) | | | | Cellulose[210] | Cellulose + CaCO$_3$[235] |
	Cellulose		Paper			
Formic acid	5.63	(± 0.31)	7.87	(± 0.30)	6.59	10.53
Furan			1.79	(± 0.28)	0.73	0.82
Glycolaldehyde	<1.00		3.16	(± 0.24)	6.69	14.32
Acetol			7.53	(± 0.78)	0.3	0.92
2-furaldehyde	<1.00		1.12	(± 0.10)	1.26	0.95
2-furan methanol			1.31	(± 0.069)	0.54	0.05
3-furan methanol			1.19	(± 0.10)	0.25	0.03
5-methyl furfural			1.68	(± 0.20)	0.24	0.3
Levoglucosenone	3.08	(± 0.26)			0.35	0.24
5-hydroxy methyl furfural	3.85	(± 0.10)	1.59	± 0.12)	2.76	2.56
Anhydrosugars	10.7	(± 1.4)	<1.00		1.43	1.40
LG	22.6	(± 3.0)	<1.00		58.78	35.73
LG (furanose)	1.20	(± 0.15)			4.08	1.88
Oligomers[‡]	44.1	(± 2.8)	63.2	(± 4.1)		

[†]only products seen in excess of 1.00% by GC identified   *wt% of mass of bio-oil

[‡]oligomers of anhydrosugars seen between 2–5 monomers in length

A large number of products were identified in the bio-oils, Table 14, alongside a large number (<30) which were present, as seen by GC, but in concentrations below the limits of detection for the GC-MS. The pyrolysis products, Scheme 67, were seen to be mainly LMW oxygenated organic compounds, furan derivatives and sugar derivatives, namely anhydrosugars such as LG. High molecular weight oligosaccharides were also observed and are thought to originate from the secondary reactions of the anhydrosugars in the latter phases of pyrolysis, section 5.1.1.[224,243,244]
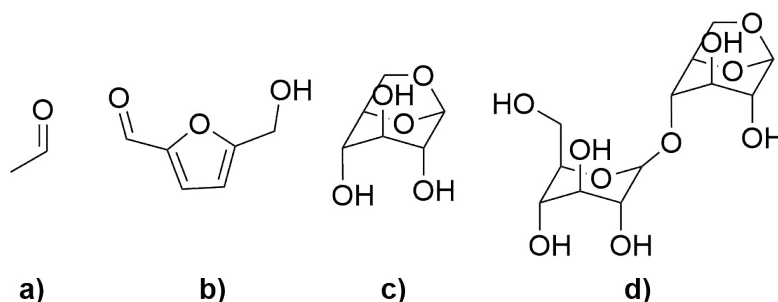
Scheme 67: Examples of products from the microwave pyrolysis of cellulose. a) is acetaldehyde, b) is 5-hydroxymethyl furfural, c) is LG and d) is an LG dimer, cellobiosan[243]

As discussed above, section 5.1.1, the primary product formed by pyrolysis of polysaccharides and their derivatives is thought to be LG.[207,210,221,222,224,243,244] The many proposed reaction pathways for the pyrolysis of cellulose are conflicting and the presented evidence for each is controversial however the general scheme which takes into account the literature arguments as a whole is shown below, Scheme 68.[17,207,222,224,243,244] This shows that LG is the main product and secondary reactions of this result in the char and LMW species also seen.
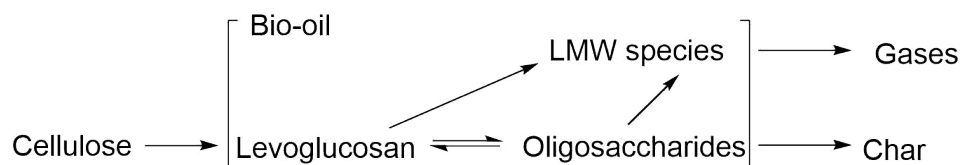
Scheme 68: General scheme depicting the pyrolysis of cellulose to produce bio-oil, char and gaseous products through LG[207,222,224,243,244]

The variation in product distribution between the pyrolysis of cellulose and that of paper can be attributed to the differences in their composition. Waste paper typically has less than 70% cellulose content and the additional mass is made up of fillers and coatings, Table 15.

Table 15: The composition of various types of paper[226]

	Composition / wt%			
	Newspaper	Office Paper	Magazine	Cardboard
Moisture	7.25	4.90	4.40	5.90
Carbohydrates	60.64	69.6	47.91	65.33
Lignin	16.82	5.78	14.19	14.86
$CaCO_3$	1.98	7.71	2.52	3.96
Ash*	9.49	7.57	28.83	9.32

*predominantly silica with other inorganics such as calcium, potassium, phosphorous, magnesium and sodium

The paper pyrolysed here was office paper and it can be seen that this paper derivative contains a high proportion of $CaCO_3$, >7%, as well as a similarly high proportion of ash, which contains a range of inorganic salts.[226] The role of these inorganics within the pyrolysis mechanism is as contentious as the mechanism itself, but the main school of thought is that they encourage the production of LMW products at the expense of LG and the other anhydrosugars. These salts can catalyse alternative pyrolysis reactions and hence an increase in these competing reactions leads to a decrease in LG yields in the presence of any or all of the observed inorganic contaminants. Magnesium, in the form of $MgCl_2$, is known to be a dehydrating agent and promotes the production of furans and levoglucosenone. Similar catalytic activity can also be associated with potassium and calcium chloride salts. The ash found in the paper has been shown to promote the formation of smaller oxygenated compounds such as formic acid and glycolaldehyde instead of the dehydration products which was suggested to be due to the inorganics being present as oxides.[235] It was observed here that the formation of small furans and C_2−−C_4 organic compounds were increased when paper was pyrolysed instead of cellulose which supports the literature findings discussed.

Depending on the inorganic salts present and their degree of Lewis acidity, scission at different bonds inside the pyranose ring are favoured. The strength of the Lewis acidity of the inorganic salt will affect which bonds it can stabilise and consequently means that scission at a wider range of positions can occur for stronger Lewis acids. Scission at C_2 or C_4 would produce glycolaldehyde and at C_3 would produce acetol **??**.[203,207,209,235]

The results indicate that optimisation is needed to improve the LG yields with particular care taken in the removal of fillers and inorganic salts present in waste paper.
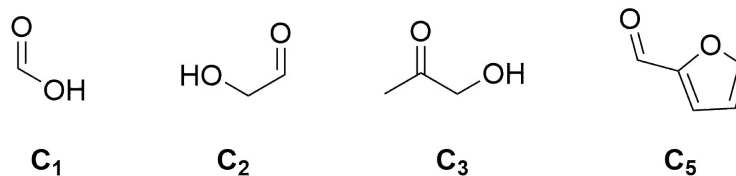
Scheme 69: Examples of LMW products from the pyrolysis of paper encouraged by the presence of inorganic salts.[209,235] C_1 — formic acid, C_2 — glycolaldehyde, C_3 — acetol and C_5 — furfural or 2-furaldehyde

5.2.1 Optimisation

Optimisation of the reaction conditions was carried out, with a number of factors being taken into consideration. The microwave power, reaction time, material loading and bio-oil extraction solvent were improved and the resulting optimal conditions were 1200 W, 18 mins, <200 °C, 200 g milled pressed waste paper and a methanol extraction solvent. The paper was milled and pressed to increase the density which improves the efficiency of heating under microwave conditions. The microwave absorber will convert the energy into heat and then dissipate it through the surrounding biomass, the higher the density, the more efficient the heating.[51] Methanol is known to be best for bio-oil and LG extraction for two main reasons; due to its small size, methanol is good at swelling the biomass/char and hence enabling the bio-oil to be extracted; also, methanol is very polar and is good at extracting the polar organic compounds such as the anhydrosugars from the biomass/char and retaining them.[245,246]

Microwave pyrolysis was carried out on waste paper under the optimised conditions and the mass balance results of this are shown in Table 16. While the fraction of total bio-oil collected is larger than the initial conditions, this is the only real improvement seen in these results and even this is not as good as it first appears as the majority of the LG will reside in the smaller, methanol fraction of the bio-oil. However, the analysis of this fraction showed that optimisation had successfully increased the yield of LG, Table 17.

In the initial tests, Section 5.2, there were many products (<30) produced in very small quantities which could not be identified but after optimisation there were fewer products in total (<30), with a larger proportion in high enough concentrations to allow identification (>60% *vs.* <50%

for the initial pyrolysis). The experimental set-up, similar to a dean-stark set-up, encouraged the evaporation and collection of LG which means it was removed from the pyrolysis conditions and hence protected from further secondary reactions. Inevitably, given its reactive nature and the harsh pyrolysis conditions, some degradation of LG occurred and these LMW products are seen as they too would have evaporated.

Table 16: Mass balance of optimised paper microwave pyrolysis

Fraction		Yield* / % (error)	
Gas		14.1	($\pm$ 0.5)
Bio-oil	methanol fraction	10.4	($\pm$ 0.8)
	aqueous fraction	34.9	($\pm$ 0.7)
Char		40.6	($\pm$ 0.6)

*wt% of inital mass

There are a wide range of investigations into LG extraction from biomass already in the literature and many with yields of up to 70%.[210,218,247,248] It is frequently reported that swift removal of LG during pyrolysis is necessary to prevent the char, residual cellulose and heat from catalysing its breakdown.[218,222,224,243,244] The most promising conditions for the production of LG hence involve, low residence times of the material and/or the LG, in the pyrolysis chamber; small sample size of material for pyrolysis, to reduce the char present for catalysis and to improve the efficiency of heating of the sample; high temperatures, to encourage evaporation of LG away from the problematic char; and low pressure, again for ease of LG removal.[218,243]

Kwon *et al.*[218] utilised a double moving belt system to achieve a very low LG residence time which resulted in not only a high LG but high bio-oil yield too. Presence of only a thin layer of cellulose on a heated belt, under vacuum, enabled LG evaporation and subsequent condensation onto a cooling belt above, moving in the opposite direction, hence removing the LG from the system. The final LG yield achieved from this method was 70.1%.[218] The combination of a sample with a high surface area, vacuum and rapid LG cooling was the key in this method.

A disadvantage of microwave pyrolysis, the method under investigation in this thesis, for this application, is that it is relatively low temperature,[50] (compared with conventional pyrolysis) and so it increases the LG residence time and hence further LG breakdown occurs. The pyrolysis of

paper in batches of ~100 g also reduces the chance of LG removal as it will likely form within the sample and too far from the surface to escape. These factors mean that this project is unlikely to reproduce, let alone improve upon, the results presented in literature but highlights that the important factors in the pyrolysis of paper are related to the experimental set-up.

Table 17: Products observed[†] by GC in bio-oil from optimised microwave pyrolysis of paper[209,210,235]

Compound	Average* / % (error)	
Acetaldehyde	1.56	(± 0.17)
Formic acid	9.99	(± 1.1)
Furan	1.15	(± 0.13)
Glycolaldehyde	1.09	(± 0.12)
Acetic acid	1.41	(± 0.15)
2-methyl furan	3.90	(± 0.43)
3-methyl furan	2.50	(± 0.27)
Acetol	2.86	(± 0.31)
2-furaldehyde	2.29	(± 0.25)
2-furan methanol	2.92	(± 0.32)
3-furan methanol	2.60	(± 0.29)
5-methyl furfural	2.19	(± 0.24)
2-hydroxy-3-methyl-2-cycltopenten-1-one	1.25	(± 0.14)
Levoglucosenone	4.16	(± 0.46)
5-hydroxy methyl furfural	4.69	(± 0.52)
Anhydrosugars	3.64	(± 0.40)
LG	31.13	(± 3.4)
LG (furanose)	<1.00	
Oligomers[‡]	<1.00	

[†]only products seen in excess of 1.00% by GC *wt% of mass of bio-oil identified

[‡]oligomers of anhydrosugars seen between 2–5 monomers in length

5.3   Conclusions

The investigations carried out into the extraction of LG from waste paper *via* pyrolysis have produced some interesting results. It was shown that microwave pyrolysis of waste paper can be applied to bio-oil production and the yield of LG can be improved by optimising the pyrolysis conditions such as microwave power, pyrolysis time and sample density. Through optimisation, the yield of LG (as wt% of initial waste paper) was increased from 1.52% up to 14.23%. These results indicate that waste paper can be an appropriate resource for the production of LG which was the aim of this project. However, high conversion of cellulose to LG is frequently reported up to 70%, and the optimised yield documented in this thesis was low in comparison.[210,218,247,248] This literature success highlights that the next steps for optimisation, beyond the afore mentioned pyrolysis conditions, should concentrate on the experimental set-up.

Removal of LG *in situ* during pyrolysis to prevent secondary reactions occurring is key for LG production. When under pyrolysis conditions, LG can polymerise to form short chain oligosaccharides, from dimers up to pentamers. From these oligomers, LMW oxygenated organics can form from bond scission within the anhydrosugar monomers.[218,222,224,243,244] Ensuring that during the process of pyrolysis the LG is removed immediately, involves both high temperature and low pressure and is aided by a small sample size or high sample surface area.[243] The reactors available for this project take relatively large amounts of sample, in batch, and pyrolysis is carried out with the aid of microwaves. The low temperature of the microwave pyrolysis and the large sample size both reduce the likelihood that the LG will evaporate and hence be removed from the pyrolysis conditions.[50] Investigation into the use of high temperature microwave technology and a flow-based system are important next steps but are avenues which could not easily be tested with the equipment available for this project.

Removal of inorganic salts from the waste paper, which are added as fillers for aesthetics as well as textural and structural reasons during the manufacturing process, is another key factor because they are known to decrease the LG yield by catalysing production of alternative LMW organics at the expense of LG.[226,235,242] While this is important, this removal should be treated as a secondary consideration behind the experimental set-up as addition of treatment steps in the pyrolysis of biomass reduces the economic and environmental feasibility of the process.[226,249]

All in all, it can be concluded that the high LG yields reported in the literature[218] are unachievable within the limits of this thesis; however the existence of such literature does provide hope that LG

is extractable from waste paper. The understanding of the mechanism and/or the removal of the fillers in waste paper can help to increase the potential of this abundant, currently under-utilised material. The direction in which study should be conducted is clear; purpose built reactors could produce LG and the possibility for fine chemical synthesis from this bio-based molecule is such that industrial applications for this process are readily identifiable.

5.4   Future Work

The synthesis of LG from cellulose pyrolysis has a great deal of potential, as demonstrated in the literature and the physical conditions of the pyrolysis have been shown to be the most important factors in its production.[210,218,247,248] With the correct pyrolysis apparatus, producing >70% LG from cellulose would be achievable as this been has previously demonstrated by Kwon *et al.*[218]. Building on their double moving belt system and focussing on the key aspects of the apparatus, high sample surface area, vacuum and rapid LG cooling, and subsequent purification of the LG from the bio-oil would be important to investigate.[218]

Optimisation to allow for the use of waste paper would be the most important next step in the investigation into the production of LG from celluose pyrolysis. This would be difficult because the effect of inorganic fillers and modifiers present in the paper would need to be assessed.[226,235,242] It would also be important to consider the varying grades of recycled paper, with emphasis on the use of low grades of paper which have been recycled a large number of times previously. The more times paper is recycled, the lower the crystallinity and the shorter the fibres of the paper become, which makes chemical attack more effective but recycling more difficult, with the economic feasability eventually ruling further recycling out as an option. Paper recycling is a highly efficient and well optimised process accounting for around 80% of the paper disposed of in the UK each year.[225] Pyrolysis of paper should not become a replacement for paper recycling but there is an opportunity for it to complement the recycling process and pick up where the recycling process begins to fail; when paper has previously been recycled many times.

Chapter 6

Concluding Remarks

The incentives for reducing the environmental impacts of the modern world encompass every aspect of life. The security that comes with ensuring the supply of all necessary chemicals from renewable resources is one important factor. However, protection of the environment and of those living in it is arguably the highest priority. To this end, it is important to reduce and ultimately aim to end the practices which lead to the release of greenhouse gases into the atmosphere, release of toxic chemicals into the water system, disposal of waste into landfill and depletion of fossil fuel reserves.

It is important for future generations that action is taken and the ideals outlined by green chemistry provide a good foundation on which to build up from. The twelve principles of green chemistry define the discipline as well as setting out basic methodologies to be followed when working in the field.[3] The focus is specifically on preventative actions to be taken, to ensure that remedial action is unnecessary.[1,4] The overall aim of this thesis was to apply these principles to improve the green chemistry credentials of the industrial surfactants market. Surfactants play an important part in the chemical industry. They are produced at an increasing rate each year, currently over 14 million tonnes, however the renewable surfactants available on the market are scarce.[58] Ultimately this was achieved in the development or improvement of two types of surfactant, alkyl polyglucosides (APGs) and sulfo-succinates, Scheme 70; utilisation of waste biomass was considered for each and the routes to these products were developed under the guidelines of clean synthesis.

a)   b)   R = C_6H_{13},
C_8H_{17},
$C_{10}H_{21}$,
$C_{12}H_{25}$ or
$C_{14}H_{29}$
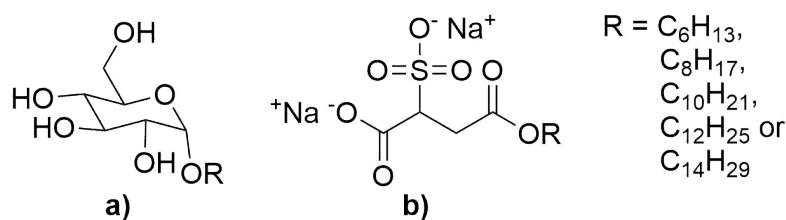
Scheme 70: The two surfactant types synthesised in this thesis, a) APGs and b) sulfo-methylene-succinates

The opportunity presented by the deficiency in the renewable surfactants market was exploited in this thesis and two avenues were investigated. One approach was to optimise the synthesis of existing renewable surfactants using starting materials obtained from waste biomass. Growing biomass for chemical production poses challenges because of the competition over arable land with crops grown for food; food production will ultimately be prioritised. Landfill use is on the rise and is not only costly and environmentally damaging but also wasteful of the chemical potential that is stored in said waste.[1] APGs have been shown to have potential for further 'green' optimisation and there is an existing market for these renewable surfactants; the synthesis currently uses glucose from edible wheat starch and triglycerides from palm oil, which has a controversial production process.[58,59]
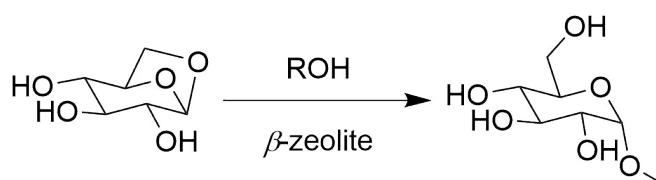
Scheme 71: The synthesis of APGs from levoglucosan (1,6-β-D-glucopyranose) (LG) investigated in this thesis, R = CH_3, C_8H_{17} or $C_{10}H_{21}$

The use of the anhydrosugar LG was investigated in this thesis, in place of glucose, for the hydrophobic head group of the APG because it is a primary pyrolysis product of cellulose.[235] Waste paper is made up of up to 70% cellulose and presents a significant waste stream which, while currently efficiently recycled, could be valorised into higher value products through chemical processes such as pyrolysis.[225,226] The results presented within demonstrated that efficient synthesis of APGs from LG could be achieved and with the use of reusable solid acid catalysis in place of traditional homogeneous acids, improvements could also be made on the environmental impacts of said synthesis, Scheme 71. This work highlights that improvements, even to processes considered as

green, can and should always be investigated. Further understanding of the mechanism of catalysis of the solid acids employed would enable the continued improvement of the APG synthesis from LG and following on from that, scale up investigations would be necessary to allow implementation of this process throughout the industry.

The second approach taken in this thesis towards the improvement of the renewable surfactants industry was the development of novel renewable surfactants with the potential for use as drop-in replacements of existing common surfactants. Sulfo-succinates represent 49% of all anionic surfactants used in a large range of applications; these include bulk household detergents and cosmetics as well as niche applications such as corrosion inhibitors and antistatic agents. [134,137] Itaconic acid (IA) is structurally similar to the maleic acid (MalA), Scheme 72, which is used in the current sulfo-succinate synthesis however is produced from the fermentation of biomass by fungi, namely *Aspergillus Terreus*. [144–146] The use of this diacid in the synthesis of surfactants produced a range of compounds, sulfo-methylene-succinates, nearly identical to the existing surfactants and hence with a high potential as direct replacements.

Scheme 72: Structure of a) bio-derived IA and b) petrochemical derived MalA [26]

The popularity of the sulfo-succinates arises from their high efficiency and so it was important to evaluate the replacements in comparison. The novel surfactants proved that they are more than capable of competing with the high reputation of the sulfo-succinates and out-performed them in the tests carried out within this thesis. The surface activity of the sulfo-methylene-succinates was not only higher, so they reduced the surface tension by a greater amount, but also faster, so the surface tension reached equilibrium quicker. These properties are useful for many applications, detergency especially, with lower surface tension bringing improved wettability to the product meaning improved fabric cleansing. [60] The sulfo-methylene-succinates also exhibited lower critical micelle concentration (CMC) values than the equivalent sulfo-succinates meaning that a lower concentration of surfactant would be necessary to produce the same product efficiency, which is beneficial for both cost and environmental reasons. The results of these tests highlighted that the implementation of green chemistry does not have to mean that product efficiency is compromised;

they emphasise that this need for renewable replacements of many commercial products is a great opportunity to improve upon the existing and should, with good reason, be viewed as a positive challenge rather than a negative burden.

Continued testing of these novel surfactants should be carried out to enable a full picture of their potential to be drawn up. Many other similar structures, such as itaconate based diesters and muconic or aconitic esters, Scheme 73, are important for investigation so that the full range of sulfo-succinates can be replaced by renewable alternatives.
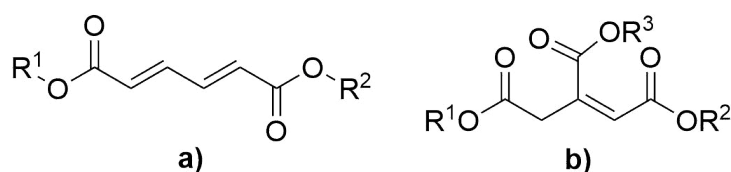
Scheme 73: Structures of a) muconic and b) aconitic esters; possible bases for further surfactant sets. R = H or alkyl

The two renewable surfactants investigated in this thesis were based on bio-derived platform molecules and therefore it was necessary to investigate the synthesis of at least one of the starting materials; in this case the LG was chosen. This glucose-based anhydrosugar is known to be obtainable from the pyrolysis of cellulosic biomass and one potential source of such biomass was identified as waste paper, this use is a higher value alternative to the current recycling options.[201,235] The research carried out into the production of LG from waste paper highlighted the challenges involved in such a process, mainly the promotion of competing reactions by contaminants that are present in the paper, some from the manufacturing process such as adhesives and fillers as well as some from consumer use such as inks. These contaminants are important to consider as they can reduce the yield of LG by up to 30% however it is also important to bear in mind that they will have an adverse effect on all the potential uses of waste paper.[230,235] The investigations in this thesis showed that there is potential in valorisation of waste paper and production of LG is possible with the right process conditions, but it also, importantly, showed that it is key for waste biomass utilisation and renewable synthesis to work together, to allow for optimisation towards the best economic output as well as towards the best environmental one.

Process optimisation is key for the use of waste paper as a chemical source and the concurrent development of syntheses from these bio-platform molecules can act as an important driver for this future work.

The aims of this project were primarily to synthesise two sets of renewable surfactants. This has been achieved successfully with the extra advantage of different approaches being applied for each. In addition the IA derived surfactants were compared to existing related surfactants and there was an indication of out-performance of the existing surfactants. The complimentary investigation into synthesis of starting materials for the renewable surfactants highlighted the importance of a whole process approach, not only to chemical synthesis but to the entire chemical industry. This project was a positive reminder of how green chemistry provides a great opportunity to existing and future chemists.

Chapter 7

Experimental

7.1 Equipment

Furnace Samples were calcined (2.5 °C min^{-1}, 400–550 °C) in a BL Barnstead Thermolyne 6000 series.

CEM Microwave Reactions carried out in the CEM microwave were performed using a CEM Discover SP Microwave Synthesizer (2.45 GHz magnetron) with in-built infra-red (IR) and fibre optic temperature sensors and an explorer automation unit.

Multipoint Reactor Radleys Discovery Technologies five point carousel stirrer hotplate.

Freeze Dryer Samples were dried using a VirTis SP Scientific sentry 2.0 freeze drier held between −105 and −110 °C under a vacuum (∼27 mT).

Hammer Mill Waste paper was milled using a Farm Feed Solutions (UK) 12 kW hammer mill with 5 mm screen.

Milestone Microwave Reactions carried out in the Milestone microwave were performed using a Milestone Rotosynth Rotative Solid-Phase Microwave Reactor (2.45 GHz magnetron) with 45° tilted rotating reaction vessel and in-built IR and fibre optic temperature sensors.

7.2 Analysis

All results were taken as an average of three data points and the error was calculated as the standard deviation over the data points used.

7.2.1 Chromatography, Spectroscopy and Spectrometry

Gas Chromatography

An Agilent Technologies 6890N network gas chromatography (GC) system was used with a 7683b series injector and flame ionisation detector (FID). The settings used for analysis by GC were as follows in Table 18.

Table 18: GC instrument settings

Injector	Detector	Column
1 μL auto sample inj.	380 °C FID temp.	ZB-5HT (5% phenyl methyl siloxane)
360 °C inj. temp.	make-up 35 mL min^{-1} N$_2$	length 30 m
25:1 split ratio	35 mL min^{-1} H$_2$	0.25 mm od
20 mL min^{-1} split flow	FID feed gas 350 mL min^{-1} air	0.25 μm id
		carrier gas flow 2 mL min^{-1} helium

Levoglucosan Surfactants The method which was used for the analysis of the levoglucosan (1,6-β-D-glucopyranose) (LG) surfactants was as follows in Table 19.

Table 19: GC temperature program for analysis of surfactants made from LG

Ramp / °C min^{-1}	Hold Temperature / °C	Hold Time / min	Total Time / min
	100	1	
40	360	1	
			8.5

Calibration curves were used for the analysis of the LG surfactants with a biphenyl internal standard (IS) and an example of such is shown below, Figure 54. It can be seen that the calibration curve does not pass through the origin which is due to the inherent nature of the FID response being an "S" shaped curve. The calibration curve shows the range of concentrations at which the response is linear. Additionally, the FID gives a different response for different molecules and a response factor, which is dependant on, among other factors, carbon content, can be determined using a calibration curve.
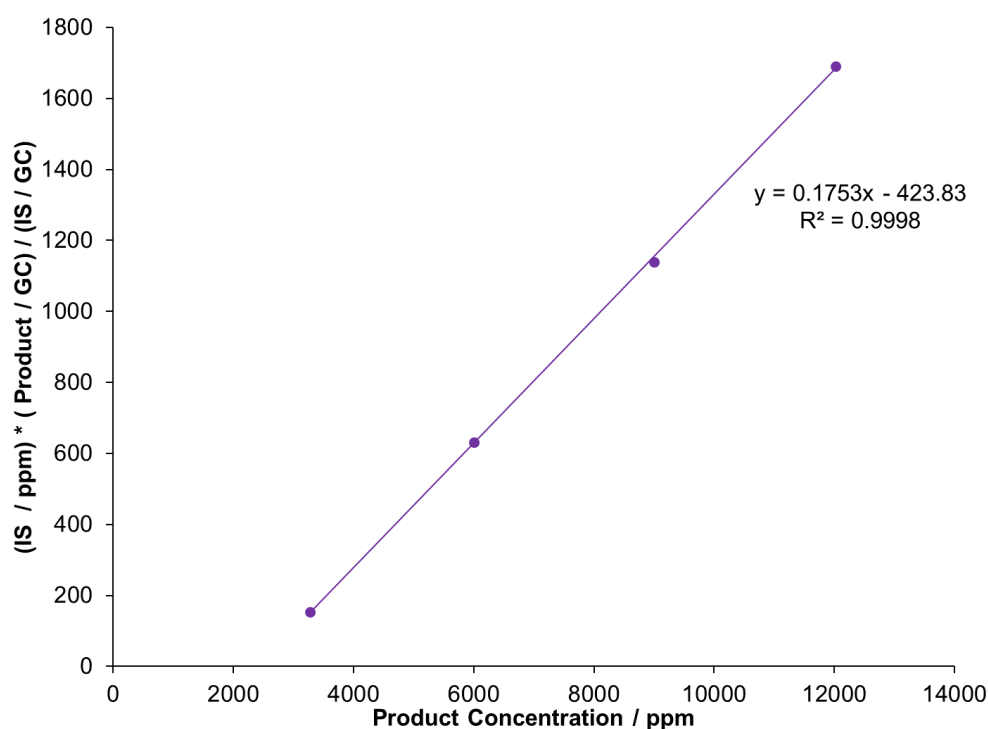
Figure 54: Example GC calibration curve for surfactants from LG against a biphenyl IS

Mass Spectrometry

A Bruker micrOTOF time of flight mass spectrometer with an electrospray ionisation (ESI) source was used for all mass spectrometry (MS) analysis.

Gas Chromatography Mass Spectrometry

Gas chromatography-mass spectrometry (GC-MS) analysis was carried out on a Perkin Elmer Clarus 500 GC with a Clarus 560S mass spectrometer equipped with an electron ionisation (EI) source and quadrupole detector. The GC specifications and method was set to match the GC-FID settings.

Supercritical Fluid Chromatography

All supercritical fluid chromatography (SFC) was carried out using a Thar SuperPure Discovery Series SFC with a Water 2995 diode array detector (DAD) and a Water 2424 evaporative light scattering detector (ELSD). The settings and columns used are detailed below in Table 20.

Table 20: SFC instrument settings

Analytical column	Separations column	Settings
Phenomenex Luna Silica	Water SunFire Silica Semi-Prep	mobile phase CO_2, 99.8% pure (BOC)
100 Å, 3 μm	100 Å, 5 μm	methanol co-solvent (7%)
50 mm × 4.6 mm	250 mm × 10 mm	column 40 °C
		flow rate 9 mL min^{-1}
		100 bar

Levoglucosan Surfactants   Calibration curves were constructed for the analysis of the LG surfactants with an azelaic acid IS and an example of such is shown below, Figure 55.
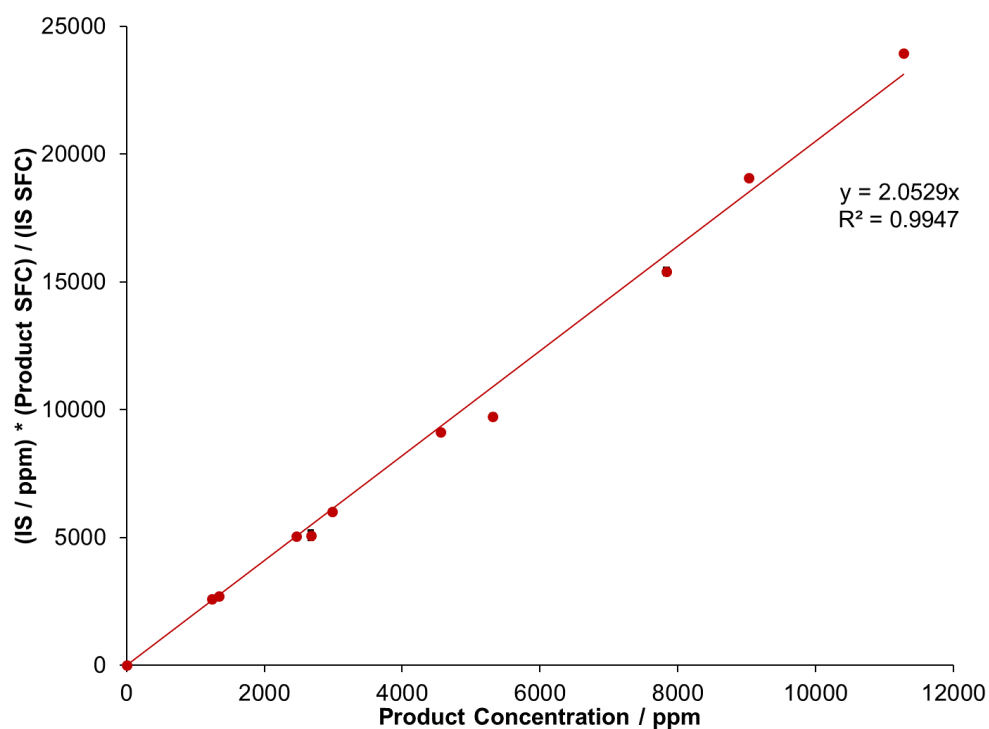
Figure 55: Example SFC calibration curve for surfactants from LG against an azelaic acid IS

Nuclear Magnetic Resonance Spectroscopy

Both ^{1}H and ^{13}C {^{1}H} nuclear magnetic resonance (NMR) spectra were recorded using a JEOL ECX 400 spectrometer. The instrument was operating at 400 MHz for ^{1}H and 100.5 MHz for ^{13}C {^{1}H}. For ^{1}H the residual protic solvent was used as a reference. The initial wait and relaxation decay were both 1 s, the pulse was 3.23 μs and 16 scans were run.

Itaconate Surfactants Calibration curves were constructed for the analysis of the itaconate surfactants and an example of such is shown below, Figure 56.
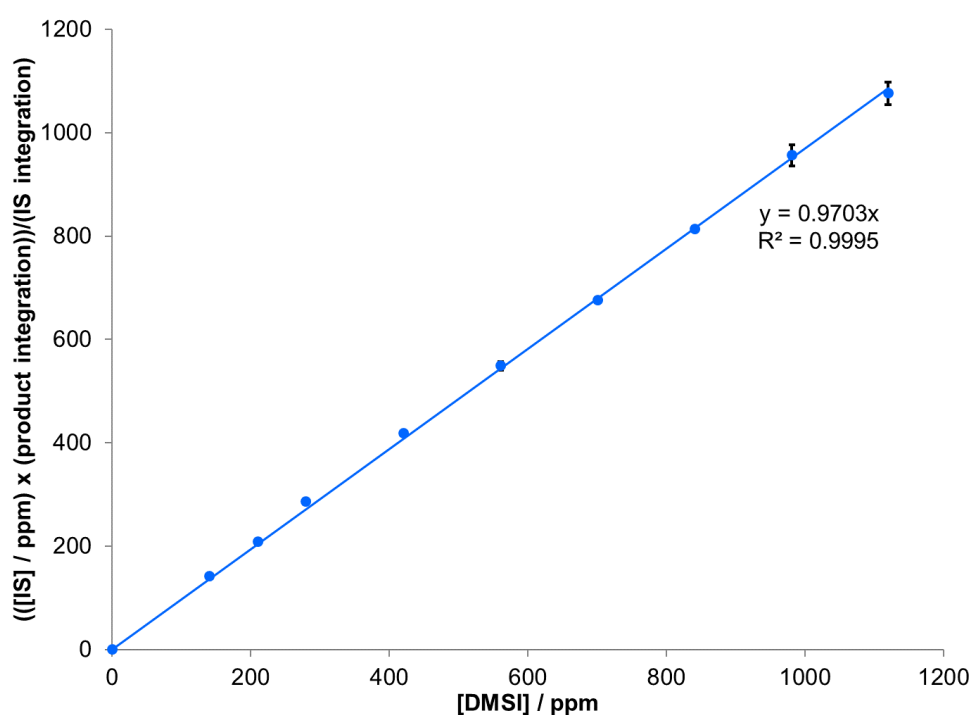
Figure 56: Example ^{1}H NMR spectroscopy calibration curve for sulfo-methylene-succinates

FT-Infra-Red Spectroscopy

Fourier transform infra-red (FT-IR) spectra in the range 4000–600 cm^{-1} were recorded using a Bruker Vertex 70 instrument equipped with a Specac Golden Gate attenuated total reflectance (ATR) accessory.

7.2.2   Catalyst Characterisation

Acidity

All samples were analysed by FT-IR spectroscopy before being charged to a sample vial (50–100 mg) containing pyridine (100–200 μL). The vials, along with a vial containing solely pyridine (1–2 cm^3) were placed (without lids) into a dessicator, with dry silica, and left overnight. All samples were then re-analysed by FT-IR spectroscopy and the pyridine stretches (1640, 1623, 1599, 1575, 1545, 1490, 1450, 1447 cm^{-1}) were evaluated for assignment of the bonding modes to the catalyst surface.

Porosimetry

Nitrogen adsorption measurements were carried out using a Micromeritics TriStar Porosimeter at 77 K. Prior to analysis, the finely ground sample was weighed (60–100 mg) into a porosimetry tube, outgassed (150 °C, 4 h) under a flow of nitrogen and then re-weighed.

7.2.3   Surfactant Characterisation

Critical Micelle Concentration

Critical micelle concentration (CMC) measurements were carried out on a Krűss force tensiometer K100 using the Wilhelmy plate method for surface tension measurement.

Dynamic Surface Tension

A Sinterface maximum bubble pressure tensiometer BPA-1S was used for analysis of the dynamic surface tension at the air-water interface.

Dynamic Interfacial Tension

A Krűss drop volume tensiometer DVT50 was used for the analysis of the dynamic interfacial tension at the oil-water interface; in this case, hexadecane was the oil present.

7.3 Levoglucosan Surfactants

7.3.1 Catalyst Activation

The catalyst was calcined in the furnace at the allotted temperature for 5 h. All solid acid catalysts were activated at 400 °C unless otherwise specified.

7.3.2 Catalyst Trials

General method used for various catalyst/alcohol combinations: LG (0.1 g, 6.17×10^{-4} mol), alcohol (10 molar equivalents (mol equiv.)) and catalyst (200 mg, 20 percent by weight (wt%)) were charged to a microwave tube (10 cm^3, snap cap) and placed in the CEM microwave. This was heated (150 W, max. temp. 220 °C, for varying reaction lengths) and analysed by GC for yield calculations. Unless specified, reaction time was 10 mins.

7.3.3 Compounds
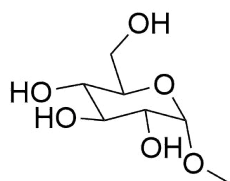
Methyl-α-D-gluco-pyranoside IR $\tilde{\nu}$ / cm^{-1} 3550 (O-H), 3300br (O-H), 2950–2850 (C-H), 1460 (C-O-Me), 1380–1340 (1°/2° O-H), 1230 (C-O-Me), 1190–1110 (C-O cyclic ether), 1060–1030 (C-O 2° OH) and 995 (C-O 1° OH); NMR δ_H / ppm (400 MHz; DMSO$-$d$_6$) 3.00 (1 H, m, C4-H), 3.13 (1 H, m, C2-H), 3.21 (3 H, s, CH_3), 3.25 (1 H, m, C5-H), 3.31 (1 H, m, C3-H), 3.38 (1 H, m, C6-OH), 3.58 (1 H, m, C6-H), 4.44 (1 H, t, ^3J = 5.9 Hz, C6-OH), 4.47 (1 H, d, ^3J = 3.7 Hz, C1-H), 4.68 (1 H, d, ^3J = 6.6 Hz, C2-OH), 4.72 (1 H, d, ^3J = 5.1 Hz, C3-OH) and 4.82 (1 H, d, ^3J = 5.9 Hz, C4-OH); δ_C / ppm (100.5 MHz; DMSO$-$d$_6$) 54.78 (1 C, C7), 61.46 (1 C, C6), 70.83 (1 C, C4), 72.48 (1 C, C2), 73.13 (1 C, C5), 73.89 (1 C, C3) and 100.17 (1 C, C1).
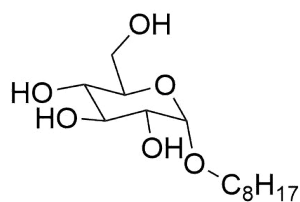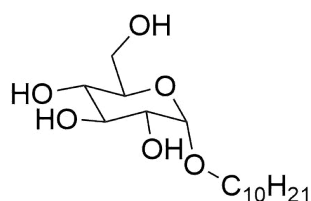
Octyl-α-D-glucopyranoside   IR $\tilde{\nu}$ / cm^{-1} 3550 (O-H), 3300br (O-H), 2950–2850 (C-H), 1460 (C-O-Me), 1380–1340 (1°/2° O-H), 1230 (C-O-Me), 1190-1110 (C-O cyclic ether), 1060–1030 (C-O 2° OH) and 995 (C-O 1° OH); NMR δ_H ppm (400 MHz; DMSO$-$d$_6$) 0.80 (3 H, t, C1-OC$_7$H$_{14}$CH_3), 1.26 (10 H, m, C1-OC$_2$H$_4$C$_5H_{10}$CH$_3$), 1.50 (2 H, m, C1-OCH$_2$CH_2C$_6$H$_{13}$), 3.00 (1 H, m, C4-H), 3.13 (1 H, m, C2-H), 3.21 (2 H, t, C1-OCH_2C$_7$H$_{15}$), 3.25 (1 H, m, C5-H), 3.31 (1 H, m, C3-H), 3.38 (1 H, m, C6-OH), 3.58 (1 H, m, C6-H), 4.44 (1 H, t, $^3J = 5.9$ Hz, C6-OH), 4.47 (1 H, d, $^3J = 3.7$ Hz, C1-H), 4.68 (1 H, d, $^3J = 6.6$ Hz, C2-OH), 4.72 (1 H, d, $^3J = 5.1$ Hz, C3-OH) and 4.82 (1 H, d, $^3J = 5.9$ Hz, C4-OH); δ_C ppm (100.5 MHz; DMSO$-$d$_6$) 14.04 (1 C, C1-OC$_7$H$_{14}$$CH_3$), 22.61 (1 C, C1-OC$_6H_{12}$$CH_2CH_3$), 25.71 (1 C, C1-OC$_2H_4$$CH_2C_5H_{11}$), 29.24 (1 C, C1-OC$_4H_8$$CH_2C_3H_7$), 29.36 (1 C, C1-OC$_3H_6$$CH_2C_4H_9$), 31.78 (1 C, C1-OC$_5H_{10}$$CH_2C_2H_5$), 32.72 (1 C, C1-OCH$_2$$CH_2C_6H_{13}$), 54.78 (1 C, C1-$CH_2C_7H_{14}$), 61.46 (1 C, C6), 70.83 (1 C, C4), 72.48 (1 C, C2), 73.13 (1 C, C5), 73.89 (1 C, C3) and 100.17 (1 C, C1).

1-methyl-septyl-α-D-glucopyranoside   IR $\tilde{\nu}$ / cm^{-1} 3550 (O-H), 3300br (O-H), 2950–2850 (C-H), 1460 (C-O-Me), 1380–1340 (1°/2° O-H), 1230 (C-O-Me), 1190–1110 (C-O cyclic ether), 1060–1030 (C-O 2° OH) and 995 (C-O 1° OH); NMR δ_H ppm (400 MHz; DMSO$-$d$_6$) 0.80–1.50 (16 H, m, C1-OCHC$_7H_{16}$), 3.00 (1 H, m, C4H), 3.13 (1 H, m, C2H), 3.21 (1 H, m, C1-OCHC$_7$H$_{16}$), 3.25 (1 H, m, C5-H), 3.31 (1 H, m, C3-H), 3.38 (1 H, m, C6-OH), 3.58 (1 H, m, C6-H), 4.44 (1 H, t, $^3J = 5.9$ Hz, C6-OH), 4.47 (1 H, d, $^3J = 3.7$ Hz, C1-H), 4.68 (1 H, d, $^3J = 6.6$ Hz, C2-OH), 4.72 (1 H, d, $^3J = 5.1$ Hz, C3-OH) and 4.82 (1 H, d, $^3J = 5.9$ Hz, C4-OH); δ_C ppm (100.5 MHz; DMSO$-$d$_6$) 14.07 (1 C, C1-OCH(CH$_3$)C$_5$H$_{10}$$CH_3$), 22.68 (1 C, C1-OCH(CH$_3$)C$_4H_8$$CH_2CH_3$), 23.39 (1 C, C1-OCH($CH_3$)C$_6H_{13}$), 25.83 (1 C, C1-OCH(CH$_3$)CH$_2$$CH_2C_4H_9$), 29.42 (1 C, C1-OCH(CH$_3$)C$_2H_4$$CH_2C_3H_7$), 31.94 (1 C, C1-OCH(CH$_3$)C$_3H_6$$CH_2C_2H_5$), 39.42 (1 C,
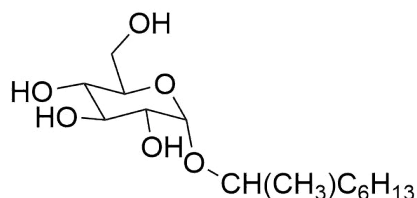
C1-OCH(CH$_3$)CH$_2$C$_5$H$_{11}$), 61.46 (1 C, C6), 68.02 (1 C, C1-CH(CH$_3$)C$_6$H$_{13}$), 70.83 (1 C, C4),

72.48 (1 C, C2), 73.13 (1 C, C5), 73.89 (1 C, C3) and 100.17 (1 C, C1).
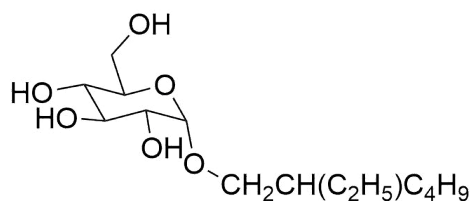
2-ethyl-hexyl-α-D-glucopyranoside   IR $\tilde{\nu}$ / cm^{-1} 3550 (O-H), 3300br (O-H), 2950–2850 (C-H),

1460 (C-O-Me), 1380–1340 (1°/2° O-H), 1230 (C-O-Me), 1190–1110 (C-O cyclic ether), 1060–1030

(C-O 2° OH) and 995 (C-O 1° OH); NMR δ_H ppm (400 MHz; DMSO$-$d$_6$) 0.80–1.50 (15 H, m,

C1-OCH$_2$C$_7$$H_{15}$), 3.00 (1 H, m, C4-$H$), 3.13 (1 H, m, C2-$H$), 3.25 (1 H, m, C5-$H$), 3.31 (1

H, m, C3-H), 3.38 (1 H, m, C6-OH), 3.51 (2 H, m, C1-OCH_2C$_7$H$_{15}$), 3.58 (1 H, m, C6-H),

4.44 (1 H, t, ^3J = 5.9 Hz, C6-OH), 4.47 (1 H, d, ^3J = 3.7 Hz, C1-H), 4.68 (1 H, d, ^3J

= 6.6 Hz, C2-OH), 4.72 (1 H, d, ^3J = 5.1 Hz, C3-OH) and 4.82 (1 H, d, ^3J = 5.9 Hz,

C4-OH); δ_C ppm (100.5 MHz; DMSO$-$d$_6$) 11.09 (1 C, C1-OCH$_2$CH(CH$_2$$CH_3$)C$_4H_9$), 14.12

(1 C, C1-OCH$_2$CH(C$_2$H$_5$)C$_3$H$_6$$CH_3$), 23.19 (1 C, C1-OCH$_2$CH(C$_2H_5$)C$_2H_4$$CH_2CH_3$), 23.43 (1

C, C1-OCH$_2$CH(CH$_2$CH$_3$)C$_4$H$_9$), 29.24 (1 C, C1-OCH$_2$CH(C$_2$H$_5$)CH$_2$$CH_2C_2H_5$), 30.23 (1 C,

C1-OCH$_2$CH(C$_2$H$_5$)CH$_2$C$_3$H$_7$), 42.07 (1 C, C1-OCH$_2$$C$H(C$_2H_5$)C$_4H_9$), 61.46 (1 C, C6), 65.15

(1 C, C1-CH$_2$CH(C$_2$H$_5$)C$_4$H$_9$), 70.83 (1 C, C4), 72.48 (1 C, C2), 73.13 (1 C, C5), 73.89 (1 C,

C3) and 100.17 (1 C, C1).

Decyl-α-D-glucopyranoside   IR $\tilde{\nu}$ / cm^{-1} 3550 (O-H), 3300br (O-H), 2950–2850 (C-H), 1460

(C-O-Me), 1380–1340 (1°/2° O-H), 1230 (C-O-Me), 1190–1110 (C-O cyclic ether), 1060–1030

(C-O 2° OH) and 995 (C-O 1° OH); NMR δ_H ppm (400 MHz; DMSO$-$d$_6$) 0.80 (3 H, t,

C1-OC$_9$H$_{18}$$CH_3$), 1.26 (14 H, m, C1-OC$_2H_4C_7$$H_{14}CH_3$), 1.50 (2 H, m, C1-OCH$_2$$CH_2C_8H_{17}$), 3.00

(1 H, m, C4-H), 3.13 (1 H, m, C2-H), 3.21 (2 H, t, C1-OCH_2C$_9$H$_{19}$), 3.25 (1 H, m, C5-H), 3.31

(1 H, m, C3-H), 3.38 (1 H, m, C6-OH), 3.58 (1 H, m, C6-H), 4.44 (1 H, t, ^3J = 5.9 Hz, C6-OH),

4.47 (1 H, d, $^3J = 3.7$ Hz, C1-H), 4.68 (1 H, d, $^3J = 6.6$ Hz, C2-OH), 4.72 (1 H, d, $^3J = 5.1$ Hz, C3-OH) and 4.82 (1 H, d, $^3J = 5.9$ Hz, C4-OH); δ_C ppm (100.5 MHz; DMSO$-$d$_6$) 14.07 (1 C, C1-OC$_7$H$_{18}$CH_3), 22.64 (1 C, C1-OC$_6$H$_{16}$CH_2CH$_3$), 25.72 (1 C, C1-OC$_2$H$_4$CH_2C$_7$H$_{15}$), 29.29 (1 C, C1-OC$_6$H$_{12}$CH_2C$_3$H$_7$), 29.41 (1 C, C1-OC$_5$H$_{10}$CH_2C$_4$H$_9$), 29.53 (1C, C1-OC$_3$H$_6$CH_2C$_6$H$_{13}$), 29.59 (1 C, C1-OC$_4$H$_8$CH_2C$_5$H$_{11}$), 31.86 (1 C, C1-OC$_7$H$_{14}$CH_2C$_2$H$_5$), 32.74 (1 C, C1-OCH_2CH$_2$C$_8$H$_{17}$), 62.95 (1 C, C1-OCH_2C$_9$H$_{19}$), 61.46 (1 C, C6), 70.83 (1 C, C4), 72.48 (1 C, C2), 73.13 (1 C, C5), 73.89 (1 C, C3) and 100.17 (1 C, C1).

7.4 Itaconate Surfactants

7.4.1 Esterification

Acids and Transesterification

Reactions were carried out in a round bottom flask (25 cm^3) equipped with magnetic stirrer, insulated Dean-Stark condenser, water cooled condenser and a stirrer hotplate with a thermocouple. The substrate (0.0154 mol), alcohol (2.2 mol equiv.), *tert-tri*-butyl phenol (TBP) (0.0807 g, 2 mol%) and *para*-toluene sulfonic acid (*p*-TSA) (0.292 g, 10 mol%) were charged to the reaction set-up and heated to temperature. After the allotted time the reaction was cooled and analysed by ^{1}H NMR spectroscopy. Hexane was added (10 cm^3) and the mixture was washed with aqueous Na$_2$CO$_3$ solution (10 cm^3, 0.15 mol dm^{-3}). The product was crystallised from the organic layer and recrystallised from hexane, both with cooling (-18 °C, 18 h) and recovered by vacuum filtration using chilled glassware.

Ring Opening of Cyclic Anhydrides

Microwave Reaction Anhydride (0.0154 mol) and alcohol (various mol equiv.) were charged to a microwave tube (10 cm^3, snap cap) and placed in the CEM microwave. This was heated (to various temperatures, for varying reaction lengths) and analysed by ^{1}H NMR spectroscopy for conversion calculations. Unless specified, conditions were 1 mol equiv. alcohol, 80 °C, 10 mins.
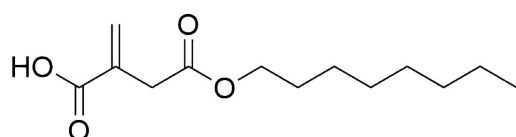
Conventional Reactions Reactions were carried out in a round bottom flask (25 cm^3) complete with magnetic stirrer flea, water cooled condenser and either a stirrer hotplate or multipoint reactor

with a thermocouple. Anhydride (0.0154 mol) and alcohol (various mol equiv.) were charged to the reaction set-up and heated to temperature (100 °C). After the 16 h the reaction was cooled and analysed by ^{1}H NMR spectroscopy. When isolation was required, the product was crystallised from the organic layer in hexane and recrystallised from a mixture of hexane and methanol (3:1 v:v), both with cooling (-18 °C, 18 h) and recovery by vacuum filtration using chilled glassware. Unless specified, 1 mol equiv. alcohol was used.

7.4.2 Sulfitation

Reactions were carried out in a round bottom flask (25 or 50 cm^3) equipped with magnetic stirrer, water cooled condenser and either a stirrer hotplate or multipoint reactor with a thermocouple. Sodium metabisulfite (SMBS) (5.70 g, 0.03 mol), water (5 g) and *iso*propyl alcohol (IPA) (5 g) were charged to the reaction set-up and once all solids were dissolved, the mixture was heated to the reaction temperature. The substrate (0.05 mol) was added and after the allotted time the reaction was analysed by ^{1}H NMR spectroscopy. IPA was removed by rotary evaporation and water was removed by freeze drying. Unless specified, conditions were 100 °C, 8 h.

7.4.3 Compounds

Mono-octyl itaconate   IR $\tilde{\nu}$ / cm^{-1} 3445br (O-H), 2920–2850 (C-H), 1738 (C=O ester), 1695 (C=O carboxylic acid), 1623 (C=C), 1075 (C-O ester), 1097 (C-O carboxylic acid); NMR δ_H / ppm (400 MHz; acetone$-$d$_6$) 0.82 (3 H, t, $^3J = 6.4$ Hz, CH_3), 1.21 (10 H, m, C$_2$H$_4$C$_5$$H_{10}CH_3$), 1.49 (2 H, m, CH$_2CH_2C_6H_{13}$), 3.25 (2 H, s, C$H_2CO_2C_8H_{17}$), 3.95 (2 H, t, $^3J = 6.6$ Hz, CH_2C$_7$H$_{15}$), 5.71 (1 H, s, HO$_2$CCH(CHH)), 6.10 (1 H, s, HO$_2$CCH(CHH)); δ_C / ppm (100.5 MHz; acetone$-$d$_6$) 14.48 (1 C, C$_7$H$_{14}$$CH_3$), 22.60 (1 C, C$_6H_{12}$$CH_2CH_3$), 25.81 (1 C, C$_2H_4$$CH_2C_5H_{11}$), 28.60 (1 C, C$_4H_8$$CH_2C_3H_7$), 29.12 (1 C, C$_3H_6$$CH_2C_4H_9$), 31.73 (1 C, C$_5H_{10}$$CH_2C_2H_5$), 37.72 (1 C, CH$_2CH_2C_6H_{13}$), 64.61 (1 C, CO$_2$$CH_2C_7H_{15}$), 128.37 (1 C, HO$_2$CCH(CH$_2$)$CH_2$), 135.44 (1 C, HO$_2CCH$(CH$_2$)), 167.81 (1 C, HO$_2$$C$CH(CH$_2$)), 171.01 (1 C, CO$_2C_8H_{17}$), 193.21 (1 C, CO$_2$H); ESI-MS *m/z* 243.1591 (MH$^+$, C$_{13}$H$_{23}$O$_4$), 265.1410 (MNa$^+$, C$_{13}$H$_{22}$NaO$_4$).
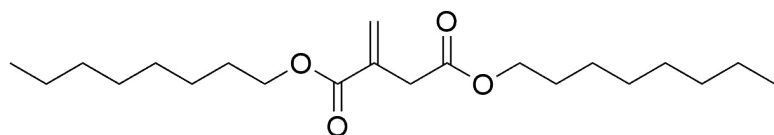
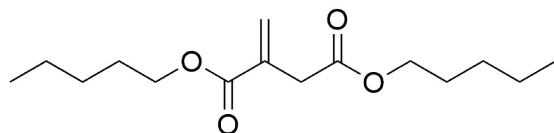**Dioctyl itaconate**   IR $\tilde{\nu}$ / cm^{-1} 2920–2850 (C-H), 1737 (C=O ester), 1637 (C=C), 1074 (C-O ester); NMR δ_H / ppm (400 MHz; acetone$-$d$_6$) 0.82 (6 H, t, $^3J = 6.4$ Hz, CH_3), 1.21 (20 H, m, CO$_2$C$_2$H$_4$C$_5$$H_{10}CH_3$), 1.49 (4 H, m, CO$_2CH_2CH_2C_6H_{13}$), 3.25 (2 H, s, C$H_2CO_2C_8H_{17}$), 3.95 (2 H, t, $^3J = 6.6$ Hz, CH$_2$CO$_2$CH_2C$_7$H$_{15}$), 4.03 (2 H, t, $^3J = 6.5$ Hz, H$_{15}$C$_7$$H_2CO_2$CCH(CH$_2$)), 5.71 (1 H, s, H$_{17}C_8CO_2$CCH(C$H$H)), 6.10 (1 H, s, H$_{17}C_8O_2$CCH(CH$H$)); δ_C / ppm (100.5 MHz; solvent) 14.48 (2 C, CO$_2$C$_7$H$_{14}$$CH_3$), 22.60 (2 C, CO$_2C_6H_{12}$$CH_2CH_3$), 25.81 (2 C, CO$_2C_2H_4$$CH_2C_5H_{11}$), 28.60 (2 C, C$_4H_8$$CH_2C_3H_7$), 29.12 (2 C, CO$_2C_3H_6$$CH_2C_4H_9$), 31.73 (2 C, CO$_2C_5H_{10}$$CH_2C_2H_5$), 37.59 (1 C, CH$_2CO_2CH_2CH_2C_6H_{13}$), 37.73 (1 C, H$_{13}C_6$$H_2CH_2CO_2$CCH(CH$_2$)), 64.42 (1 C, CH$_2CO_2$$CH_2C_7H_{15}$), 65.87 (1 C, H$_{15}C_7H_2$$CO_2$CCH(CH$_2$)), 128.37 (1 C, CH$_2CO_2C_8H_{17}$), 135.44 (1 C, H$_{17}C_8O_2$CCH(CH$_2$)), 167.81 (1 C, H$_{17}C_8O_2$$C$CH(CH$_2$)), 171.01 (1 C, CH$_2$$CO_2C_8H_{17}$), 193.21 (1 C, H$_{17}C_8O_2$$C$CH(CH$_2$)); ESI-MS m/z 355.2787 (MH$^+$, C$_{21}$H$_{39}$O$_4$), 265.1410 (MNa$^+$, C$_{21}$H$_{38}$NaO$_4$).
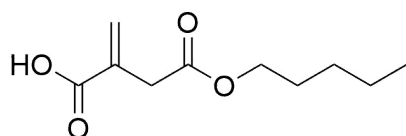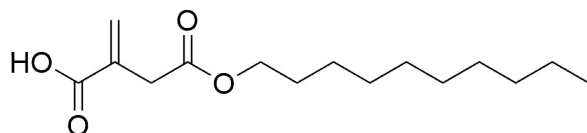

Monopentyl itaconate   IR $\tilde{\nu}$ / cm^{-1} 3442br (O-H), 2920–2850 (C-H), 1733 (C=O ester), 1708 (C=O carboxylic acid), 1624 (C=C), 1084 (C-O ester), 1089 (C-O carboxylic acid); NMR δ_H / ppm (400 MHz; acetone$-$d$_6$) 0.79 (3 H, t, $^3J = 6.9$ Hz, CH_3), 1.18 (4 H, m, CO$_2$C$_2$H$_4$C$_2$$H_4CH_3$), 1.51 (2 H, m, CO$_2CH_2CH_2C_3H_5$), 3.24 (2 H, s, C$H_2CO_2C_5H_{11}$), 3.95 (2 H, t, $^3J = 6.5$ Hz, CO$_2$CH_2C$_4$H$_9$), 5.69 (1 H, s, HO$_2$CCH(CHH)), 6.18 (1 H, s, HO$_2$CCH(CHH)); δ_C / ppm (100.5 MHz; acetone$-$d$_6$) 14.30 (1 C, CO$_2$C$_4$H$_8$$CH_3$), 22.56 (1 C, CO$_2C_2H_4$$CH_2C_2H_5$), 28.26 (1 C, CO$_2C_3H_6$$CH_2CH_3$), 32.55 (1 C, CH$_2CO_2CH_2CH_2C_3H_7$), 61.09 (1 C, CH$_2CO_2$$CH_2C_4H_9$), 128.34 (1 C, CH$_2CO_2C_5H_{11}$), 135.43 (1 C, H$_{11}C_5O_2$CCH(CH$_2$)), 167.81 (1 C, H$_{11}C_5O_2$$C$CH(CH$_2$)), 171.09 (1 C, CH$_2$$CO_2C_5H_{11}$), 193.15 (1 C, HO$_2$$C$CH(CH$_2$)); ESI-MS m/z 201.1051 (MH$^+$, C$_{10}$H$_{17}$O$_4$), 223.0921 (MNa$^+$, C$_{10}$H$_{16}$NaO$_4$).
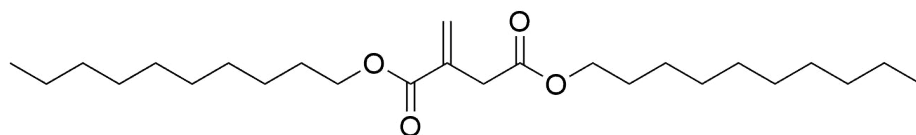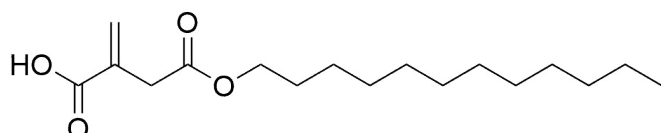
Dipentyl itaconate IR $\tilde{\nu}$ / cm^{-1} 2920–2850 (C-H), 1738 (C=O ester), 1636 (C=C), 1078 (C-O ester); NMR δ_H / ppm (400 MHz; acetone$-d_6$) 0.79 (6 H, t, $^3J = 6.9$ Hz, CH_3), 1.18 (8 H, m, CO$_2$C$_2$H$_4$C$_2$H$_4$CH$_3$), 1.51 (4 H, m, CO$_2$CH$_2$CH_2C$_3$H$_5$), 3.24 (2 H, s, CH_2CO$_2$C$_5$H$_{11}$), 3.95 (2 H, t, $^3J = 6.5$ Hz, CH$_2$CO$_2$CH_2C$_4$H$_9$), 4.01 (2 H, t, $^3J = 6.6$ Hz, H$_9$C$_4$H$_2$CO$_2$CCH(CH$_2$)CH$_2$CO$_2$C$_5$H$_{11}$), 5.69 (1 H, s, H$_{11}$C$_5$O$_2$CCH(CHH)), 6.18 (1 H, s, H$_{11}$C$_5$O$_2$CCH(CHH)); δ_C / ppm (100.5 MHz; acetone$-d_6$) 14.30 (2 C, CO$_2$C$_4$H$_8$$CH_3$), 22.56 (2 C, CO$_2C_2H_4$$CH_2C_2H_5$), 28.26 (2 C, CO$_2C_3H_6$$CH_2CH_3$), 32.55 (1 C, CH$_2CO_2CH_2$$CH_2C_3H_7$), 32.74 (1 C, H$_7C_3H_2$$CH_2CO_2$CCH(CH$_2$)), 61.09 (1 C, CH$_2CO_2$$CH_2C_4H_9$), 62.34 (1 C, H$_9C_4H_2CO_2$$C$CH), 128.34 (1 C, CH$_2CO_2C_5H_{11}$), 135.43 (1 C, H$_{11}C_5O_2$CCH(CH$_2$)), 167.81 (1 C, H$_{11}C_5O_2$$C$CH), 171.09 (1 C, CH$_2$$CO_2C_5H_{11}$), 193.15 (1 C, H$_{11}C_5O_2$$C$CH(CH$_2$)); ESI-MS m/z 257.1689 (MH$^+$, C$_{15}$H$_{27}$O$_4$), 279.1638 (MNa$^+$, C$_{15}$H$_{26}$NaO$_4$).
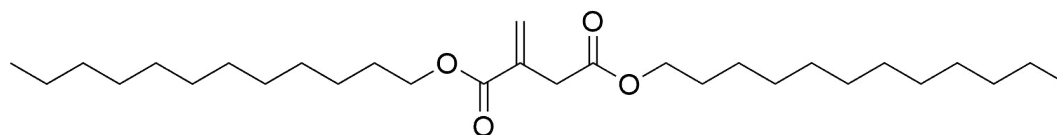

Monodecyl itaconate IR $\tilde{\nu}$ / cm^{-1} 3448br (O-H), 2920–2850 (C-H), 1735 (C=O ester), 1707 (C=O carboxylic acid), 1622 (C=C), 1076 (C-O ester), 1097 (C-O carboxylic acid); NMR δ_H / ppm (400 MHz; acetone$-d_6$) 0.79 (3 H, t, $^3J = 6.9$ Hz, CH_3), 1.20 (14 H, m, CO$_2$C$_2$H$_4$C$_7$H$_{14}$CH$_3$), 1.51 (2 H, m, CO$_2$CH$_2$CH_2C$_8$H$_{17}$), 3.24 (2 H, s, CH_2CO$_2$C$_{10}$H$_{21}$), 3.95 (2 H, t, $^3J = 6.5$ Hz, CO$_2$CH_2C$_9$H$_{19}$), 5.65 (1 H, s, HO$_2$CCH(CHH)), 6.19 (1 H, s, HO$_2$CCH(CHH)); δ_C / ppm (100.5 MHz; acetone$-d_6$) 14.07 (1 C, CO$_2$C$_9$H$_{18}$$CH_3$), 22.64 (1 C, CO$_2C_8H_{16}$$CH_2CH_3$), 25.72 (1 C, CO$_2C_2H_4$$CH_2C_7H_{15}$), 29.29 (1 C, CO$_2C_6H_{12}$$CH_2C_3H_7$), 29.41 (1 C, CO$_2C_5H_{10}$$CH_2C_4H_9$), 29.53 (1 C, CO$_2C_3H_6$$CH_2C_6H_{13}$), 29.59 (1 C, CO$_2C_4H_8$$CH_2C_5H_{11}$), 31.86 (1 C, C$_7H_{14}$$CH_3C_2H_5$), 32.74 (1 C, CO$_2CH_2CH_2C_8H_{17}$), 62.95 (1 C, CO$_2$$CH_2C_9H_{19}$), 128.47 (1 C, CH$_2CO_2C_{10}H_{21}$), 135.40 (1 C, HO$_2$CCH(CH$_2$)), 167.80 (1 C, HO$_2$$C$CH(CH$_2$)), 171.00 (1 C, CH$_2$$CO_2C_{10}H_{21}$), 193.79 (1 C, HO$_2$$C$CH(CH$_2$)); ESI-MS m/z 271.1898 (MH$^+$, C$_{15}$H$_{27}$O$_4$), 293.1728 (MNa$^+$, C$_{15}$H$_{26}$NaO$_4$.
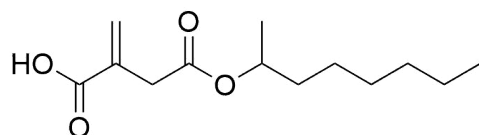
Didecyl itaconate   IR $\tilde{\nu}$ / cm^{-1} 2920–2850 (C-H), 1737 (C=O ester), 1623 (C=C), 1074 (C-O ester); NMR δ_H / ppm (400 MHz; acetone$-$d$_6$) 0.79 (6 H, t, ^3J = 6.9 Hz, CH_3), 1.20 (28 H, m, CO$_2$C$_2$H$_4$C$_7$$H_{14}CH_3$), 1.51 (4 H, m, CO$_2CH_2CH_2C_8H_{17}$), 3.24 (2 H, s, C$H_2CO_2C_{10}H_{21}$), 3.95 (2 H, t, ^3J = 6.5 Hz, CH$_2$CO$_2$CH_2C$_9$H$_{19}$), 4.02 (2 H, t, ^3J = 6.6 Hz, H$_{19}$C$_9$$H_2CO_2$CCH(CH$_2$)), 5.65 (1 H, s, H$_{21}C_{10}O_2$CCH(C$H$H)), 6.19 (1 H, s, H$_{21}C_{10}O_2$CCH(CH$H$)); δ_C / ppm (100.5 MHz; acetone$-$d$_6$) 14.07 (2 C, CO$_2$C$_9$H$_{18}$$CH_3$), 22.64 (2 C, CO$_2C_8H_{16}$$CH_2CH_3$), 25.72 (2 C, CO$_2C_2H_4$$CH_2C_7H_{15}$), 29.29 (2 C, CO$_2C_6H_{12}$$CH_2C_3H_7$), 29.41 (2 C, CO$_2C_5H_{10}$$CH_2C_4H_9$), 29.53 (2 C, CO$_2C_3H_6$$CH_2C_6H_{13}$), 29.59 (2 C, CO$_2C_4H_8$$CH_2C_5H_{11}$), 31.86 (2 C, C_7H$_{14}CH_3C_2H_5$), 32.69 (1 C, CH$_2CO_2CH_2$$CH_2C_8H_{17}$), 32.74 (1 C, H$_{17}C_8H_2$$CCH_2CO_2$CCH(CH$_2$)), 61.95 (1 C, CH$_2CO_2$$CH_2C_9H_{19}$), 62.95 (1 C, H$_{19}C_9H_2$$CO_2$CCH(CH$_2$)), 128.47 (1 C, CH$_2CO_2C_{10}H_{21}$), 135.40 (1 C, H$_{21}C_{10}O_2$CCH(CH$_2$)), 167.80 (1 C, H$_{21}C_{10}O_2$$C$CH(CH$_2$)), 171.00 (1 C, CH$_2$$CO_2C_{10}H_{21}$), 193.79 (1 C, H$_{21}C_{10}O_2$$C$CH(CH$_2$)); ESI-MS m/z 411.3494 (MH$^+$, C$_{25}$H$_{47}$O$_4$), 433.3338 (MNa$^+$, C$_{25}$H$_{46}$NaO$_4$.


Monododecyl itaconate   IR $\tilde{\nu}$ / cm^{-1} 3443br (O-H), 2920–2850 (C-H), 1736 (C=O ester), 1703 (C=O carboxylic acid), 1623 (C=C), 1076 (C-O ester), 1095 (C-O carboxylic acid); NMR δ_H / ppm (400 MHz; acetone$-$d$_6$) 0.80 (3 H, t, ^3J = 6.6 Hz, CH_3), 1.20 (18 H, m, CO$_2$C$_2$H$_4$C$_9$$H_{19}CH_3$), 1.51 (2 H, m, CO$_2CH_2CH_2C_{10}H_{21}$), 3.26 (2 H, s, C$H_2CO_2C_{12}H_{25}$), 3.95 (2 H, t, ^3J = 6.4 Hz, CO$_2$CH_2C$_{11}$H$_{23}$), 5.69 (1 H, s, HO$_2$CCH(CHH)), 6.08 (1 H, s, HO$_2$CCH(CHH)); δ_C / ppm (100.5 MHz; acetone$-$d$_6$) 14.11 (1 C, CH$_3$), 22.77 (1 C, CO$_2$C$_{10}$H$_{20}$$CH_2CH_3$), 29.91 (1 C, CO$_2C_2H_4$$CH_2C_9H_{19}$), 29.46 (1 C, CO$_2C_8H_{16}$$CH_2C_3H_7$), 29.59 (1 C, CO$_2C_3H_6$$CH_2C_8H_{17}$), 29.76 (4 C, CO$_2C_4H_8$$C_4H_8C_4H_9$), 32.03 (1 C, CO$_2C_9H_{18}$$CH_2C_2H_5$), 32.88 (1 C, CO$_2CH_2$$CH_2C_{10}H_{21}$), 62.87 (1 C, CO$_2$$CH_2C_{11}H_{23}$) 128.61 (1 C, CH$_2CO_2C_{12}H_{25}$), 135.44 (1 C, CH(CH$_2$)CO$_2$H), 167.88 (1 C, CH(CH$_2$)CO$_2$H), 171.09 (1 C, CO$_2C_{12}H_{25}$), 193.25 (1 C, CO$_2$H); ESI-MS m/z 299.2163 (MH$^+$, C$_{17}$H$_{31}$O$_4$), 321.2045 (MNa$^+$, C$_{17}$H$_{30}$NaO$_4$.

Didodecyl itaconate IR $\tilde{\nu}$ / cm^{-1} 2920–2850 (C-H), 1745 (C=O ester), 1639 (C=C), 1072 (C-O ester); NMR δ_H / ppm (400 MHz; acetone$-$d$_6$) 0.80 (6 H, t, ^3J = 6.6 Hz, CH_3), 1.20 (36 H, m, CO$_2$C$_2$H$_4$C$_9H_{19}$CH$_3$), 1.51 (4 H, m, CO$_2$CH$_2$CH_2C$_{10}$H$_{21}$), 3.26 (2 H, s, H_2CO$_2$C$_{12}$H$_{25}$), 3.95 (2 H, t, ^3J = 6.4 Hz, CH$_2$CO$_2$CH_2C$_{11}$H$_{23}$), 4.02 (2 H, t, ^3J = 6.4 Hz, H$_{23}$C$_{11}$$H_2CO_2$CCH(CH$_2$)), 5.69 (1 H, s, H$_{25}C_{12}O_2$CCH(C$H$H)), 6.08 (1 H, s, H$_{25}C_{12}O_2$CCH(CH$H$)); δ_C / ppm (100.5 MHz; acetone$-$d$_6$) 14.11 (2 C, CH$_3$), 22.77 (2 C, C$_{10}$H$_{20}$$CH_2CH_3$), 29.91 (2 C, CO$_2C_2H_4$$CH_2C_9H_{19}$), 29.46 (2 C, CO$_2C_8H_{16}$$CH_2C_3H_7$), 29.59 (2 C, CO$_2C_3H_6$$CH_2C_8H_{17}$), 29.76 (8 C, C$_4H_8$$C$$_4H_8C_4H_9$), 32.03 (2 C, CO$_2C_9H_{18}$$CH_2C_2H_5$), 32.88 (1 C, CH$_2CO_2CH_2$$CH_2C_{10}H_{21}$), 32.92 (1 C, H$_{21}C_{10}$$H_2CH_2CO_2$CCH), 62.87 (1 C, CH$_2CO_2$$CH_2C_{11}H_{23}$), 62.95 (1 C, H$_{23}C_{11}H_2$$CO_2$CCH), 128.61 (1 C, CH$_2CO_2C_{12}H_{25}$), 135.44 (1 C, CH(CH$_2$)CO$_2C_{12}H_{25}$), 167.88 (1 C, CHCO$_2C_{12}H_{25}$), 171.09 (1 C, CH$_2$$CO_2C_{12}H_{25}$), 193.25 (1 C, CH$CO_2C_{12}H_{25}$); ESI-MS m/z 467.4075 (MH$^+$, C$_{29}$H$_{55}$O$_4$), 489.3924 (MNa$^+$, C$_{29}$H$_{54}$NaO$_4$.

Mono-1-methyl-septyl itaconate IR $\tilde{\nu}$ / cm^{-1} 3450br (O-H), 2920–2850 (C-H), 1733 (C=O ester), 1704 (C=O carboxylic acid), 1624 (C=C), 1079 (C-O ester), 1100 (C-O carboxylic acid); NMR δ_H / ppm (400 MHz; acetone$-$d$_6$) 1.45–0.76 (16 H, m, CO$_2$CH(CH_3)C$_6$$H_{13}$), 3.19 (2 H, s, C$H_2CO_2C_8H_{17}$), 4.75 (1 H, m, CO$_2CH$(CH$_3$)C$_6H_{13}$), 5.65 (1 H, s, HO$_2$CCH(CH$H$)), 6.15 (1 H, s, HO$_2$CCH(C$H$H)); δ_C / ppm (100.5 MHz; acetone$-$d$_6$) 14.07 (1 C, CO$_2$CH(CH$_3$)C$_5$H$_{10}$$CH_3$), 22.68 (1 C, CO$_2$CH(CH$_3$)C$_4H_8$$CH_2CH_3$), 23.39 (1 C, CO$_2$CH($CH_3$)C$_6H_{13}$), 25.83 (1 C, CO$_2$CH(CH$_3$)CH$_2$$CH_2C_4H_9$), 29.42 (1 C, CO$_2$CH(CH$_3$)C$_2H_4$$CH_2C_3H_7$), 31.94 (1 C, CO$_2$CH(CH$_3$)C$_3H_6$$CH_2C_2H_5$), 39.42 (1 C, CH(CH$_3$)$CH_2C_5H_{11}$), 68.02 (1 C, CH(CH$_3$)C$_6H_{13}$), 128.39 (1 C, CH$_2CO_2C_8H_{17}$), 135.41 (1 C, HO$_2$CCH(CH$_2$)), 167.82 (1 C, HO$_2$CCH(CH$_2$)), 171.56 (1 C, CH$_2$$CO_2C_8H_{17}$), 193.64 (1 C, HO$_2$$C$CH(CH$_2$)); ESI-MS m/z 243.1591 (MH$^+$, C$_{13}$H$_{23}$O$_4$), 265.1410 (MNa$^+$, C$_{13}$H$_{22}$NaO$_4$).
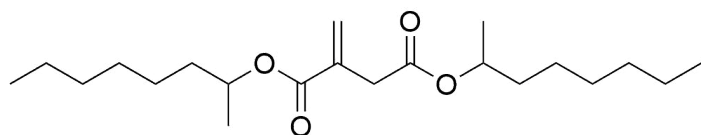
Di-1-methyl-septyl itaconate　IR $\tilde{\nu}$ / cm^{-1} 2920–2850 (C-H), 1728 (C=O ester), 1624 (C=C), 1072 (C-O ester); NMR δ_H / ppm (400 MHz; acetone$-$d$_6$) 1.45–0.76 (32 H, m, CO$_2$CH(CH_3)C$_6H_{13}$), 3.19 (2 H, s, CH_2CO$_2$C$_8$H$_{17}$), 4.75 (1 H, m, CH$_2$CO$_2$CH(CH$_3$)C$_6$H$_{13}$), 4.84 (1 H, m, H$_{13}$C$_6$(H$_3$C)HCO$_2$CCH(CH$_2$)), 5.65 (1 H, s, H$_{17}$C$_8$O$_2$CCH(CHH)), 6.15 (1 H, s, H$_{17}$C$_8$O$_2$CCH(CHH)); δ_C / ppm (100.5 MHz; acetone$-$d$_6$) 14.07 (2 C, CO$_2$CH(CH$_3$)C$_5$H$_{10}$$CH_3$), 22.68 (2 C, CO$_2$CH(CH$_3$)C$_4H_8$$CH_2CH_3$), 23.39 (2 C, CO$_2$CH($CH_3$)C$_6H_{13}$), 25.83 (2 C, CO$_2$CH(CH$_3$)CH$_2$$CH_2C_4H_9$), 29.42 (2 C, CO$_2$CH(CH$_3$)C$_2H_4$$CH_2C_3H_7$), 31.94 (2 C, CO$_2$CH(CH$_3$)C$_3H_6$$CH_2C_2H_5$), 39.42 (1 C, CH$_2CO_2$CH(CH$_3$)CH$_2C_5H_{11}$), 39.98 (1 C, H$_{11}C_5H_2$$C$(H$_3$C)HCO$_2CCHC$H2CH$_2$), 68.02 (1 C, CH(CH$_2$)CH$_2CO_2$$C$H(CH$_3$)C$_6H_{13}$), 68.15 (1 C, H$_{13}C_6$(H$_3$C)H$CO_2$CCH), 128.39 (1 C, CH$_2CO_2C_8H_{17}$), 135.41 (1 C, H$_{17}C_8O_2$CCH(CH$_2$)), 167.82 (1 C, H$_{17}C_8O_2$$C$CH), 171.56 (1 C, CH$_2$$CO_2C_8H_{17}$), 193.64 (1 C, H$_{17}C_8O_2$$C$CH(CH$_2$)); ESI-MS m/z 355.2787 (MH$^+$, C$_{21}$H$_{39}$O$_4$), 265.1410 (MNa$^+$, C$_{21}$H$_{38}$NaO$_4$).
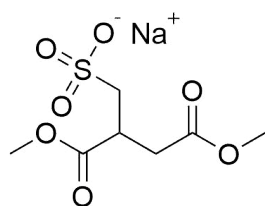
Dimethyl sulfo-methylene-succinate　IR $\tilde{\nu}$ / cm^{-1} 2920–2850 (C-H), 1734 (C=O ester), 1406 (C-S), 1347 (S=O), 1080 (C-O ester), 1049 (S=O); NMR δ_H / ppm (400 MHz; acetone$-$d$_6$) 2.75 (2 H, m, CH_2SO$_3$), 3.05 (1 H, m, CHCH$_2$SO$_3$), 3.19 (2 H, m, CH_2CO$_2$CH$_3$), 3.57 (3 H, s, CH(CH$_2$SO$_3$)CO$_2$CH_3), 3.61 (3 H, s, CH$_2$CO$_2$CH_3); δ_C / ppm (100.5 MHz; acetone$-$d$_6$) 34.88 (1 C, CH$_2$SO$_3$), 38.10 (1 C, CHCH$_2$SO$_3$), 51.44 (1 C, CH$_2$CO$_2$CH$_3$), 52.51 (1 C, CHCO$_2$$CH_3$), 52.97 (1 C, CH$_2CO_2$$CH_3$), 174.14 (1 C, CH(CH$_2SO_3$)$CO_2CH_3$), 175.60 (1 C, CH$_2$$CO_2CH_3$); ESI-MS m/z 239.0231 (M$^-$, C$_7$H$_{11}$O$_7$S).

Sulfo-methylene-succinic acid   IR $\tilde{\nu}$ / cm^{-1} 3442br (O-H), 2920–2850 (C-H), 1600 (C=O carboxylate salt), 1400 (C-S), 1359 (S=O), 1325 (C-O carboxylate salt), 1050 (S=O); NMR δ_H / ppm (400 MHz; acetone$-$d$_6$) 2.69 (2 H, m, CH_2SO$_3$), 2.99 (1 H, dd, $^3J = 13.7$, 6.9 Hz, CHHCO$_2$H), 3.06 (1 H, m, CH), 3.19 (1 H, dd, $^3J = 13.7$, 5.5 Hz, CHHCO$_2$H); δ_C / ppm (100.5 MHz; acetone$-$d$_6$) 35.58 (1 C, CH$_2$SO$_3$), 38.75 (1 C, CH), 51.69 (1 C, CH$_2$CO$_2$H), 176.21 (1 C, CHCO$_2$H), 177.68 (1 C, CH$_2$$CO_2$H); ESI-MS m/z 210.9918 (M$^-$, C$_5$H$_7$O$_7$S).
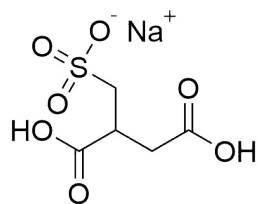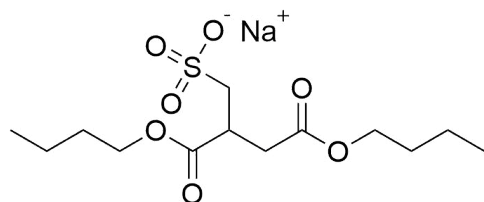
Dibutyl sulfo-methylene-succinate   IR $\tilde{\nu}$ / cm^{-1} 2920–2850 (C-H), 1738 (C=O ester), 1403 (C-S), 1350 (S=O), 1084 (C-O ester), 1053 (S=O); NMR δ_H / ppm (400 MHz; acetone$-$d$_6$) 0.75 (6 H, t, $^3J = 7.3$ Hz, CH_3), 1.22 (4 H, m, CO$_2$C$_2$H$_4$CH_2CH$_3$), 1.47 (4 H, m, CO$_2$CH$_2$CH_2C$_2$H$_5$), 2.76 (2 H, m, CH_2SO$_3$), 3.03 (1 H, m, CH), 3.18 (2 H, m, C)H_2CO$_2$C$_4$H$_9$), 3.98 (2 H, t, $^3J = 6.9$ Hz, CH(CH$_2$SO$_3$)CO$_2$CH_2C$_3$H$_7$), 4.00 (2 H, t, $^3J = 6.9$ Hz, CH$_2$CO$_2$CH_2C$_3$H$_7$); δ_C / ppm (100.5 MHz; acetone$-$d$_6$) 14.41 (2 C, CH$_3$), 28.26 (2 C, CH$_2$CH$_3$), 32.60 (1 C, CH(CH$_2$SO$_3$)CO$_2$CH$_2$$CH_2C_2H_5$), 32.74 (1 C, CH$_2CO_2CH_2$$CH_2C_2H_5$), 34.88 (1 C, CH$_2SO_3$), 38.10 (1 C, CH), 51.44 (1 C, CH$_2$CO$_2$C$_4$H$_9$), 52.51 (1 C, CH(CH$_2$SO$_3$)CO$_2$$CH_2C_3H_7$), 52.97 (1 C, CH$_2CO_2$$CH_2C_3H_7$), 176.24 (1 C, CH(CH$_2SO_3$)$CO_2C_4H_9$), 178.09 (1 C, CH$_2$$CO_2C_4H_9$); ESI-MS m/z 323.1170 (M$^-$, C$_{13}$H$_{23}$O$_7$S).

Mono-octyl sulfo-methylene-succinate   IR $\tilde{\nu}$ / cm^{-1} 3446br (O-H), 2920–2850 (C-H), 1738 (C=O ester), 1593 (C=O carboxylate salt), 1407 (C-S), 1339 (S=O), 1328 (C-O carboxylate salt), 1098 (C-O ester), 1049 (S=O); NMR δ_H / ppm (400 MHz; acetone$-$d$_6$) 0.82 (3 H, t, $^3J = 6.4$ Hz, CH_3), 1.21 (10 H, m, CO$_2$C$_2$H$_4$C$_5$$H_{10}CH_3$), 1.49 (2 H, m, CO$_2CH_2CH_2C_6H_{13}$), 2.76 (2 H, m, C$H_2SO_3$), 3.05 (1 H, m, C$H$), 3.26 (2 H, m, C$H2CO_2C_8H_{17}$), 3.95 (2 H, t, $^3J = 6.6$ Hz, CO$_2$CH_2C$_7$H$_{15}$), δ_C / ppm (100.5 MHz; acetone$-$d$_6$) 14.48 (1 C, CO$_2$C$_7$H$_{14}$CH_3), 22.60 (1 C, CO$_2$C$_6$H$_{12}$CH_2CH$_3$), 25.81 (1 C, CO$_2$C$_2$H$_4$CH_2C$_5$H$_{11}$), 28.60 (1 C, CO$_2$C$_4$H$_8$CH_2C$_3$H$_7$), 29.12 (1 C, CO$_2$C$_3$H$_6$CH_2C$_4$H$_9$), 31.73 (1 C, CO$_2$C$_5$H$_{10}$CH_2C$_2$H$_5$), 34.88 (1 C, CH_2SO$_3$), 37.72 (1 C, CO$_2$CH$_2$CH_2C$_6$H$_{13}$), 38.10 (1 C, CH), 51.44 (1 C, CH_2CO$_2$C$_8$H$_{17}$), 64.61 (1 C, CO$_2$CH_2C$_7$H$_{15}$), 174.14 (1 C, CH$_2$CO_2C$_8$H$_{17}$), 195.60 (1 C, HO$_2$CCH(CH$_2$SO$_3$)); ESI-MS m/z 323.1170 (M$^-$, C$_{13}$H$_{23}$O$_7$S).
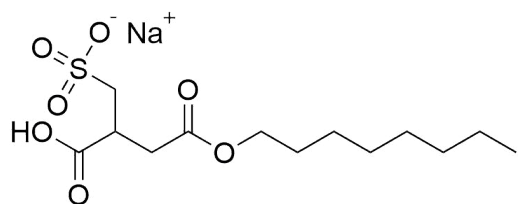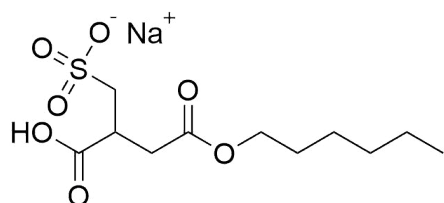
Monohexyl sulfo-methylene-succinate   IR $\tilde{\nu}$ / cm^{-1} 3443br (O-H), 2920–2850 (C-H), 1739 (C=O ester), 1608 (C=O carboxylate salt), 1410 (C-S), 1348 (S=O), 1325 (C-O carboxylate salt), 1098 (C-O ester), 1046 (S=O); NMR δ_H / ppm (400 MHz; acetone$-$d$_6$) 0.86 (3 H, t, $^3J = 6.6$ Hz, CH_3), 1.28 (6 H, m, CO$_2$C$_2$H$_4$C$_3$$H_6CH_3$), 1.52 (2 H, m, CO$_2CH_2CH_2C_4H_9$), 2.71 (2 H, m, C$H_2SO_3$), 3.00 (1 H, m, C$HCH_2SO_3$), 3.18 (2 H, m, C$H2CO_2C_6H_{13}$), 3.96 (2 H, t, $^3J = 6.3$ Hz, CO$_2$CH_2C$_5$H$_{11}$), δ_C / ppm (100.5 MHz; acetone$-$d$_6$) 14.08 (1 C, CH_3), 22.75 (1 C, CO$_2$C$_4$H$_8$CH_2CH$_3$), 25.59 (1 C, CO$_2$C$_2$H$_4$CH_2C$_3$H$_7$), 31.80 (1 C, CO$_2$C$_3$H$_6$CH_2C$_2$H$_5$), 32.79 (1 C, CO$_2$CH$_2$CH_2C$_4$H$_9$), 34.88 (1 C, CH_2SO$_3$), 38.10 (1 C, CH), 51.44 (1 C, CH_2CO$_2$C$_6$H$_{13}$), 52.97 (1 C, CO$_2$CH_2C$_5$H$_{11}$), 176.24 (1 C, CO_2H), 178.09 (1 C, CO_2C$_6$H$_{13}$); ESI-MS m/z 295.0857 (M$^-$, C$_{11}$H$_{19}$O$_7$S).

Monodecyl sulfo-methylene-succinate   IR $\tilde{\nu}$ / cm^{-1} 3435br (O-H), 2920–2850 (C-H), 1739 (C=O ester), 1592 (C=O carboxylate salt), 1408 (C-S), 1346 (S=O), 1325 (C-O carboxylate salt), 1095 (C-O ester), 1049 (S=O); NMR δ_H / ppm (400 MHz; acetone−d$_6$) 0.82 (3 H, t, $^3J = 6.4$ Hz, CH_3), 1.21 (14 H, m, CO$_2$C$_2$H$_4$C$_7$$H_{14}CH_3$), 1.49 (2 H, m, CO$_2CH_2CH_2C_8H_{17}$), 2.76 (2 H, m, C$H_2SO_3$), 3.05 (1 H, m, C$HCH_2SO_3$), 3.26 (2 H, m, C$H2CO_2C_{10}H_{21}$), 3.95 (2 H, t, $^3J = 6.6$ Hz, CO$_2$CH_2C$_9$H$_{19}$), δ_C / ppm (100.5 MHz; acetone−d$_6$) 14.07 (1 C, CO$_2$C$_9$H$_{18}$$CH_3$), 22.64 (1 C, CO$_2C_8H_{16}$$CH_2CH_3$), 25.72 (1 C, CO$_2C_2H_4$$CH_2C_7H_{15}$), 29.29 (1 C, CO$_2C_6H_{12}$$CH_2C_3H_7$), 29.41 (1 C, CO$_2C_5H_{10}$$CH_2C_4H_9$), 29.53 (1 C, CO$_2C_3H_6$$CH_2C_6H_{13}$), 29.59 (1 C, CO$_2C_4H_8$$CH_2C_5H_{11}$), 31.86 (1 C, CO$_2C_7H_{14}$$CH_3C_2H_5$), 32.74 (1 C, CO$_2CH_2CH_2C_8H_{17}$), 34.88 (1 C, CH$_2SO_3$), 38.10 (1 C, CH), 51.44 (1 C, CH$_2$CO$_2$C$_4$H$_9$), 52.97 (1 C, CH$_2$CO$_2$CH$_2$C$_9$H$_{19}$), 176.24 (1 C, CH(CH$_2$SO$_3$)CO$_2$H), 178.09 (1 C, CH$_2$$CO_2C_{10}H_{21}$); ESI-MS *m/z* 351.1483 (M$^-$, C$_{15}$H$_{27}$O$_7$S).
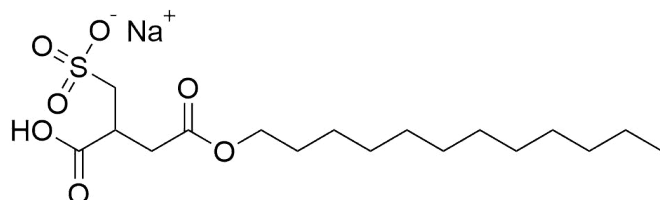
Monododecyl sulfo-methylene-succinate   IR $\tilde{\nu}$ / cm^{-1} 3442br (O-H), 2920–2850 (C-H), 1733 (C=O ester), 1599 (C=O carboxylate salt), 1402 (C-S), 1348 (S=O), 1317 (C-O carboxylate salt), 1084 (C-O ester), 1059 (S=O); NMR δ_H / ppm (400 MHz; acetone−d$_6$) 0.82 (3 H, t, $^3J = 6.4$ Hz, CH_3), 1.21 (18 H, m, CO$_2$C$_2$H$_4$C$_9$$H_{18}CH_3$), 1.49 (2 H, m, CO$_2CH_2CH_2C_{10}H_{21}$), 2.76 (2 H, m, C$H_2SO_3$), 3.05 (1 H, m, C$HCH_2SO_3$), 3.26 (2 H, m, C$H2CO_2C_{12}H_{25}$), 3.95 (2 H, t, $^3J = 6.6$ Hz, CO$_2$CH_2C$_{11}$H$_{23}$), δ_C / ppm (100.5 MHz; acetone−d$_6$) 14.11 (1 C, CH_3), 22.77 (1 C, CO$_2$C$_{10}$H$_{20}$$CH_2CH_3$), 25.91 (1 C, CO$_2C_2H_4$$CH_2C_9H_{19}$), 29.46 (1 C, CO$_2C_8H_{16}$$CH_2C_3H_7$), 29.59 (1 C, CO$_2C_3H_6$$CH_2C_8H_{17}$), 29.76 (4 C, CO$_2C_4H_8$$C_4H_8C_4H_9$), 32.03 (1 C, CO$_2C_9H_{18}$$CH_2C_2H_5$), 32.88 (1 C, CH$_2CH_2C_{10}H_{21}$), 34.88 (1 C, C$H_2SO_3$), 38.10 (1 C, C$H$), 51.44 (1 C, C$H_2CO_2C_{12}H_{25}$), 52.97 (1 C, C$H_2CO_2CH_2C_{11}H_{23}$), 176.24 (1 C, CO$_2$H), 178.09 (1 C, CO$_2C_{12}H_{25}$); ESI-MS *m/z* 379.1774 (M$^-$, C$_{17}$H$_{31}$O$_7$S).
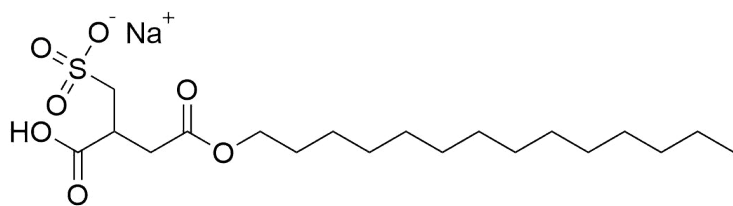
Monotetradecyl sulfo-methylene-succinate IR $\tilde{\nu}$ / cm^{-1} 3445br (O-H), 2920–2850 (C-H), 1736 (C=O ester), 1593 (C=O carboxylate salt), 1400 (C-S), 1356 (S=O), 1327 (C-O carboxylate salt), 1094 (C-O ester), 1043 (S=O); NMR δ_H / ppm (400 MHz; acetone$-d_6$) 0.82 (3 H, t, ^3J = 6.4 Hz, CH_3), 1.21 (22 H, m, $CO_2C_2H_4C_{11}H_{22}CH_3$), 1.49 (2 H, m, $CO_2CH_2CH_2C_{12}H_{25}$), 2.76 (2 H, m, CH_2SO_3), 3.05 (1 H, m, CHCH$_2$SO$_3$), 3.26 (2 H, m, C$H2$CO$_2$C$_{14}$H$_{29}$), 3.95 (2 H, t, ^3J = 6.6 Hz, CO$_2$CH_2C$_{13}$H$_{27}$), δ_C / ppm (100.5 MHz; acetone$-d_6$) 14.13 (1 C, CH_3), 22.77 (1 C, CO$_2$C$_{12}$H$_{24}$CH_2CH$_3$), 25.91 (1 C, CO$_2$C$_2$H$_4$CH_2C$_{11}$H$_{23}$), 29.47 (1 C, CO$_2$C$_{10}$H$_{20}$CH_2C$_3$H$_7$), 29.59 (1 C, C$_3$H$_6$CH_2C$_{10}$H$_{21}$), 29.79 (6 C, C$_4$H$_8$C$_6$H$_{12}$C$_4$H$_9$), 32.03 (1 C, CO$_2$C$_{11}$H$_{22}$CH_2C$_2$H$_5$), 32.86 (1 C, CH_2CH$_2$C$_{12}$H$_{25}$), 34.88 (1 C, CH_2SO$_3$), 38.10 (1 C, CH), 51.44 (1 C, CH_2CO$_2$C$_{14}$H$_{29}$), 52.97 (1 C, CH$_2$CO$_2$CH_2C$_{13}$H$_{27}$), 176.24 (1 C, CO_2H), 178.09 (1 C, CO_2C$_{14}$H$_{29}$); ESI-MS m/z 407.2109 (M$^-$, C$_{19}$H$_{35}$O$_7$S).

Mono-octyl sulfo-succinate IR $\tilde{\nu}$ / cm^{-1} 3448br (O-H), 2920–2850 (C-H), 1733 (C=O ester), 1600 (C=O carboxylate salt), 1402 (C-S), 1344 (S=O), 1330 (C-O carboxylate salt), 1101 (C-O ester), 1049 (S=O); NMR δ_H / ppm (400 MHz; acetone$-d_6$) 0.80 (3 H, t, ^3J = 6.9 Hz, CH_3), 1.23 (10 H, m, CO$_2$C$_2$H$_4$C$_5$H$_{10}$CH$_3$), 1.58 (2 H, m, CO$_2$CH$_2$CH_2C$_6$H$_{13}$), 2.90 (2 H, m, C$H2$CHSO$_3$), 3.94 (1 H, m, CH), 4.05 (2 H, t, ^3J = 6.6 Hz, CO$_2$CH_2C$_7$H$_{15}$), δ_C / ppm (100.5 MHz; acetone$-d_6$) 14.48 (1 C, CO$_2$C$_7$H$_{14}$CH_3), 22.60 (1 C, CO$_2$C$_6$H$_{12}$CH_2CH$_3$), 25.81 (1 C, CO$_2$C$_2$H$_4$CH_2C$_5$H$_{11}$), 28.60 (1 C, CO$_2$C$_4$H$_8$CH_2C$_3$H$_7$), 29.12 (1 C, CO$_2$C$_3$H$_6$CH_2C$_4$H$_9$), 31.73 (1 C, CO$_2$C$_5$H$_{10}$CH_2C$_2$H$_5$), 33.21 (1 C, CH_2CO$_2$C$_8$H$_{17}$), 37.73 (1 C, CO$_2$CH$_2$CH_2C$_6$H$_{13}$), 53.57 (1 C, CO$_2$CH_2C$_7$H$_{14}$), 61.68 (1 C, CH), 169.73 (1 C, CH(SO$_3$)CO_2H), 173.14 (1 C, CO_2C$_8$H$_{17}$); ESI-MS m/z 309.1013 (M$^-$, C$_{12}$H$_{21}$O$_7$S).
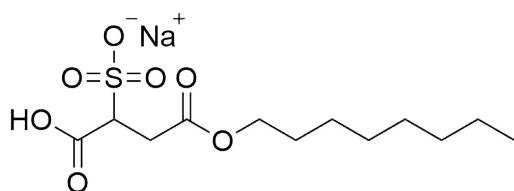
Monodecyl sulfo-succinate   IR $\tilde{\nu}$ / cm^{-1} 3450br (O-H), 2920–2850 (C-H), 1730 (C=O ester), 1598 (C=O carboxylate salt), 1408 (C-S), 1344 (S=O), 1325 (C-O carboxylate salt), 1091 (C-O ester), 1049 (S=O); NMR δ_H / ppm (400 MHz; acetone$-$d$_6$) 0.85 (3 H, t, ^3J = 6.9 Hz, CH_3), 1.25 (14 H, m, $CO_2C_2H_4C_7H_{14}CH_3$), 1.56 (2 H, m, $CO_2CH_2CH_2C_8H_{17}$), 2.96 (2 H, m, C$H2$CHSO$_3$), 3.91 (1 H, m, CHSO$_3$), 4.03 (2 H, t, ^3J = 6.6 Hz, $CO_2CH_2C_9H_{19}$), δ_C / ppm (100.5 MHz; acetone$-$d$_6$) 14.11 (1 C, CH_3), 22.77 (1 C, $CO_2C_8H_{16}CH_2CH_3$), 29.91 (1 C, $CO_2C_2H_4CH_2C_7H_{15}$), 29.46 (1 C, $CO_2C_6H_{12}CH_2C_3H_6$), 29.59 (1 C, $CO_2C_5H_{10}CH_2C_4H_9$), 29.76 (1 C, $CO_2C_3H_6CH_2C_6H_{13}$), 32.03 (1 C, $CO_2C_4H_8CH_2C_5H_{11}$), 32.88 (1 C, $CO_2C_7H_{14}CH_2C_2H_5$), 33.21 (1 C, $CH_2CO_2C_{10}H_{21}$), 34.56 (1 C, $CO_2CH_2CH_2C_8H_{17}$), 53.57 (1 C, $CO_2CH_2C_9H_{19}$), 61.68 (1 C, CH), 169.73 (1 C, $CH(SO_3)CO_2H$), 173.14 (1 C, $CH_2CO_2C_{10}H_{21}$); ESI-MS m/z 337.1282 (M$^-$, $C_{14}H_{25}O_7S$).

Monododecyl sulfo-succinate   IR $\tilde{\nu}$ / cm^{-1} 3442br (O-H), 2920–2850 (C-H), 1734 (C=O ester), 1594 (C=O carboxylate salt), 1402 (C-S), 1344 (S=O), 1325 (C-O carboxylate salt), 1097 (C-O ester), 1050 (S=O); NMR δ_H / ppm (400 MHz; acetone$-$d$_6$) 0.80 (3 H, t, ^3J = 6.9 Hz, CH_3), 1.23 (18 H, m, $CO_2C_2H_4C_9H_{18}CH_3$), 1.58 (2 H, m, $CO_2CH_2CH_2C_{10}H_{21}$), 2.90 (2 H, m, C$H2$CO$_2$C$_{12}$H$_{25}$), 3.94 (1 H, m, CHSO$_3$), 4.05 (2 H, t, ^3J = 6.6 Hz, $CO_2CH_2C_{11}H_{23}$), δ_C / ppm (100.5 MHz; acetone$-$d$_6$) 14.11 (1 C, CH_3), 22.77 (1 C, $CO_2C_{10}H_{20}CH_2CH_3$), 25.91 (1 C, $CO_2C_2H_4CH_2C_9H_{19}$), 29.46 (1 C, $CO_2C_8H_{16}CH_2C_3H_7$), 29.59 (1 C, $CO_2C_3H_6CH_2C_8H_{17}$), 29.76 (4 C, $CO_2C_4H_8C_4H_8C_4H_9$), 32.03 (1 C, $CO_2C_9H_{18}CH_2C_2H_5$), 32.88 (1 C, $CO_2CH_2CH_2C_{10}H_{21}$), 33.21 (1 C, $CH_2CO_2C_{12}H_{25}$), 53.57 (1 C, $CO_2CH_2C_{11}H_{23}$), 61.68 (1 C, CH), 169.73 (1 C, $CH(SO_3)CO_2H$), 173.14 (1 C, $CH_2CO_2C_{12}H_{25}$); ESI-MS m/z 365.1639 (M$^-$, $C_{16}H_{29}O_7S$).
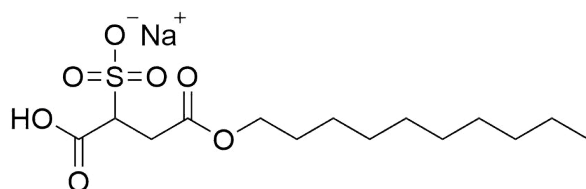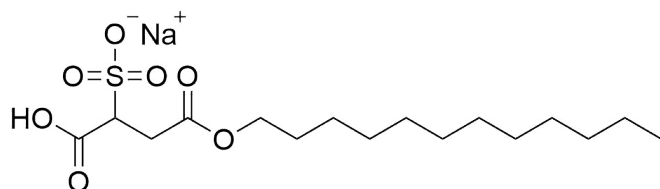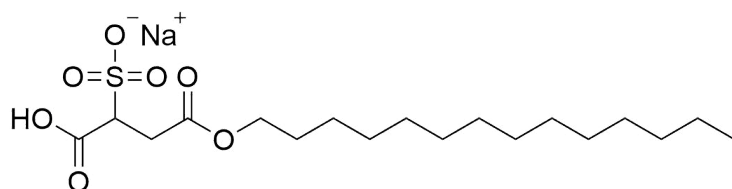
Monotetradecyl sulfo-succinate   IR $\tilde{\nu}$ / cm^{-1} 3442br (O-H), 2920–2850 (C-H), 1733 (C=O ester), 1602 (C=O carboxylate salt), 1404 (C-S), 1339 (S=O), 1330 (C-O carboxylate salt), 1095 (C-O ester), 1052 (S=O); NMR δ_H / ppm (400 MHz; acetone$-$d$_6$) 0.80 (3 H, t, ^3J = 6.9 Hz, CH_3), 1.23 (22 H, m, CO$_2$C$_2$H$_4$C$_{11}$$H_{22}CH_3$), 1.58 (2 H, m, CO$_2CH_2CH_2C_{12}H_{25}$), 2.90 (2 H, m, C$H2CO_2C_{14}H_{29}$), 3.94 (1 H, m, C$HSO_3$), 4.05 (2 H, t, ^3J = 6.6 Hz, CO$_2$CH_2C$_{13}$H$_{27}$), δ_C / ppm (100.5 MHz; acetone$-$d$_6$) 14.13 (1 C, CH_3), 22.77 (1 C, CO$_2$C$_{12}$H$_{24}$CH_2CH$_3$), 25.91 (1 C, CO$_2$C$_2$H$_4$CH_2C$_{11}$H$_{23}$), 29.47 (1 C, CO$_2$C$_{10}$H$_{20}$CH_2C$_3$H$_7$), 29.59 (1 C, C$_3$H$_6$CH_2C$_{10}$H$_{21}$), 29.79 (6 C, C$_4$H$_8$C$_6$H$_{12}$C$_4$H$_9$), 32.03 (1 C, CO$_2$C$_{11}$H$_{22}$CH_2C$_2$H$_5$), 32.86 (1 C, CO$_2$CH$_2$CH_2C$_{12}$H$_{25}$), 33.21 (1 C, CH_2CO$_2$C$_{14}$H$_{25}$), 53.57 (1 C, CH$_2$C$_{13}$H$_{27}$), 61.68 (1 C, CH), 169.73 (1 C, CO_2H), 173.14 (1 C, CH$_2$CO_2C$_{14}$H$_{29}$); ESI-MS m/z 393.1952 (M$^-$, C$_{18}$H$_{33}$O$_7$S).

7.5   Paper Pyrolysis

7.5.1   Paper *vs.* Cellulose

Milled office paper or microcrystalline cellulose (0.7 g) was charged to a microwave tube (10 cm^3, snap cap) and placed in the CEM microwave. This was heated (250 W, <250 °C, <5 mins) in open vessel mode with a syringe (glass, 100 cm^3) inserted into the tube to measure the gaseous products. Once cooled, the char was washed with methanol (3 × 5 cm^3) to extract the bio-oil which was analysed by GC-FID and GC-MS for quantification and identification. The gaseous products could not be efficiently collected and analysed with the equipment available.

7.5.2   Optimisation

Milled office paper was pressed with water into bricks and then left to dry before being cut into pieces (1 cm × 1 cm). The pieces of pressed paper (100 g) and water (10 g) were charged to the Milestone microwave complete with two condensers (one room temperature and one water cooled) and two collection flasks. The biomass was heated (<1200 W, <200 °C, <100 mbar, 18

mins) and once cool, the reactor and char were washed with methanol. The mass balance for the pyrolysis was calculated and the aqueous and organic fractions of bio-oil were analysed by GC-FID and GC-MS for quantification and identification.

Abbreviations

150Z zeolite150 (Al:Si molar ratio 150:1)

25Z zeolite25 (Al:Si molar ratio 25:1)

30Z zeolite30 (Al:Si molar ratio 30:1)

AE atom economy

Al-MC aluminium pillared montmorillonite clay

Al:Si alumina:silica molar ratio

AOT-1 Aerosol-OT-1

APG alkyl polyglucoside

API active pharmaceutical ingredient

ATR attenuated total reflectance

BA Brönsted acid

BPR Biocidal Product Regulation

c400 °C calcined at 400 °C

c550 °C calcined at 550 °C

CA citraconic acid

CLP Classification, Labelling and Packaging of substances and mixtures

CMC critical micelle concentration

DAD diode array detector

DAIC dialkyl itaconate

DASMS dialkyl sulfo-methylene-succinate

DBIC dibutyl itaconate

DGP decyl-α-D-glucopyranoside

DMIC dimethyl itaconate

DMMF 2-(dimethoxymethyl)-5-(methoxymethyl)furan

DMSMS dimethyl sulfo-methylene-succinate

DOCC dioctyl citraconate

DOIC dioctyl itaconate

DOMC dioctyl mesaconate

DOSMS dioctyl sulfo-methylene-succinate

E-R Eley-Rideal

EFAL extra-framework aluminium

EI electron ionisation

ELSD evaporative light scattering detector

ESI electrospray ionisation

FDCA 2,5-furan dicarboxylic acid

FID flame ionisation detector

FT-IR fourier transform infra-red

GC gas chromatography

GC-MS gas chromatography-mass spectrometry

H-β-Z H-β-zeolite

HDF 5-(hydroxymethyl)-2-(dimethoxymethyl)furan

HLB hydrophilic-lipophilic balance

HMF 5-hydroxymethyl furfural

IA itaconic acid

IAnh itaconic anhydride

IPA *iso*propyl alcohol

IR infra-red

IS internal standard

L-H Langmuir-Hinshelwood

LA Lewis acid

LG levoglucosan (1,6-β-D-glucopyranose)

LMW low molecular weight

MA mesaconic acid

MAIC monoalkyl itaconate

MalA maleic acid

MalAnh maleic anhydride

MASMS monoalkyl sulfo-methylene-succinate

MASSC monoalkyl sulfo-succinate

MDSMS monodecyl sulfo-methylene-succinate

MGP methyl-α-D-glucopyranoside

MI/PMI (process) mass intensity

MK10 montmorillonite clay K10

MK30 montmorillonite clay K30

MKSF montmorillonite clay KSF

MOCC mono-octyl citraconate

MOIC mono-octyl itaconate

mol equiv. molar equivalents

MOMC mono-octyl mesaconate

MOSMS mono-octyl sulfo-methylene-succinate

MS mass spectrometry

MTDSMS mono-tetradecyl sulfo-methylene-succinate

MW microwave

NMR nuclear magnetic resonance

OE optimum efficiency

PAcid phosphoric acid (H_3PO_4)

PEF polyethylene furandicarboxylate

PET polyethylene terephthalate

p-**TSA** *para*-toluene sulfonic acid

PVC polyvinyl chloride

r.t. room temperature

RDS rate determining step

REACH Registration, Evaluation, Authorisation and Restriction of Chemicals

RME reaction mass efficiency

scCO$_2$ supercritical CO_2

SDOSS sodium dioctyl sulfo-succinate

SDS sodium dodecyl sulfate

SFC supercritical fluid chromatography

SMBS sodium metabisulfite

SZ sulfated zirconia

TAcid tungstosilicic acid ($H_4[W_{12}SiO_{40}]$)

TBP *tert-tri*-butyl phenol

TOF turnover frequency

U.S. D.O.E. United States Department of Energy

UC uncalcined

WI waste intensity

WP waste percentage

wt% percent by weight

References

[1] C. O. Tuck, E. Perez, I. T. Horvath, R. A. Sheldon and M. Poliakoff, *Science (80-.).*, 2012, **337**, 695–699.

[2] J. H. Clark, *Green Chem.*, 1999, **1**, 1–8.

[3] P. T. Anastas and J. C. Warner, *Green Chemistry: Theory and Practice*, Oxford University Press, Oxford, UK, 1st edn., 1998.

[4] R. A. Sheldon, *Green Chem.*, 2014, **16**, 950–963.

[5] P. Gallezot, *Chem. Soc. Rev.*, 2012, **41**, 1538–1558.

[6] C. Lin, L. A. Pfaltzgraff, L. Herrero-Davila, E. B. Mubofu, A. Solhy, P. J. Clark, A. Koutinas, N. Kopsahelis, K. Stamatelatou, F. Dickson, S. Thankappan, M. Zahouily, R. Brocklesby and R. Luque, *Energy Environ. Sci.*, 2013, **6**, 426–464.

[7] *IPCC 5th Assessment Report. Climate Change 2013, Intergovernmental Panel on Climate Change. Working Group 1 Technical Report: The Physical Science Basis*, Cambridge University Press, Cambridge, UK, 2013.

[8] M. Hagens and J. J. Middelburg, *Geochim. Cosmochim. Acta*, 2016, **187**, 334–349.

[9] D. Tonini, V. Martinez-Sanchez and T. F. Astrup, *Environ. Sci. Technol.*, 2013, **47**, 8962–8969.

[10] E. U. Commission, *Environment fact sheet: REACH - a new chemicals policy for the EU*, 2006.

[11] *Regulation (EC) No 1907/2006 of the European Parliament and of the Council of 18 December 2006 concerning the Registration, Evaluation, Authorisation and Restriction of Chemicals (REACH)*, 2006, `http://data.europa.eu/eli/reg/2006/1907/oj`.

[12] *Regulation (EC) No 1272/2008 of the European Parliament and of the Council of 16 December 2008 on classification, labelling and packaging of substances and mixtures*, 2008, `http://data.europa.eu/eli/reg/2008/1272/oj`.

[13] E. U. Commission, *Classifying and Labelling Chemicals: A brief guide to the classification and labelling of chemicals in the EU*, 2014.

[14] *Regulation (EU) No 528/2012 of the European Parliament and of the Council of 22 May 2012 concerning the making available on the market and use of biocidal products*, 2012, `http://data.europa.eu/eli/reg/2012/528/oj`.

[15] J. BeMiller and R. Whistler, *Starch: Chemistry and Technology*, Elsevier, Burlington, USA, 3rd edn., 2009.

[16] J. Fan, M. De Bruyn, V. L. Budarin, M. J. Gronnow, P. S. Shuttleworth, S. Breeden, D. J. Macquarrie and J. H. Clark, *J. Am. Chem. Soc.*, 2013, **135**, 12728–12731.

[17] H. B. Mayes and L. J. Broadbelt, *J. Phys. Chem. A*, 2012, **116**, 7098–7106.

[18] H. V. Scheller and P. Ulvskov, *Annu. Rev. Plant Biol.*, 2010, **61**, 1–720.

[19] R. Vanholme, B. Demedts, K. Morreel, J. Ralph and W. Boerjan, *Plant Physiol.*, 2010, **153**, 895–905.

[20] R. Wojcieszak, F. Santarelli, S. Paul, F. Dumeignil, F. Cavani and R. V. Gonçalves, *Sustain. Chem. Process.*, 2015, **3**, 9–20.

[21] S. P. Teong, G. Yi and Y. Zhang, *Green Chem.*, 2014, **16**, 2015–2026.

[22] J. P. M. Sanders, J. H. Clark, G. J. Harmsen, H. J. Heeres, J. J. Heijnen, S. R. a. Kersten, W. P. M. van Swaaij and J. a. Moulijn, *Chem. Eng. Process. Process Intensif.*, 2012, **51**, 117–136.

[23] B. Erickson, Nelson and P. Winters, *Biotechnol. J.*, 2012, **7**, 176–185.

[24] J. H. Clark, V. Budarin, T. Dugmore, R. Luque, D. J. Macquarrie and V. Strelko, *Catal. Commun.*, 2008, **9**, 1709–1714.

[25] G. Fogassy, P. Ke, F. Figueras, P. Cassagnau, S. Rouzeau, V. Courault, G. Gelbard and C. Pinel, *Appl. Catal. A Gen.*, 2011, **393**, 1–8.

[26] T. Werpy and G. Petersen, *Top Value Added Chemicals from Biomass. Volume I, US Department of Energy Technical Report, Golden, CO*, 2004.

[27] Y. Akanuma, S. E. M. Selke and R. Auras, *Int. J. Life Cycle Assess.*, 2014, **19**, 1238–1246.

[28] A. J. J. E. Eerhart, A. P. C. Faaij and M. K. Patel, *Energy Environ. Sci.*, 2012, **5**, 6407–6422.

[29] G. J. M. Gruter and F. Dautzenberg, *EP Pat., 1834951 A1*, 2007.

[30] G. J. M. Gruter and F. Dautzenberg, *EP Pat., 1834950 A1*, 2007.

[31] L. Martino, N. Guigo, J. G. van Berkel, J. J. Kolstad and N. Sbirrazzuoli, *Macromol. Mater. Eng.*, 2016, **301**, 586–596.

[32] J. Britton, S. B. Dalziel and C. L. Raston, *Green Chem.*, 2016, **18**, 2193–2200.

[33] V. L. Budarin, P. S. Shuttleworth, J. R. Dodson, A. J. Hunt, B. Lanigan, R. Marriott, K. J. Milkowski, A. J. Wilson, S. W. Breeden, J. Fan, E. H. K. Sin and J. H. Clark, *Energy Environ. Sci.*, 2011, **4**, 471–479.

[34] J. H. Clark, D. J. Macquarrie and J. Sherwood, *Green Chem.*, 2012, **14**, 90–93.

[35] E. Goos, U. Riedel, L. Zhao and L. Blum, *Energy Procedia*, 2011, **4**, 3778–3785.

[36] J. A. Hyatt, *J. Org. Chem.*, 1984, **49**, 5097–5101.

[37] Y. D. Fomin, V. N. Ryzhov, E. N. Tsiok and V. V. Brazhkin, *Phys. Rev. E - Stat. Nonlinear, Soft Matter Phys.*, 2015, **91**, 1–5.

[38] Y. Wan, P. Chen, B. Zhang, C. Yang, Y. Liu, X. Lin and R. Ruan, *J. Anal. Appl. Pyrolysis*, 2009, **86**, 161–167.

[39] P. T. Anastas, M. M. Kirchhoff and T. C. Williamson, *Appl. Catal. A Gen.*, 2001, **221**, 3–13.

[40] P. Atkins, T. L. Overton, J. P. Rourke, M. T. Weller and F. A. Armstrong, 2014.

[41] J. Šmidrkal, M. Tesařová, I. Hrádková, M. Berčíková, A. Adamčíková and V. Filip, *Food Chem.*, 2016, **211**, 124–129.

[42] R. A. Sheldon, *Pure Appl. Chem.*, 2000, **72**, 1233–1246.

[43] S. R. Kirumakki, N. Nagaraju and S. Narayanan, *Appl. Catal. A Gen.*, 2004, **273**, 1–9.

[44] R. Koster, B. V. D. Linden, E. Poels and A. Bliek, *J. Catal.*, 2001, **204**, 333–338.

[45] W. Liu and C. Tan, *Ind. Eng. Chem. Res.*, 2001, **40**, 3281–3286.

[46] S. Miao and B. H. Shanks, *J. Catal.*, 2011, **279**, 136–143.

[47] M. R. Altiokka and A. Çitak, *Appl. Catal. A Gen.*, 2003, **239**, 141–148.

[48] J. González-Rivera, I. R. Galindo-Esquivel, M. Onor, E. Bramanti, I. Longo and C. Ferrari, *Green Chem.*, 2014, **16**, 1417–1425.

[49] Á. Szabolcs, M. Molnár, G. Dibó and L. T. Mika, *Green Chem.*, 2013, **15**, 439–445.

[50] P. Shuttleworth, V. Budarin, M. Gronnow, J. H. Clark and R. Luque, *J. Nat. Gas Chem.*, 2012, **21**, 270–274.

[51] D. J. Macquarrie, J. H. Clark and E. Fitzpatrick, *Biofuels, Bioprod. Biorefining*, 2012, **6**, 549–560.

[52] B. Krieger-Brockett, *Res. Chem. Intermed.*, 1994, **20**, 39–49.

[53] V. L. Budarin, J. H. Clark, B. A. Lanigan, P. Shuttleworth, S. W. Breeden, A. J. Wilson, D. J. Macquarrie, K. Milkowski, J. Jones, T. Bridgeman and A. Ross, *Bioresour. Technol.*, 2009, **100**, 6064–6068.

[54] P. Nuss and K. H. Gardner, *Int. J. Life Cycle Assess.*, 2013, **18**, 603–612.

[55] X. Hu and C.-Z. Li, *Green Chem.*, 2011, **13**, 1676–1679.

[56] L. A. Pfaltzgraff, M. De Bruyn, E. C. Cooper, V. Budarin and J. H. Clark, *Green Chem.*, 2013, **15**, 307–314.

[57] A. M. Balu, V. Budarin, P. S. Shuttleworth, L. A. Pfaltzgraff, K. Waldron, R. Luque and J. H. Clark, *ChemSusChem*, 2012, **5**, 1694–1697.

[58] P. Foley, A. Kermanshahi pour, E. S. Beach and J. B. Zimmerman, *Chem. Soc. Rev.*, 2012, **41**, 1499–1518.

[59] J. Guilbot, S. Kerverdo, A. Milius, R. Escola and F. Pomrehn, *Green Chem.*, 2013, **15**, 3337–3354.

[60] L. S. Hirst, *Fundamentals of Soft Matter Science*, CRC Press, Boca Raton, 1st edn., 2013.

[61] A. L. Jones, *Soft Condensed Matter*, Oxford University Press, New York, 13th edn., 2013.

[62] N. Hashimoto, K. Kawaguchi and K. Yoshioka, *J. Oleo Sci.*, 2015, **64**, 191–196.

[63] Y. Okada, T. Banno, K. Toshima and S. Matsumura, *J. Oleo Sci.*, 2009, **58**, 519–528.

[64] A. Gassama, C. Ernenwein, A. Youssef, M. Agach, E. Riguet, S. Marinković, B. Estrine and N. Hoffmann, *Green Chem.*, 2013, **15**, 1558–1566.

[65] W. V. Rybinski and K. Hill, *Angew. Chemie Int. Ed.*, 1998, **37**, 1328–1345.

[66] W. Wei, F. Feng, B. Perez, M. Dong and Z. Guo, *Green Chem.*, 2015, **17**, 3475–3489.

[67] J. Xu, F. Cao, T. Li, S. Zhang and C. Gao, *J. Surfactants Deterg.*, 2016, **19**, 373–379.

[68] T. Kawase, Y. Nagase and T. Oida, *J. Oleo Sci.*, 2016, **65**, 45–59.

[69] L. Zhi, Q. Li, Y. Li and Y. Song, *Colloids Surfaces A Physicochem. Eng. Asp.*, 2013, **436**, 684–692.

[70] W. Smułek, A. Zdarta, M. Milewska and E. Kaczorek, *Toxicol. Environ. Chem.*, 2016, **98**, 13–25.

[71] D. Malferrari, N. Armenise, S. Decesari, P. Galletti and E. Tagliavini, *ACS Sustain. Chem. Eng.*, 2015, **3**, 1579–1588.

[72] C. Damez, S. Bouquillon, D. Harakat, F. Hénin, J. Muzart, I. Pezron and L. Komunjer, *Carbohydr. Res.*, 2007, **342**, 154–162.

[73] D. Pérusse, J. P. Guégan, H. Rolland, J. Guilbot and T. Benvegnu, *Green Chem.*, 2016, **18**, 1664–1673.

[74] X. Zhu, R. T. Dere, J. Jiang, L. Zhang and X. Wang, *J. Org. Chem.*, 2011, **76**, 10187–10197.

[75] T. Hosoya, H. Kawamoto and S. Saka, *Carbohydr. Res.*, 2006, **341**, 2293–2297.

[76] N. M. Bennett, S. S. Helle and S. J. B. Duff, *Bioresour. Technol.*, 2009, **100**, 6059–6063.

[77] S. S. Choi, M. C. Kim and Y. K. Kim, *J. Anal. Appl. Pyrolysis*, 2011, **90**, 56–62.

[78] A. D. McNaught and A. Wilkinson, *IUPAC. Compendium of Chemical Terminology (the "Gold Book")*, Blackwell Scientific Publications, Oxford, 2nd edn., 1997.

[79] L. Chen, X. Li, J. C. Rooke, Y. Zhang, X. Yang, Y. Tang, F. Xiao and B. Su, *J. Mater. Chem.*, 2012, **22**, 17381–17403.

[80] C. Baerlocher, L. McCusker and D. Olson, *Atlas of Zeolite Framework Types*, Elsevier B.V., Amsterdam, 6th edn., 2007.

[81] J. B. Higgins, R. B. LaPierre, J. L. Schlenker, A. C. Rohrman, J. D. Wood, G. T. Kerr and W. R. Rohrbaugh, *Zeolites*, 1988, **8**, 446–452.

[82] M.-l. Gou, R. Wang, Q. Qiao and X. Yang, *Catal. Commun.*, 2014, **56**, 143–147.

[83] H. Fujita, T. Kanougi and T. Atoguchi, *Appl. Catal. A Gen.*, 2006, **313**, 160–166.

[84] E. Derouane, J. Védrine, R. R. Pinto, P. Borges, L. Costa, M. Lemos, F. Lemos and F. R. Ribeiro, *Catal. Rev.*, 2013, **55**, 454–515.

[85] J. Weitkamp and M. Hunger, in *Introd. to Zeolite Sci. Pract.*, ed. J. Cejka, H. van Bekkum, A. Corma and F. Schuth, Elsevier, Oxford, 3rd edn., 2007, vol. 168, ch. 22, pp. 787–835.

[86] N. Kaur and D. Kishore, *J. Chem. Pharm. Res.*, 2012, **4**, 991–1015.

[87] B. Caglar, O. Cubuk, E. Demir, F. Coldur, M. Catir, C. Topcu and A. Tabak, *J. Mol. Struct.*, 2015, **1089**, 59–65.

[88] L. Jankovič and P. Komadel, *J. Catal.*, 2003, **218**, 227–233.

[89] C. Breen, A. T. Deane and J. J. Flynn, *Clay Miner.*, 1987, **22**, 169–178.

[90] R. S. Drago and N. Kob, *J. Phys. Chem.*, 1997, **101**, 3360–3364.

[91] N. Katada, J. I. Endo, K. I. Notsu, N. Yasunobu, N. Naito and M. Niwa, *J. Phys. Chem. B*, 2000, **104**, 10321–10328.

[92] K. Saravanan, B. Tyagi and H. C. Bajaj, *Indian J. Chem. - Sect. A Inorganic, Phys. Theor. Anal. Chem.*, 2014, **53**, 799–805.

[93] D. Farcasiu, J. Q. Li and S. Cameron, *Appl. Catal. A Gen. Catal. A Gen.*, 1997, **154**, 173–184.

[94] B. M. Reddy, P. M. Sreekanth and P. Lakshmanan, *J. Mol. Catal. A Chem.*, 2005, **237**, 93–100.

[95] K. Hill, A. Behler, M. Biermann, H. C. Raths, M. E. Saint Victor and G. Uphues, *Surfactants Sci. Ser.*, 2001, **100**, 1–44.

[96] A. Milius and B. Brancq, *OCL*, 1995, **2**, 177–182.

[97] E. Jurado, M. Fernandez-Serrano, J. Nunez-Olea, M. Lechuga, J. L. Jimenez and F. Rios, *Water Environ. Res.*, 2011, **83**, 154–161.

[98] S. Iglauer, Y. Wu, P. Shuler, Y. Tang and W. A. Goddard III, *Tenside Surfactants Deterg.*, 2010, **47**, 87–97.

[99] F. Zhang, W. Gu, P. Xu, S. Tang, K. Xie, X. Huang and Q. Huang, *Waste Manag.*, 2011, **31**, 1333–1338.

[100] Y. Qin, G. Zhang, J. Zhang, Y. Zhao and J. Zhao, *J. Surfactants Deterg.*, 2006, **9**, 227–230.

[101] R. Sirsam, D. Hansora and G. A. Usmani, *J. Inst. Eng. Ser. E*, 2016, 1–15.

[102] H. Shi, A. N. Migues and S. M. Auerbach, *Green Chem.*, 2014, **16**, 875–884.

[103] T. M. Aida, Y. Sato, M. Watanabe, K. Tajima, T. Nonaka, H. Hattori and K. Arai, *J. Supercrit. Fluids*, 2007, **40**, 381–388.

[104] G. Yang, E. A. Pidko and E. J. M. Hensen, *J. Catal.*, 2012, **295**, 122–132.

[105] X. Hu, L. Wu, Y. Wang, D. Mourant, C. Lievens, R. Gunawan and C.-Z. Li, *Green Chem.*, 2012, **14**, 3087–3098.

[106] X. Hu, C. Lievens, A. Larcher and C. Z. Li, *Bioresour. Technol.*, 2011, **102**, 10104–10113.

[107] L. Hu, Z. Wu, J. Xu, Y. Sun, L. Lin and S. Liu, *Chem. Eng. J.*, 2014, **244**, 137–144.

[108] L. Zhou, L. Wu, H. Li, X. Yang, Y. Su, T. Lu and J. Xu, *J. Mol. Catal. A Chem.*, 2014, **388**-**389**, 74–80.

[109] X. Hu, R. J. M. Westerhof, L. Wu, D. Dong and C.-Z. Li, *Green Chem.*, 2015, **17**, 219–224.

[110] B. Girisuta, L. P. B. M. Janssen and H. J. Heeres, *Green Chem.*, 2006, **8**, 701–709.

[111] J. Zhang and E. Weitz, *ACS Catal.*, 2012, **2**, 1211–1218.

[112] H. Kimura, M. Nakahara and N. Matubayasi, *J. Phys. Chem. A*, 2013, **117**, 2102–2113.

[113] M. N. Timofeeva, *Appl. Catal. A Gen.*, 2003, **256**, 19–35.

[114] T. Okuhura, T. Nishimura, H. Watanabe and M. Misono, *J. Mol. Catal. A Chem.*, 1992, **247**, 247–256.

[115] R. Mokaya and W. Jones, *J. Catal.*, 1997, **172**, 211–221.

[116] C. R. Reddy, Y. S. Bhat, G. Nagendrappa and B. S. Jai Prakash, *Catal. Today*, 2009, **141**, 157–160.

[117] K. T. Wan, B. Khouw and M. E. Davis, *J. Catal.*, 1996, **158**, 311–326.

[118] C. Morterra and G. Cerrato, *Phys. Chem. Chem. Phys.*, 1999, **1**, 2825–2831.

[119] C. Morterra, G. Cerrato, F. Pinna and G. Meligrana, *Top. Catal.*, 2001, **15**, 53–61.

[120] V. Tabernero, C. Camejo, P. Terreros, M. D. Alba and T. Cuenca, *Materials (Basel).*, 2010, **3**, 1015–1030.

[121] K.-Y. Kwak, M.-S. Kim, D.-W. Lee, Y.-H. Cho, J. Han, T. S. Kwon and K.-Y. Lee, *Fuel*, 2014, **137**, 230–236.

[122] S. A. Bagshaw and R. P. Cooney, *Chem. Mater.*, 1993, **5**, 1101–1109.

[123] K. S. W. Sing, *Adv. Colloid Interface Sci.*, 1998, **76-77**, 3–11.

[124] K. Sing, *Colloids Surfaces A Physicochem. Eng. Asp.*, 2001, **187-188**, 3–9.

[125] K. S. W. Sing, *Colloids Surfaces A Physicochem. Eng. Asp.*, 2004, **241**, 3–7.

[126] S. Brunauer, P. H. Emmett and E. Teller, *J. Am. Chem. Soc.*, 1938, **60**, 309–319.

[127] E. P. Barrett, L. G. Joyner and P. P. Halenda, *J. Am. Chem. Soc.*, 1951, **73**, 373–380.

[128] L. G. Joyner, E. P. Barrett and R. Skold, *J. Am. Chem. Soc.*, 1951, **73**, 3155–3158.

[129] P. Komadel and J. Madejova, *Handbook of Clay Science*, Elsevier, Oxford, 1st edn., 2006.

[130] K. S. W. Sing, D. H. Everett, R. A. W. Haul, L. Moscou, R. A. Pierotti, J. Rouquerol and T. Siemieniewska, *Pure Appl. Chem.*, 1985, **57**, 603–619.

[131] M. Khalfaoui, S. Knani, M. A. Hachicha and A. B. Lamine, *J. Colloid Interface Sci.*, 2003, **263**, 350–356.

[132] F. Rouquerol, J. Rouquerol, K. S. W. Sing, P. Llewellyn and G. Maurin, *Adsorption by Powder and Porous Solids. Principles, Methodology and Applications*, Elsevier, Oxford, 2nd edn., 2014.

[133] M. Thommes, K. Kaneko, A. V. Neimark, J. P. Olivier, F. Rodriguez-Reinoso, J. Rouquerol and K. S. W. Sing, *Pure Appl. Chem.*, 2015, **87**, 1051–1069.

[134] V. K. Tyagi, *J. Oleo Sci.*, 2006, **55**, 429–439.

[135] A. M. Al-Sabagh, E. M. S. Azzam, S. A. Mahmoud and N. E. A. Saleh, *J. Surfactants Deterg.*, 2007, **10**, 3–8.

[136] W. Johnson Jr., B. Heldreth, W. F. Bergfeld, D. V. Belsito, R. A. Hill, C. D. Klaassen, D. C. Liebler, J. G. Marks Jr., R. C. Shank, T. J. Slaga, P. W. Snyder and F. A. Andersen, *Int. J. Toxicol.*, 2015, **34**, 70S–83S.

[137] A. Adewuyi, A. D. Adesina and R. A. Oderinde, *Adv. Chem.*, 2014, 1–7.

[138] V. Singh and R. Tyagi, *J. Surfactants Deterg.*, 2016, **19**, 111–118.

[139] K. Baczko, X. Chasseray and C. Larpent, *J. Chem. Soc. Perkin Trans. 2*, 2001, 2179–2188.

[140] H. V. Patil, R. D. Kulkarni and S. Mishra, *Int. J. Chem. Chem. Eng.*, 2013, **3**, 69–74.

[141] S. Baup, *Ann Chim Phys*, 1837, **19**, 29–38.

[142] J. Ding, B. Song, C. Wang, J. Xu and Y. Wu, *J. Surfactants Deterg.*, 2011, **14**, 43–49.

[143] J. Lian, M. Garcia-Perez and S. Chen, *Bioresour. Technol.*, 2013, **133**, 183–189.

[144] A. M. Medway and J. Sperry, *Green Chem.*, 2014, **16**, 2084–2101.

[145] P. Bonnarme, B. Gillet, A. M. Sepulchre, C. Role, J. C. Beloeil and C. Ducrocq, *J. Bacteriol.*, 1995, **177**, 3573–3578.

[146] T. Willke and K. D. Vorlop, *Appl. Microbiol. Biotechnol.*, 2001, **56**, 289–295.

[147] R. N. Ram and I. Charles, *Tetrahedron*, 1997, **53**, 7335–7340.

[148] T. Kawabata, T. Mizugaki, K. Ebitani and K. Kaneda, *Tetrahedron Lett.*, 2003, **44**, 137–140.

[149] A. León, E. Abuin, E. Lissi, L. Gargallo and D. Radić, *J. Colloid Interface Sci.*, 1987, **115**, 529–534.

[150] R. A. Prasath and S. Ramakrishnan, *J. Polym. Sci. Part A Polym. Chem.*, 2005, **43**, 3257–3267.

[151] W. D. Emmons and G. A. Frank, *US Pat., 3 541 138*, 1970.

[152] A. Leon, L. Gargallo, D. Radic and A. Horta, *Polymer (Guildf).*, 1991, **32**, 761–763.

[153] K. Naitohj, Y. Ishii and K. Tsujii, *J. Phys. Chem.*, 1991, **95**, 7915–7918.

[154] A. Parsons, *Keynotes in Organic Chemistry*, Wiley-Blackwell, Chichester, 2nd edn., 2014.

[155] C. R. Reddy, P. Iyengar, G. Nagendrappa and B. S. J. Prakash, *Catal. Letters*, 2005, **101**, 87–91.

[156] J. H. Clark, E. M. Fitzpatrick, D. J. MacQuarrie, L. a. Pfaltzgraff and J. Sherwood, *Catal. Today*, 2012, **190**, 144–149.

[157] Y. Zhu, Z. Hua, Y. Song, W. Wu, X. Zhou, J. Zhou and J. Shi, *J. Catal.*, 2013, **299**, 20–29.

[158] L. Li, S. Liu, J. Xu, S. Yu, F. Liu, C. Xie, X. Ge and J. Ren, *J. Mol. Catal. A Chem.*, 2013, **368-369**, 24–30.

[159] T. J. Farmer, Y. Bai, M. De Bruyn, J. Clark, J. R. Dodson, M. Honoré, I. Ingram, M. Naguib, A. C. Whitwood and M. North, *Green Chem.*, 2016, **18**, 3945–3948.

[160] J. K. West, A. B. Brennan, A. E. Clark, M. Zamora and L. L. Hench, *J. Biomed. Mater. Res.*, 1998, **41**, 8–17.

[161] E. Sagot, D. S. Pickering, X. Pu, M. Umberti, T. B. Stensboel, B. Nielsen, M. Chapelet, J. Bolte, T. Gefflaut and L. Bunch, *J. Med. Chem.*, 2008, **51**, 4093–4103.

[162] P. Ferraboschi, S. Casati, P. Grisenti and E. Santaniello, *Tetrahedron*, 1994, **50**, 3251–3258.

[163] W. Markownikow, *Chem. Ber.*, 1880, **13**, 1844–1845.

[164] Y. Kita, S. Akai, N. Ajimura, M. Yoshigi, T. Tsugoshi, H. Yasuda and Y. Tamura, *J. Org. Chem.*, 1986, **51**, 4150–4158.

[165] R. L. Shriner, S. G. Ford and L. J. Roll, *Org. Synth.*, 1931, **11**, 70–71.

[166] M. Kuchar, M. Poppova, H. Zunova, E. Knezova, V. Vosatka and M. Prihoda, *Collect. Czechoslov. Chem. Commun.*, 1994, **59**, 2705–2713.

[167] R. P. Linstead and J. T. W. Mann, *J. Chem. Soc.*, 1931, 726–740.

[168] M. Sakai, *Bull. Chem. Soc. Jpn.*, 1976, **49**, 219–223.

[169] M. Sakai, *Bull. Chem. Soc. Jpn.*, 1977, **50**, 1232–1234.

[170] G. Cody, N. Boctor, R. Hazen, J. Brandes, H. J. Morowitz and H. Yoder, *Geochim. Cosmochim. Acta*, 2001, **65**, 3557–3576.

[171] M. Carlsson, C. Habenicht, L. C. Kam, M. J. Antal, Jr., N. Bian, R. J. Cunningham and M. Jones, Jr., *Ind. Eng. Chem. Res.*, 1994, **33**, 1989–1996.

[172] T. J. Farmer, R. L. Castle, J. H. Clark and D. J. Macquarrie, *Int. J. Mol. Sci.*, 2015, **16**, 14912–14932.

[173] T. J. Farmer, J. H. Clark, D. J. Macquarrie, J. K. Ogunjobi and R. L. Castle, *Polym. Chem.*, 2016, **7**, 1650–1658.

[174] T. Salavati-fard, S. Caratzoulas and D. J. Doren, *J. Phys. Chem. A*, 2015, **119**, 9834–9843.

[175] I. S. Zope, A. Dasari and G. Camino, *Mater. Chem. Phys.*, 2015, **157**, 69–79.

[176] T. Parangi, B. Wani and U. Chudasama, *Appl. Catal. A Gen.*, 2013, **467**, 430–438.

[177] R. Ellson, R. Stearns, M. Mutz, C. Brown, B. Browning, D. Harris, S. Qureshi, J. Shieh and D. Wold, *Comb. Chem. High Throughput Screen.*, 2005, **8**, 489–498.

[178] A. Luzar and D. Chandler, *J. Chem. Phys.*, 1993, **98**, 8160–8173.

[179] D. B. Wong, K. P. Sokolowsky, M. I. El-Barghouthi, E. E. Fenn, C. H. Giammanco, A. L. Sturlaugson and M. D. Fayer, *J. Phys. Chem. B*, 2012, **116**, 5479–5490.

[180] J. Kisielewski and D. Robertson, *US Pat., 7 985 396 B2*, 2011.

[181] W. Spormann, B. Durkheim and J. Heiuke, *US Pat., 3 361 524*, 1968.

[182] S. L. Bean, M. D. Dulik and R. J. Wilson, *US Pat., 4 844 880*, 1989.

[183] W. M. Zolotoochin, J. P. Metziner and D. M. Hansen, *US Pat., 5 753 200*, 1998.

[184] M. S. Kharasch, E. M. May and F. R. Mayo, *J. Org. Chem.*, 1938, **3**, 175–192.

[185] S. C. Bright, C. E. Stubbs and L. Thompson, *J. Appl. Chem. Biotechnol.*, 1975, **25**, 901–912.

[186] M. Morton and H. Landfield, *J. Am. Chem. Soc.*, 1952, **74**, 3523–3526.

[187] T. D. Stewart and L. H. Donnally, *J. Am. Chem. Soc.*, 1932, **54**, 3559–3569.

[188] M. S. Kharasch, H. Engelmann and F. Mayo, *J. Am. Chem. Soc.*, 1937, **989**, 288–302.

[189] E. Hayon, a. Treinin and J. Wilf, *J. Am. Chem. Soc.*, 1972, **94**, 47–57.

[190] T. L. Brown, E. LeMay Jr., B. E. Bursten, C. Murphy, P. Woodward, S. Langford, D. Sagatys and A. George, in *Chem. Cent. Sci.*, ed. K. Millar, Pearson Australia, Frenchs Forest, 3rd edn., 2014, ch. 17, pp. 678–732.

[191] M. G. Khublaryan, in *Encycl. Life Support Syst.*, ed. M. G. Khublaryan, EoLSS Publishers Co. Ltd., Oxford, 1st edn., 2009, ch. 4, pp. 257–277.

[192] T. Kurten, T. Berndt and F. Stratmann, *Atmos. Chem. Phys.*, 2009, **9**, 3357–3369.

[193] D. Moller, *Chemistry of the Climate System*, Walter de Gruyter & Co., Berlin, 1st edn., 2010.

[194] H. Hung and M. R. Hoffmann, *Environ. Sci. Technol.*, 2015, **49**, 13768–13776.

[195] W. Pasiuk-Bronikowska, T. Bronikowski and M. Ulejczyk, *J. Atmos. Chem.*, 2003, **44**, 97–111.

[196] G. N. Smith, R. Kemp, J. C. Pegg, S. E. Rogers and J. Eastoe, *Langmuir*, 2015, **31**, 13690–13699.

[197] C. R. McElroy, A. Constantinou, L. C. Jones, L. Summerton and J. H. Clark, *Green Chem.*, 2015, **17**, 3111–3121.

[198] E. N. Kolesnikova and N. A. Glukhareva, *Russ. J. Phys. Chem. A*, 2009, **83**, 2119–2121.

[199] Y. Minegishi, K. Aigami and H. Arai, *J. Japanese Oil Chem. Soc.*, 1975, **24**, 237–340.

[200] T. Hosoya, H. Kawamoto and S. Saka, *J. Anal. Appl. Pyrolysis*, 2008, **83**, 71–77.

[201] L. Wang, R. Templer and R. J. Murphy, *Bioresour. Technol.*, 2012, **120**, 89–98.

[202] Y.-c. Lin, J. Cho, G. a. Tompsett, P. R. Westmoreland and G. W. Huber, *J. Phys. Chem.*, 2009, **113**, 20097–20107.

[203] F. Shafizadeh, *J. Anal. Appl. Pyrolysis*, 1982, **3**, 283–305.

[204] V. L. Budarin, J. H. Clark, B. A. Lanigan, P. Shuttleworth and D. J. Macquarrie, *Bioresour. Technol.*, 2010, **101**, 3776–3779.

[205] A. G. W. Bradbury, Y. Sakai and F. A. Shafizadeh, *J. Appl. Polym. Sci.*, 1979, **23**, 3271–3280.

[206] M. J. Antal Jr and G. Varhegyi, *Ind. Eng. Chem. Res.*, 1995, **34**, 703–717.

[207] J. Piskorz, D. Radlein and D. Scott, *J. Anal. Appl. Pyrolysis*, 1986, **9**, 121–137.

[208] H. Kawamoto, M. Murayama and S. Saka, *J. Wood Sci.*, 2003, **49**, 469–473.

[209] R. Vinu and L. J. Broadbelt, *Energy Environ. Sci.*, 2012, **5**, 9808–9826.

[210] P. R. Patwardhan, J. A. Satrio, R. C. Brown and B. H. Shanks, *J. Anal. Appl. Pyrolysis*, 2009, **86**, 323–330.

[211] H. Kawamoto, W. Hatanaka and S. Saka, *J. Anal. Appl. Pyrolysis*, 2003, **70**, 303–313.

[212] G. R. Ponder, G. N. Richards and T. T. Stevenson, *J. Anal. Appl. Pyrolysis*, 1992, **22**, 217–229.

[213] A. N. Kislitsyn, Z. M. Rodionovo, V. I. Savinykh and A. V. Gusev, *Zhurnal Prikl. Khimii*, 1971, **44**, 2518–2524.

[214] A. M. Pakhomov, *Russ. Chem. Bull.*, 1958, **6**, 1525–1527.

[215] D. J. Gardiner, *J. Chem. Soc. C*, 1966, 1473–1476.

[216] K. Kato, *Agric. Biol. Chem.*, 1967, **31**, 657–663.

[217] O. P. Golova, A. M. Andrievskaya, E. A. Pakhomov and N. M. Merlis, *Russ. Chem. Bull.*, 1957, **6**, 399–401.

[218] G. J. Kwon, D. Y. Kim, S. Kimura and S. Kuga, *J. Anal. Appl. Pyrolysis*, 2007, **80**, 1–5.

[219] M. J. Antal Jr, G. Varhegyi and E. Jakabi, *Ind. Eng. Chem. Res.*, 1998, **37**, 1267–1275.

[220] X. Bai, P. Johnston and R. C. Brown, *J. Anal. Appl. Pyrolysis*, 2013, **99**, 130–136.

[221] D. S. T. A. G. Radlein, A. Grinshpun, J. Piskorz and D. S. Scott, *J. Anal. Appl. Pyrolysis*, 1987, **12**, 39–49.

[222] F. Ronsse, X. Bai, W. Prins and R. C. Brown, *Environ. Prog. Sustain. Energy*, 2012, **31**, 256–260.

[223] X. Zhang, W. Yang and W. Blasiak, *J. Anal. Appl. Pyrolysis*, 2012, **96**, 110–119.

[224] H. Kawamoto, H. Morisaki and S. Saka, *J. Anal. Appl. Pyrolysis*, 2009, **85**, 247–251.

[225] G. Magnaghi, *Recovered Paper Market in 2010, BIR Paper Division Technical Report, Brussels, Belgium*, 2010.

[226] L. Wang, M. Sharifzadeh, R. Templer and R. J. Murphy, *Energy Environ. Sci.*, 2012, **5**, 5717–5730.

[227] A. Mansikkasalo, R. Lundmark and P. Söderholm, *For. Policy Econ.*, 2014, **38**, 17–29.

[228] A. Blanco, R. Miranda and M. C. Monte, *For. Syst.*, 2013, **22**, 471–483.

[229] *Directive 2008/98/EC of the European Parliament and of the Council of 19 November 2008 on waste and repealing certain Directives*, 2008, `http://data.europa.eu/eli/dir/2008/98/oj`.

[230] A. Iosip, A. Dobon, M. Hortal and E. Bobu, *Int. J. Life Cycle Assess.*, 2012, **17**, 1050–1058.

[231] D. Rajput, S. S. Bhagade, S. P. Raut, R. V. Ralegaonkar and S. A. Mandavgane, *Constr. Build. Mater.*, 2012, **34**, 470–475.

[232] L. Wang, R. Templer and R. J. Murphy, *Appl. Energy*, 2012, **99**, 23–31.

[233] Z. Zhang, D. J. Macquarrie, M. De Bruyn, V. L. Budarin, A. J. Hunt, M. Gronnow, J. Fan, P. S. Shuttleworth, J. H. Clark and A. S. Matharu, *Green Chem.*, 2014, **17**, 260–270.

[234] S. W. Breeden, J. H. Clark, T. J. Farmer, D. J. Macquarrie, J. S. Meimoun, Y. Nonne and J. E. S. J. Reid, *Green Chem.*, 2012, **15**, 72–75.

[235] P. R. Patwardhan, J. A. Satrio, R. C. Brown and B. H. Shanks, *Bioresour. Technol.*, 2010, **101**, 4646–4655.

[236] J. Piskorz, D. S. Radlein, D. S. Scott and S. Czernik, *J. Anal. Appl. Pyrolysis*, 1989, **16**, 127–142.

[237] G. N. Richards, *J. Anal. Appl. Pyrolysis*, 1987, **10**, 251–255.

[238] N. Shimada, H. Kawamoto and S. Saka, *J. Anal. Appl. Pyrolysis*, 2008, **81**, 80–87.

[239] N. Shimada, H. Kawamoto and S. Saka, *Carbohydr. Res.*, 2007, **342**, 1373–1377.

[240] J. B. Paine, Y. B. Pithawalla and J. D. Naworal, *J. Anal. Appl. Pyrolysis*, 2008, **83**, 37–63.

[241] M. Müller-Hagedorn, H. Bockhorn, L. Krebs and U. Müller, *J. Anal. Appl. Pyrolysis*, 2003, **68-69**, 231–249.

[242] M. Kleen and G. Gellerstedt, *J. Anal. Appl. Pyrolysis*, 1995, **35**, 15–41.

[243] P. R. Patwardhan, D. L. Dalluge, B. H. Shanks and R. C. Brown, *Bioresour. Technol.*, 2011, **102**, 5265–5269.

[244] X. Bai, P. Johnston, S. Sadula and R. C. Brown, *J. Anal. Appl. Pyrolysis*, 2013, **99**, 58–65.

[245] L. J. Kuo, B. E. Herbert and P. Louchouarn, *Org. Geochem.*, 2008, **39**, 1466–1478.

[246] P. Louchouarn, L. J. Kuo, T. L. Wade and M. Schantz, *Atmos. Environ.*, 2009, **43**, 5630–5636.

[247] M. Essig, G. N. Richards and E. Schench, in *Cellul. Wood-Chemistry Technol.*, ed. C. Schuerch, John Wiley and Sons Inc., New York, 1st edn., 1989, ch. 4, pp. 841–862.

[248] F. Shafizadeh, R. H. Furneaux, T. G. Cochran, J. P. Scholl and Y. Sakai, *J. Appl. Polym. Sci.*, 1979, **23**, 3525–3539.

[249] Q. Zhang, M. Benoit, K. De Oliveira Vigier, J. Barrault, G. Jegou, M. Philippe and F. Jerome, *Green Chem.*, 2013, **15**, 963–969.